Phytochemical and pharmacological study of *Hypericum triquetrifolium* TURRA

Dissertation

submitted to the Faculty of Chemistry and Pharmacy,
University of Regensburg for the degree of
Doctor of Natural Sciences (Dr. rer. nat.)

presented by

Ilya B. Volkov

from Holon, Israel

2017

The present work was carried out from October 2013 until October 2016 under the supervision of Prof. Dr. Jörg Heilmann at the Pharmaceutical Biology department, Institute of Pharmacy, Faculty of Chemistry and Pharmacy, University of Regensburg.

Dissertation submitted on: 2nd December, 2016

Day of oral presentation: 10th February, 2017

Examination committee:	Prof. Dr. Sigurd Elz	(Chairperson)
	Prof. Dr. Jörg Heilmann	(First examiner)
	Prof. Dr. Michael Decker	(Second examiner)
	PD Dr. Birgit Kraus	(Third examiner)

Fortune favours the bold.

— Virgil, “The Aeneid”

Acknowledgements

My deepest and most sincere thank you first goes to Prof. Dr. Jörg Heilmann for accepting me to your working group. It was a great pleasure to work on your department, to learn tons of new things, not only biological, chemical, biochemical, analytical, pharmaceutical, etc., but also to discover a whole new world all around me. I am extremely grateful for your kindness, support, taking time, sharing ideas, explanations and the fact you did care.

PD Dr. Birgit Kraus, many thanks for taking your time and, what is much more important, patience, for teaching and explaining how things in cell culture work. It was an unforgettable experience and I loved it a lot. Thank you for your inspiration, I do highly appreciate that.

Dr. habil. Guido Jürgenliemk, thank you for leading me in the right direction, both during the studies and during the Bioanalytik Praktikum. Thank you for your kind and fruitful advises, knowledge and willingness to help.

Dr. Sebastian Schmidt, without you all this would not have been possible. Thank you for your patience, wise advises, for sharing attainments, thoughts and experience. I'm also grateful for your kind help in proofreading!

Gabi Brunner, for keeping everything in perfect and strict order and letting know where the things are. The Department never functions the same without you! Thank you for open column teaching and taking time in explanations about useful cell culture tricks, as well as insuring me with extra cells available. Anne Grasshuber for helping in practice with students, for your kindness and enormous help by extraction. I wish you nothing, but the very best!

Hedwig Ohli, our dear secretary, for helping in being accepted to the department, for helping with the accommodation, for all the messy but necessary administrative things.

Central Analytical Department of the University of Regensburg: Fritz Kastner and Dr. Ilya Schenderowitch for taking NMR spectra; Josef Kiermaier and Wolfgang Söllner for taking MS spectra. PD Dr. Axel Dürkop (Institute of Analytical Chemistry, Chemo- and Biosensorik) for measuring CD-spectra and telling stories about the Uni's history.

Mrs. Michal Monosov (Hebrew University Botanical Gardens on Mt. Scopus, Jerusalem) and Mrs. Hagar Leschner (The Israeli National Herbarium, Hebrew University, Givat-Ram, Jerusalem) for your magical and kind help in finding, verifying and transporting the herb material to Germany.

My dearest lab Mädls – Katharina Schiller and Eva Lotter for all your help, sincere laughs, Bavarian language and tradition lessons (I red a bissl Boarisch und des is a guad so! ☺), Budapest drinks and walks, cartoons, die 3 Besoffskis, TV commercials, Christmas songs, Regina & Garbo Filmtheaters, etc. for creating the coolest lab spirit one could have ever dreamt to have – you are unequivocally a true enco-co-couraging!

Julianna Ziegler, for joint bus trips to Munich, advises and notes along the work and proofreading! I wish you all the good luck with your *Hypericum* sp.!

Dr. Edna E. Makule (Arusha, Tanzania), for your inspiration and advices, for patience, help and explanations, for always bringing the sun with you. Very much appreciated!

Sebastian Schwindl, for your recommendations and discoveries in cell culture, NMR and optical rotation.

My department colleagues Christian Zeh, Stefan Wiesneth, Sina Malenke, Dr. Monika Untergehrer, Dr. Tri-Hieu Nguen (Vietnam), Dr. Beata Kling, Dr. Marcel Flemming, Dr. Petr Jirásek, Dr. Rosi Scherübl – thank you for the inspiration, it was a great pleasure to work with you! Sebastian Pitzl, thank you very much for your suggestions and permission to reprint the unpublished data of your master thesis for comparison reasons. Good luck with your PhD work!

Our international guest scientists Carlo and Sylvia (Vinece, Italy), Angeliki, Arthemis and Ariola (Athens, Greece) and Filip (Novi Sad, Serbia). I hope you had a lot of fun with 2D-NMR spectra!

Dr. Parsekev Nedialkov (Sofia, Bulgaria) and Dr. Peter Lorenz from „Wala“ for great time at the GA-2015 conference in Budapest, for fruitful discussions and wise advises.

My interns Svetlana Reichert, Rafael Rager and Marcell Kaljanac for teaching me something new.

I am extremely thankful to all the people, who inspired and supported me mentally during these years and helped me in performing this work. Among them, almighty and unbeliveable Per Gessle, charming and cute Helena Josefsson, kind and touching Marie Fredriksson + Mazarinerna, SOAP and Gyllene Tider rockaboom guys and all the people from the Rox world, who have been lightening my everyday path during the recent 20 years. My gorgeous muse Eva Gaëlle Green and Susan Sarandon, Geoffrey Rush, Cate Blanchett, Sir Ian McKellen, Dame Judi Dench, Kevin Spacey, Tom Hanks and many others, who share their unlimited magic and spread the world with their sincere art and encouraged me all this time.

My best friends Dr. Ilya Alexeev, Alexander Grigoruk and Sergey Dulin for your endless support and inspiration, for your ideas, honesty, warmth, sand of south oceans and spirit of Samui. I promise you to explore Sumatra one day and find *Rafflesia arnoldii* at last. My dearest Mr. Vladislav Braginsky for supporting me during all these years, for your kindness and understanding; I sincerely wish you all the good luck in everything you do. Frau Alexandra Gutzmer for friendly meows, cakes, photos, cafes and walks.

Dr. med. dent. Vladimir and Ludmila Reboudé + the family for their financial and unlimited moral support. You have always been my back and I will never have enough words to thank you properly for what you have done for me. I extremely appreciate you being by my side.

Dipl.-Ing. Zeev and Liora Kotel + the family for your wise advises and supporting my beginnings. For believing and not letting me alone, even if I was not right.

My dearest parents, Dipl.-Ing. Boris and Irina Volkov (+ Manya) for your support, for your investments in my education, for taking care of me, for wishing me nothing but the best, for your endless love. The current work is dedicated to you.

I would also like to thank my Eugen for your love, patience and support. I don’t know where I would’ve been without you. Thank you for your compassion and sincerity. I look forward to discover a whole new world together.

Publications list

Poster

Ilya Volkov, Sebastian Schmidt, Jörg Heilmann (2015): Isolation and structure elucidation of acylphloroglucinols from *Hypericum triquetrifolium* TURRA. *Planta Medica*, 16(81): PM_85. DOI: 10.1055/s-0035-1565462.

63rd International Congress and Annual Meeting of the Society for Medicinal Plant and Natural Product Research (GA2015). Budapest, Hungary, 23–27, August 2015

Content

1 Introduction

1.1 Genus *Hypericum* L.

1.1.1 General information and classification

Genus *Hypericum* belongs to family Hypericaceae JUSSIEU and comprises nearly 500 various species (Crockett and Robson, 2011), which can be found in almost all parts of the Earth, excluding polar regions, deserts and tropical lowlands (Schütt and Schulz, 2007). The earliest reference to *Hypericum* belongs to the II century BC (Robson, 2003) and new species are being discovered even today (Ely et al., 2015).

Family Hypericaceae is well described by (Stevens, 2007) and is divided in three tribes:

I. **Tribe Vismieae** CHOISY (1821)
   1. *Vismia* VAND. – ca. 52 species
   2. *Harungana* LAMARK – 50 species in 7 groups

II. **Tribe Hypericeae** CHOISY (1821)
   3. *Hypericum* L. – 420 species
   4. *Lianthus* N. ROBSON – 1 species
   5. *Triadenum* RAF. – 6 species
   6. *Thornea* BREEDLOVE & MCCLINTOCK – 2 species
   7. *Santomasia* N. ROBSON – 1 species

III. **Tribe Cratoxyleae** BENTHAM (1862)
   8. *Cratoxylum* BLUME – 6 species
   9. *Eliea* CAMBESS. – 1 species

Several years ago the family Hypericaceae was not defined as independent family, but was included in Clusiaceae (Guttiferae). The modern systematic classification of the genus *Hypericum* can be observed from **Tab. 1** (§ 1.1.3.3).

A large number of species in one single genus caused a great need for further and deeper classification. Therefore, additional taxonomical units in frames of a genus are used: subgenus, sections and series. British botanist Norman Keith Bonner Robson (b. 1928) produced a worldwide taxonomic monograph of genus *Hypericum* between 1977 and 2012 (Robson, 1977; Robson, 2002; Robson 2003). This work is constantly updated and edited through the time, presenting today 30 sections and 6 sub-sections (6a, 9a-e).

According to Robson, the division of the genus to sections is based on morphological, geographical and phylogenetical principals. All these unite in chemotaxonomy, thus emphasizing relative species. **Fig. 1** represents connections between the sections of the genus.

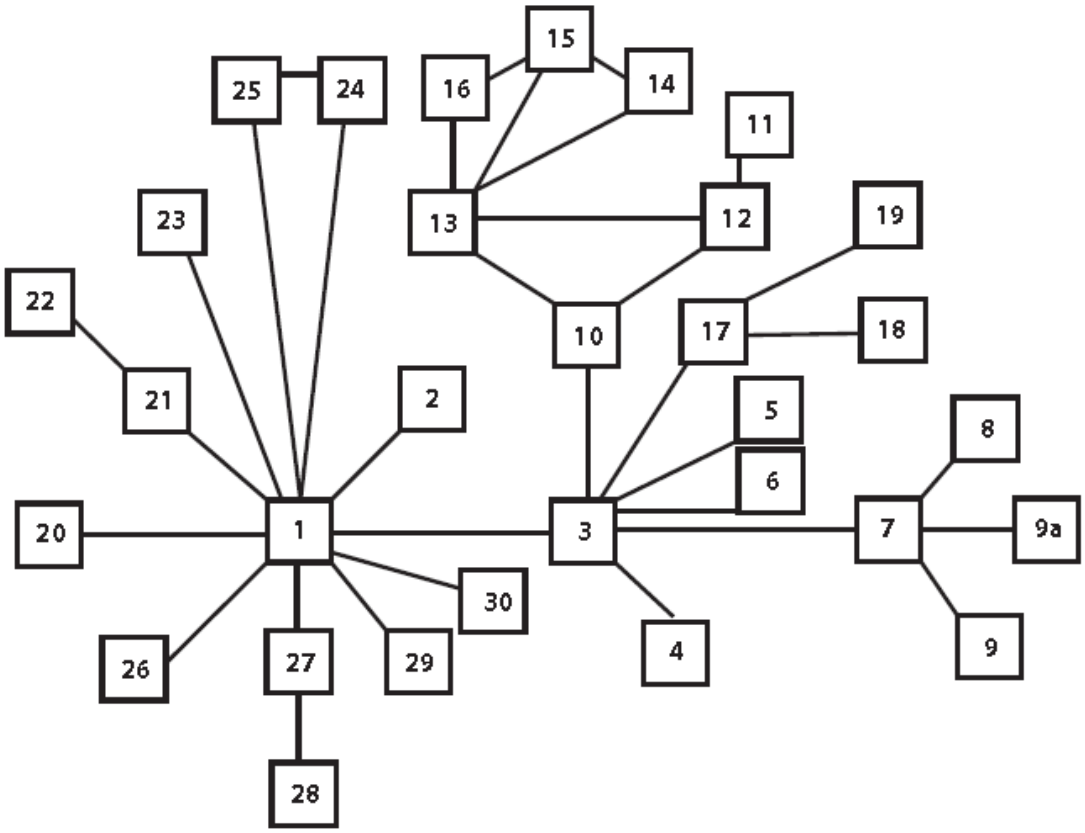

Fig. 1. Phylogenetic tree of genus *Hypericum*
(Sections according to Robson, 1977) (Nürk, 2011)

A complex mixture of bioactive secondary metabolites in several *Hypericum* species makes them valuable as herbal drugs (Crockett et al., 2005; Mártonfi et al., 2006; Crockett et al., 2010). A lot of species are used in traditional medicine in different countries all over the world. A few examples include:

- In Europe *Hypericum* sp. was used since the ancient times. Pedanius Dioscorides and Pliny the Elder described its healing and emmenagogue properties (Plinius Secundus, 1967). *H. perforatum* was famous in European herbal medicine (AMR, 2004; Hahn, 1992), and was first noted as a remedy for melancholy and madness in British folk medicine since XVII century (Culpeper, 1652). Until today the genus is used in Italian traditional medicine (Idolo et al., 2010).

- In Traditional Chinese Medicine (TCM) *H. perforatum* is known as *Guan Ye Lian Qiao*, originating from "Ben Cao Gang Mu Shi Yi" by Zhao Xue-Min (1765). It is used to reduce fever, eliminate toxins, stop bleeding, relief muscles pain and treat depression (Chen and Chen, 2012). At least 30 different representatives of the genus are being used in the TCM (Zhou et al., 2011).
- In Middle East species of the genus *Hypericum* are used in Iranian Traditional Medicine for wounds and old sores treatment (Mosaddegh et al., 2012; Ghorbani, 2005), as well as in Turkey (Altundag and Ozturk, 2011; Cakilioglu et al., 2011) and India (Kumar et al., 2007).
- *H. connatum* is used in traditional Brazilian medicine as tonic and astringent (Correa, 1984). In southern Brazil it is used against oral lesions, frequently caused by herpes viruses (Mentz et al., 1997).

1.1.2 Section 9 *Hypericum* L.

Section 9 is called *Hypericum* and comprises 42 species. It is divided in two subsections (**Fig. 2**): subsect. 1. *Hypericum* (widespread) and subsect. 2. *Erecta* (Japan, Taiwan, eastern China). Subsection 1 *Hypericum* is divided in series 1. *Hypericum* (species 1-12) and series 2. *Senanensia* (species 13-19, Japan, Korea, China).

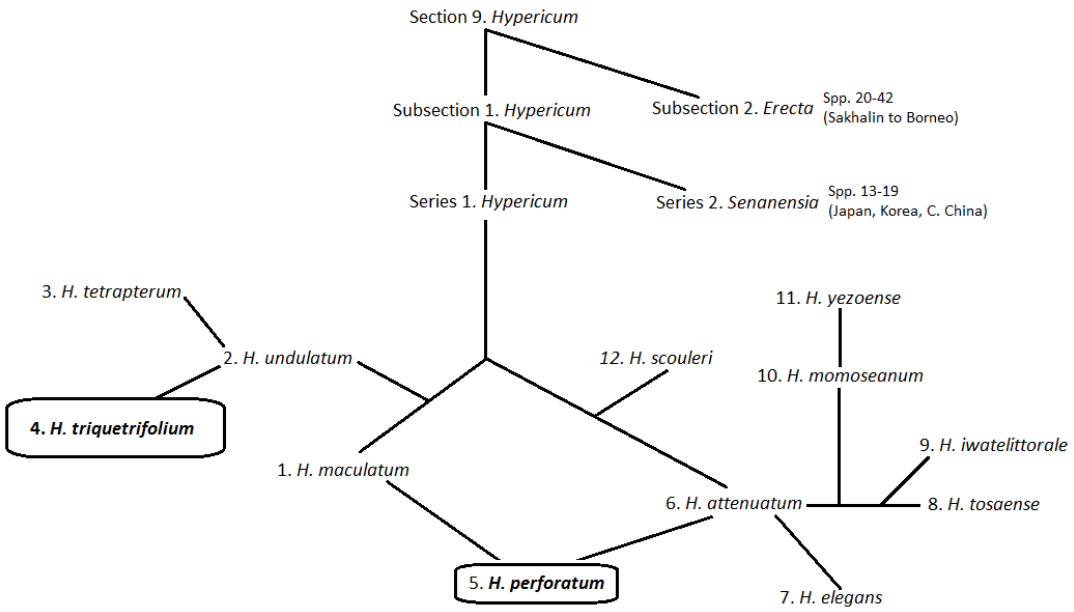

Fig. 2. Phylogenetic tree for section 9, subsect. 1, series 1. Simplified. (Robson, 2002)

As clearly seen from **Fig. 2**, Section 9, Subsection 1, Series 1 comprises 12 species, among which the most famous member of the family – *H. perforatum* (Common St. John's Wort) – finds place. This herb is being widely studied and investigated even until today and is nowadays successfully used in both traditional and officinal medicine to treat depression (Bongiorno and LoGiudice, 2010). In Germany it is prescribed to treat mild to moderate depression, especially in children (Dörks et al., 2013*;* Fegert et al., 2006). However, there are data collected in clinical trials which showed, that it was superior to placebo in patients with major depression, as effective as standard antidepressants and had fewer side-effects (Linde et al., 2008). This is the only *Hypericum* species, which is approved in several countries for medicinal use in humans as a "true medicine" and not as a dietary supplement. Therefore, its chemotaxonomical relatives are of a great scientific interest to be well studied, since they might be as potent and useful in medicine, as *H. perforatum* itself or even more.

1.1.3 *Hypericum triquetrifolium* Turra

Also known as *H. crispum* L.

1.1.3.1 Geography and ecology

H. triquetrifolium was first described by Italian botanist Antonio Turra (1736 – 1797) from Vicenza.

The species is native to mostly eastern Mediterranean region, but can also be found in wild nature in Spain (Málaga and Andalucía), Gibraltar, Balearic Islands (Menorca), south France, south Italy, Sicily, Malta, Tunisia, Algeria, Libya (Cyrenaica), Montenegro, Albania, Greece (mainland and islands), Crete, Cyprus, Turkey, north Syria, Lebanon (coast and lower mountains), Israel, Jordan, Egypt (Sinai), Iraq and north-west Iran (Robson, 2002). The herb has been naturalised in Australia. (**Fig. 3**)

H. triquetrifolium is listed as a "principal" weed in Tunisia and a "common" weed in Lebanon (Holm et al., 1979). In these and other countries of the Middle East, it is a weed of cereals, orchards, vineyards and waste places. It has established a small infestation in Australia, where it is listed as a noxious weed (Parsons and Cuthbertson, 1992). It is poisonous to livestock (NGRP, 2002). The plant spreads by both seeds and rhizome fragments following cultivation.

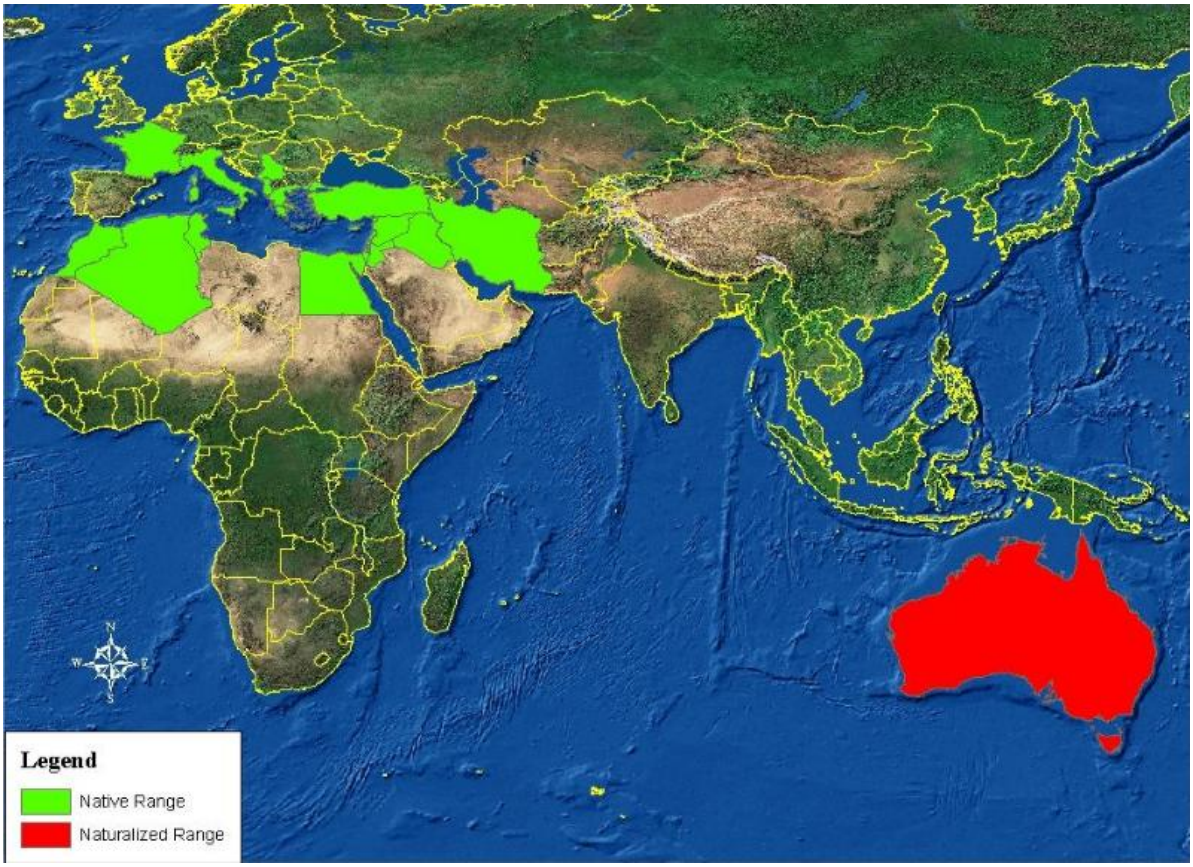

Fig. 3. Native and naturalized distribution of *H. triquetrifolium* (Fowler, 2002)

1.1.3.2 Etymology

The word "*Hypericum*" is a Latin name of the genus, which most probably derives from Greek language. It consists of two parts: "hyper-" (Υπερ, above) and "eikōn" (εἰκών, image) (Robson, 2003). The Greek word "Eikōn" is the likely origin of "icon", which is generally a flat panel painting depicting Jesus Christ, Mary, saints and/or angels, which is venerated among Orthodox Churches. Therefore, *Hypericum* might have been the herb, hanging "above the image", protecting it and the house from bad spirits. English common name for the genus is St. John's Wort ("Tutsan" is another one, but rarely used), as well as German – Johanniskraut.

The species name "*triquetrifolium*" literary means "leaves of three planes". English common names of *H. triquetrifolium* are: Wavy-leaf St. John's wort, Curled leaf St. John's wort, Tangled Hypericum or Tumble St. John's-wort.

English name “St. John’s Wort” is usually referred to John the Baptist, because the herb usually starts blooming at the end of June, when Midsummer or St. John's Day is celebrated (Hahn, 1992).

In Hebrew its scientific name is “*Péra mesul’sál’*”, which means “curled hypericum”.

Russian name of the herb is “*Zverobóy*”, which literary means “he, who kills animals” (from *zver’* – animal and *ubóy* – slaughter). This may also explain its poisonousness to livestock (§ 1.1.3.1).

1.1.3.3 Botanical and taxonomical description

H. triquetrifolium is a perennial herb 15-77 cm tall, erect to decumbent, with a dense tangle of thin branches, glabrous but spotted with small black glands. Sap is resinous. It has deep vertical roots and a shallow rhizome system from which new shoots are produced. Leaves are opposite, sessile, simple, 5-15 mm long, the base clasping the stem. Margins of the leaf are wavy, undulate, also with small black translucent glands. Flowers are yellow, 8-14 mm across, shortly stalked in clusters of two to five at the end of branches, with five free petals. Stamens are many in three groups. Sepals are 2 mm long, ovate, without glands. Fruit is a three-celled dry capsule, 3-5 mm long with numerous small brown seeds (**Fig. 4**), 1.5-1.8 mm long, slightly curved, with a pitted surface (Robson, 2002).

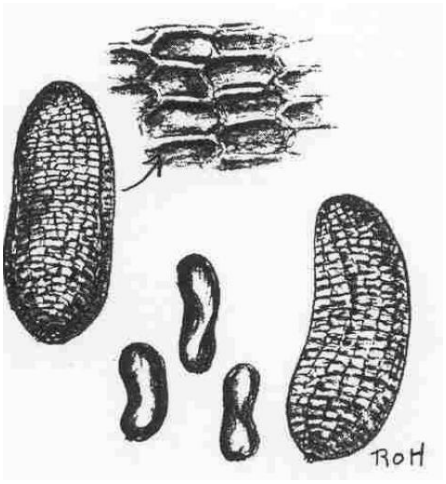

Fig. 4. *H. triquetrifolium* seed (Reed, 1977)

Generally the herb flowers from May to September, however the blossom peak happens from mid-June until end of July.

Photos **Fig. 5-8**, as well as paintings **Fig. 9-10** give better vision of the herb.

Modern taxonomy of the herb is presented in the following **Tab. 1**:

Tab. 1. Scientific classification of *H. triquetrifolium* TURRA

Scientific classification	
Domain:	Eukaryota
Kingdom:	Plantae
	Streptophyta
Subkingdom:	Embryophyta
	Spermatophyta
Division:	Angiosperms (= Magnoliophyta)
	Eudicots
Class:	Magnoliopsida
Subclass:	Rosids
Order:	Malpighiales
Family:	Hypericaceae
Subfamily:	Hypericoideae
Tribe:	Hypericeae
Genus:	*Hypericum*
Section:	9. *Hypericum*
Subsection:	1. *Hypericum*
Series:	1. *Hypericum*
Species:	4. ***Hypericum triquetrifolium*** TURRA

Numbers of section, subsection, series and species – according to **Fig. 2**.

Fig. 5. *H. triquetrifolium* in wild nature on 4th July 2016, Golan Heights (Israel)

Fig. 6. *H. triquetrifolium* in wild nature on 4th July 2016, Golan Heights (Israel)

Fig. 7. Flowers of *H. triquetrifolium* in wild nature on 4th July 2016, Golan Heights (Israel)

Fig. 8. Flowers of *H. triquetrifolium* in wild nature, 28th August 2012, Golan Heights (Israel)

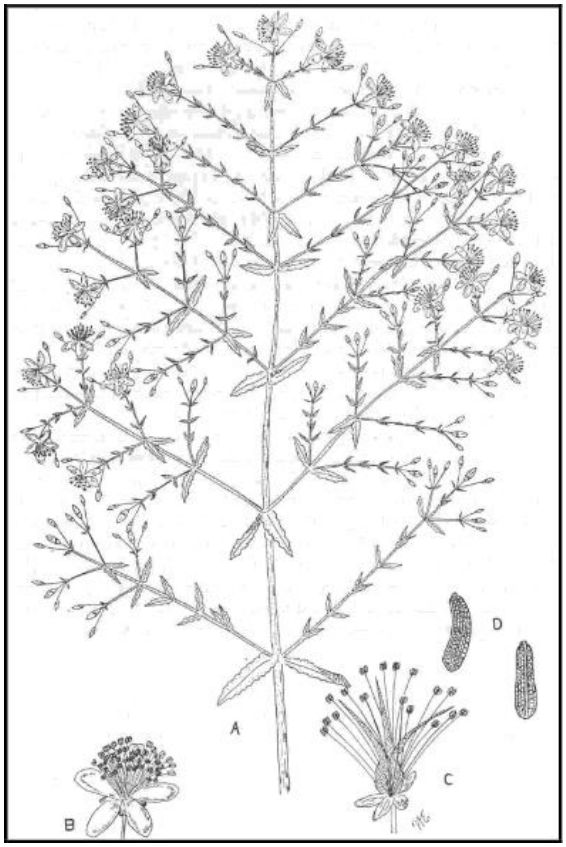

Fig. 9. *H. triquetrifolium* (Abu-Irmaileh, 1982) **Fig. 10.** *H. triquetrifolium* (Edgecombe, 1970)

1.1.3.4 Phytochemistry and pharmacology

Until today the plant was widely investigated on its essential oil composition. Overall, 109 compounds were identified. Among them sesquiterpene hydrocarbons (α-humulene, cis-calamenene, δ-cadinene, bicyclogermacrene, eremophilene, β-caryophyllene, (E)-γ-bisabolene), monoterpene hydrocarbons (α-pinene), oxygenated sesquiterpenes (caryophyllene oxide), oxygenated monoterpenes (<1%) and others (Rouis Z. et al., 2012; Yuce and Bagci, 2012; Karim et al., 2007). Recent studies of Iranian species proved the presence of germacrene-D, β-caryophyllene, δ-cadinene, *trans*-β-farnesene, α-humulene, β-selinene, γ-cadinene and *trans*-phytol, which were the major constituents of the oil (Sajjadi et al., 2015).

Phenolic compounds are found as well: mostly flavonoids – rutin (= quercetin-3-O-α-L-rhamnopyranosyl-(1→6)-β-D-glucopyranoside), hyperoside (= quercetin-3-O-galactoside), apigetrin (= apigenin-7-O-glucoside), kaempferol, quercitrin, quercetin and amentoflavone

(Cirak et al., 2011), and also I3, II8-biapigenin, astragalin (= kaempferol-3-O-glucoside), (-)-epicatechin (Conforti et al., 2002). Confirmed are naphthodianthrones (so called *hypericins*): hypericin, pseudohypericin, protohypericin and protopseudohypericin, as well as 4 acylphloroglucinols: hyperforin and adhyperforin (Alali and Tawaha, 2009) and most recently discovered adhyperfirin and hyperibine J (**Fig. 11**) (Mitsopoulou et al., 2015). Fatty acids, namely α-linolenic acid (C18:3), linoleic acid (C18:2), oleic acid (C18:1), palmitic acid (C16:0) and stearidonic acid (C18:4) were isolated from Tunisian resources of *H. triquetrifolium* (Hosni et al., 2007).

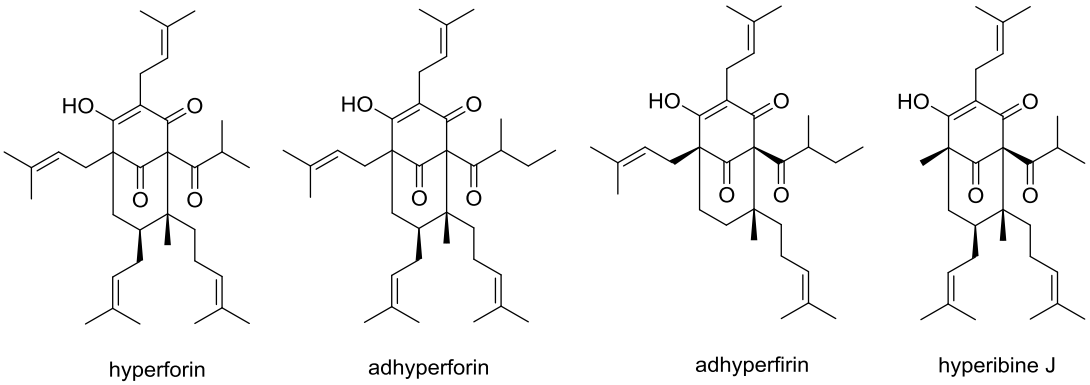

Fig. 11. Acylphloroglucinols isolated from *H. triquetrifolium* TURRA.

Hypericins are one of the principle components in many species of the genus *Hypericum*. They are responsible for large number of biological effects: antimicrobial (García et al., 2015), antiviral (Hudson et al., 1991) and antiretroviral (Stevenson and Lenard, 1993), stress-relieving and antidepressant effects (Wang et al., 2010) and many others. An exhaustive and comprehensive review on the biological effects of hypericins can be found in (Karioti and Bilia, 2010).

Extensive literature review revealed, that the only one non-*Hypericum* herb known today to accumulate hypericin as well as pseudohypericin, is Haronga or *Harungana madagascariensis* LAMARCK EX POIRET from the same family Hypericaceae (tribe Vismieae, § 1.1.1). These compounds were extracted from the herb's leaves (Fisel et al., 1966; Hölzl und Petersen, 2003).

H. triquetrifolium is believed to be potent against retroviruses, because of the high content of naphthodianthrones (Stojanovic et al., 2013). Essential oil of collected in Tunisia *H. triquetrifolium* shows "good antibacterial", "promising antifungal", "significant

anticandidal" and low cytotoxic effect and did not show any antiviral activity against Coxsackievirus B3 (Rouis et al., 2013). Israeli study suggests that the herb probably exerts anti-inflammatory effects through the suppression of TNF-α and iNOS expressions (Saad at al., 2011). In Sulforhodamine B assay the I3, II8-biapigenin isolated from the methanolic extract exhibited strong cytotoxic activity with a certain degree of selectivity against different cell types (Conforti et al., 2007). Plant extract shows promising antimicrobial activity (Al-Bakri and Afifi, 2007). Greek scientists observed "the highest cytotoxic activity" on brine shrimps (LC_{50} = 22 mg/mL) and good antioxidant activity *in vitro* (Couladis et al., 2002). Anti-inflammatory effect on rats by *H. triquetrifolium* extract was also shown (Ozturk et al., 2002). Lyophilized extract exhibits antinociceptive activity in mice (Apaydin et al., 1999).

1.1.4 Acylphloroglucinols

Acylphloroglucinols form a diverse class of secondary metabolites, which can be found in various plants, marine and microorganisms all around the Earth. They possess a diverse structure, as well as strong and highly versatile biological activity. There are almost 1000 unique compounds known and more are being elucidated and described every year (Singh and Bharate, 2006).

For genus *Hypericum* more than 300 phloroglucinols are known (Schmidt and Heilmann, 2013). Probably the most famous of them is hyperforin (**Fig. 11**), found in *Hypericum perforatum* in larger amounts, which is widely used today in officinal medicine. It has also been found in other *Hypericum* species.

1.1.4.1 Biosynthesis of acylphloroglucinols

Phloroglucinols are polyketides which derive from the acetate-malonate pathway. As such, a CoA-activated aromatic or aliphatic starter acid (acetyl-, propionyl-, butyryl-, isobutyryl-, 2-methylbutyryl-CoA) reacts with 3 molecules of malonyl-CoA, which serves as an extender acid (Avato, 2005). This intermolecular decarboxylative Claisen condensation is catalyzed by an enzyme called polyketide synthase (Type III PKS). Via the formation of an intermediate polyketide, which cyclise through the intramolecular Dieckmann condensation, an acylphloroglucinol backbone is built. It undergoes then a subsequent prenylation: a special enzyme prenyltransferase (PT) catalyses the reaction of addition of dimethylallyl pyrophosphate (DMAPP) to the main molecule. Thus a (poly-) prenylated acylphloroglucinol is formed. Several prenyl-/geranyl- chains may also cyclise, forming bi- or polycyclic derivatives. A proposed acylphloroglucinol biosynthesis pathway on example of hyperforin was described by working group of Prof. Dr. Ludger Beerhues (Institute for Pharmaceutical Biology, University of Braunschweig, Germany) and is shown on **Fig. 12** below.

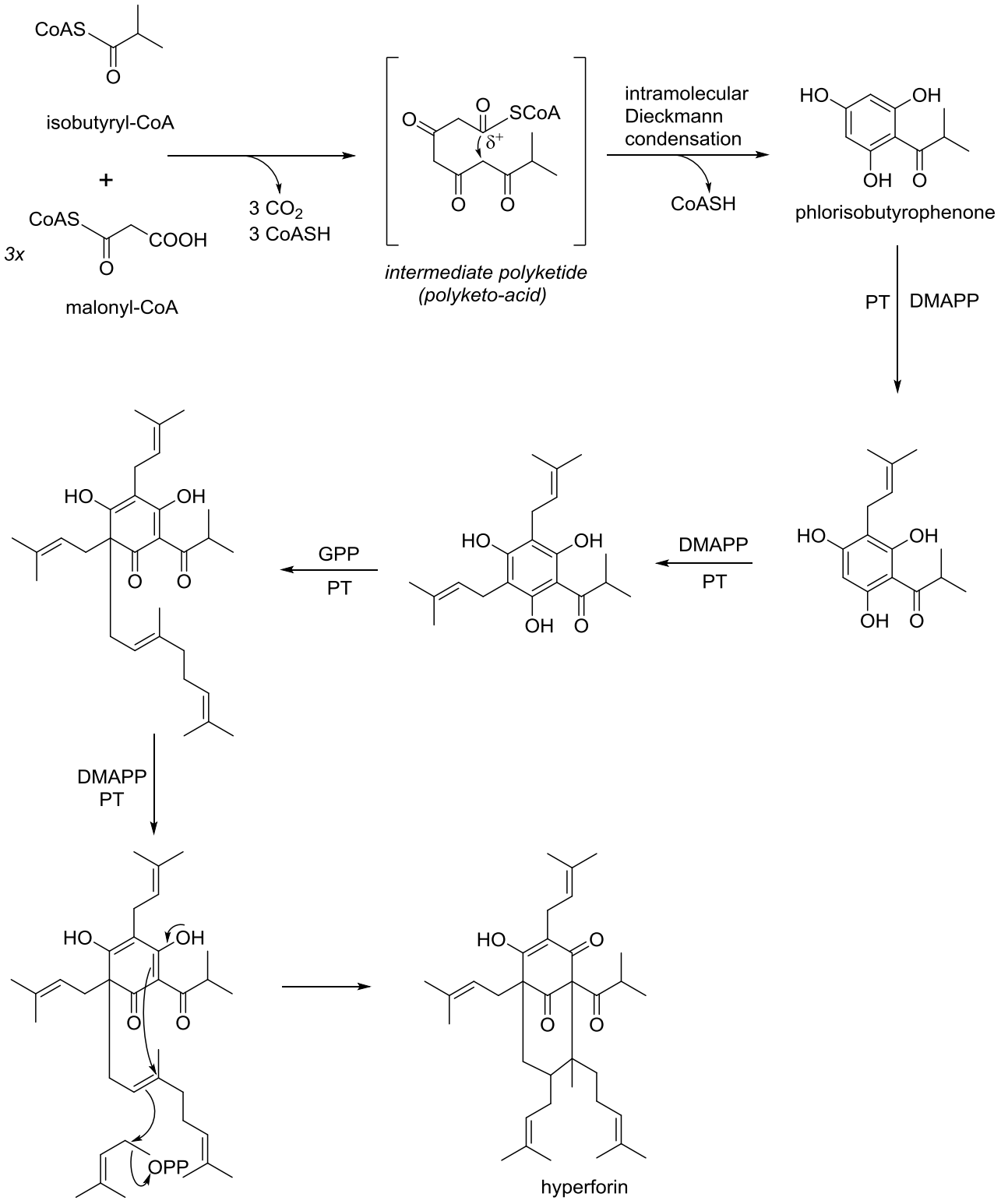

Fig. 12. Proposed biosynthesis of hyperforin (Beerhues, 2006), modified. (Klingauf et al., 2005; Dakanali and Theodorakis, 2011)

DMAPP biosynthesis simplified scheme may be observed from **Fig. 13**. In nature two possible biosynthesis pathways exist: via MVA (primarily in plants and in rare insects) or via DOXP/MEP pathway (characteristic for algae, cyanobacteria, as well as for *Mycobacterium tuberculosis* and malaria parasites). Both pathways result in two isomers: DMAPP or IPP. The latter is relatively un-reactive, that is why a special enzyme IPP-isomerase turns it into a more-reactive electrophile DMAPP, which, in turn, plays important role in prenylated acylphloroglucinols biosynthesis (**Fig. 12**).

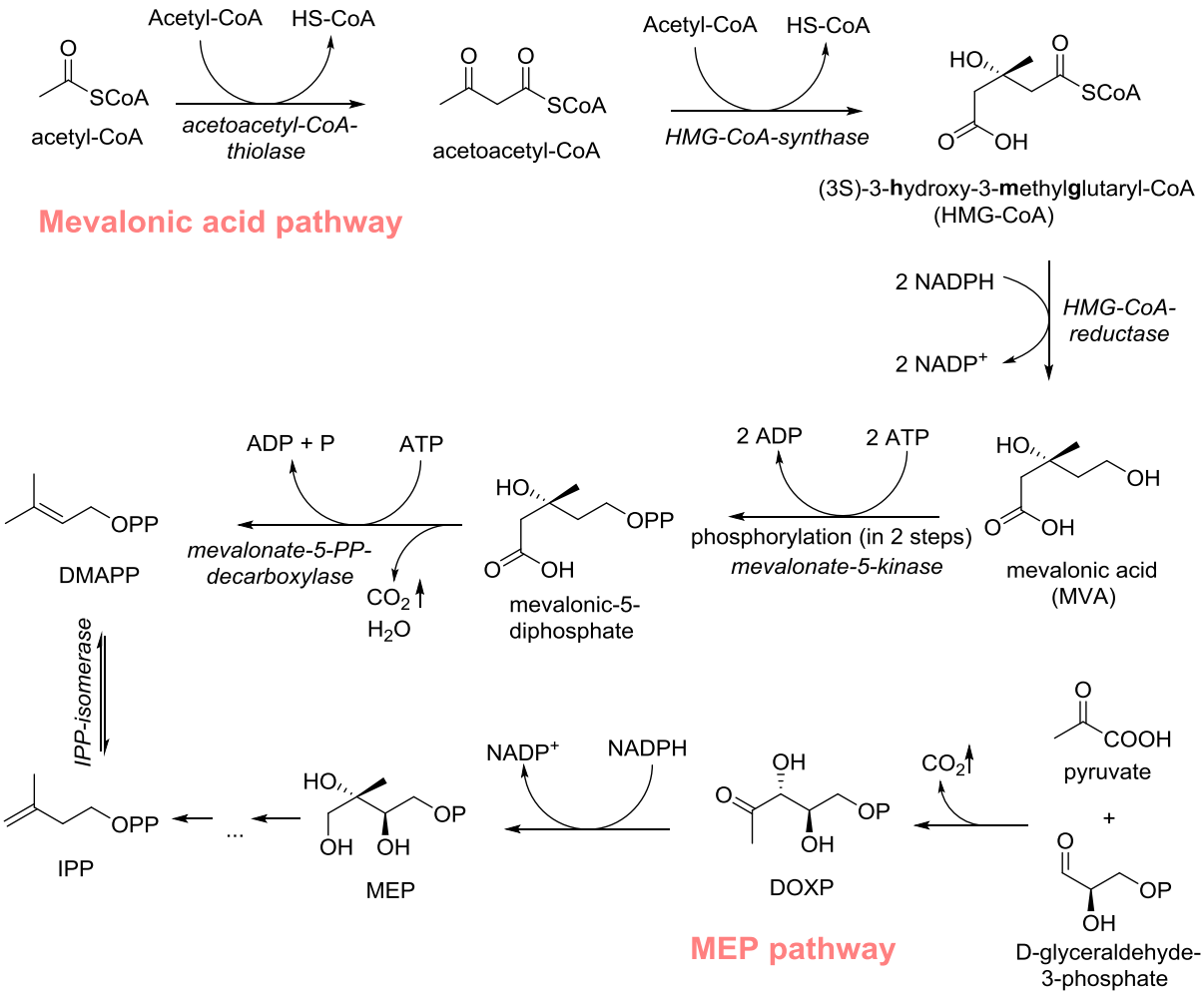

Fig. 13. Mevalonate and non-mevalonate pathways of DMAPP's biosynthesis (Zurbriggen et al., 2012). Simplified, modified.

1.1.4.2 Structural diversity and classification of acylphloroglucinols

Great number and broad structural variety of acylphloroglucinols makes it really difficult to present a clear and unambiguous classification. Two big reviews have been prepared and help better understand the entire depth of the question. The first one by (Singh and Bharate, 2006) describes phloroglucinols, discovered not only in plants, but also in other organisms. The second one by (Schmidt and Heilmann, 2013) focuses on acylphloroglucinols isolated from *Hypericum*. And even in the latter case, dedicated to the herbs of only one genus, the classification is not so easy and unequivocal.

Essentially the compounds can be divided into mono-, bi-, tri-, tetrameric, etc. They can also be mono-, bi- and polycyclic (**MPAPs** – monocyclic polyprenylated acylphloroglucinols; **BPAPs** – bicyclic polyprenylated acylphloroglucinols; **PPAPs** – polycyclic polyprenylated acylphloroglucinols). They can also be C- or O- prenylated or geranylated, methylated, methoxylated, with sugars, with aliphatic or aromatic starter acid. Isoprene and geranyl chains can cyclise in ortho- or para- position to starter acid and thus form either 5-ring (furan) or 6-ring (pyran) derivatives (**Fig. 16**). Even epoxy and hemiacetal phloroglucinols do exist. Of course, all these possibilities may be combined together and build a very complicated single compound (**Fig. 14**).

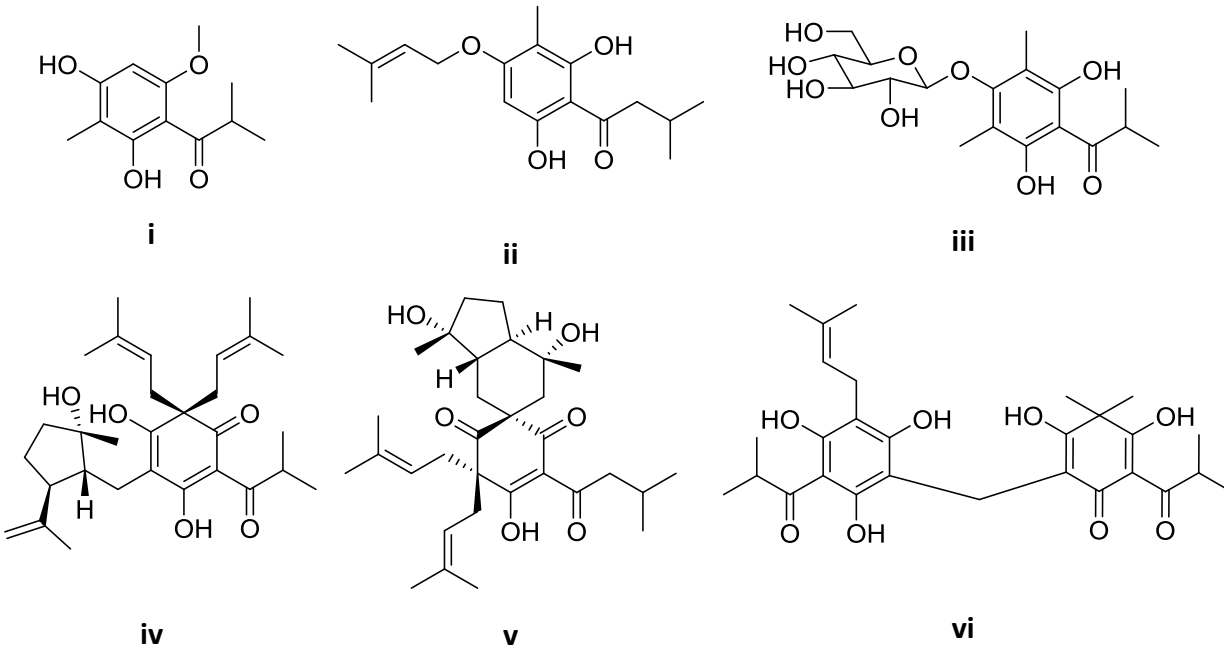

i – C- and O-methylated, non-prenylated. From *H. beanii* (Shiu and Gibbons, 2006)
ii – O-prenylated, C-methylated. From *H. calycinum* (Decosterd et al., 1991)

iii – O-glycoside, C-methylated. From *H. japonicum* (Wu et al., 1998)
iv – C-prenylated with 5-ring adduct. From *H. ascyron* (Hashida, 2008) and *H. riparium* (Tala, 2015)
v – C-prenylated, spiro-condenced. From *H. henryi* (Yang, 2015b)
vi – Dimeric, C-prenylated, C-methylated. From *H. uliginosum* (Parker and Johnson, 1968)

Fig. 14. Examples of MPAPs' structural diversity.

Structure diversity not only determines herb's biological activity, but is also genetically determined and therefore plays an important role in its chemotaxonomical classification. Herbs from each section of the genus comprise typical types of phloroglucinols and let Norman Robson inter alia classify the plants respectively (Robson 1977; Robson 2002). As an example, herbs from sections 14 and 15 accumulate only acylphloroglucinols, which can be described as monocyclic O-glycosides, while section 10 has only O-prenylated or geranylated compounds; and species from section 13 form polycyclic compounds of undefined type. As opposed to described sections, sections 3, 9 and 9c are rich in quite various types and cannot be characterised by one specific acylphloroglucinol type.

Principal classification of monomeric bi- and polycyclic acylphloroglucinols were proposed by (Dakanali and Theodorakis, 2011). Scientists define four classes, namely A, B(I), B(II) and C.

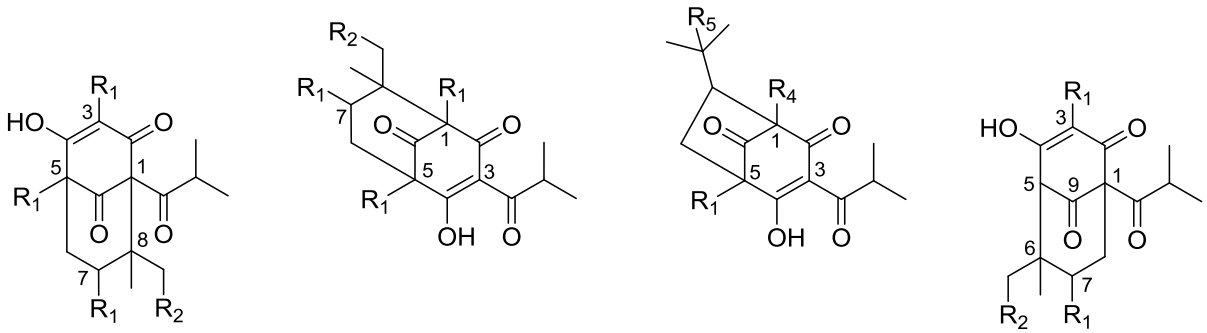

Fig. 15. Classification of BPAPs and PPAPs (Dakanali and Theodorakis, 2011). Simplified.

Fig. 15 clearly shows the difference between compounds of types A, B(I) and C, which are characterized by a highly oxygenated bicyclo[3.3.1]nonane-2,4,9-trione, while type B(II) is

based on bicycle[3.2.1]octane-2,4,8-trione skeleton. Each skeleton can be prenylated or geranylated, as well as the prenyl/geranyl chains may cyclize to form tri- or polycyclic compounds of furano-, chroman-, chromene- type, etc. Possible cyclization on example of A-type can be observed from **Fig. 16**.

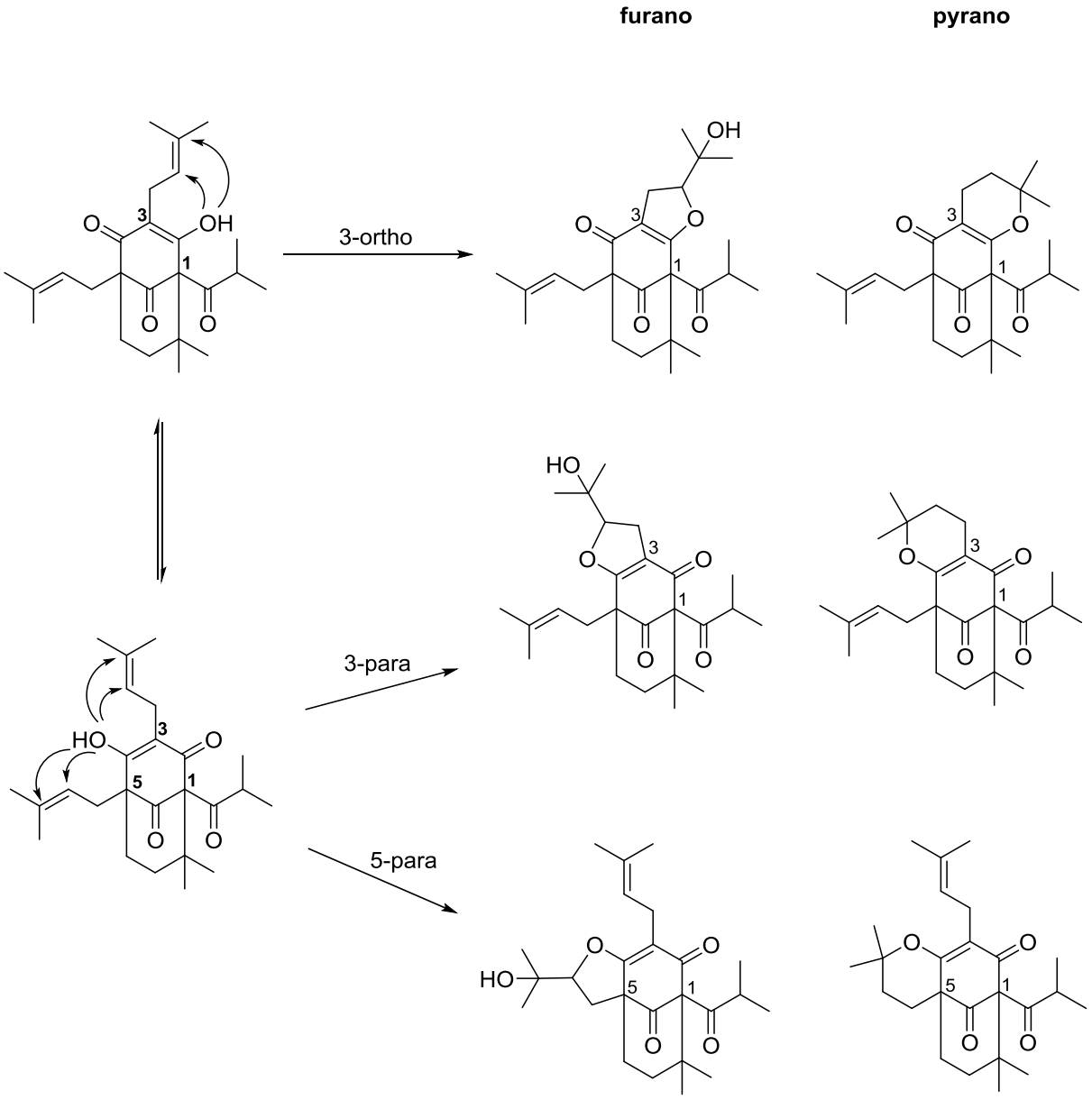

Fig. 16. Possible cyclization and formation of furano- or pyrano- PPAPs derivatives on example of Type-A acylphloroglucinol. Simplified. (Schmidt and Heilmann, 2013)

Presented in **Fig. 16** possible biosynthesis processes let one classify the compounds not only according to their scaffolds, but also in accordance with their additional customizations.

1.1.4.3 Biological properties of acylphloroglucinols

Almost all newly discovered acylphloroglucinols are being studied *in vitro* on their biological and pharmacological effects. These do vary a lot and present a vast palette of different kinds. Most common effects and activities include:

- antidepressant (Stein et al., 2012; Jensen et al., 2001)
- antiproliferative (Schmidt et al., 2012; Pinhatti et al., 2013; Sun et al., 2014)
- cytotoxic (Chen et al., 2011; Liu et al., 2013)
- antinociceptive (Stolz et al., 2014)
- antioxidative (Wu et al., 2008; Alfaro et al., 2014; Sun et al., 2014)
- larvicidal (Mitsopoulou et al., 2014)
- antiangiogenic (Schmidt, 2013)
- antimicrobial (Tanaka et al., 2011)
- anti-inflammatory (Crockett et al., 2008)
- analgesic (Stolz et al., 2016)
- antiviral (Piccinelli et al., 2005; Hu et al., 2016)
- anti-HIV (Fobofou et al., 2015)
- neuroprotective (Gao et al., 2016)
- antifungal (Tanaka et al., 2008)
- cyclooxygenase-1 and -2 inhibition (Henry et al., 2009) and many others.

1.2 Neurodegenerative diseases

1.2.1 Introduction

EU Joint Programme – Neurodegenerative Disease Research (JPND Research) defines neurodegenerative disease as an umbrella term for a range of conditions which primarily affect the neurons in the human brain.

Neurodegenerative disorders (NDs) are incurable today, although neurons do replicate and differentiate in mammalian brain during the whole life (Danielson et al., 2016; Zhao et al., 2008; Dranovsky et al., 2011). Problems caused may affect movement (ataxias) or mental health (dementias). Cognitive abilities, such as memory or decision making are also harmed.

Number of NDs is great. Among most common diseases are:

- Alzheimer's disease (AD)
- Parkinson's disease
- Huntington's disease
- amyotrophic lateral sclerosis (ALS)
- Creutzfeldt-Jakob disease (CJD)
- primary progressive aphasia
- progressive supranuclear palsy
- and many others.

NDs are very important issue especially of the western world; it is being taken serious care in all developed countries. In both EU and USA there are numerous institutes and funds, which closely cooperate in order to discover a secure and effective medicine for NDs. To name a few, EuroPa is the European Cooperative Network for Research, Diagnosis and Therapy of Parkinson's Disease. European Huntington's disease Network (EHDN), European and Allied Countries Collaborative Study Group of CJD (EUROCJD) with local offices in the UK, Spain, France, Italy, Canada and USA, as well as US National Institute of Neurological Disorders and Stroke – are only a few examples of how broad and deep is the research on NDs conducted today.

According to EuroStat, the rise of the median age of population in 28 EU countries from 2004 to 2014 composes ca. 7% (39.5 years in 2004 *versus* 42.2 years in 2014). These data show the population doesn't get younger as time passes and with the development of medicinal technology, preventive diagnostics and medication and rise of overall life quality, there will

be more aged people, than it would have been 10 or 20 years ago. Age, i.e. changes undergoing in a human organism with the flow of time, are a part of not till the end known reasons, leading to NDs (Hung et al., 2010).

Public health department of European Commission quotes the data, calculated by (Olesen et al., 2012), which say that total European cost of brain disorders in 2010 estimated € 798 billion, affecting more than a third of the continental population. Compared to year 2004, when 127 million adults were affected by disorders of the brain in the EU member states, Iceland, Norway and Switzerland € 386 billion were spent (Andlin-Sobocki et al., 2005). A doubling of costs in 6 years shows significant increase of the patients, as well as a strong growing necessity to obtain an efficient preventive drug.

Constant works on AD costs estimation and its' influence on the state's economy are performed in the USA (Meek et al., 1998), China (Keogh-Brown et al., 2015), Sweden (Åkerborg et al., 2016), Czech Republic (Marešová et al., 2015) and other countries. The inferences are unfavourable: expenses are growing at full pelt.

All the facts, mentioned above prove the need to further and deeper investigate these group of diseases, broaden research and discovering a potent and safe medicines to prevent and treat the pathological conditions.

1.2.2 Aetiology of neurodegenerative disorders

When talking about NDs, it is usually meant that CNS, i.e. brain is hurt. The great variety of illnesses does not, however, have the same origin and may appear through a number of different factors, processes and conditions.

The most widespread disorder is AD, followed by Parkinson's (Elbaz et al., 2016). A bit less common, but not less important include Huntington's, CJD, ALS, epilepsy, migraine and chronic pain and many others. NDs may have common whence, as well as their aetiology might be very much different and is not well known and clear until today. For example, one most recent study even proposes, that AD is not a single disease, but a group of diseases, which have absolute different aetiology (Ben-Gedalya et al., 2015). Still there are a lot of argues and discussions on this matter and the consensus is far away.

While a lot of researches are conducted all over the world, different scientific groups name different factors as the cause of concrete disease. In short, the aetiology is very complicated and not always unequivocal. In the following **Tab. 2** an overview with a few examples is presented. Both similarities and differences in developing of these pathologic states can be noted.

Tab. 2. Overview of NDs aetiologies.

NDs	Cause	Source
Alzheimer's	oxidative stress	Cacciapuoti, 2016 Moulton and Yang, 2012
	mitochondrial dysfunction, accumulation of abnormally folded Aβ protein, which build senile plaques in brain	Hashimoto et al., 2003
	genetic predisposition	Wilson et al., 2011 Gatz et al., 2006
	cholinergic hypothesis: reduced production of acetylcholine	Francis et al., 1999
	hyperphosphorylated tau protein connects to other tau proteins and forms neurofibrillary tangle inside nerve cells – its structure is being damaged and the cell dies	Goedert et al., 1991 Iqbal et al., 2005
	herpes simplex virus Type I	Itzhaki and Wozniak, 2008
	metals like Cu, Zn, Al, Fe are being discussed to be one of the initiators of the disease	Brewer, 2012
	lack of sleep	Mander et al., 2015
	age-related myelin breakdown in the brain	Bartzokis, 2011
	obesity	Ballard et al., 2011
	smoking	Cataldo et al., 2010
	less daily computer use	Silbert et al., 2016
	environment and ecology	Moulton and Yang, 2012
	head injuries, depression, hypertention	Burns and Iliffe, 2009
	1) mutations: amino acid proline is being replaced in both prions and in presenilin 1 protein. Its functional interaction with chaperone protein cyclophilin B is impaired. Presenilin 1 fails to fold properly. Attenuation of γ-secretase activity and impairment of mitochondrial distribution and function. 2) aging	Ben-Gedalya et al., 2015
	transmissible Alzheimer's theory, prions	Abbott, 2016

Parkinson's	accumulation of iron	Medeiros et al., 2016
	increased production of ROS and RNS	
	inflammatory markers	
	oxidative stress	Cacciapuoti, 2016
	1) Aβ and α -synuclein oligomers might damage the mitochondrial membrane 2) mitochondrial damage might promote Aβ and α-synuclein aggregation 3) Aβ oligomers and α-synuclein might interact in disturbing mitochondrial function	Hashimoto et al., 2003
	influence of the surroundings, ecology	Noyce et al., 2012
	genetic factors (in ca. 15% of patients)	Samii et al., 2004
Huntington's	accumulation of misfolded proteins in neuronal cytosol and nuclei	Cummings and Zoghbi, 2000; Muchowski, 2002
	genetic mutation in *HTT* gene on the short arm of chromosome 4; cytosine-adenine-guanine (CAG) trinucleotide repeat.	Walker, 2007
	autosomal dominant inheritance	
ALS	genetics (5-10% of cases are directly inherited from parents): defect on chromosome 21, which codes for superoxide dismutase	Kiernan et al., 2011 Battistini et al., 2010
	90% are classified as having sporadic disease but how do people get ill is still not clear	Kiernan et al., 2011
	oxidative stress	Cacciapuoti, 2016
	people with ASL have higher levels of glutamate in their serum and spinal fluid, but it is not the sole cause of the disease	Al-Chalabi and Leigh, 2000
DLB	mitochondrial dysfunction and abnormal accumulation of α-synuclein in neuronal cell bodies, axons, and synapses	Hashimoto et al., 2003
CJD	1) Alzheimer-type Aβ pathology, prions 2) transmissible theory	Frontzek, 2016
	aging	Ben-Gedalya et al., 2015

As clearly seen from **Tab. 2** above, oxidative stress in general is one of the most important factors, leading to different NDs. It can be expressed in several ways, e.g. through elevation of ROS levels or damaging important cellular macromolecules like lipids, proteins and DNA (Cacciapuoti, 2016).

Medication therapy of the NDs is debatable. For example, as of April 2016 there are 408 open clinical trials (in comparison to 315 cases in 2014) to understand the mechanisms and evaluate drugs for AD treatment. These data are provided by online service *clinicaltrials.gov*, which is an agency of the US National Institutes of Health. Tens of approaches are being

tested, including among others immunotherapy to Aβ (Dodel et al., 2010), use of statins (Whitfield, 2007), antibiotics (Loeb et al., 2004), antiviral agents (Itzhaki and Wozniak, 2008) and even intranasal insulin (Freiherr et al., 2013; Vandal et al., 2014). Tetrahydrocannabinol (THC) was also asserted to inhibit AChE and therefore reduce Aβ plaque formation (Eubanks et al., 2006).

Most recent successful discoveries. Some of the researches are fruitful and already do show interesting results. An Australian study proposes not yet a full cure, but significant improvement – AD patients may restore their memory by removing Aβ proteins with the help of scanning ultrasound (Leinenga and Götz, 2015). Scientists from MIT under the supervision of the Nobel Prize-winning Professor Susumu Tonegawa propose the memory retrieval by activating engram cells in mouse models of early stages of AD (Roy et al., 2016). Working groups from UCSF Gladstone Institutes in San Francisco reveals a mechanism of tau protein toxicity and memory loss in AD. Also involved is a memory-associated **KI**dney/**BRA**in (KIBRA) protein. This discovery may also help to restore memory in AD patients (Tracy et al., 2016).

Working group of Prof. Fischer from the Bar-Ilan University (Ramat-Gan, Israel) reports successful treatments of AD causing factors – oxidative stress and Aβ – first in culture, later in mice (Danino et al., 2015), however it is still too early to talk about treating the AD in all the patients.

The Buck Institute (California, USA) research showed that vitamin D3 induces expression of SKN-1 target gene, influences the proteins insolubility and therefore prevents toxicity, caused by human Aβ (Mark et al., 2016). That is why it can also be used as an effective solution to treat NDs.

Worldwide famous *Ice Bucket Challenge* flash mob, which went around the Earth mainly in August 2014, resulted in collecting more than 100 million US dollars from donations. This helped scientists from 38 various research institutes worldwide in discovering that single mutations in NEK1 gene are responsible for developing the ALS (Kenna et al., 2016). Further genome studies identify C21orf2 as an additional gene associated with ALS risk. Besides that MOBP and SCFD1 are also named as risk loci (van Rheenen et al., 2016).

1.2.3 Glutamate-induced neurotoxicity

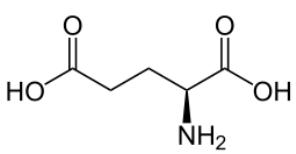

Fig. 17. Glutamic acid

Not the last role in causing an oxidative stress belongs to glutamate (Glu), an important and abundant excitatory neurotransmitter in CNS (Meldrum, 2000; Zhang et al., 2016). Glutamate or glutamic acid (**Fig. 17**) is an α-amino acid, used in the biosynthesis of proteins. It is non-essential in humans, which means the body can synthesize it. Glu is contributing to normal neural transmission, development, differentiation, and plasticity (Kritis et al., 2015). It is involved in cognition, i.e. memory and learning (Yang et al., 2011). At the same time pathologically elevated levels of glutamic acid are harmful for the CNS and may incur toxicity and oxidative stress, which in turn develop various acute and chronic diseases of the brain, including ischemia and NDs, like Parkinson's or AD (Lipton and Rosenberg, 1994; Mattson and Magnus, 2006).

Glutamate expresses its toxicity in 2 possible pathways:

1) **NMDA-mediated excitotoxicity.** Ionotropic glutamate receptors (i.e. NMDA-, AMPA- or kainate receptors) mediate the excitotoxicity through Ca^{2+} influx and ROS concentration during the cell death. Glutamate activates the receptor, Ca^{2+} flows into the cell: its high concentrations in cytoplasm provokes arachidonic acid cascade, which results in NO, O_2• radicals' production (Choi, 1988; Coyle and Puttfarcken, 1993) and release of lysosomal enzymes. Excitotoxicity is associated with most common NDs, as well as with stroke and traumatic brain injury (Kritis et al., 2015).
2) **Oxytosis.** Oxidative glutamate toxicity is not mediated by receptors (e.g. in cells, which do not have any NMDA receptors). It is initiated by high concentrations of Glu in the intercellular space (**Fig. 18**). As such, Glu/cystine antiporter system in cell membrane is being blocked. It results in cystine (oxidized dimer of cysteine) uptake inhibition, lowered levels of cysteine and glutathione (GSH) synthesis suppression. Cysteine is the rate-limiting factor in cellular GSH biosynthesis. GSH is also an important intracellular antioxidant, preventing cells from damage, caused by ROS (Pompella et al., 2003).

   Since the GSH level in the cell is low, ROS production is mild on initial stages (5-10 fold increase), followed by an explosive boost (200-400 fold increase) from mitochondria with

the course of time. The cell undergoes an oxidative stress (Murphy et al., 1989; Tan et al., 1998b).

Second increase of ROS levels causes 12-LOX activation and consequently sGC, which is responsible for conversion of GTP into cGMP (Tan et al., 2001). The latter activates the cGMP-dependent Ca^{2+} channels. Ca^{2+} flows drastically into the cell and its accumulation in cytoplasm is a major downstream event in glutamate-induced cell death cascade (Tan et al., 1998a).

Ca^{2+} ions are deleterious for the cells, since they lead to disturbance of the mitochondrial membrane potential, which in turn leads to ATP synthesis inhibition. Ca^{2+} also disturbs electron transport chain – this directs to ROS increasing production.

Further studies of oxytosis were continued by (Fukui et al., 2009). Early stages (8-12 h) are characterised by necrosis, followed by apoptosis afterwards (16-24 h). The latter is defined by release of AIF from damaged mitochondria (it catalyses DNA fragmentation), activation of MAPK cascades and other processes. Important apoptosis parameters, e.g. cytochrome C release or depolarisation of mitochondrial membrane do not, however, happen (Tan et al., 2001), thus the word “oxytosis” describes the cascade better, than regular necrosis or apoptosis (Kling, 2015).

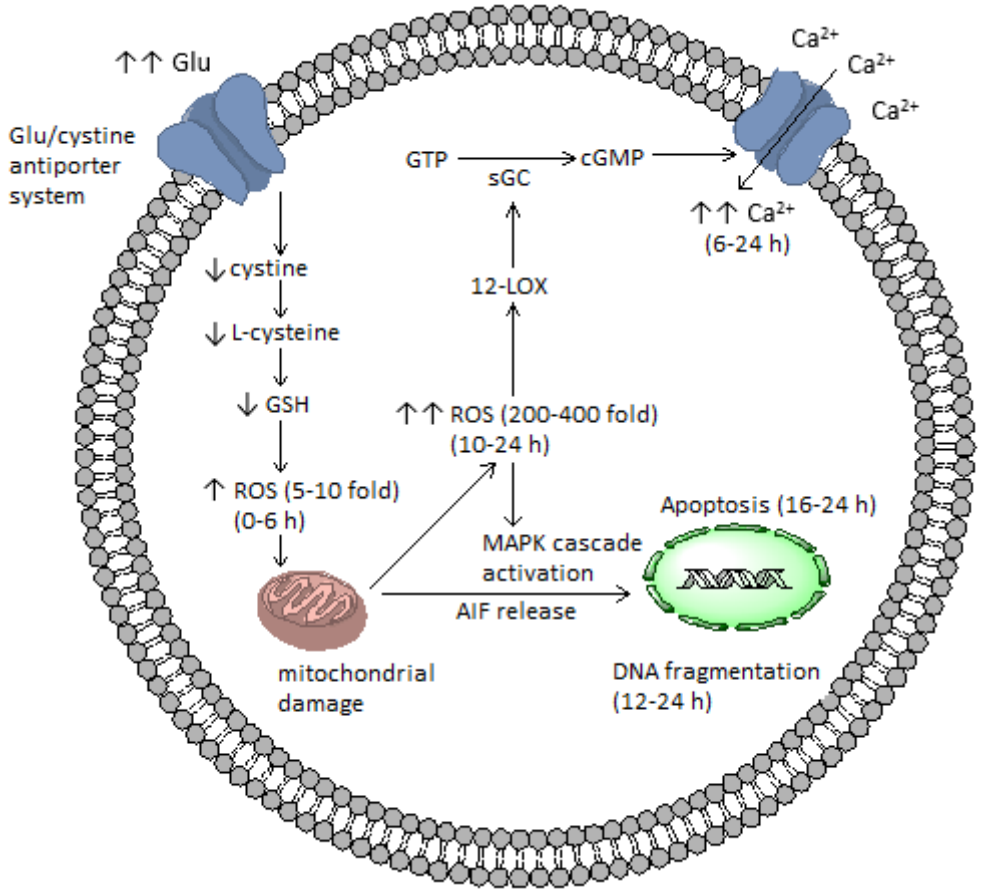

Fig. 18. Glutamate-induced toxicity in HT-22 cells, proposed by (Fukui et al., 2009; Tan et al., 1998a; Maher and Schubert, 2000).

There are several defence mechanisms exerted by a number of secondary metabolites of natural origin. A study by (Ishige et al., 2001) confirms that flavonoids protect the cell from an oxidative stress via three different mechanisms:

- preventing the GSH decrease (quercetin, fisetin)
- blocking ROS production (quercetin, vitamin E, kaempferol, galangin, luteolin)
- inhibiting Ca^{2+} influx (flavonol)

Important discovery of this work is that quercetin along with fisetin increase GSH levels in HT-22 cells both in the presence and absence of Glu. This allows the use of quercetin as positive control in Glu-induced toxicity tests on HT-22 cells, which do not possess NMDA receptors (Zaulyanov et al., 1999), so the assays conducted with them show oxytosis toxicity and not excitotoxicity.

1.2.4 Role of *Hypericum* in treating NDs

Hypericum is being widely studied to medicate NDs. Standardized extract enriched in hyperforin from *H. perforatum* along with quercetin were suggested to provide better therapeutic advantage for the management of Parkinson's disease (Gómez del Rio et al., 2013). Phenolic compounds (quercetin, kaempferol and biapigenin) isolated from the same herb may be used in prevention of Parkinson's disease (Vieira et al., 2011). Yet another recent study confirms the feasibility of using *H. perforatum* and its main constituent hyperforin in AD therapy (Griffith et al., 2016). Complex plant extract from *H. perforatum* may restore or improve microglial viability and attenuate amyloid-β (Aβ) mediated toxicity in AD (Kraus et al., 2007), which is closely connected to the following scientific investigation. Acylphloroglucinol hyperforin itself also influences the Aβ-induced neurotoxicity and may be used a putative therapeutic agent to fight the AD (Dinamarca et al., 2006).

Tetrahydrohyperforin, a semi-synthetic hyperforin derivative, generates neuroprotective effects and prevents memory loss in double transgenic mice modelling AD (Montecinos-Oliva et al., 2015). The same study proposes that tetrahydrohyperforin is an agonist of the TRPC3/6/7 subfamily of channels in cytomembrane. The compound may increase Ca^{2+} concentrations in the cell (§ 1.2.3) and generates stronger synaptic responses, which might be compensating the effects of amyloid-β oligomers. Aβ is a peptide of 39–42 amino acids which is involved in AD as the main component of the amyloid plaques found in the brains of Alzheimer patients (Ittner and Götz, 2011; Nussbaum et al., 2013; LaFerla et al., 2007). Since hyperforin selectively activates TRCP6 channels while TRPC1/3/4/5 channels remained unaffected (Leuner et al., 2007), TRPC6 is the most likely candidate to be targeted by tetrahydrohyperforin. However, the lack of an atomic resolution structure of any TRPC channel doesn't let any rational drug design for these channels at the moment.

Almost all studies focus on and represent mostly one and the most famous member of the genus, i.e. *H. perforatum*, which makes other *Hypericum* species interesting for investigation and comparison, whether they can also be potent in treating any NDs.

However, some rare studies on other species exist. Research on neurotoxicity and neuroprotection of organically synthesized acylphloroglucinols (Sun et al., 2014) in

compination with derivatives isolated from *H. empetrifolium* (Schmidt, 2013) was conducted on HT-22 cells in Glu-induced toxicity assays by (Pitzl et al., 2015).

Chinese scientists elucidated polycyclic prenylated acylphloroglucinols from *Hypericum scabrum* and proved their neuroprotective effects on Glu-induced toxicity in SK-N-SH cells. Investigated compounds exhibited significant neuroprotection at 10 µM (Gao et al., 2016).

Most recent study focuses on *Hypericum uralum* from Tibet and northwest of Yunnan Province, PRC. Isolated from this herb 1,9-*seco*-BPAPs hyperuralones C and D were examined against acetylcholinesterase (AChE) using the Ellman method (Ellman et al., 1961) and exhibited moderate AChE inhibitory activities (Zhang et al., 2015).

1.3 Aim of the present work

1.3.1 Isolation of acylphloroglucinols from *H. triquetrifolium*

Being wide and successfully used for ages in traditional medicine by different peoples in its native Mediterranean region, *H. triquetrifolium* looks very promising to be scientifically investigated and deeper studied. Until now only 4 acylphloroglucinol derivatives were isolated, therefore, exploring the herb's secondary metabolites is of a great interest. Acylphloroglucinols possess strong and highly diverse biological activity – they are of a great medicinal importance. Moreover, the isolated acylphloroglucinols may prove and confirm chemotaxonomic connections and family ties in frames of the species and section 9 *Hypericum*.

With the use of NMR-guided fractionating strategy acylphloroglucinol derivatives are to be isolated, their structure is to be elucidated and confirmed with MS. Newly discovered substances should be characterised by their physico-chemical constants, such as UV wavelength maxima, CD spectroscopy and specific rotation.

1.3.2 Testing the isolated substances on neuroprotection

Almost all the acylphloroglucinol derivatives isolated from *Hypericum* species show diverse and strong bioactivity *in vitro* (Schmidt, 2013; Zhou et al., 2014; Fobofou et al., 2015; Dos Santos et al., 2015). Taking into consideration close relative phylogenetic bonds between *H. triquetrifolium* and *H. perforatum*, as well as the wide and successful use of the later (§ 1.1.2), studying the influence of the isolated acylphloroglucinols on the CNS, i.e. neuroprotection assay is of a great interest and importance.

Further recent pharmacological investigations on medicinal botanicals prove high potential of nature secondary metabolites in treating Glu-caused oxidative stress in HT-22 cells (Lee et al., 2015; Dos Santos et al., 2016).

A study of neuroprotection of organically synthesised phloroglucinols was conducted at the University of Regensburg. The work showed that the investigated substances, especially those with catechol structure, possess neuroprotective properties (Pitzl et al., 2015). Evaluating the pharmacological activity of acylphloroglucinols with another structure, i.e. PPAPs in particular and comparing the studies' data would be of a great interest.

2 Materials and methods

2.1 Phytochemical methods

All the glassware, devices and software (**Tab. 3**), solvents and chemicals (**Tab. 4**), as well as phytochemical methods described in this chapter refer to and were used for the extraction of the plant, isolation of pure compounds, their analysis and characterisation.

2.1.1 Devices, vessels and software

Table 3. Glassware, devices and software for the phytochemical methods.

Device	Model	Manufacturer
Analytical weights	R 160 P	Sartorius, Göttingen
CD Spectropolarimeter	J-710	Jasco, Groß-Umstadt
CPC	SPOT centrifugal partition chromatography	Armen, Saint-Ave (FR)
	Pump: 515 HPLC	Waters (US)
	Fractions collector: 2211 Superrac Racks: Type B2	LKB, Bromma (SE)
Flash Chromatography	Spot Liquid Chromatography Flash Armen Glider Flash V 2.3 (Software)	Armen, Saint-Ave (FR)
Glass-frit-adapter	top female Joint: ST/NS 29/32 bottom male Joint: ST/NS 29/32	self-made at the University's blowing shop, Regensburg
Glass pipettes	0.1 mL, 0.2 mL, 0.5 mL, 1 mL, 2 mL, 5 mL, 10 mL, 20 mL	Brand, Wertheim
HPLC semi-preparative	ProStar 410 (Autosampler) 210 (Both pumps) 335 (DAD) 701 (Fractions collector) Galaxie 1.9.302.952 (Software)	Varian, Darmstadt
HPLC syringe for manual injection	Gas Tight Syringe 2.5 mL Cat. no. 549-0537	VWR, manufactured for VWR-Leuven, Belgium in (JP)
Laboratory film	Parafilm® "M" 4 in. x 125 ft. roll Cat. no. PM996	Bemis, Neenah, WI (US)
Mass spectrometer	UPLC-HRMS: Q-TOF 6540 UHD	Agilent, Darmstadt
Measuring flasks	5 mL, 10 mL, 25 mL	Brand, Wertheim
Measuring cylinder	25-500 mL	Brand, Wertheim
Mill	Yellow line A10	IKA-Werke, Staufen
NMR tubes	507HP	Norell, Landisville (US)
NMR spectrometer	Avance 300	Bruker, Ettlingen
	Avance 400	
	Avance III 600	
NMR software	TopSpin 3.2	Bruker, Ettlingen

Painting software	ChemDraw Professional 15.0	Perkin Elmer, Waltham (US)
Pasteur glass pipettes, disposable	150 mm (Cat. no. 612-1701) 230 mm (Cat. no. 612-1702)	VWR, Fontenay-sous-Bois (FR)
Polarimeter	P8000-PT	Krüss, Hamburg
Precision balances	LE4202S	Sartorius, Göttingen
Quartz cuvettes	QS; 10,00 mm	Hellma, Müllheim
Rotation evaporator	Laborta 4003-control	Heidolph, Schwabach
Round-bottom flask	100, 250, 500 and 1000 mL	Schott Duran, Wertheim/Main
Snap-cap glass vial	5 mL, 40x20 mm, 18 mm snap cap Cat. no. 548-0555	VWR, Darmstadt
Syringe	1 mL Norm-Ject® tuberculin Luer Cat. no. 4010-200V0	Henke Sass Wolf, Tuttlingen
	10 mL (12 mL) Norm-Ject® Luer Lot 4A27048	Henke Sass Wolf, Tuttlingen
Syringe filter	Perfect Flow®, pore size 0.2 µm	Wicom, Maienfeld
UV spectrophotometer	Cary 50 Scan Cary WinUV 3.00(182) (Software)	Varian, Darmstadt
Ultra-sound water bath	Ultrasonic cleaner	VWR, Darmstadt

2.1.2 Chemicals and solvents

Table 4. Chemicals and solvents used in phytochemical methods

	Specification and quality mark	**Manufacturer**
Acetonitrile	gradient grade for liquid chromatography (LiChrosolv®) Cat. no. 1.00030.2500	Merck, Darmstadt
Acetic acid	100% anhydrous for analysis (glacial) Cat. no. 1.00063.2500	Merck, Darmstadt
p-Anisaldehyde	4-Methoxybenzaldehyde 98% Cat. no. A88107	Aldrich, Steinheim
Chloroform-d_1	99.8 atom-% D (deuterated) Cat. no. 151823	Sigma-Aldrich (CH)
Ethanol	absolute, ≥ 99.8% Cat. no. 32205	Sigma-Aldrich, Steinheim
Ethyl acetate	for analysis Cat. no. 10386320	Fisher, Loughborough (UK)
n-Hexane	for analysis Cat. no. 24580.324	VWR, Fontenay-sous-Bois (FR)
Methanol	HSL grade Cat. no. 670485	CSC Jäklechemie, Nürnberg
	for analysis Cat. no. M/4000/17	Fischer, Loughborough (UK)
	gradient grade for liquid chromatography (LiChrosolv®)	Merck, Darmstadt

	Cat. no. 1.06007.2500	
Petroleum ether	isohexan 56/62, HSL grade Cat. no. 650065	CSC Jäklechemie, Nürnberg
RP-18	LiChroprep® RP-18 (25-40 µm) for liquid chromatography Cat. no. 1.09303.0100	Merck, Darmstadt
CSi-gel	Geduran® Si 60 for column chromatography (0.063-0.200 mm) Cat. no. 1.10832.9025	Merck, Darmstadt
Sulfuric acid	95-97% GR for analysis Cat. no. 1.00731.1000	Merck, Darmstadt
Water	0.055 – 0.062 µS/cm obtained upon occurrence from Astacus LS	MembraPure, Bodenheim

2.1.3 Plant material

The flowering air parts of *Hypericum triquetrifolium* TURRA were collected on 23rd July, 2012 along the Highway 91 between Ortal and Ein Zivan on Golan Heights, Israel. Approximate GPS coordinates are 33°05'22.8"N 35°47'18.7"E.

The place where to find the plant was advised by Mrs. Michal Monosov, a curator of The Botanical Garden for Israeli Flora of the Hebrew University of Jerusalem on Mount Scopus. The plant material was identified and collected by the author of the present work and verified by Mrs. Hagar Leschner, collection manager of the National Israeli Herbarium of the Hebrew University (Berman building, Edmond J. Safra campus in Givat Ram, Jerusalem). The herb was dried under the RT (ca. 28 °C), stored at -80 °C for pest control and sent to Regensburg, Germany, via regular post.

Voucher specimens number HUJ-131843, HUJ-131844 and HUJ-131845 were deposited at the National Israeli Herbarium of the Hebrew University of Jerusalem in Givat Ram.

2.1.4 Extraction of plant material

Air-dried aerial parts of *Hypericum triquetrifolium* TURRA (1023.5 g) were cut manually with scissors, then powdered and extracted by percolation with petroleum ether HSL grade (7.5 L) yielding 32.7 g crude extract (PE) after solvent evaporation.

2.1.5 Fractioning and isolation

2.1.5.1 Flash Chromatography

The raw PE extract was separated several times using Flash chromatography. Generally, first separation steps (fractions of larger quantities, more than 1000 mg) were conducted on Si-gel, later steps (and smaller quantities, less than 1000 mg) – with RP-18 material. Fraction, which should have undergone the separation, was mixed with some quantity of stationary phase powder (ca. 2 – 3 times more than the weight of the fraction) and ca. 50-100 mL of solvent (hexane or MeOH). It was then rotated with a glass-frit-adapter on water bath evaporator under low-pressure to dry powder. The dried probe, mixed with the stationary phase, was placed into the pre-column. Two types of columns were used: pre- and main-column, both manually packed (**Tab. 5**).

Table 5. Manually packed columns for Flash chromatography

№	Type	Amount of stationary phase	Packed volume	Cartouche type
Si-gel				
1	pre-	ca. 25 g	ca. 62 mL	SVF D26, Götec (Germany)
2	main-	ca. 90 g	ca. 228 mL	SVP D40, Merck Chimie SAS (France)
RP-18 material				
3	pre-	ca. 4 g	ca. 11 mL	SVF D26, Götec (Germany)
4	main-	ca. 30 g	ca. 74 mL	

Before the columns were installed, the device was purged with working solvents for 5-10 min in order to remove air bubbles from the cables and the device. Then both pre- and main columns were installed into the Flash chromatograph and washed with 2-3 volumes of solvents (linear gradient, starting conditions). Afterwards the dry mixture of the fraction to be separated with stationary phase was placed in pre-column, and separation method started. When the running programme was over, columns were washed for ca. 15 min with 100% MeOH or EtOAc (Si-gel and RP-18 respectively), **Tab. 6**.

Table 6. Methods and solvents for Flash chromatography

Method	Mobile phase	Gradient, %	Time, min	Flow, mL/min	Collection volume, mL
Si-gel					
Flash_1	Hexane-EtOAc	0 → 100 EtOAc	0-60	20	10
Flash_2		100 MeOH	60-75	10	10
Flash_3	EtOAc-MeOH	0 → 100 MeOH 100 MeOH	0-80 80-110	20	10
RP-18					
Flash_4	Water-MeOH	70 MeOH 70 → 90 MeOH 90 MeOH 90 → 100 MeOH 100 MeOH 100 EtOAc	0-20 20-25 25-40 40-45 45-65 65-80	10	7.5
Flash_5		80 MeOH 80 → 90 MeOH 90 MeOH 90 → 100 MeOH 100 MeOH 100 EtOAc	0-15 15-20 20-35 35-40 40-60 60-70	15	7.5
Flash_6	H_2O-MeOH	35 MeOH 35 → 40 MeOH 40 → 60 MeOH 60 → 75 MeOH 75 MeOH 100 EtOAc	0-5 5-10 20-35 35-40 60-65 65-75	10	5

Methods Flash_1 and Flash_3 occurred with two Si-gel columns (№ 1 and 2, **Tab. 5**), while method Flash_2 was performed with only one small SVF D26 type column, 2/3 filled with Si-gel as stationary phase. Flash_4, Flash_5 and Flash_6 were conducted with both pre- and main columns (№ 3 and 4, **Tab. 5**).

2.1.5.2 Fractions control

2.1.5.2.1 Thin-layer chromatography (TLC)

To control the obtained fractions and sub-fractions, etc. as well as to evaluate the results of separation (e.g. after CPC or Flash chromatography), TLC was performed. The main characteristic substance factor, describing this method is R_f, retardation factor. R_f is the ratio of the distance travelled by the centre of a spot to the distance travelled by the solvent front. The solvent system for the TLC analysis is considered ideal, when the investigated

compounds migrate on the plate between R_f values 0.3-0.8. Compounds distributed on the plate after the evaluation can be detected in daylight or in UV light, as well as detected with the use of various spray reagents.

For this work Si-gel coated aluminium 20 x 20 cm plates were cut as appropriate. The sample (10 µl, concentration 1 mg/mL) was applied with a capillary (micro pipette) manually on the TLC plate and dried with common hair drier. Twin trough chamber was used to develop the plates. Chamber was filled with sufficient volume of the developing solvents mixture and well closed in order to bare the constant quantity of vapours inside.

- mobile phase: hexane – EtOAc – acetic acid = 70:28:2

Two sheets of filter paper were also placed inside to maintain the solvent's vapours in all the volume of the chamber equable. A TLC plate with the applied probes was placed inside the filled chamber until the solvent reaches the front line. The plate was then dried in the laboratory hood with common drier and photographed (daylight, 254 and 366 nm). Derivatization was performed with AAR (subsequent heating 100 °C, ca. 5 min on a heat plate, until the spots are clearly developed on the plate) and immediately after that, pictures were taken (daylight and 366 nm). Specifications for TLC implements are described in **Tab. 7**.

- AAR: anisaldehyde 0.5 mL, CH_3COOH 10 mL, MeOH 85 mL, H_2SO_4 5 mL (Wagner et al., 1983)

Table 7. TLC implements

Instrument	Specification	Manufacturer
Heat plate	Thermoplate S	Desaga, Nümbrecht
Linomat	Linomat 5 for sample application Syringe 100 µL Photo documentation: Reprostar 3 Software: WinCats 1.4.2	CAMAG, Muttenz (CH)
Micro Pipettes	Hirschmann® ringcaps® Duran® 250 pcs (10 µL) Cat. no. 9600110	Hirschmann, Eberstadt
	BLAUBRAND® intraMARK 250 pcs (20 µL) Cat. no. 7087 18	Brand, Wertheim
TLC chamber	Twin Trough chamber 20 x 20 cm	Camag, Muttenz (CH)
TLC devices	Linomat 5 (Application); Reprostar 3 (Documentation) WinCats 1.4.9.2001 (Software)	Camag, Muttenz (CH)
TLC plates	Pre-coated aluminium TLC-sheets ALUGRAM® Xtra SIL G/UV_{254} silica gel 60, 20 x 20 cm Cat. no. 818333	Macherey-Nagel, Düren
	Silica gel 60 RP-18 F_{254S} aluminium sheets, 20x20 cm Cat. no. 1.05554.0001	Merck, Darmstadt

For making overview TLC of high quality, an automatic sample applicator device (Linomat 5 by CAMAG) was used. It sprays the liquid probe (20 µL) with nitrogen onto a TLC plate in a form of a band. Filling the syringe with probe solution, installing the syringe into the Linomat, taking it out and rinsing happened manually. All other operations were done automatically. A TLC plate with the applied probes was dried and placed into a TLC chamber as usual, following the common procedures, described above.

Performing TLCs after Flash column chromatography or after CPC in order to evaluate the separation results and unite the obtained test-tubes in sub-fractions appropriately, probes were applied on the TLC plate directly from each test-tube. Concentration of the applied probe in this case could not be measured.

2.1.5.2.2 ^{1}H-NMR spectroscopy

In order to choose the correct fractions for further separation, ^{1}H-NMR experiments were conducted with every fraction and sub-fraction obtained (*NMR-guided fractionation*). Each fraction or its part was solved in ca. 0.65 mL $CDCl_3$, filled in a special NMR-test-tube with a cap and a proton spectrum was measured on Brucker Avance 300 at 300.13 MHz, 295 K.

Software TopSpin 3.2 was used to read the results, analyse and interpret the spectra. (§ 2.1.6.1)

2.1.5.3 Centrifugal Partition Chromatography

This method refers to liquid-liquid chromatography techniques and is based on two immiscible liquid phases which are united together and form a two-phase system. CPC has being widely used for isolation and purification of natural products for almost 50 years (Friesen et al., 2015). This method let one get a very high selectivity, and also unlike traditional column chromatography, stationary phase is every time new, so it cannot be fouled and thus worsening the separation quality.

In order to find an optimal solvent system for the separation, several known CPC conditions previously used for isolation of acylphloroglucinols from various *Hypericum* species were tested. The most suitable results were chosen for separation of PE-3 and PE-5 (**Tab. 8**) – this means, the fraction to be separated should be solved in both upper and lower phases equally and should be distributed identically in a parallel run on the same TLC plate (**Fig. 19** and **Fig. 20**). In both cases, during the main run in ascending mode the upper phase (organic, non-polar) was a mobile phase, while the lower phase (polar) served as a stationary one.

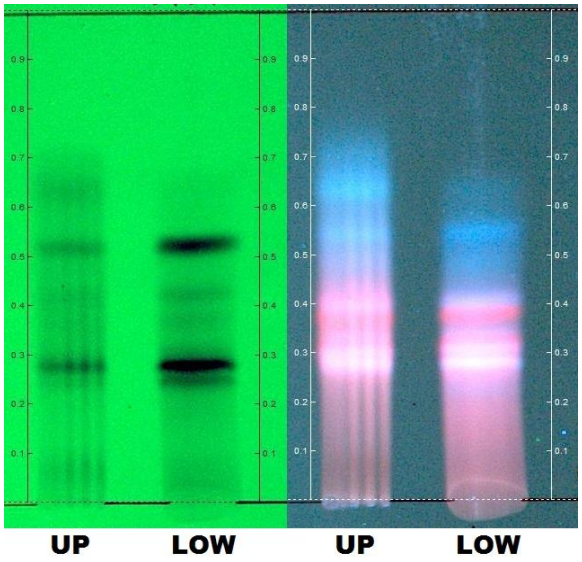

Fig. 19. TLC test of the optimal solvent mixture for CPC for fraction PE-3 (**Tab. 8**).
UP – PE-3 solved in upper phase, **LOW** – PE-3 solved in lower phase.
Left: 254 nm, right: 366 nm.
Si-gel; hexane – EtOAc – acetic acid = 70:28:2

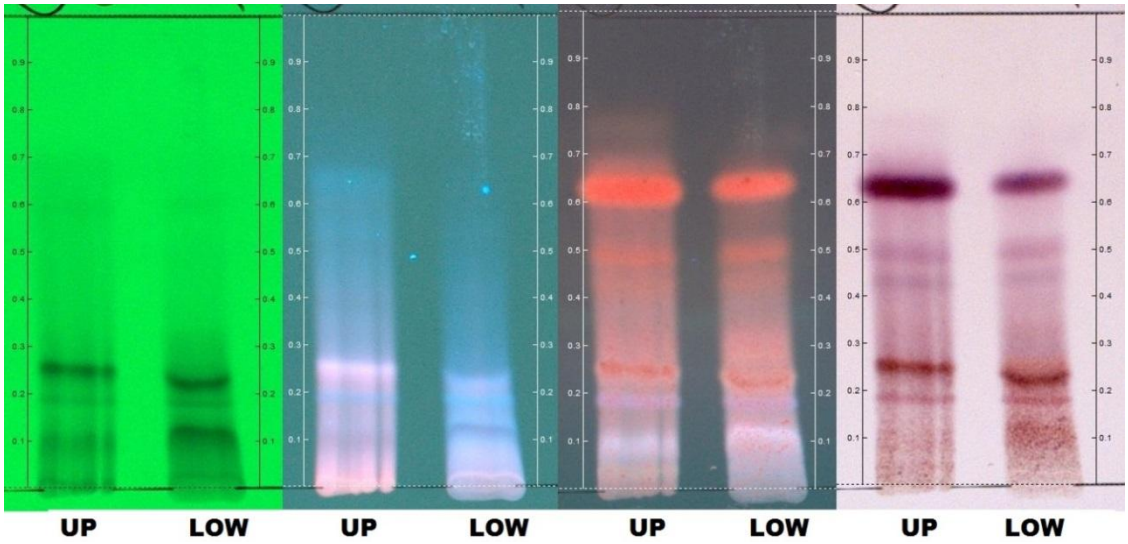

Fig. 20. TLC test of the optimal solvent mixture for CPC for fraction PE-5 (**Tab. 8**).
UP – PE-5 solved in upper phase, **LOW** – PE-5 solved in lower phase.
From left to right: 254 nm, 366 nm. 366 nm AAR, daylight AAR.
Si-gel; hexane – EtOAc – acetic acid = 70:28:2; derivatisation with AAR

Table 8. Conditions for CPC separation

Fraction	Solvents mixture	Flow	Collection volume	Rotation speed	Previously used by
PE-3	hexane 8 MeCN 5 MeOH 2	5 mL/min	7.5 mL/test-tube	800 RPM	Rocha et al., 1995
PE-5	hexane 83 EtOH 67 EtOAc 33 H_2O 17				Decosterd et al., 1989

Prior to perform a CPC separation, solvent systems were prepared. All the solvents in designated proportions were united together in a separatory funnel. After intensive manual shaking the mixture was left alone for several seconds until the distinct border between two phases appeared. Both phases were separated, each one collected in a separate flask.

The lower (stationary) phase was pumped into a rotor in sufficient quantity. It was followed by an upper (mobile) phase, at CPC rotation speed 800 rpm. The pumping of the upper phase continued until the equilibrium between both phases was reached. It was noted in a measuring cylinder, where the eluted lower phase was collected and its level remained steady. An extract fraction to be separated was well solved in a 50:50 mixture of upper and lower phases (1 g/4 mL of the mixture). The sample was injected in CPC manually with a 10

mL Luer syringe, right after that the separation process began. The eluent was collected in glass test-tubes in the automatic fraction collector.

With parallel TLC control, 300 test-tubes were collected in ascending mode. When no eluent spots were detected on a TLC plate, the CPC device was switched to the descending mode and 150 more test-tubes were collected. According to the TLC control, test tubes were united in sub-fractions, which were later purified with semi-preparative HPLC.

2.1.5.4 Semi-preparative HPLC

This was the last step in elucidating pure compounds. Fractions to be purified were solved in the solvents mixture equal to the starting conditions of the method, or in 100% MeCN. Solved fractions were filtrated through syringe filters with pore size 0.2 µm. Filtrated fractions were manually injected into an HPLC loop at room temperature. Concentration of the fractions injected was 10 mg/mL. Injection volume was ca. 250 µL each time (2.5 mg pro run). The separation was conducted on two columns (**Tab. 9**) with following conditions (**Tab. 10**).

Table 9. Columns for semi-preparative RP-HPLC

№	Name	Particles size	Dimensions	Manufacturer
1	Eclipse XDB-C18	5 µm	9.4 x 250 mm	Agilent Technologies (USA)
2	Vertex Eurosphere-100 C18	7 µm	16 x 250 mm	Dr. Ing. H. Knauer GmbH, Berlin

Table 10. Separation solvents systems for semi-preparative HPLC

Method	Column	Solvents	Gradient, %	Time, min	Flow, mL/min
HPLC_1	1	H_2O-MeCN	80 → 100 MeCN	0-30	3
HPLC_2	1	MeCN	100 MeCN	0-45	3
HPLC_3	1	MeCN-MeOH	60 → 100 MeOH	0-30	2
HPLC_4	1	MeCN-MeOH	70 → 100 MeOH	0-30	2
HPLC_5	2	MeOH-MeCN	70 MeCN	0-30	5
HPLC_6	2	H_2O-MeCN	80 MeCN	0-50	10

Collection of the fractions, i.e. corresponding peaks, seen on the monitor, occurred manually into the test-tubes. Results of several runs were united according to their retention time, wave length maximum and absorption similarities. The solvent from the united fractions was evaporated under constant nitrogen flow (overnight, laboratory hood, room temperature), then the fractions were weighted and NMR spectra were measured.

2.1.6 Structure elucidation and substances' characterisation

In order to characterise and describe the newly isolated substances, common spectroscopic and spectrometric methods were used, including:

- NMR – Nuclear Magnetic Resonance
- MS – Mass spectrometry
- Polarimetry – optical rotation
- UV-Spectra
- CD – Circular dichroism

Some of them (for example, 2D-NMR) are used to elucidate the structure of the newly isolated compound. Other methods, like MS may confirm the formula. CD-spectra help in determination of an absolute configuration, while other methods characterise the substance and may serve in future as a guiding landmark in discovering and characterising other similar compounds.

2.1.6.1 NMR spectroscopy

Fractions and sub-fractions underwent the ^{1}H-NMR analysis in order to detect putative acylphloroglucinols whereas pure compounds were subjected to extensive NMR analyses to establish their structure. Each separate fraction or compound was solved in ca. 0.65 mL deuterated chloroform $CDCl_3$ and placed in an NMR-tube so that the height of the solvent in the tube was not less than 4 cm.

1D- and 2D experiments were measured at the Central Analytical department, Faculty of Chemistry and Pharmacy, University of Regensburg, Germany. Spectra were recorded at 298 K, 600.25 MHz for ^{1}H-NMR and 150.95 MHz for ^{13}C-NMR.

All the conducted NMR experiments may be divided in several groups:

1) One dimensional:
    - ^{1}H-NMR
    - ^{13}C-NMR
2) Two dimensional:
    a. Heteronuclear (^{1}H, ^{13}C):

- HSQC – **H**eteronuclear **S**ingle **Q**uantum **C**oherence
- HMBC – **H**eteronuclear **M**ultiple **B**ond **C**orrelation

b. Homonuclear (^{1}H, ^{1}H):

- COSY – **Co**rrelated **s**pectroscop**y**
- NOESY – **N**uclear **O**verhauser **E**nhancement **S**pectroscop**y**

In ^{1}H-NMR spectrum various multiplets can be noted. They refer to the number of protons, according to the so called "*n+1 rule*", where *n* is the number of neighbouring protons and multiplet refers to the investigated proton. In case of doublets (d), doublet of doublets (dd), triplets (t), sextets (sext.), septets (sept.), etc. a "*coupling constant*" (*J*, Hz) can be defined.

After obtaining a ^{13}C-NMR spectrum, a list of all the carbons may be printed out. With the help of HSQC experiment all the direct C-H bonds can be allocated. In this case one can observe blue and green cross-peaks (colours may depend on the software individual customizations). The first ones refer to either =CH– or –CH_3 groups, while the latter shows –CH_2– groups. Quaternary carbons do not have any cross-peaks with any protons in this case, of course, because they cannot be connected with each other. HMBC shows then heteronuclear bonds between carbons and protons, which are maximum ^4J far from each other. HMBC experiments were also particularly useful in determining quaternary carbons with very weak signals on ^{13}C spectra or those, which didn't show any visible signals at all. In this case HMBC allows seeing cross-peaks correlations between respective proton and quaternary carbon, thus enabling to confirm the bond.

Homonuclear experiments, such as COSY show *geminal* (twins) (bonded to one and the same carbon, like in –C**H$_2$**– group) or *vicinal* (neighbours) protons (each of them is bonded to the neighbouring carbon, like in –C**H**=C**H**–). NOESY helps to establish a relative stereochemistry configuration, based on correlations of protons, which are less than 5 Å far from each other in space.

2.1.6.2 Mass spectrometry

Mass experiments were conducted at the Mass spectrometry department of the Central Analytical division, Chemical-Pharmaceutical faculty, University of Regensburg, Germany. Moleculat weight and formula were obtained from high-resolution electrospray ionisation

spectra (ESI-HRMS), which were measured in positive or negative mode on Q-TOF 6540 UHD (Agilent).

From the molecular ions M^+ and quasi- or pseudo-molecular ions like, for example, $[M + H]^+$ or $[M - H]^-$ and with the help of high-resolution precise determination of molecular weight and elemental composition analysis, an empirical formula of the investigated compound may be obtained (Budzikiewicz und Schäfer, 2012).

2.1.6.3 Polarimetry

Each one of the isolated substances was solved in MeOH HPLC grade (final concentration 0.5 mg/mL, which equals 0.05 g/100 mL) and placed with a Pasteur pipette in a special cuvette (1 dm length) of the polarimeter. The measurements were conducted by room temperature with pure solvent as a reference solution. Wave length equals 589.0 nm, which corresponds with the D-line of sodium's light. The specific rotation is calculated according to the formula 1 (Rücker et al., 2008):

Formula 1. Calculation of optical rotation:

$$[\alpha]_D^T = \frac{100 \cdot a}{c \cdot l}$$

where:

[α] – specific rotation
T – temperature in the moment of measurement, °C
D – D-line of sodium's light, 589.0 nm
α – measured rotation, °
c – concentration of the measured substance, 0.05 g/100 mL
l – pathlength of the cuvette, dm

The polarimetry data, presented for each substance is an arithmetic mean value from six successional measurements with an interval of 4 seconds.

2.1.6.4 UV-Visible spectroscopy

Each one of the isolated substances were solved in MeOH HPLC grade (final concentration = 0.6 mg/10mL) and placed in a special quartz cuvette for UV spectroscopy. This solution was

measured on UV spectrophotometer (λ = 200-800 nm, RT) with pure MeOH HPLC grade as a reference solution.

The measurement gives the absorption maxima value. With its help the molar attenuation coefficient can be calculated, using a formula 2, resulting from Beer–Lambert law.

Formula 2. Calculation of molar attenuation coefficient:

$$\varepsilon = \frac{A}{c \cdot l}$$

where:

ε – molar attenuation coefficient, $L \cdot mol^{-1} \cdot cm^{-1}$
A – absorption
c – molar concentration, mol/L
l – pathlength, 1 cm

By describing the isolated substances, the data is presented by wave length value in nm, as well as by logarithmical form of the molar attenuation coefficient (log ε).

2.1.6.5 CD spectroscopy

For measurement of circular dichroism, a substance was solved in MeOH p.a. to give a 200 µM solutiuon, filled in a quartz cuvette and measured on CD spectropolarimeter at room temperature with pure solvent as a reference. CD spectra graphs were constructed in Microsoft® Excel (relation of molar ellipticity from the wave length). Calculation of the molar ellipticity is possible, using the following equation (Rücker et al., 2008):

Formula 3. Calculation of molar ellipticity:

$$[\theta]_M = \frac{\theta \cdot M}{100 \cdot c \cdot l}$$

where:

$[\theta]_M$ – molar ellipticity, $° \cdot cm^2 \cdot dmol^{-1}$
θ – ellipticity, °
M – molar mass, g/mol
c – concentration, g/mL
l – pathlength, 0.1 dm

2.2 Cell culture methods

The following chapter describes devices, expendables and software (**§ 2.2.1**), chemicals and reagents (**§ 2.2.2**), as well as culture mediums and other solutions (**§ 2.2.3**) used in cell culture experiments during the course of the present work.

2.2.1 Devices, expendables and software

Autoclave	Autoklav 23, Melag, Berlin
	Varioklav 500, H+P, Oberschleißheim
Centrifuge	Megafuge 1.0 R Heraeus Sepatech, Heraeus Holding, Hanau
Cell culture flask	75 cm^2, 250 mL, PS, red filter cap, sterile Cat. no. 658-175, Greiner Bio-One GmbH, Frickenhausen
Cryovials	2 mL, Greiner Bio-One, Frickenhausen
Falcon centrifuge tubes	15 mL Cellstar® tubes (Cat. no. 188 271) 50 mL Cellstar® tubes (Cat. no. 227 261), TPP, Trasadingen (CH)
Filter, sterile	Syringe filter PES 0.45 µm (Cat. no. 99745), TPP, Trasadingen (CH)
Haemocytometer	Neubauer improved, Brang, Wertheim
Incubator	NU-5500 E, NUAIRE, Plymouth (USA)
Laminar flow cabinet	HERASafeKS, Thermo, Langenselbold
Microtiter plate	Tissue culture Testplate 96F, Art. 92096, TPP, Trasadingen (CH)
Microscopes (inverted light)	CKX41SF, Olympus, Hamburg
	PrimoVert with camera and monitor, Zeiss, Göttingen
Mixer	Vortex Genius 3, IKA, Staufen
Pasteur glass pipettes	230 mm (Cat. no. 612-1702), VWR, Darmstadt Heat-sterilized at 200°C during 3 h prior to use.
Photometer (plate reader)	SpectraFluor Plus, Tecan, Crailsheim; Xfluor4 v 4.40 (software)
Pipette tips	200 µL, 1000 µL, Sarstedt, Nümbrecht; 10 µL, Axygen, Union City (USA). Pipette tips were autoclaved prior to use.
Pipettes	2.5 Reference (0.1-2.5 µL), 10 Reference (2.5-10 µL) 100 Research (10-100 µL), 1000 Research (100-100 µL) 100 Research, 8-channel (10-100 µL), Eppendorf, Hamburg
Pipettor	Accu jet® pro, Brand, Wertheim
Safe lock tubes	Micro-centrifuge tubes for high g-force 1.5 mL natural, VWR, Radnor, PA (USA) (Cat. no. 211-0015)
	Safe lock tubes 2 mL, Eppendorf, Hamburg
Serologic pipettes	5 mL (Cat. no. 606 180), 10 mL (Cat. no. 607 180) Greiner, Frickenhausen
Syringe	1 mL Norm-Ject® Tuberkulin Luer (Cat. no. 4010-200V0) Henke Sass Wolf, Tuttlingen
Ultrapure water supplier	Astacus LS, MembraPure, Bodenheim
Vacuum pump	N 811 KT.18, KNF Neuberger, Freiburg
Water bath	WB22, Memmert, Schwabach

2.2.2 Chemicals and reagents

Reagents	Specifications and manufacturer
DMEM	Dulbecco's Modified Eagle Medium, DMEM (1x) [+] 4.5 g/L D-Glucose, [+] L-Glutamine, [-] Pyruvate Cat. no. 41965-039 (500 mL), Cat. no. 41965-062 (10 x 500 mL) Gibco®, Life Technologies, Paisley (UK). Stored at 4 °C Used as DMEM + 10% FCS HI
DMSO	Dimethyl sulfoxide for molecular biology 100 mL, ≥ 99.5% Art. A994.1, Carl Roth GmbH, Karlsruhe
FCS	Fetal calf serum, Superior, LOT 1305 C; Biochrom, Berlin. Stored at -20 °C Used as FCS HI, heat-inactivated: water bath 56 °C, 30 min
Glutamate	Monosodium-L-glutamate, purity ≥ 99% (HPLC) Cat. no. 6445, Merk, Darmstadt
MTT	3-(4,5-dimethylthiazol-2-yl)-2,5-diphenyl tetrazolium bromide Thiazolyl Blue Tetrazolium Bromide Cat. no. M2128-5G, Sigma, St. Louis, MO (USA). Stored at 4 °C
PBS	Dulbecco's Phosphate Buffered Saline (w/o $CaCl_2$, $MgCl_2$) Cat. no. D8537, Sigma life sciences, Steinheim. Stored at 4 °C
Quercetin	3,3',4',5,7-pentahydroxyflavone, dehydrate Lot 14H0957, Sigma chemical Co., St. Louis, MO (USA)
SDS	Sodium dodecyl sulfate, 92.5 – 100.5% based on total alkyl sulfate content basis. Sigma-Aldrich, St. Louis, MO (USA). Cat. no. L5750-1KG
Trypsin/EDTA	10x solution (0.5%/0.2%, w/v) in PBS, Cat. no. L 2153, Biochrom, Berlin
Trypan blue	3-3'-dimethyl-4,4'-bis-(5-amino-4-hydroxy-2,7-disulfonaphtyl-3-azo)-[1,1'-biphenyl], dye content ca. 37%, Sigma-Aldrich, Taufkirchen

2.2.3 Culture mediums and other solutions

Medium	Components	Quantities
Freezing medium for cryovials	DMEM	70%
	FCS	20%
	DMSO	10%
Growth medium	DMEM	500 mL
	FCS HI	50 mL

Solution	Specifications	Stored at
Glu solution	1 M stock solution in PBS, sterile filtered	-20 °C
MTT solution	4 mg/mL MTT in PBS	-20 °C
SDS solution	10% (m/v) in millipore water	RT
Quercetin solution	50 mM stock solution in DMSO, sterile filtered	-20 °C
Trypan blue	0.4% (w/v) solution in PBS	4 °C
Trypsin/EDTA	10% (v/v) solution in PBS	4 °C

2.2.4 Cells

For the assays conducted in frames of this work, HT-22 cells were used (**Fig. 21**). This is a glutamate-sensitive immortalized mouse hippocampal sub-line, derived from parent HT4 cells. Immortalization was performed with temperature sensitive SV40 T-antigen. (Davis and Maher, 1994; Maher and Davis, 1996; Morimoto and Koshland, 1990)

Since HT-22 cells do not possess ionotropic NMDA receptors (Maher and Davis, 1996), Glu-induced neurotoxicity occurs only via oxidative path. Therefore, Glu-induced, receptor mediated, excitotoxicity cell death pathway can be excluded (Kling, 2015) (§ 1.2.3, **Fig. 18**). In the course of the present work these cells were used for modelling and studying neurotoxicity and neuroprotection effects of the isolated acylphloroglucinol from *H. triquetrifolium.*

The HT-22 cells were kindly supplied by the Max Plank Institute of Psychiatry, Munich (Germany).

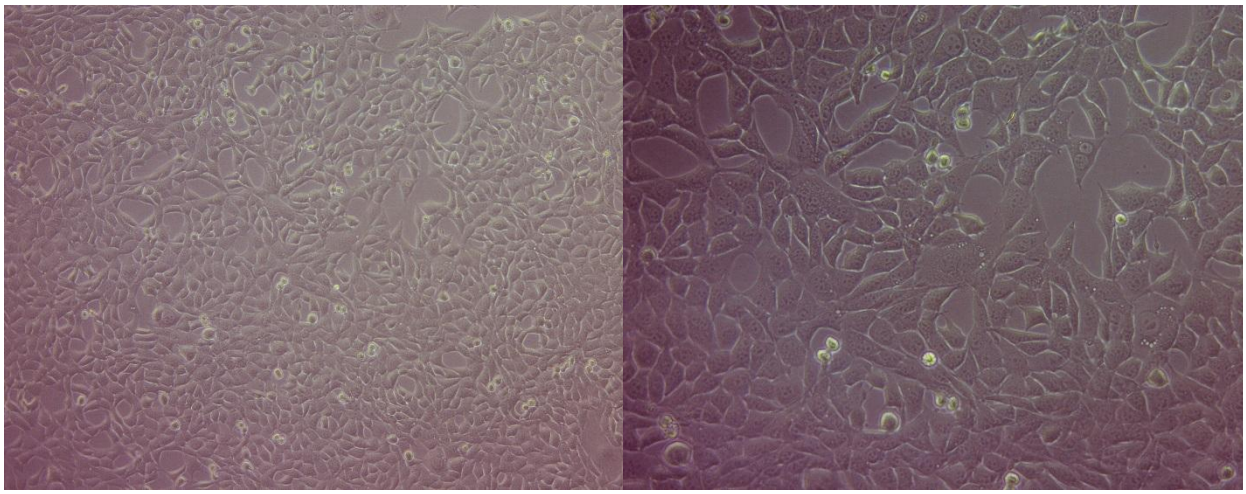

Fig. 21. Microscopic photograph of HT-22 cells (PX+8+3). Enlargement 10x (left), 20x (right). Photo edit: Dipl.-Ing. Igor Zeiger.

2.2.5 Basic principles

All the conducted experiments with HT-22 cells were performed under sterile conditions in a laminar flow cabinet following common cell culture procedures. (Schmitz, 2011) DMEM and PBS were warmed up to 37 °C on water bath prior to use. Trypsin and trypan blue solutions were left for 15-20 min to warm up at RT.

DMEM is a growth medium suitable for HT-22 cells. It combines carbonate buffer, all the necessary nutritional chemicals for the cells, as well as pH indicator phenol red (pH of fresh DMEM is 7.1). When cells remain in the growth medium too long, their acidic waste products lower the pH value, which results in colour change of the medium. Red solution becomes orange and then yellow. Normally, this should not happen if cells are cultivated and splitted correctly. Furthermore, heat-inactivated FCS 50 mL was added to 500 mL growth medium DMEM bottle, making the final medium more rich in nutritional elements for cells, than the DMEM alone (§ 2.2.3).

Thawing. HT-22 cells are kept in cryovials in a liquid nitrogen storage tank (temperature under atmospheric pressure is between ca. -210 °C and -196 °C). One cryovial contains 1.8 mL freezing medium with about 1-2 million cells. The freezing medium for HT-22 cells consists of 70% DMEM + 20% FCS + 10% DMSO. FCS prevents crystallisation and restrains the clash. DMSO inhibits crystallisation as well, but in high concentrations it is very poisonous for the cells when they are defrosted. Therefore, after quick defrosting in a 37 °C water bath (in a beaker), cell suspension was diluted with 8 mL growth medium (1:5) and centrifuged at 700 rpm (92 x g) for 4 min. Supernatant was removed and the remaining cells were suspended with 2 mL growth medium, which was then transferred to 18 mL fresh medium in a 75 cm^2 culture flask. The flask was then placed in an incubator and fresh medium was exchanged in 2 days.

Cultivation of HT-22 cells happened in incubator with the following conditions: temperature = 36.7 °C, CO_2 level = 5%, humidity = 95%. Density and growth of the cells were observed under the microscope five times a week.

Splitting of the cells occurred 3 times a week at around 80% confluence in order to keep the constant level of metabolic activity and their division efficiency. On Mondays and Wednesdays they were splitted in ratio 1:5 (for two days) and on Fridays 1:10 (for three days). For this purpose, growth medium from the culture flask was aspired with Pasteur pipette and the cells were washed with 10 mL PBS. Then 1 m of serine protease trypsin in EDTA was added. Since the cells are firmly hold on the internal surface of the culture flask with protein tails, which are stabilised with Ca^{2+} and Mg^{2+}, EDTA complexes the ions and the enzyme functions better. (Boxberger, 2007) The culture flask was placed into incubator for 1

min until trypsin takes effect. Gentle clapping on the culture flask also helped to detach the cells. Then an excess of 9 mL of growth medium were added to the flask to dilute trypsin and stop its impact. The cells were well suspended and transferred into a falcon tube, then centrifuged at 700 rpm (92 x g) during 4 min. The supernatant was removed and cells were suspended in 5 mL fresh growth medium. In case of 1:5 splitting, 1 mL of this suspension was added to 19 mL growth medium in a new culture bottle. When the cells were splitted in ratio 1:10, just 0.5 mL of the suspension was taken and dispensed in 19.5 mL growth medium. The cells in the flask were observed under the microscope and placed in incubator. Remaining in the falcon centrifuge tube cells were then used for further experiments (see below), or casted away if there was no need of immediate use.

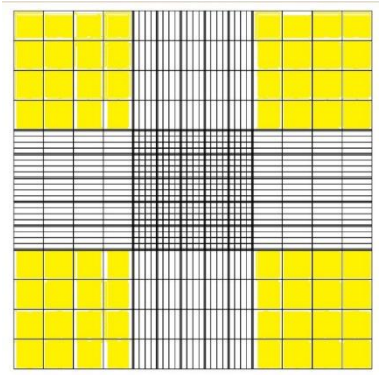

Fig. 22. Neubauer haemocytometer counting area

Estimating the cells quantity was performed using those ones, which were left in a falcon tube after the splitting (see above). Several drops of the suspension were taken to an Eppendorf 1.5 mL safe lock tube and 20 µL of this liquid was mixed in ratio 1:1 with 20 µL of diazo dye trypan blue solution (0.04 g in 10 mL PBS) (**Fig. 23**). An aliquot of this mixture (10 µl) was placed under a glass lid into a Neubauer haemocytometer. Living cells do not let the trypan blue solution through their undamaged cell membranes and therefore remain uncoloured, whereas the dead cells take the dye. Only living cells were counted in 4 corner 4x4 squares (yellow coloured, see **Fig. 22**). An arithmetic mean was calculated, multiplied by two (because of the 1:1 dilution factor with trypan blue) and then multiplied by 10^4 (counting chamber conversion factor). The final value meant the quantity of cells in 1 mL suspension in the falcon tube.

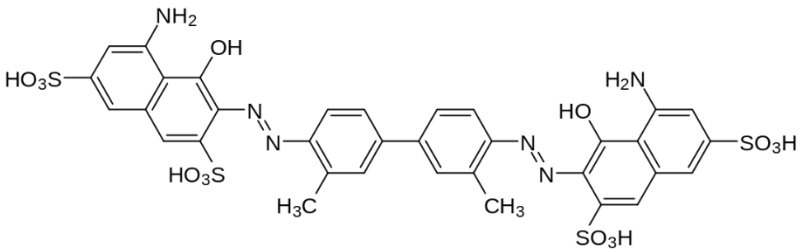

Fig. 23. Trypan blue (also known as diamine blue and Niagara blue)

Substances. Previously isolated substances with elucidated structure were tested on HT-22 cells. Having being kept in glass vials, sealed with Parafilm® "M" laboratory film, each substance was transferred to a safe lock tube, dried under the nitrogen flow and weighted. Weighting occurred six times, after which an arithmetical mean was estimated and used for further calculations.

Stock solutions preparation. Dried and weighted substances were solved in DMSO 99.5% for molecular biology in order to obtain a 0.1 M stock solution. These were stored in safe lock tubes at -20 °C.

2.2.6 MTT assay

MTT assay is a useful and simple method to evaluate the quantity of living cells after toxicity/protection test. Since HT-22 cells do not possess ionotropic NMDA receptors, Glu-induced neurotoxicity occurs in this case via oxytosis pathway (§ 1.2.3). Experiments were conducted in two stages:

1) During the first stage, substances were tested on cells and their toxicity, i.e. neurotoxicity was observed. In this case they were compared to untreated cells in growth medium and pure solvent (0.05% DMSO) as control.
2) On the second stage, tested substances were mixed with glutamate (5 mM Glu pro well) and should have protected the cells against ruinous activity of the latter. This time, the effects of the tested substances were compared to that of quercetin (positive control), since it is well known to protect neurons in low µM concentrations (Dok-Go et al., 2003). Glu acted as negative control and untreated cells in growth medium were considered as 100%.

After a usual splitting, quantity of HT-22 cells in 1 mL growth medium was counted and calculated (§ 2.2.5). 96-well microtiter plates were used for the assay. Outer 36 wells were filled with only pure growth medium, whereas the internal 60 wells were used for the test. Cells were seeded in each one of these 60 internal wells in quantity of ca. 5000 cells in 100 µL growth medium pro well. The microtiter plate with the cells was left in an incubator (t = 36.7 °C, CO_2 level = 5%, humidity = 95%) for 24 hours.

Investigated substance was solved in DMSO (max. 0.05%) to prepare a 0.1 M stock solution (kept in freezer), which was then diluted with growth medium to prepare a serial dilution with concentrations of 1, 5, 10 and 25 µM. The following controls were used to compare and analyse the data:

- Untreated cells in growth medium (as 100%)
- 25 µM quercetin/DMSO + 5 mM Glu in growth medium as positive control
- 5 mM Glu/PBS in growth medium as negative control

Impact of DMSO on the cells was studied separately (§ 3.2.1).

After the cells were seeded and incubated for 24 hours, the supernatant was removed. 100 µL of each 1-25 µM solution was subsequently placed in corresponding wells of the plate (6 wells for each solution), which was left in incubator for additional 24 hours after that.

On the next day an MTT solution was prepared. Usually being stored in freezer, it has to be defrosted in water bath at 37 °C. Defrosted MTT solution (c = 4 mg/mL in PBS) was diluted with growth medium in ratio 1:10.

Microtiter plate was taken out of the incubator and the applied substances were substituted with the MTT 1:10 diluted solution. The plate was once again placed in the incubator for 3 hours, during which the yellow tetrazolium MTT salt was reduced to insoluble violet-blue formazan crystals (**Fig. 24**).

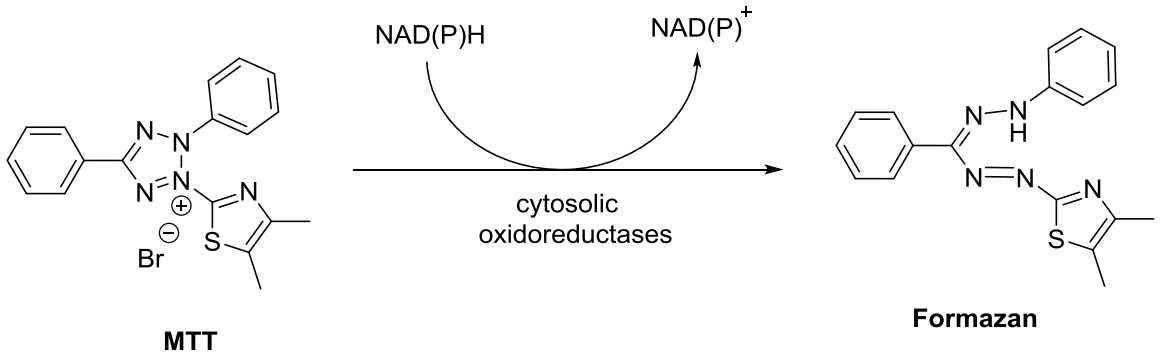

Fig. 24. Reduction of MTT salt (yellow) to formazan (violet-blue) mainly occurs by cytosolic NADH- and NADPH-dependent oxidoreductases, as well as by mitochondrial reductases of metabolically active and viable cells. (Berridge et al., 1993; Berridge et al., 2005; Kling, 2015)

After 3 hours 10% water solution of sodium dodecylsulfat (SDS) (100 µL pro well) replaced the MTT one. It destroys cell membranes (and, as a result, the cells themselves) and solves formazan crystals. Microtiter plate was left for the night at RT in a dark place (because formazan can be photolabile) and on the next day the intensity of colouring was measured photometrically at 560 nm.

Evaluation of results occurred in two ways, depending on the test:

1) For neurotoxicity assay, untreated cells were used as 100% and an influence of the investigated substance on the HT-22 cells was expressed as percent to the number of untreated cells. Theoretically it might be expected, that the substances' toxicity will rise with the increase of their concentration, although desirable is the constant high level of viable cells after the assay, which tends to 100% (untreated cells level).
2) For neuroprotection assay, untreated cells were used as 100% as well, but also 5 mM Glu and 25 µM quercetin (positive control) were used as controls. The tested substance in different concentrations was added to the cells along with Glu to observe its protecting properties in spite of a simultaneous impairment action of the amino acid. Data obtained on the impact of the tested compounds is compared to these three controls. Desirable are substances, which protect neuronal HT-22 cells on the same level as quercetin or better.

Impact of the solvent. All the tested compounds were solved in DMSO in order to prepare 0.1 M stock solutions, which were later diluted to the tested concentrations. In order to ensure the absence of any DMSO's impact on the cells, three independent successive MTT-assays (§ 2.2.6) with only pure cells and DMSO in concentrations 0.05%, 0.025% and 0.01% (in growth medium) were conducted (§ 3.2.1).

2.2.7 Statistical analysis

All experiments were conducted in hexaplicate and repeated three or more times independently from each other. The results are expressed as an arithmetic mean ± standard deviation, in % as a relation to 100% untreated cells. Statistical analysis was performed with Prism® 5.03 for Windows (GraphPad Software Inc., La Jolla, CA, USA) using one-way analysis of variances (ANOVA) to determine significant differences. Post hoc analysis was done using

the Dunnett's test. Statistical significance levels: $p < 0.05$ (*), $p < 0.01$ (**) and $p < 0.001$ (***). For significance test in neurotoxicity assays all results were compared to the untreated cells control, while in neuroprotection assays all results were compared to 5 mM Glu negative control.

3 Results and Discussion

3.1 Phytochemical experiments

3.1.1 Isolation strategy

Talking about isolation strategies in general, three most common ones should be mentioned:

- TLC-guided fractionation
- NMR-guided fractionation
- Bioactivity-guided fractionation

Each one of them has its own advantages and disadvantages. For example, **TLC-guided fractionation** is a simple analytical method, which is cheap, easy and quickly to perform. On the other side, the spots can overlay on the plate, thus hiding and/or falsifying the results. Furthermore, the R_f values and spots' colours are not specific constants to characterise a substance undoubtedly and unequivocally.

NMR-guided fractionation may help in detecting compounds, while the ppm region is specific for certain functional groups. As an example and a guideline for all the isolated substances in the course of the present work, prenylated acylphloroglucinols may be detected according to several characteristic attributes (examples, **Fig. 25**):

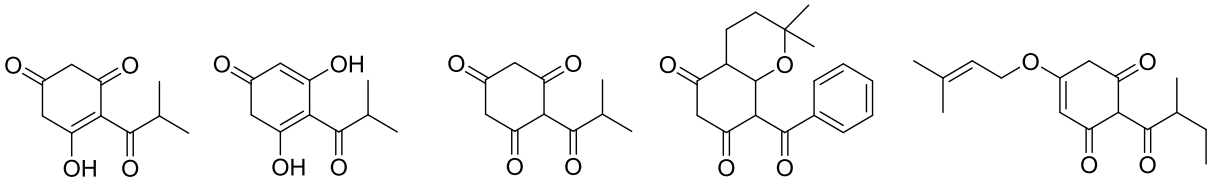

Fig. 25. Examples of structure elements with lacking or varying "down field shifted" hydrogen bonds in NMR-guided isolation strategy for acylphloroglucinols.

- Specific "*down field*" singlets at δ_H > 13-15 ppm, usually 17-19 ppm. These do correlate with the hydrogen bond between the –OH group in the main phloroglucinol ring and =O of the starter acid (**i**) (also **Fig. 63**, § 3.1.3.1). In case of two –OH groups in ortho-position to a starter acid (**ii**), signal value will be "high field shifted" (ca. δ_H 11-15 ppm), because the keto-group is able to build hydrogen bonds with them both.

However, absence of these signals doesn't confirm the absence of acylphloroglucinols in the investigated probe (**iii-v**).

- Characteristic are also triplets at ca. δ_H 5.00 ppm, which may indicate a =CH– group proton of the isoprene or geranyl rest (**v**). Exceptions from the rule are compounds, which are neither prenylated, nor geranylated or contain a cyclized side chain (**i-iv**).
- Several compounds have been biosynthesized with isobutyryl CoA as a starter acid (**i-iii**). In this case, a clear septet (ca. δ_H 2.50 – 3.50 ppm; δ_C 38-45 ppm), representing the aliphatic methine proton, as well as two doublets for each of the $–CH_3$ groups (ca. δ_H 1.10 ppm) can be clearly observed. In representatives containing a 2-methylbutyryl coA as starter acid (**v**), the methin proton will resonate as a sextet. A doublet (ca. δ_H 1.10 ppm) and a triplet (ca. δ_H 0.85 ppm) will be observed for the $–CH_3$ groups. In case of aromatic starter acid (**iv**), its protons' signals will find place at around δ_H 7.00 ppm.
- Signals of isoprene chains' $–CH_3$ groups (**v**) often show themselves as intensive high singlets at ca. δ_H 1.50 – 1.75 ppm, however these values may vary.
- One can also obtain ^{13}C-NMR spectra to confirm the presence of an acylphloroglucinol. In this case, there should be a different number of down field shifted signals (ca. δ_C 187-212 ppm), corresponding to the carbonyl carbons of the keto-groups (**i-v**).

In addition to the exceptions described above, some other disadvantages lie in the fact that signals' intensity of the crude extract spectrum do not always correlate with the quantity of the compounds in the probe.

Unlike two previous strategies, **bioactivity-guided fractionation** always leads to an isolation of biologically active compounds. However, it is usually more expensive and takes more time, if compared to TLC- or NMR-guided methods. It is not also sensible to the fact that new, i.e. previously unknown compounds may possess different biological activity. It should be considered, that an extract or mixture of compounds may possess much higher biological activity, than that of one pure substance because of synergism.

While performing the current work, NMR-guided strategy was used, thus resulting in isolation of 20 compounds, including acylphloroglucinols and their possible precursors.

Those isolated in sufficient quantities were tested for neurotoxicity and neuroprotection *in vitro*.

3.1.2 Fractionation and isolation

Obtained as described in § 2.1.4 a petroleum ether crude extract, **PE** (18.68 g) from *H. triquetrifolium* TURRA (^{1}H-NMR, **Fig. 26**), was divided in four equal parts in order to undergo the first separation step on Si-gel Flash column chromatography. This was done because of the limited columns' capacity. Mobile phase was used as described in method Flash_1 (§ 2.1.5.1).

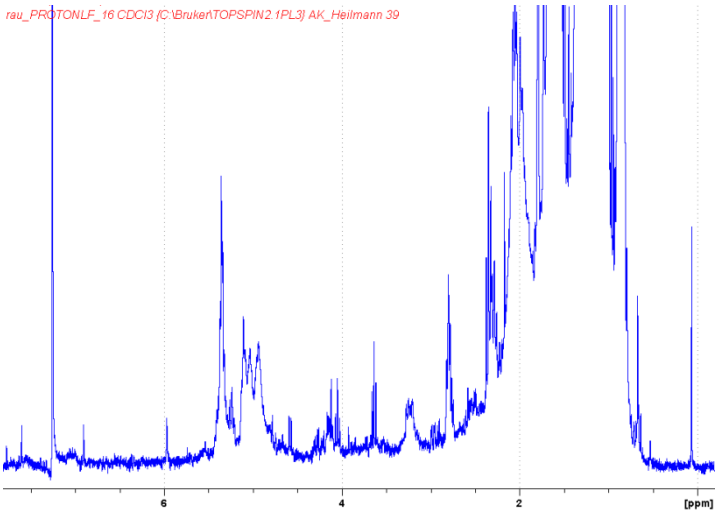

Fig. 26. ^{1}H-NMR of crude PE extract (300.13 MHz, 295 K)

The separation resulted in 6 fractions. Four identical subsequent runs were checked by TLC- and NMR-fractions control. These allowed uniting equal corresponding fractions from each of the four runs together. Principal separation scheme of PE extract is presented in **Fig. 27**.

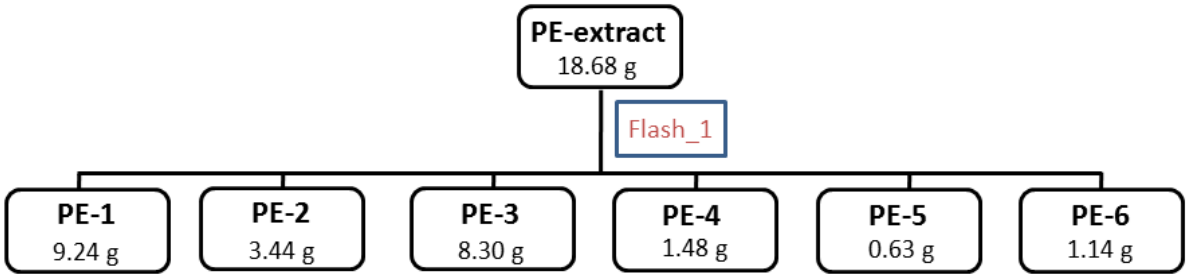

Fig. 27. Separation scheme for crude PE extract.

Weights and volumes of sub-fractions, obtained after Flash fractionation of PE extract of *H. triquetrifolium*.

Flash 1: PE-1 0.59 g, 100 mL; PE-2 0.74 g, 140 mL; PE-3 0.54 g, 210 mL; PE-4 0.34 g, 190 mL; PE-5 0.28 g, 430 mL; PE-6 0.31 g, 70 mL

Flash 2: PE-1 3.69 g, 300 mL; PE-2 1.03 g, 110 mL; PE-3 1.36 g, 300 mL; PE-4 0.25 g, 160 mL; PE-5 0.17 g, 190 mL; PE-6 0.08 g, 180 mL

Flash 3: PE-1 5.31 g, 380 mL; PE-2 0.88 g, 100 mL; PE-3 2.35 g, 280 mL; PE-4 0.29 g, 190 mL; PE-5 0.14 g, 190 mL; PE-6 0.56 g, 250 mL

Flash 4: PE-1 3.25 g, 380 mL; PE-2 1.07 g, 100 mL; PE-3 1.80 g, 280 mL; PE-4 0.28 g, 190 mL; PE-5 0.13 g, 190 mL; PE-6 0.57 g, 300 mL

3.1.2.1 Fractionation of PE-2

Separation scheme of PE-2 can be observed from **Fig. 28**.

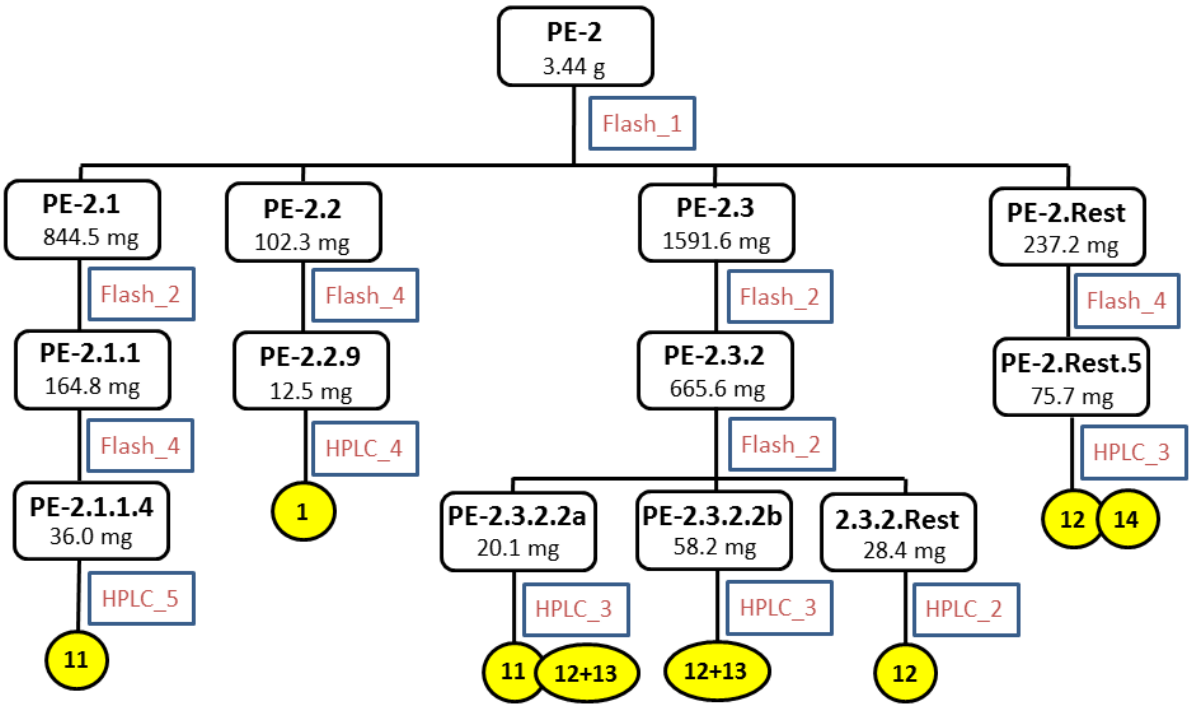

Fig. 28. Separation scheme of PE-2.

PE-2 (3.44 g) was separated with Flash chromatography on Si-gel (method Flash_1), giving 6 fractions (PE-2.1 844.5 mg, 190 mL; PE-2.2 102.3 mg, 130 mL; PE-2.3 1591.6 mg, 250 mL; PE-2.4 459.0 mg, 190 mL; PE-2.5 218.9 mg, 440 mL; PE-2.Rest 237.2 mg, 300 mL) in 150 test-tubes (10 mL/each). The overview TLC on Si-gel for these fractions is presented on **Fig. 29**.

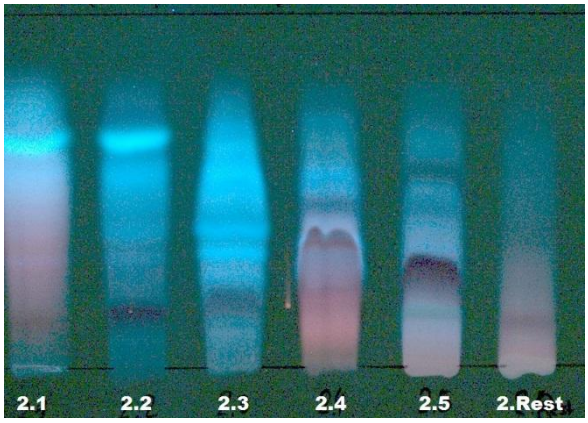

Fig. 29. TLC of PE-2.1–2.Rest (366 nm)
Si-gel; hexane – EtOAc – acetic acid = 70:28:2

Fractions PE-2.2, PE-2.3 and PE-2.5 show dark, almost black-blue bands at R_f 0.16, 0.19 and 0.30 respectively. They are characteristic for phenolic compounds and may point on the presence of some acylphloroglucinols in the probe (Schmidt, 2013).

PE-2.1 (844.5 mg, 190 mL eluted) was separated with Flash column chromatography on Si-gel (method Flash_2), giving 6 sub-fractions (PE-2.1.1 164.8 mg, 120 mL; PE-2.1.2 390.6 mg, 80 mL; PE-2.1.3 35.9 mg, 50 mL; PE-2.1.4 18.0 mg, 60 mL; PE-2.1.5 9.4 mg, 70 mL; PE-2.1.Rest 31.0 mg, 320 mL) in 70 test tubes (10 mL/each), out of which **PE-2.1.1** (164.8 mg, 120 mL eluted) was subsequently separated on RP-18 Flash column chromatography (method Flash_4), giving 6 sub-fractions (PE-2.1.1.1 5.2 mg, 285 mL; PE-2.1.1.2 4.9 mg, 75 mL; PE-2.1.1.3 21.5 mg, 75 mL; PE-2.1.1.4 36.0 mg, 135 mL; PE-2.1.1.5 5.3 mg, 158 mL; PE-2.1.1.Rest 67.9 mg, 75 mL) in 107 test tubes (7.5 mL/each). According to its ^{1}H-NMR spectrum (**Fig. 30**), fraction PE-2.1.1.4 looked very promising regarding a search for acylphloroglucinols: characteristic "*down field*" signals at δ_H 19.00 ppm and 10.00 ppm suggesting an intramolecular hydrogen bond, a septet resonating at 2.95 ppm represents the aliphatic methine proton of the isobutyric starter acid, as well as 2 doublets at 0.99 and 1.02 ppm may depict both $-CH_3$ groups. Additional singlets at 1.15 and 1.70 ppm may stand for isoprene rests' $-CH_3$ groups. **PE-2.1.1.4** (36.0 mg, 135 mL eluted) was purified on semi-

preparative HPLC (method HPLC_5) giving (+)-yezo'otogirin C (**11**) (t_R 15.8 min; λ_{max} 211, 302 nm; **Fig. 30**).

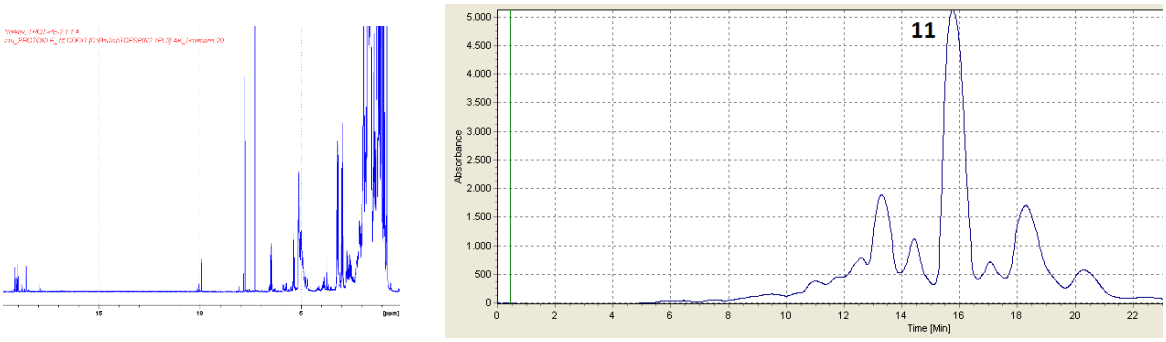

Fig. 30. PE-2.1.1.4 ^{1}H-NMR (300.13 MHz, 295 K) (left)
HPLC chromatogram at 211 nm, HPLC_5 (right)

PE-2.2 (102.3 mg, 130 mL eluted) was separated by Flash chromatography on RP-18 (method Flash_4), giving 11 sub-fractions (PE-2.2.1 18.3 mg, 158 mL; PE-2.2.2 14.6 mg, 53 mL; PE-2.2.3 13.6 mg, 120 mL; PE-2.2.4 17.3 mg, 45 mL; PE-2.2.5 63.0 mg, 30 mL; PE-2.2.6 41.3 mg, 90 mL; PE-2.2.7 32.7 mg, 38 mL; PE-2.2.8 7.0 mg, 23 mL; PE-2.2.9 12.5 mg, 53 mL; PE-2.2.10 7.1 mg, 105 mL; PE-2.2.Rest 43.6 mg, 90 mL) from 107 test tubes (7.5 mL each). Because of its clear "*down field*" signals on ^{1}H-NMR spectrum, fraction **PE-2.2.9** (12.5 mg, 53 mL eluted) was chosen for further HPLC purification (method HPLC_4), resulting in triquetriborin (**1**) (t_R 22.0 min; λ_{max} 205, 243, 287 nm; **Fig. 31**).

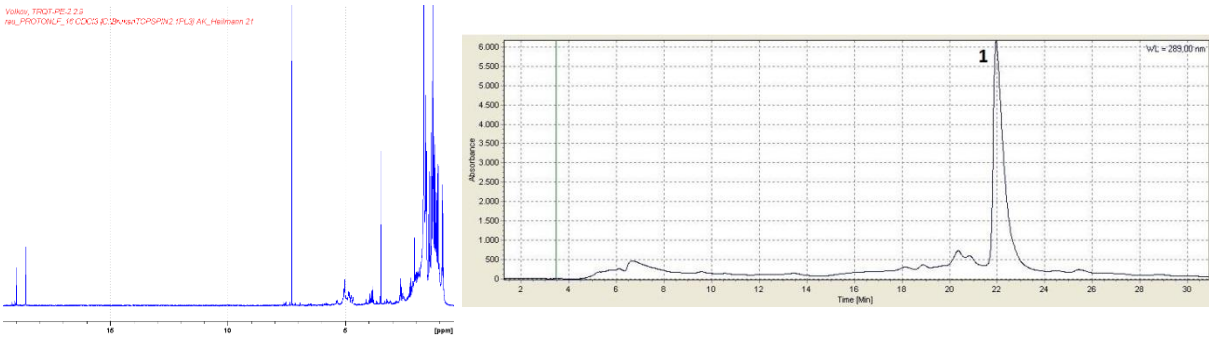

Fig. 31. PE-2.2.9 ^{1}H-NMR (300.13 MHz, 295 K) (left)
HPLC chromatogram at 289 nm, HPLC_4 (right)

PE-2.3 (1591.6 mg, 250 mL eluted) was separated with Flash column chromatography on Si-gel (method Flash_2), giving 5 sub-fractions (PE-2.3.1 40.3 mg, 110 mL; PE-2.3.2 665.6 mg, 110 mL; PE-2.3.3 232.7 mg, 90 mL; PE-2.3.4 79.9 mg, 190 mL; PE-2.3.Rest 63.2 mg, 200 mL) in 70 test tubes (7.5 mL each). The fraction with the highest quantity, **PE-2.3.2** (665.6 mg,

110 mL eluted) (**Fig. 32**) was once again separated with Si-gel Flash chromatography (method Flash_2), resulting in 70 test tubes (7.5 mL each), which were combined to 7 sub-fractions (PE-2.3.2.1 7.0 mg, 100 mL; PE-2.3.2.2a 20.1 mg, 20 mL; PE-2.3.2.2b 58.2 mg, 20 mL; PE-2.3.2.3 299.1 mg, 80 mL; PE-2.3.2.4 35.1 mg, 90 mL; PE-2.3.2.5 18.4 mg, 140 mL; PE-2.3.2.Rest 28.4 mg, 250 mL).

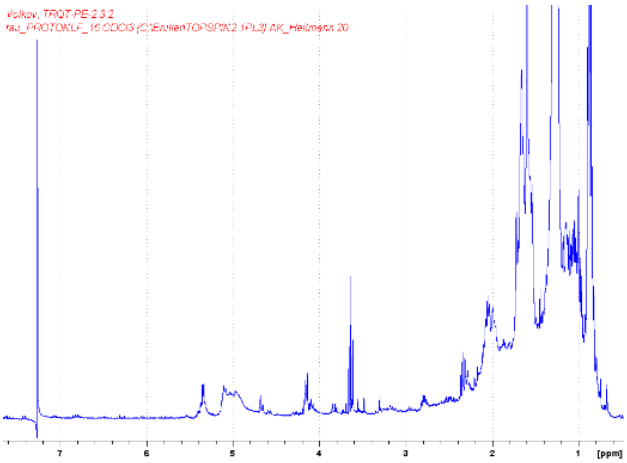

Fig. 32. ^{1}H-NMR of PE-2.3.2 (300.13 MHz, 295 K)

PE-2.3.2.2a (20.1 mg, 20 mL eluted) was purified on semi-preparative HPLC (method HPLC_3) giving a mixture of triquetriirinon A and B (**12+13**) (t_R 9.9 min; λ_{max} 207, 294 nm) and (+)-yezo'otogirin C (**11**) (t_R 16.0 min; λ_{max} 210 nm) (**Fig. 33**).

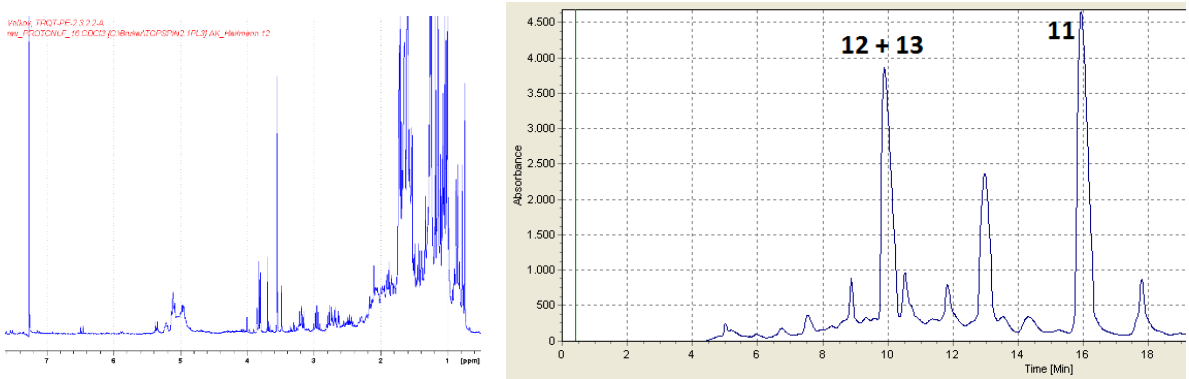

Fig. 33. PE-2.3.2.2a ^{1}H-NMR (300.13 MHz, 295 K) (left)
HPLC chromatogram at 209 nm, HPLC_3 (right)

PE-2.3.2.2b (58.2 mg, 20 mL eluted) was purified on semi-preparative HPLC (method HPLC_3) giving a mixture of triquetriirinon A and B (**12+13**) (t_R 9.8 min; λ_{max} 207 nm; **Fig. 34**). Right as in the case of sub-fraction PE-2.3.2.2a these both compounds couldn't be separated and eluted together.

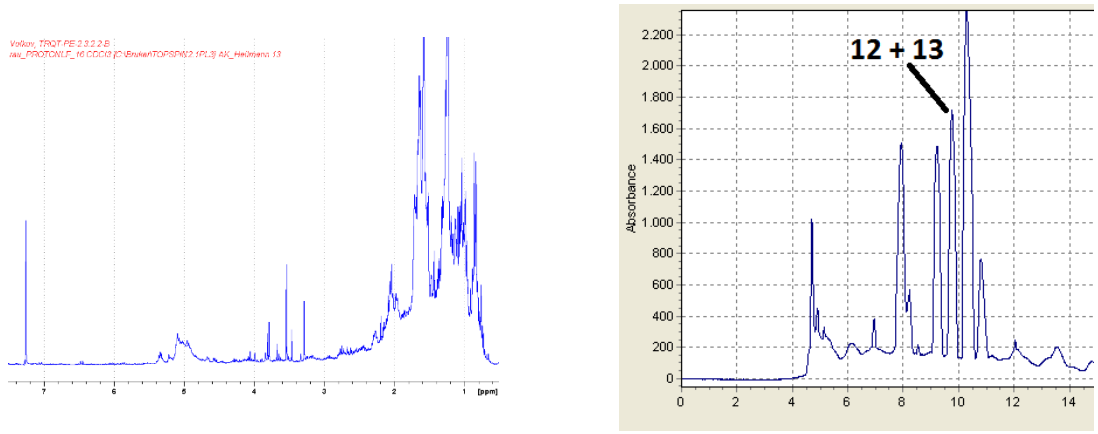

Fig. 34. PE-2.3.2.2b ^{1}H-NMR (300.13 MHz, 295 K) (left)
HPLC chromatogram at 210 nm, HPLC_3 (right)

PE-2.3.2.Rest (28.4 mg, 250 mL eluted) was purified by semi-preparative HPLC (method HPLC_2, time = 15 min) giving pure triquetriirinon A (**12**) (t_R 9.0 min; λ_{max} 203, 216, 280 nm; **Fig. 35**).

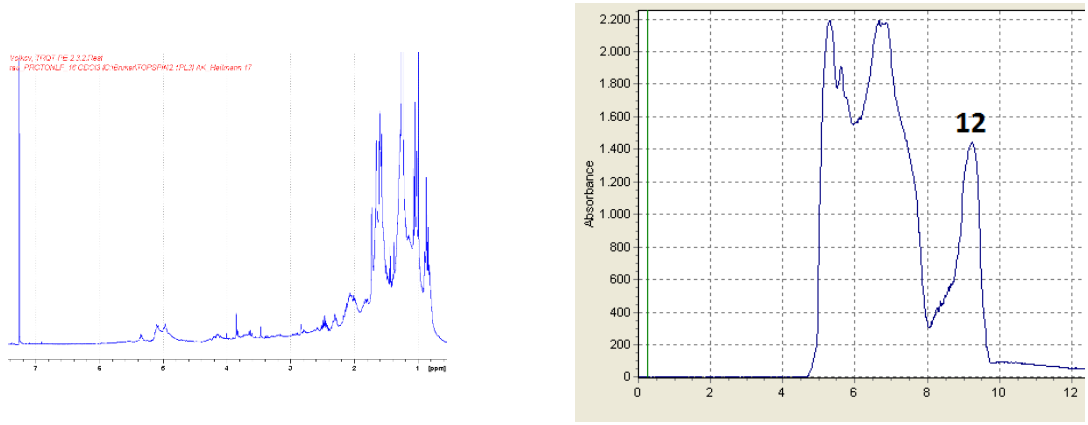

Fig. 35. PE-2.3.2.Rest ^{1}H-NMR (300.13 MHz, 295 K) (left)
HPLC chromatogram at 202 nm, HPLC_2 (right)

PE-2.Rest (237.2 mg, 300 mL eluted) (**Fig. 36**) was separated with Flash on RP-18 (method Flash_4), giving 7 fractions (PE-2.Rest.1 45.3 mg, 210 mL; PE-2.Rest.2 6.2 mg, 90 mL; PE-2.Rest.3 14.4 mg, 53 mL; PE-2.Rest.4 5.5 mg, 30 mL; PE-2.Rest.5 75.7 mg, 120 mL; PE-2.Rest.6 27.7 mg, 210 mL; PE-2.Rest.Rest 21.3 mg, 90 mL) in 107 test-tubes (7.5 mL each). Fraction **PE-2.Rest.5** (75.7 mg, 120 mL eluted) was subsequently purified on semi-preparative HPLC (method HPLC_3) yielding triquetriirinon A (**12**) (t_R 10.3 min; λ_{max} 213, 282 nm) and triquetriirinon C (**14**) (t_R 11.3 min; λ_{max} 205, 248, 323 nm) (**Fig. 37**).

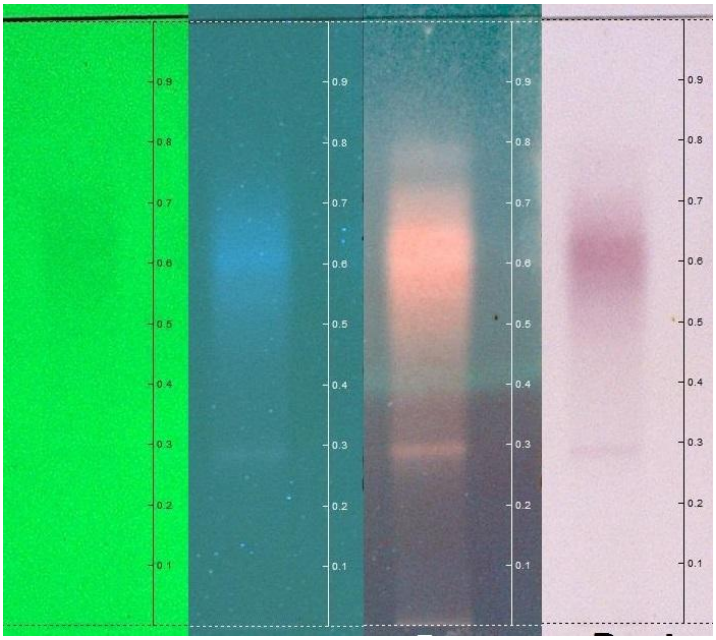

Fig. 36. TLC of PE-2.Rest
From left to right: 254 nm, 366 nm, 366 nm AAR, daylight AAR.
Si-gel; hexane – EtOAc – acetic acid = 70:28:2

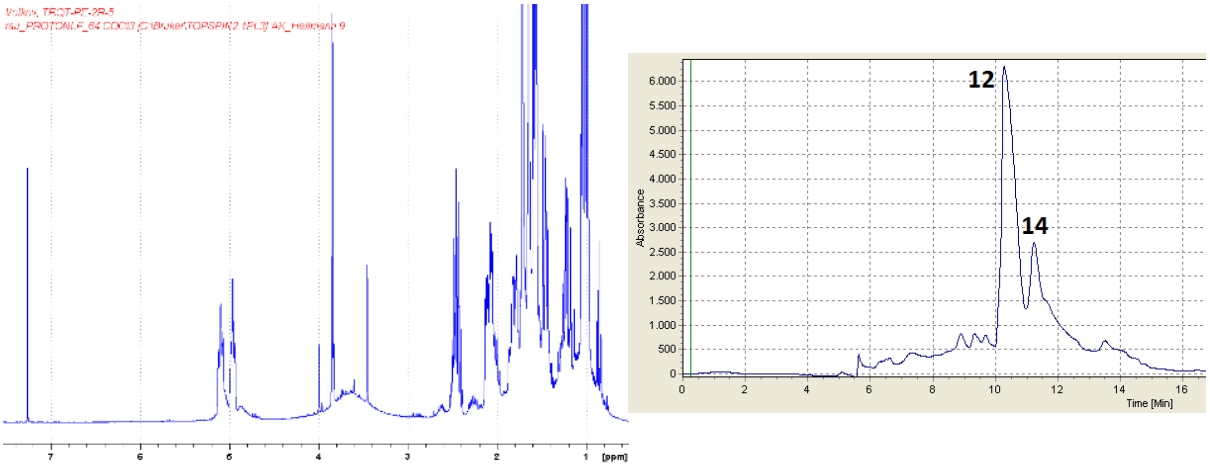

Fig. 37. PE-2.Rest.5 ^{1}H-NMR (300.13 MHz, 295 K) (left)
HPLC chromatogram at 211 nm, HPLC_3 (right)

3.1.2.2 Fractionation of PE-3

Separation scheme of PE-3 can be observed from **Fig. 38**.

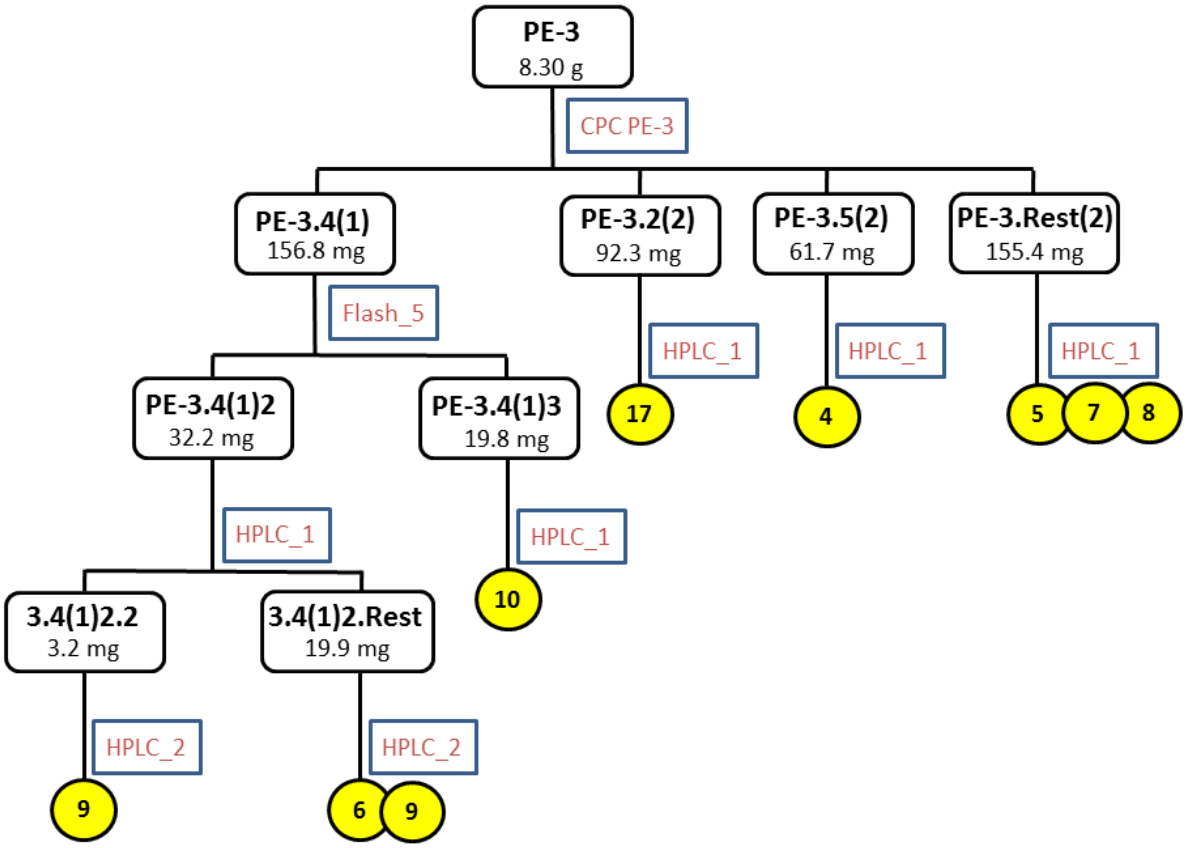

Fig. 38. Separation scheme of PE-3.

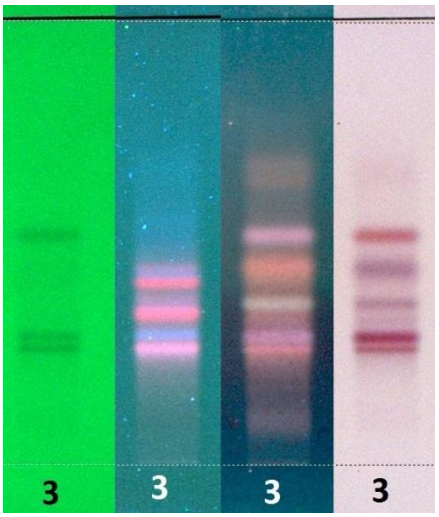

Fig. 39. TLC on Si-gel of PE-3
(from left to right: 254 nm, 366 nm,
366 nm AAR, daylight AAR)
hexane – EtOAc – acetic acid = 70:28:2

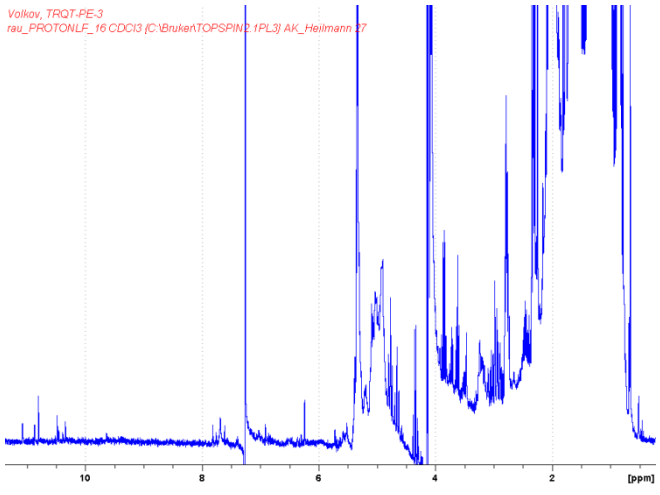

Fig. 40. ^{1}H-NMR of PE-3 (300.13 MHz, 295 K)

Fraction **PE-3** looked very promising in search for acylphloroglucinols according to its TLC (**Fig. 39**) and ^{1}H-NMR spectrum (**Fig. 40**). Characteristic "*down field shifted*" signals, as well as blue bands at R_f ca. 0.31 and 0.53 (366 nm) point on the presence of desirable chemicals in the probe.

PE-3 (8.30 g) was separated using CPC (**Tab. 8**, § 2.1.5.3). Because the loading quantity into a CPC device is limited, the separation occurred in four runs, namely "0", "1", "2" and "3". TLC- and NMR- control of the sub-fractions revealed identical results for runs 0-3. However similar corresponding sub-fractions were not united. Their subsequent fractionating occurred separately.

After each CPC separation run, 8 sub-fractions were obtained. According to their ^{1}H-NMR spectra and overview TLCs four fractions were chosen for later separation: from run 1 – PE-3.4(1) and from run 2 – PE-3.2(2), PE-3.5(2) and PE-3.Rest(2). TLCs of the sub-fractions obtained after CPC on the example of run 2 are presented in **Fig. 41**.

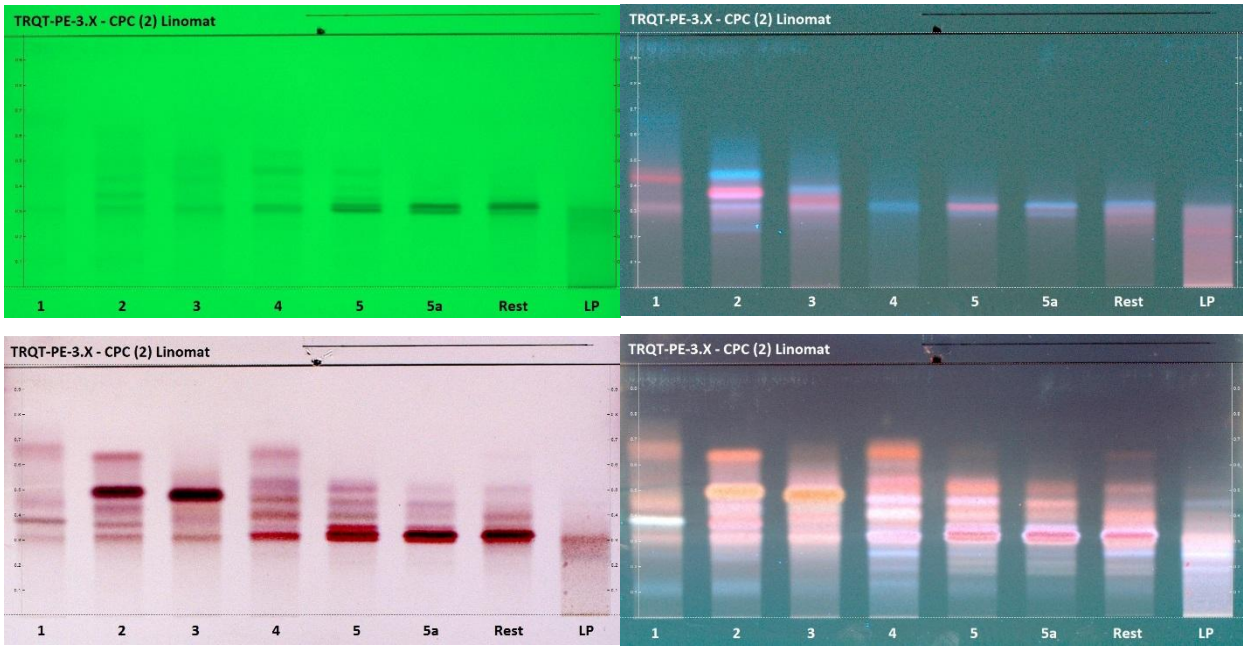

Fig. 41. TLC. Example of sub-fractions of PE-3 after separation on CPC, shown is run 2.
Up left: 254 nm; up right: 366 nm; down left: daylight AAR; down right: 366 nm AAR
Bands from left to right: PE-3.1 – 3.5, 3.5a, 3.Rest and "lower phase wash" sub-fraction
Si-gel; hexane – EtOAc – acetic acid = 70:28:2

Weight and volume of sub-fractions, obtained during the run "1" CPC of PE-3: PE-3.1(1) 461.3 mg, 330 mL; PE-3.2(1) 75.2 mg, 180 mL; PE-3.3(1) 46.4 mg, 135 mL; PE-3.4(1) 156.8 mg, 480 mL; PE-3.5(1) 104.6 mg, 255 mL; PE-3.Rest(1) 151.2 mg, 1433 mL; PE-3.LP(1) 72.54 mg, 788 mL. Fraction PE-3.LP(1) was obtained during the wash of the CPC with the descending mode.

Weight and volume of sub-fractions, obtained during the run "2" CPC of PE-3: PE-3.1(2) 655.3 mg, 293 mL; PE-3.2(2) 92.3 mg, 158 mL; PE-3.3(2) 73.0 mg, 255 mL; PE-3.4(2) 127.7 mg, 360 mL; PE-3.5(2) 61.7 mg, 180 mL; PE-3.5a(2)-110.6 mg, 255 mL; PE-3.Rest(2) 155.4 mg, 1313 mL; PE-3.LP(2) 121.9 mg, 795 mL. Fraction PE-3.LP(2) was obtained during the wash of the CPC with the descending mode.

PE-3.4(1) (156.8 mg, 480 mL eluted) underwent a Flash column chromatography separation on RP-18 (method Flash_5), giving seven fractions in 140 test tubes (7.5 mL/each).

Weight and volume of sub-fractions, obtained during the Flash separation of PE-3.4(1): PE-3.4(1)0 12.6 mg, 98 mL; PE-3.4(1)1 24.9 mg, 53 mL; PE-3.4(1)2 32.2 mg, 135 mL; PE-3.4(1)3 19.8 mg, 120 mL; PE-3.4(1)4 6.9 mg, 75 mL; PE-3.4(1)5 16.5 mg, 420 mL; PE-3.4(1)Rest 6.4 mg, 150 mL. It was decided to purify fractions PE-3.4(1)-2 and PE-3.4(1)-3 on semi-preparative HPLC.

PE-3.4(1)-2 (32.2 mg, 135 mL eluted) was separated using method HPLC_1, but according to ^{1}H-NMR spectra all three obtained sub-fractions were not pure enough to conduct 2D-NMR experiments (**Fig. 42**): PE-3.4(1)2.1 (t_R 10.8 min), PE-3.4(1)2.2 (t_R 11.2 min) and the rest was collected in PE-3.4(1)2.Rest. It was then decided to additionally purify these sub-fractions with another HPLC method.

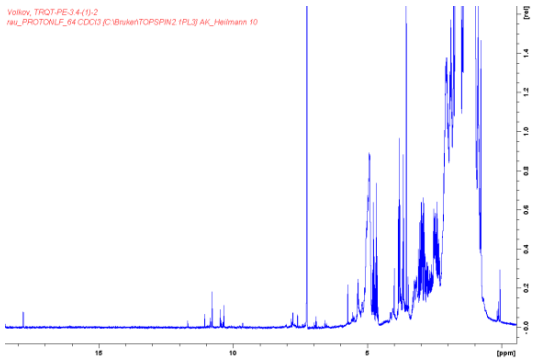

Fig. 42. ^{1}H-NMR of PE-3.4(1)-2 (300.13 MHz, 295 K)

PE-3.4(1)-2.2 (3.2 mg; t_R 11.2 min) was purified on semi-preparative HPLC (method HPLC_2) giving triquetriroxettin (**9**) (t_R 7.7 min; λ_{max} 202, 274 nm; **Fig. 43**).

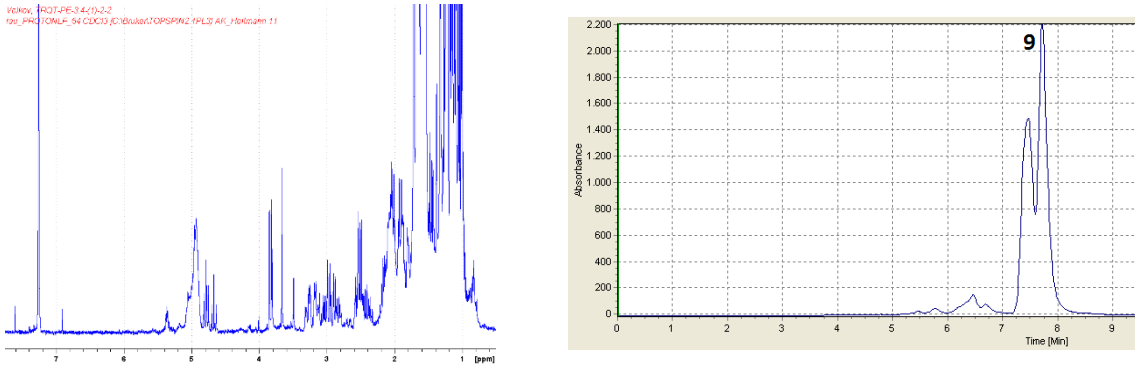

Fig. 43. PE-3.4(1)-2.2 ^{1}H-NMR (300.13 MHz, 295 K) (left)
HPLC chromatogram at 274 nm, HPLC_2 (right)

PE-3.4(1)-2.Rest (19.9 mg) was purified on semi-preparative HPLC (method HPLC_2) giving triquetrireboudin B (**6**) (t_R 9.6 min; λ_{max} 207 nm) and triquetriroxettin (**9**) (t_R 8.4 min; λ_{max} 202, 274 nm) (**Fig. 44**).

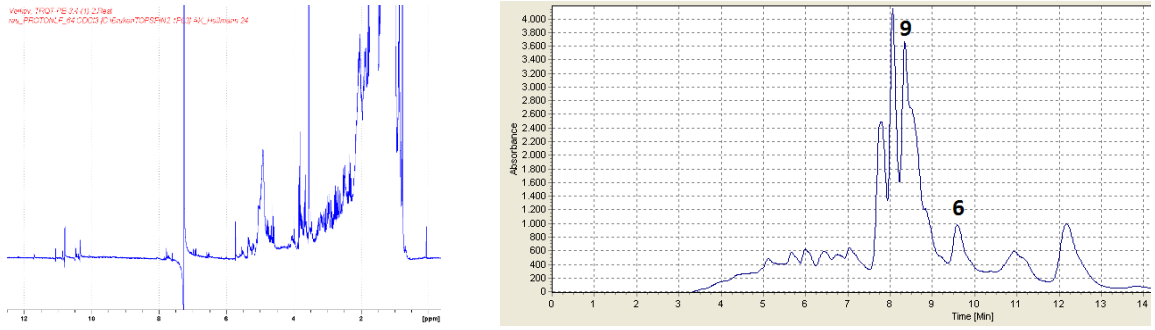

Fig. 44. PE-3.4(1)-2.Rest ^{1}H-NMR (300.13 MHz, 295 K) (left)
HPLC chromatogram at 276 nm, HPLC_2 (right)

PE-3.4(1)-3 (19.8 mg, 120 mL eluted) was purified on semi-preparative HPLC (method HPLC_1) giving triquetribavarin (**10**) (t_R 10.2 min; λ_{max} 203, 279 nm; **Fig. 45**).

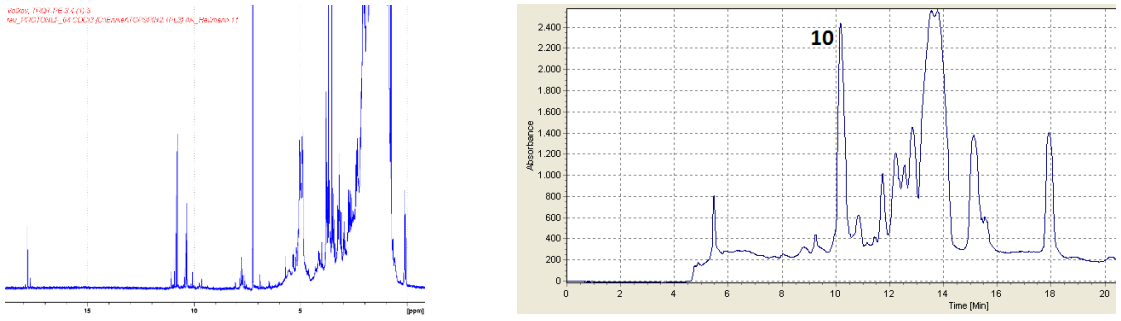

Fig. 45. PE-3.4(1)-3 ^{1}H-NMR (300.13 MHz, 295 K) (left)
HPLC chromatogram at 203 nm, HPLC_1 (right)

PE-3.2(2) (92.3 mg, 158 mL eluted) was purified on semi-preparative HPLC (method HPLC_1) giving linoleic acid (**17**) (t_R 16.3 min; λ_{max} 206 nm; **Fig. 46**).

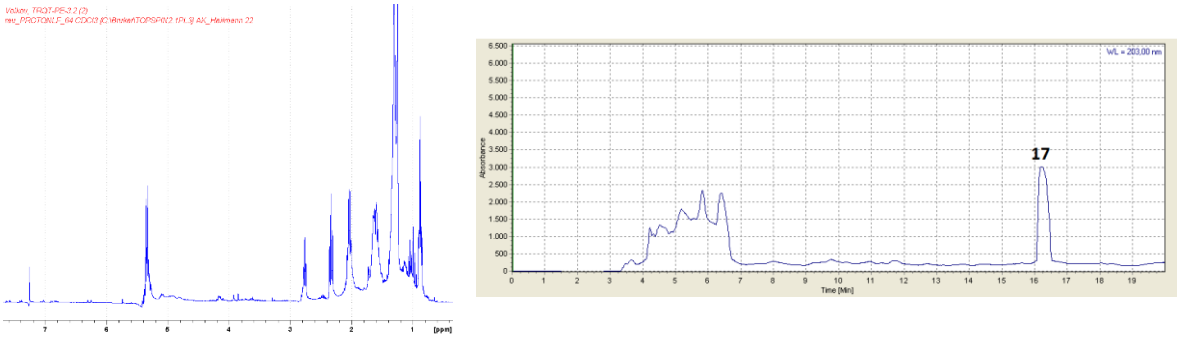

Fig. 46. PE-3.2(2) ^{1}H-NMR (300.13 MHz, 295 K) (left)
HPLC chromatogram at 203 nm, HPLC_1 (right)

PE-3.5(2) (61.7 mg, 180 mL eluted) was purified on semi-preparative HPLC (method HPLC_1) giving triquetrireboudin A (**4**) (t_R 8.2 min; λ_{max} 210, 276 nm; **Fig. 47**).

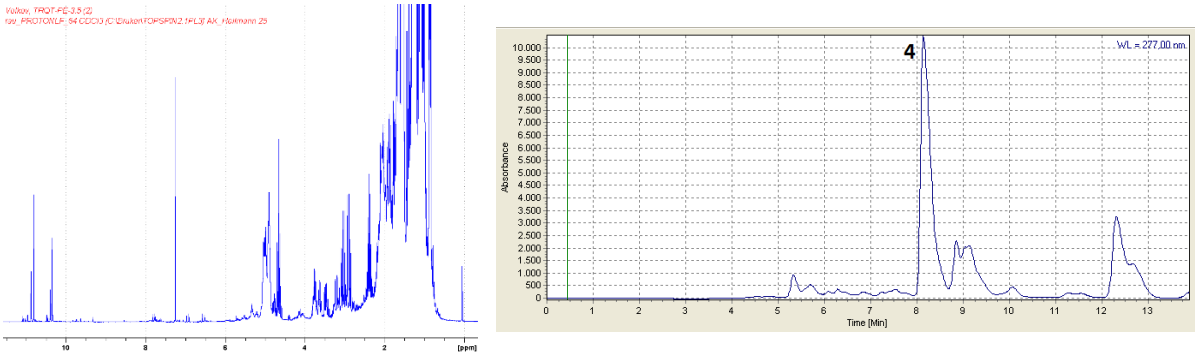

Fig. 47. PE-3.5(2) ^{1}H-NMR (300.13 MHz, 295 K) (left)
HPLC chromatogram at 277 nm, HPLC_1 (right)

PE-3.Rest(2) (155.4 mg, 1313 mL eluted) was purified on semi-preparative HPLC (method HPLC_1) giving triquetrikotelin A (**7**) (t_R 9.6 min; λ_{max} 215, 268 nm), triquetrikotelin B (**8**) (t_R 10.8 min; λ_{max} 203, 268 nm) and triquetrireboudin Aa (**5**) (t_R 15.6 min; λ_{max} 216, 276 nm) (**Fig. 48**).

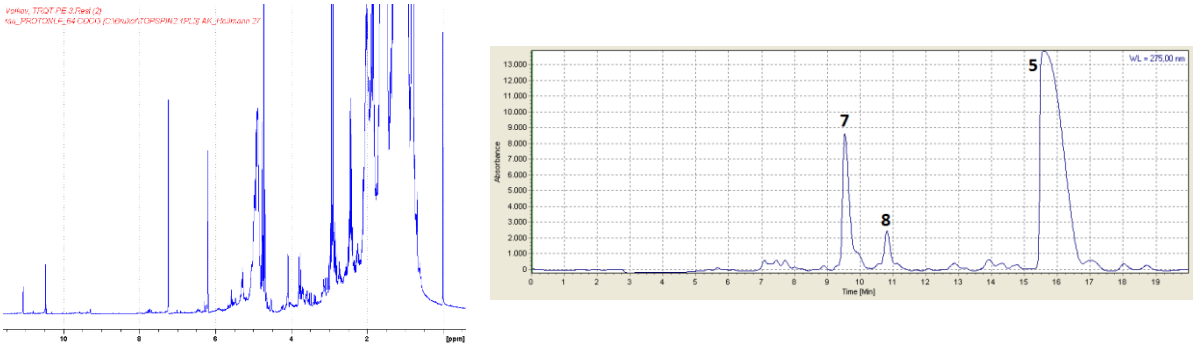

Fig. 48. PE-3.Rest(2) ^{1}H-NMR (300.13 MHz, 295 K) (left)
HPLC chromatogram at 275 nm, HPLC_1 (right)

3.1.2.3 Fractionation of PE-4

Separation scheme of PE-4 can be observed from **Fig. 49**.

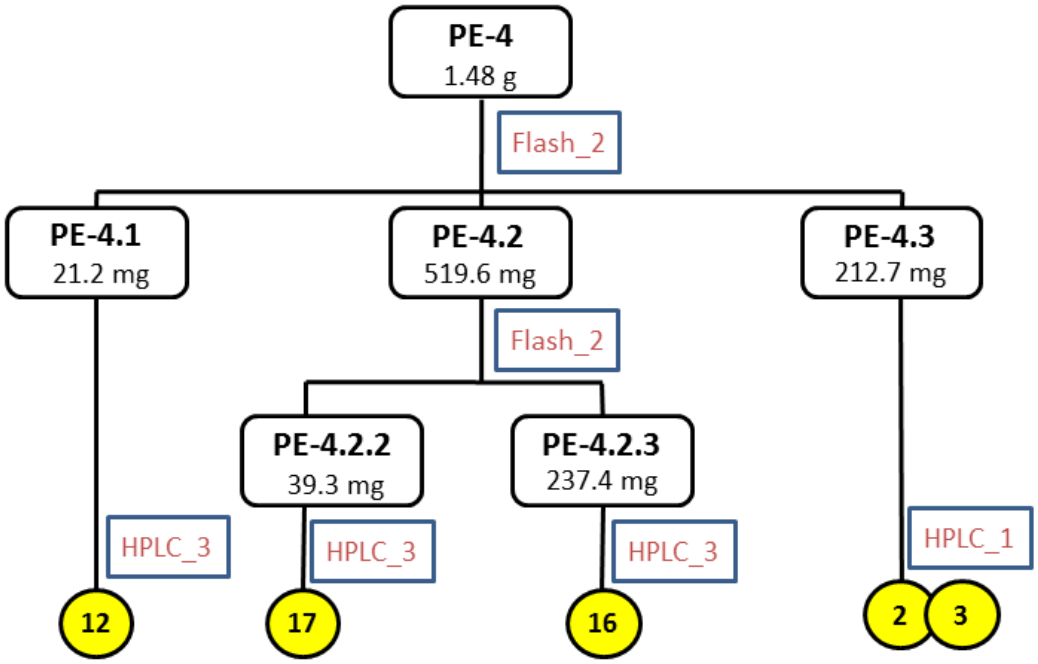

Fig. 49. Separation scheme of PE-4.

PE-4 (1.48 g) was first separated with Si-gel Flash chromatography (method Flash_2). The process resulted in 4 fractions (PE-4.1 21.2 mg, 150 mL; PE-4.2 519.6 mg, 230 mL; PE-4.3 212.7 mg, 220 mL; PE-4.Rest 142.0 mg, 100 mL) in 70 test tubes (10 mL/each).

PE-4.1 (21.2 mg, 150 mL eluted) was purified on semi-preparative HPLC (method HPLC_3) giving triquetriirinon A (**12**) (t_R 10.8 min; λ_{max} 204, 284 nm; **Fig. 50**).

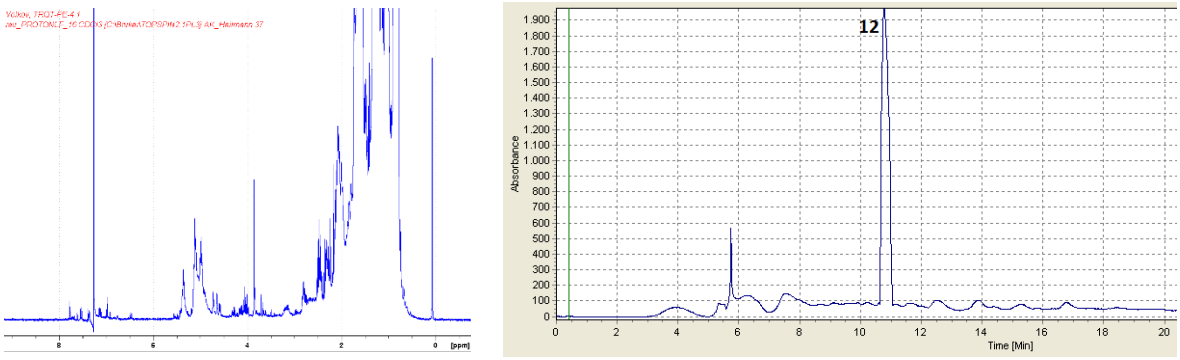

Fig. 50. PE-4.1 ^{1}H-NMR (300.13 MHz, 295 K) (left)
HPLC chromatogram at 204 nm, HPLC_3 (right)

PE-4.2 (519.6 mg, 230 mL eluted) was separated using Flash column chromatography on Si-gel (method Flash_2). Obtained are 5 sub-fractions (PE-4.2.1 152.2 mg, 130 mL; PE-4.2.2 39.3 mg, 110 mL; PE-4.2.3 237.4 mg, 260 mL; PE-4.2.4 8.3 mg, 100 mL; PE-4.2.Rest 44.6 mg, 100 mL) in 70 test-tubes (10 mL/each).

PE-4.2.2 (39.3 mg, 110 mL eluted) was purified on semi-preparative HPLC (method HPLC_3) giving linoleic acid (**17**) (t_R 12.6 min; λ_{max} 203, 211, 273 nm; **Fig. 51**).

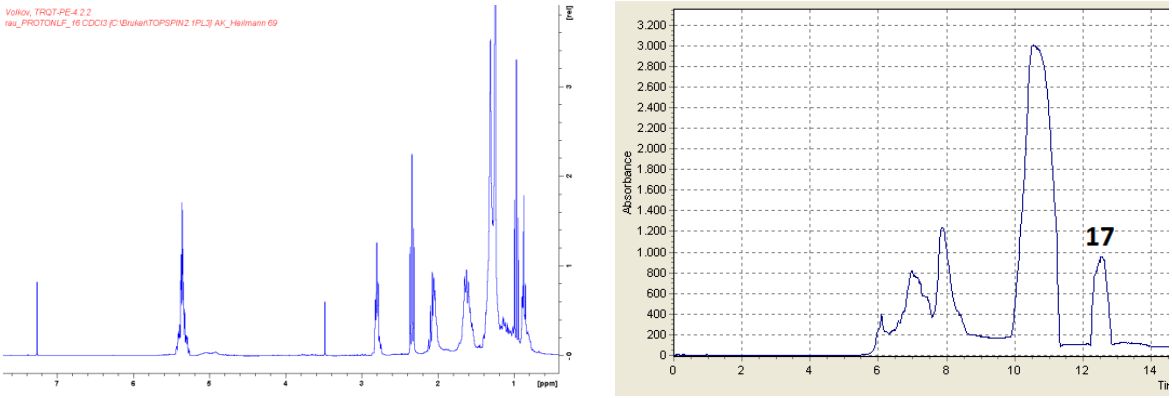

Fig. 51. PE-4.2.2 (300.13 MHz, 295 K) (left)
HPLC chromatogram at 203 nm, HPLC_3 (right)

PE-4.2.3 (237.4 mg, 260 mL eluted) was purified on semi-preparative HPLC (method HPLC_3) giving α-linolenic acid (**16**) (t_R 10.6 min; λ_{max} 204, 273 nm; **Fig. 52**).

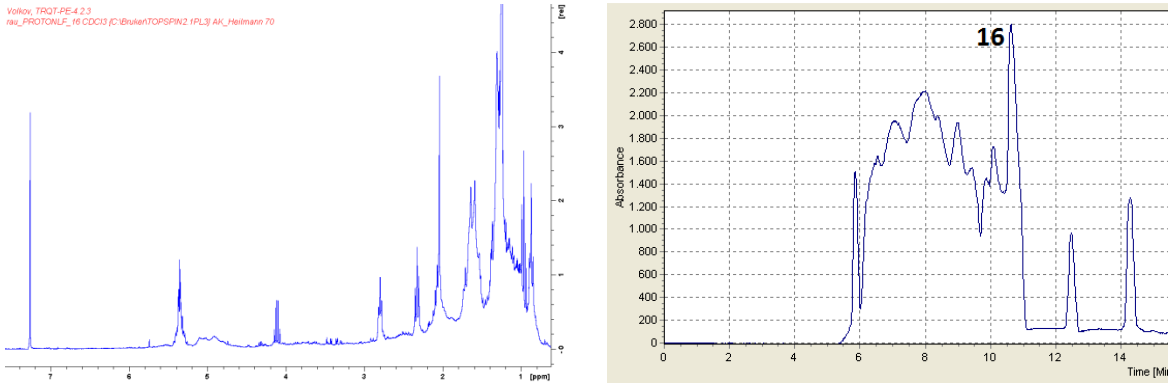

Fig. 52. PE-4.2.3 ^{1}H-NMR (300.13 MHz, 295 K) (left)
HPLC chromatogram at 202 nm, HPLC_3 (right)

PE-4.3 (212.7 mg, 220 mL eluted) was chosen because of the characteristic "*down field shifted*" signal at ca. δ_H 18.30 ppm (**Fig. 53**), which could have denoted the presence of an acylphloroglucinol. The fraction was purified on semi-preparative HPLC (method HPLC_1, time = 50 min) giving triquetrijakobin A (**2**) (t_R 29.8 min; λ_{max} 203, 244, 322 nm) and triquetrijakobin B (**3**) (t_R 30.7 min; λ_{max} 203, 245, 322 nm) (**Fig. 53**).

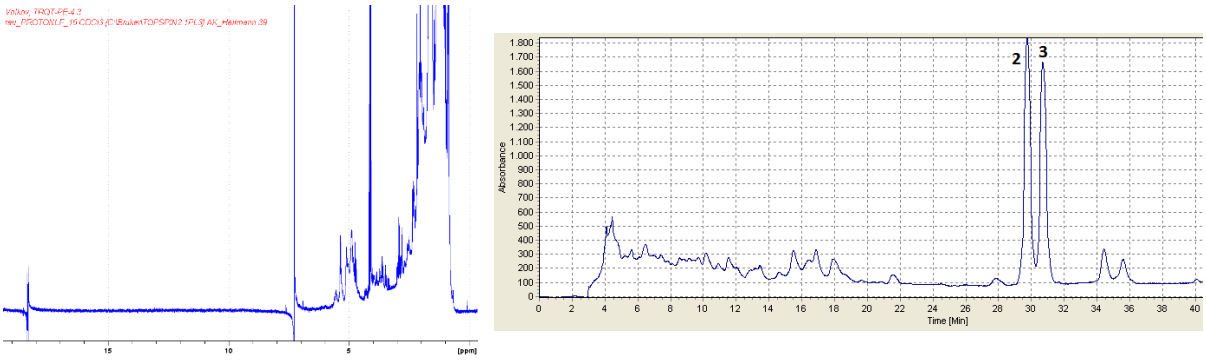

Fig. 53. PE-4.3 ^{1}H-NMR (300.13 MHz, 295 K) (left)
HPLC chromatogram at 203 nm, HPLC_1 (right)

3.1.2.4 Fractionation of PE-5

Separation scheme of PE-5 can be observed from **Fig. 54**.

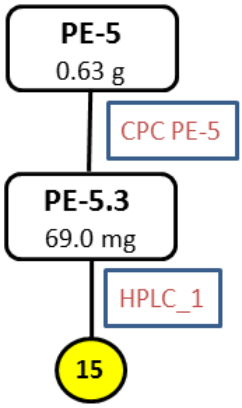

Fig. 54. Separation scheme of PE-5.

Fraction **PE-5** was selected for further separation according to characteristic blue bands at R_f ca. 0.27 (366 nm) on a Si-gel TLC plate (**Fig. 55**), as well as because of the clear signals in "*down field*" on its ^{1}H-NMR spectrum, meaning the possible presence of acylphloroglucinols (**Fig. 56**).

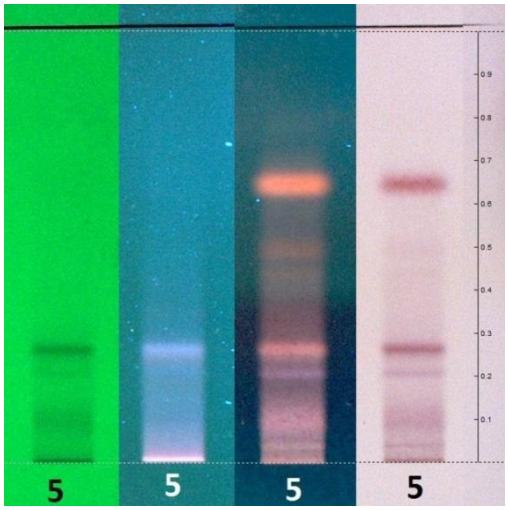

Fig. 55. TLC on Si-gel of PE-5.
From left to right: 254 nm, 366 nm, 366 nm AAR, daylight AAR.
hexane – EtOAc – acetic acid = 70:28:2

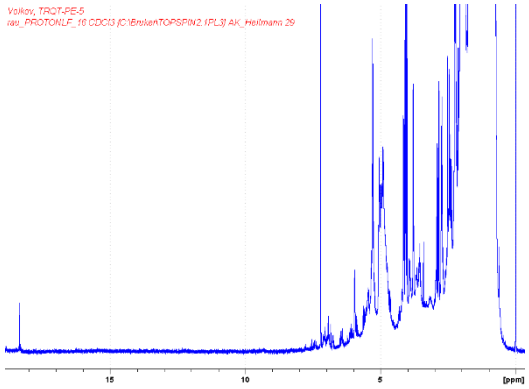

Fig. 56. ^{1}H-NMR of PE-5 (300.13 MHz, 295 K)

PE-5 (0.63 g) was separated with CPC. Several systems previously used in various *Hypericum* species were tested, just as for the fraction PE-3. The most suitable solvent mixture

appeared to be hexane : EtOH : EtOAc : H_2O = 83 : 67 : 33 : 17 (Decosterd et al., 1989). With the conditions described in **Tab. 8**, § 2.1.5.3, nine sub-fractions were obtained (**Fig. 57**).

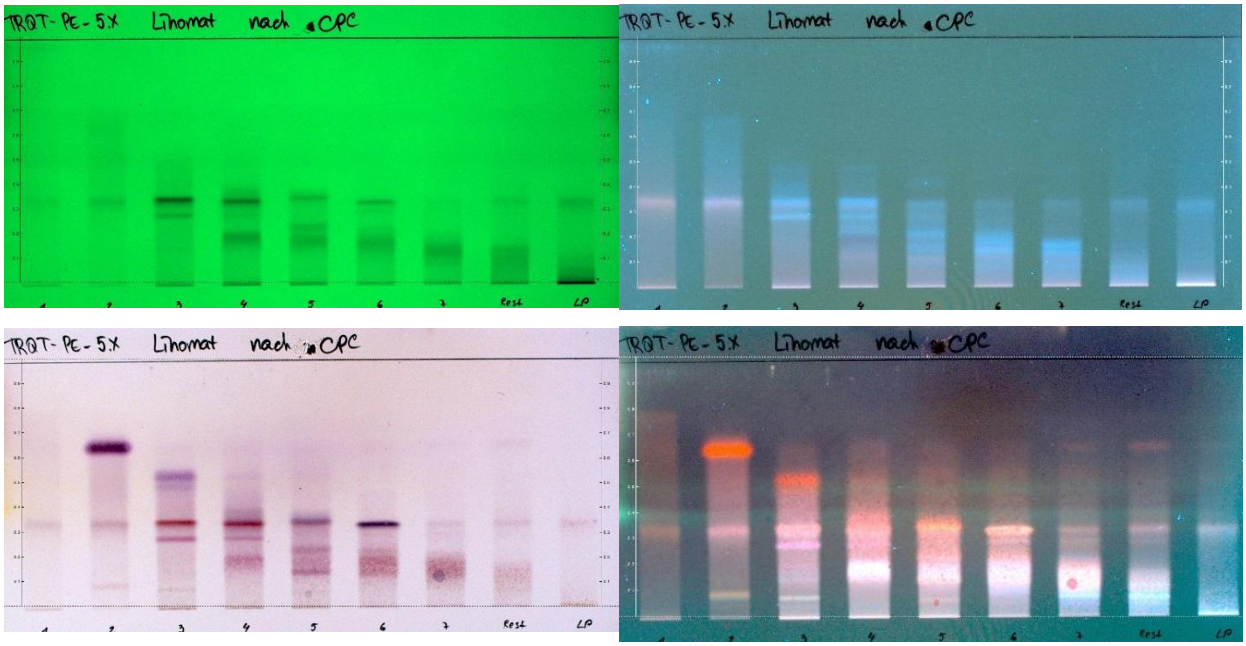

Fig. 57. TLC, PE-5 sub-fractions after CPC separation.
Left up: 254 nm; right up: 366 nm; left down: daylight AAR; right down: 366 nm AAR
Bands from left to right: PE-5.1 – 5.7, 5.Rest and "lower phase wash" sub-fraction.
Si-gel; hexane – EtOAc – acetic acid = 70:28:2

After CPC run of PE-5 eight fractions (PE-5.1 3.8 mg, 75 mL; PE-5.2 210.9 mg, 83 mL; PE-5.3 69.0 mg, 68 mL; PE-5.4 84.9 mg, 195 mL; PE-5.5 32.3 mg, 135 mL; PE-5.6 48.4 mg, 323 mL; PE-5.7 30.5 mg, 405 mL; PE-5.Rest 27.0 mg, 975 mL) in 300 test-tubes (7.5 mL/each) were obtained.

Each obtained sub-fraction underwent ^{1}H-NMR measurement for fractions control. From which, sub-fraction PE-5.3 looked promising in quest of acylphloroglucinols because of characteristic down-field signal and signals for probable isoprene-chain proton at ca. δ_H 5.00 ppm (**Fig. 58**).

PE-5.3 (69.0 mg, 68 mL eluted) underwent the last purification step with semi-preparative HPLC (method HPLC_1). Triquetriirinon D (**15**) was isolated (t_R 15.9 min; λ_{max} 202, 274 nm; **Fig. 58**).

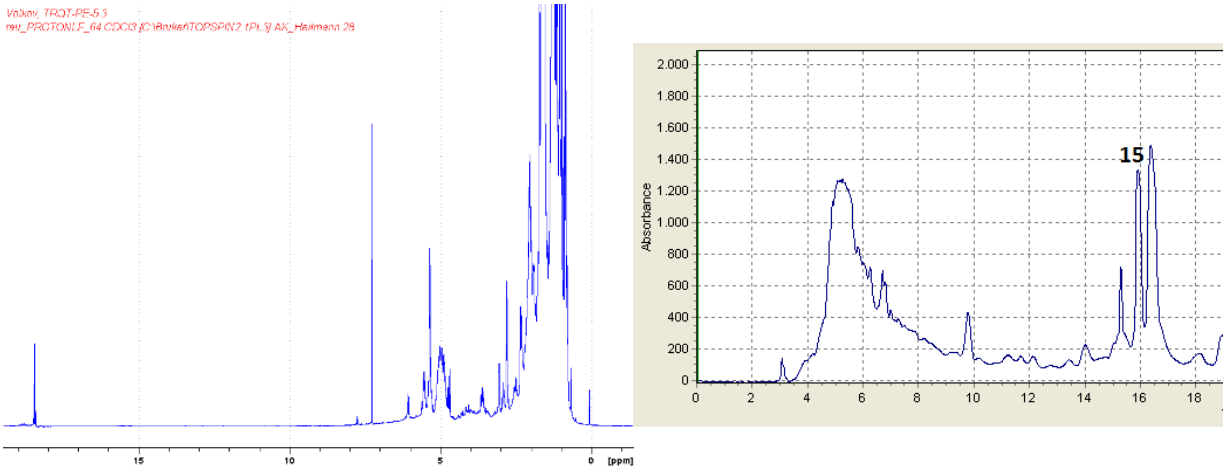

Fig. 58. PE-5.3 ^{1}H-NMR (300.13 MHz, 295 K) (left)
HPLC chromatogram at 202 nm, HPLC_1 (right)

3.1.2.5 Fractionating of methanolic extract

The study of methanolic extract (**ME**) obtained from *H. triquetrifolium* was conducted in frames of a PhD-student-guided internship practice of Mr. Marcell Kaljanac on Pharmaceutical Biology department (University of Regensburg) (internship mentor: Ilya B. Volkov). The aim of this part of work was to elucidate some flavonoids and thus characterise the herb not only with its nonpolar constituents.

The fractionation of ME occurred with the same NMR-guided strategy. In this case, important landmarks on ^{1}H-NMR spectra were:

- Signals at ca. δ_H 7.00 ppm, usual for protons in aromatic rings
- Signals at δ_H 3.00 – 4.00 ppm, usual for sugars (in case of glycosides)

Obtained as described in § 2.1.4 **ME** extract (189.47 g) was used for partial research. 6.6 g of crude ME extract was separated on Si-gel Flash column chromatography, giving 5 fractions (**Fig. 59**). **ME-3** (897.5 mg) was separated with RP-18 Flash chromatography, resulting in 11 sub-fractions. **ME-3.3** (265.7 mg) was finally purified on preparative HPLC (RP-18) (method HPLC_6), yielding in **18** and **19+20**.

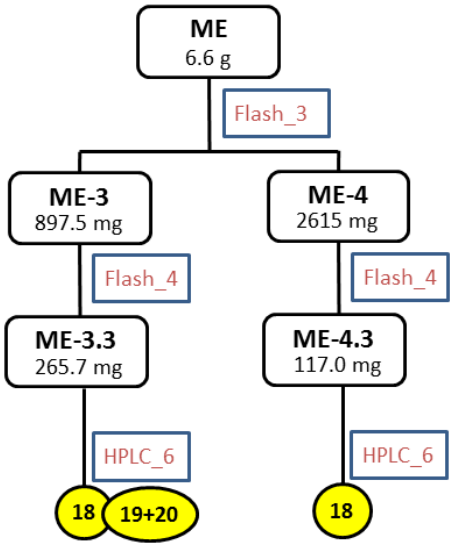

Fig. 59. Separation scheme of crude methanolic extract (ME).

ME-4 (2615.0 mg) was separated on RP-18 Flash chromatography, giving 7 sub-fractions. **ME-4.3** (117.0 mg) was finally purified on preparative RP-18 HPLC (method HPLC_6), resulting in **18**.

3.1.3 Structure elucidation and characterisation of isolated compounds

Structure elucidation was conducted using 1D- and 2D-NMR experiments (^{1}H, ^{13}C, HSQC, HMBC, COSY and NOESY). MS experiments confirmed the structure. In order to characterise the substances, specific rotation, UV- and CD-spectra were also measured, recorded and calculated.

3.1.3.1 General principles in structure elucidation

There is of course a vast variety of different approaches on how to determine a molecule structure according to its 2D-NMR spectra. The following approximate algorithm was used during the course of the present work (see also § 2.1.6.1):

The List. The list of all ^{13}C signals (i.e. the list of all the carbons belonging to the compound) was printed out and each carbon was correlated to the respective hydrogen according to the HSQC experiment, thus making direct bonds clear, as well as marking whether the carbon is quaternary or refers to a $–CH_3$, $–CH_2–$ or $=CH–$ group. Multiplicity of hydrogens was also noted using a ^{1}H-NMR signal list.

Isoprene chain. Typical triplets in ^{1}H-NMR spectrum at ca. δ_H 5.00 ppm were chosen to indicate a prenyl side chain. They should represent a proton of an isoprene based side chain (=C**H**– group) as the value is shifted towards the "*down field*". HMBC and COSY helped in determination of the atoms consequence in the chain. $–CH_2–$ groups' protons show HMBC correlations with a carbon at ca. δ_C 38-42 ppm, which is usually referred to the main core of the molecule (**Fig. 60**).

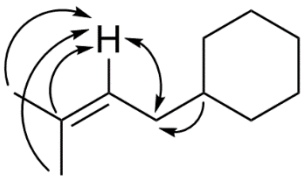

Fig. 60. Isoprene rest on a six membered ring (2D NMR correlations).

Starter acid. Keto group – quaternary carbon, connected to an oxygen with a double bond, usually resonates in acylphloroglucinols at ca. δ_C 197-218 ppm in a ^{13}C spectrum (**Fig. 61, a**). In HMBC it is clearly "seen" by a proton of the methine carbon, which multiplicity is either usually a septet (isobutyryl) (**Fig. 62**) or less often a pseudo-sextet (2-methylbutyryl). In case of isobutyryl both $–CH_3$ groups are characterised by two doublets at ca. δ_H 1.10 ppm each, while in 2-methylbutyryl starter acid there's an additional $–CH_2–$ group and thus the terminal $–CH_3$ group resonated as a triplet at ca. δ_H 0.85 ppm (**Fig. 61, b**).

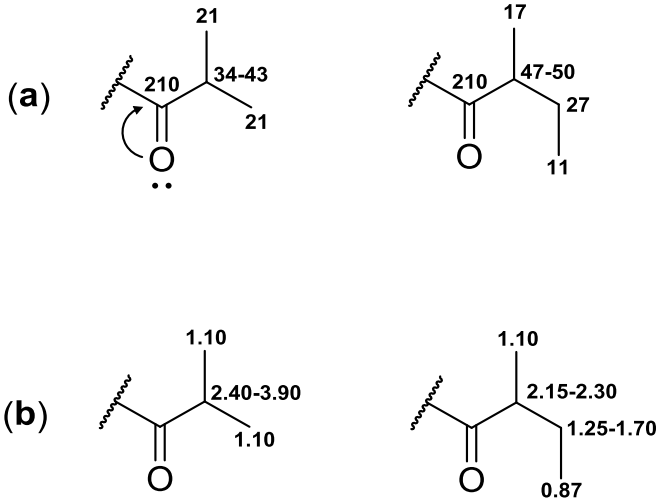

Fig. 61. Starter acid's approximate δ_C (**a**) and δ_H (**b**) values, ppm. Differences can be noted between isobutyryl (left) and 2-methylbutyryl (right).

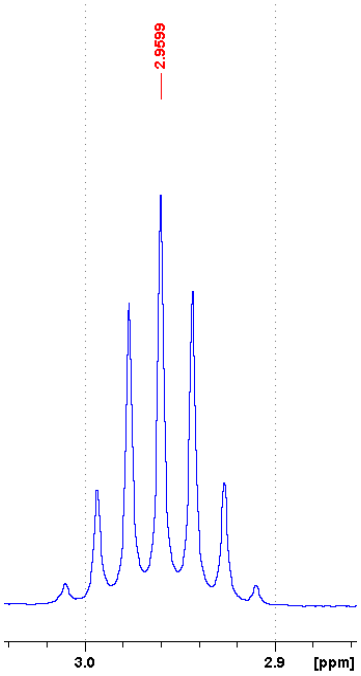

Fig. 62. Example of a characteristic septet at δ_H 2.96, indicating an aliphatic methine proton in an isobutyryl side chain. (300.13 MHz, 295 K).

Intramolecular hydrogen bonds. Many acylphloroglucinols (not all though, § 3.1.1) build characteristic intramolecular hydrogen bonds, which can be clearly seen seen in a ^{1}H-NMR spectra as "*down field shifted*" signals at ca. δ_H 14-19 ppm. This happens between –OH group of the main phloroglucinol skeleton and oxygen from the starter acid's keto group (**Fig. 63**).

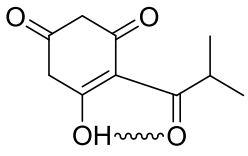

Fig. 63. Intramolecular hydrogen bond

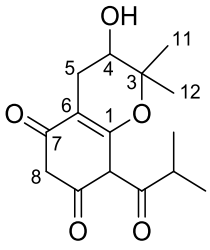

Fig. 64. Undetectable hydroxyl group (in position 4)

Undetectable hydroxyl groups. During the elucidation process some uncertainties in pyran ring occurred. In HSQC C-4 (**Fig. 64**) was identified as a methine carbon. Both the carbon and the proton directly connected to it possess unusually high chemical shift values: ca. δ_C 94

ppm, δ_H 4.65 ppm. This let suggesting the presence of an ether group directly coupled to the carbon in position 4. However, HMBC showed only correlations between the atoms in position 4 and those in positions 1, 3, 5, 6, 11 and 12. No further correlations (i.e. those, lying beyond the proposed oxygen out of the pyran ring) in an HMBC experiment were noted in order to prolong the chain further. This in turn let hypothesizing the presence of a hydroxyl group, connected to C-4. High resolution MS experiments (HRESIMS) when the molecular formula was calculated, later confirmed the presence of an –OH group in this position, which was indeed not visible in any 1D- or 2D-NMR experiment most probably due to deuterium exchange with the solvent.

Molecule's main core was elucidated using usual correlations in HMBC and COSY experiments. Relative stereochemistry was defined via NOESY.

3.1.3.2 Prenylated acylphloroglucinols

Compound 1 (Triquetriborin)

Tab. 11. ^{1}H and ^{13}C data in $CDCl_3$ (^{1}H-NMR 600 MHz, ^{13}C-NMR 150 MHz, 298 K)

C/H	δ_C	δ_H mult (*J* in Hz)
1	56.1	
2	199.6	
3	144.8	
4	194.3	
5	69.9	
6	50.7	
7	39.4	1.76 (1H, m)
8	40.4	1.95 (1H, m)
		2.24 (1H, d, 14.5)
9	208.5	
10	17.5	1.32 (3H, s)
11	18.7	1.24 (3H, s)
1‘	207.4	
2‘	35.0	3.85 (1H, sept)
3‘	18.5	1.20 (3H, d, 6.7)
4‘	18.9	1.06 (3H, d, 6.8)
1‘‘	25.7	1.77 (1H, m)
		2.66 (1H, m)
2‘‘	119.7	4.76 (1H, t)
3‘‘	134.3	
4‘‘	25.9	1.55 (3H, m)
5‘‘	18.1	1.66 (3H, s)
1‘‘‘	29.2	1.93 (1H, m)
		2.05 (1H, m)
2‘‘‘	124.2	4.84 (1H, t)
3‘‘‘	133.0	
4‘‘‘	25.8	1.66 (3H, s)
5‘‘‘	17.6	1.40 (3H, s)
1‘‘‘‘	35.8	1.38 (1H, m)
		1.15 (1H, m)
2‘‘‘‘	22.5	1.81 (1H, m)
		1.89 (1H, m)
3‘‘‘‘	123.8	5.02 (1H, t, 7.0)
4‘‘‘‘	132.0	
5‘‘‘‘	17.7	1.57 (3H, m)
6‘‘‘‘	25.6	1.66 (3H, s)
4-OH		18.57 (1H, s)

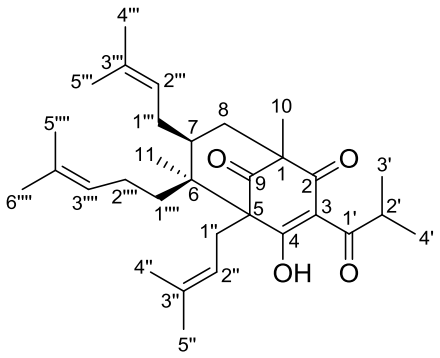

^{13}C-NMR spectrum showed 31 carbons related to the measured probe. According to an HSQC spectrum, 11 carbons are referred as quaternary, 3 as =CH–, 2 as aliphatic methines, 5 as –CH_2– and 10 as –CH_3 groups. A "*down field shifted*" signal at δ_H 18.57 ppm refers to the characteristic hydrogen bond between the hydroxyl group of the phloroglucinol main core and the keto group of the starter acid. The latter was unequivocally defined as activated isobutyric acid due to a very clear septet at δ_H 3.85 ppm (C-2') and two doublets at δ_H 1.06 ppm and 1.20 ppm, representing two –CH_3 groups (C-3', C-4').

Unusual high values of quaternary carbons in position 3 and 4 (δ_C 144.8 ppm and 194.3 ppm respectively) let suggesting the presence of an enol. Presence of a quaternary C-3 let suggesting the cyclisation appears between C-1→C-5 and not C-5→C-3.

In the HMBC spectrum the protons of the –CH_3 group (δ_H 1.32 ppm) are clearly correlated with both keto groups in the main phloroglucinol core (**Fig. 65**). This proved that the methyl group (C-10) is connected to C-1.

Further HMBC correlations of the –CH_3 group (δ_H 1.24 ppm, C-11) with quaternary carbon C-5 (δ_C 69.9 ppm) (**Fig. 66**) and lacking correlations with protons at C- 8, let to the suggestion that the cyclisation of an isoprene rest was realized from C-1 to C-5 and not *vice versa*.

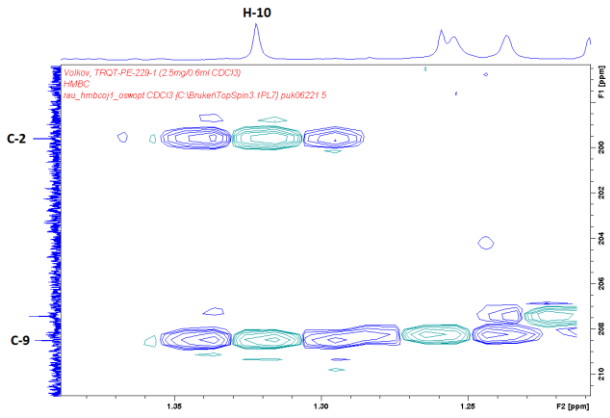

Fig. 65. Part of HMBC spectrum of **1**: correlation between H-10 and C-2 and C-9.

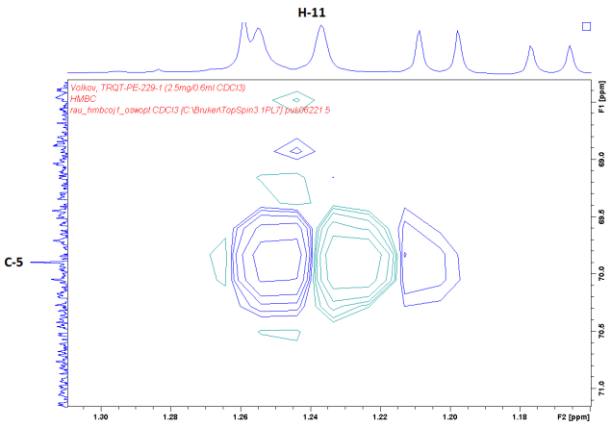

Fig. 66. Part of HMBC spectrum of **1**: correlation between H-11 and C-5.

Structure elucidation of substitution pattern regarding the isoprene chains started with the proton at ca. δ_H 5.00 ppm and were realized with the help of HMBC and COSY experiments.

Cross peaks between atoms in positions 1'', 1''' and 1'''' helped connecting the aliphatic chains to the phloroglucinol core in positions 5, 7 and 6 respectively.

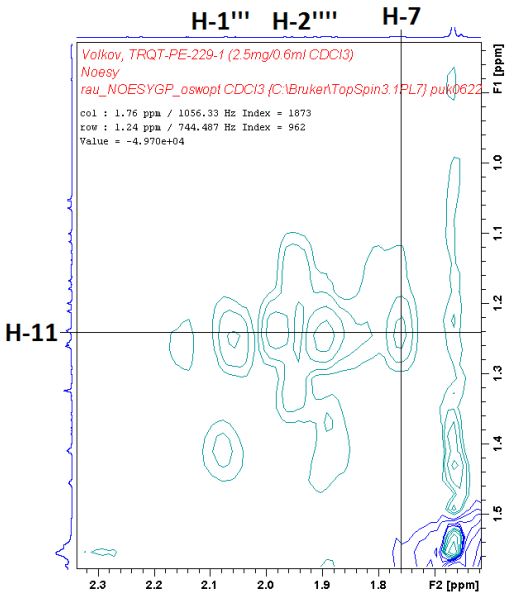

Fig. 67. Part of NOESY spectrum of **1**: correlation between H-11 and H-7.

NOESY experiments helped in defying relative stereochemistry (example, **Fig. 67**). Molecular formula was established as $C_{31}H_{47}O_4$ by HRESIMS (*m/z* 483.3469 $[M+H]^+$). The hitherto not known compound was identified as (6S, 7S)-4-hydroxy-1,6-dimethyl-3-isobutyryl-5,7-bis(3-methylbut-2-en-1-yl)-6-(4-methylpent-3-en-1-yl)-bicyclo-[3.3.1]non-3-ene-2,9-dione and was given a trivial name **Triquetriborin**. Experimental CD spectrum for 1 is presented on **Fig. 68**.

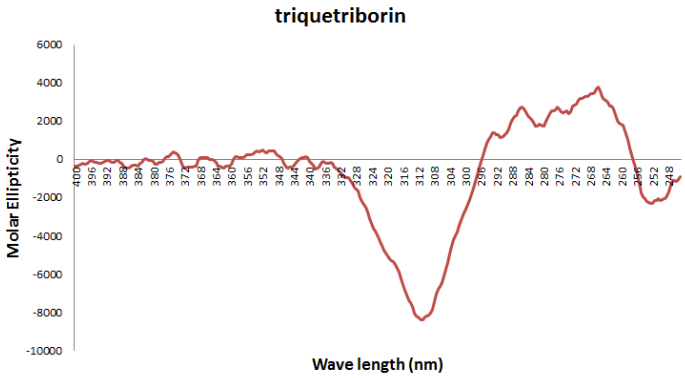

Fig. 68. Experimental CD spectrum of **1.**

Compounds 2 and 3 (Triquetrijakobin A and B)

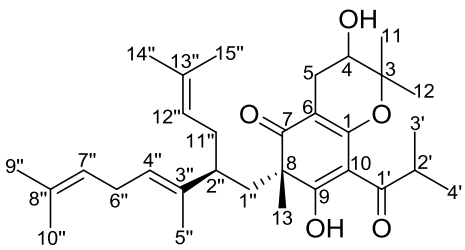

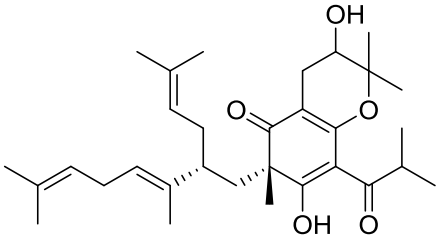

Tab. 12. ^{1}H and ^{13}C data in $CDCl_3$ (^{1}H-NMR 600 MHz, ^{13}C-NMR 150 MHz, 298 K)

	(**2**) Triquetrijakobin A		(**3**) Triquetrijakobin B	
C/H	δ_C	δ_H mult (*J* in Hz)	δ_C	δ_H mult (*J* in Hz)
1	168.8		168.8	
3	71.8		71.5	
4	92.4	4.71 (1H, dd, 8.5, 10.3)	92.4	4.74 (1H, t, 9.5)
5	26.7	2.86 (1H, m)	26.6	2.90 (2H, dd, 4.5)
		2.96 (1H, m)		
6	108.0		108.0	
7	205.4		205.6	
8	56.3		56.4	
9	192.4		192.4	
10	100.3		100.3	
11	25.6	1.33 (3H, s)	25.9	1.33 (3H, s)
12	24.5	1.25 (3H, m)	24.4	1.25 (3H, s)
13	28.5	1.29 (3H, s)	28.8	1.30 (3H, s)
1’	197.9		197.7	
2’	34.5	3.62 (1H, sept)	34.5	3.62 (1H, sept)
3’	20.6	1.23 (3H, d, 6.9)	19.6	1.23 (3H, d, 6.8)
4’	18.8	1.20 (3H, d, 6.7)	19.8	1.20 (3H, d, 6.8)
1’’	41.5	2.06 (1H, dd, 3.3, 13.6)	41.2	2.08 (1H, m)
		2.19 (1H, m)		2.18 (1H, m)
2’’	46.6	1.97 (1H, m)	46.7	1.91 (1H, m)
3’’	136.4		137.0	
4’’	126.3	4.85 (1H, t, 6.3)	125.8	4.82 (1H, t)
5’’	11.6	1.30 (3H, s)	11.6	1.32 (3H, s)
6’’	26.7	2.18 (1H, m)	26.7	2.14 (1H, m)
		2.53 (1H, m)		2.55 (1H, m)
7’’	122.9	4.91 (1H, m)	122.9	4.90 (1H, m)
8’’	131.6		132.0	
9’’	17.7	1.54 (3H, s)	17.8	1.53 (3H, s)
10’’	25.60	1.66 (3H, s)	25.6	1.64 (3H, s)
11’’	32.3	1.91 (2H, m)	32.4	1.90 (2H, m)
12’’	122.8	4.90 (1H, m)	122.8	4.88 (1H, m)
13’’	131.5		131.5	
14’’	17.9	1.60 (3H, s)	17.9	1.54 (3H, s)
15’’	25.7	1.63 (3H, s)	25.7	1.62 (3H, s)
9-OH		18.33 (s)		18.30 (s)

^{13}C-NMR spectrum of **2** comprises 31 atoms, of which 11 carbons are quaternary, 6 are =CH–, 4 are –CH_2– and 10 –CH_3 groups. A "*down field shifted*" signal at δ_H 18.33 ppm refers to the –OH group linked to the carbonyl group of the starter acid via hydrogen bond. Only one further keto group resonated at δ_C 205.4, indicating that the third oxygen of the main phloroglucinol core is either involved into a cyclization or an ether group.

HMBC correlations proved the "3-ortho-pyrano" cyclisation type of this compound (**Fig. 16**, § 1.1.4.2). Three isoprene rests, unusually connected to each other form an aliphatic side chain, connected to the main core in position 8. Starter acid was confirmed as activated isobutyric acid with a septet at δ_H 3.62 ppm for a methine proton and two doublets at δ_H 1.20 ppm and δ_H 1.23 ppm for both –CH_3 groups.

Aliphatic side chain was confirmed according to HMBC and COSY experiments. Important to note is, that this substituent consists of two chains, a long (1'' – 10'') and a short one (11'' – 15''). Although the long chain consists of 10 carbons, it is due to the displaced position of one double bond not a geranyl chain. Diagnostic correlations occur within the protons H-4'', H-6'' and H-7'' (**Fig. 69**) thus confirming H-6'' lies between two double bonds; in case of a geranyl side chain, this double bond would have lied between H-2''and H-3''.

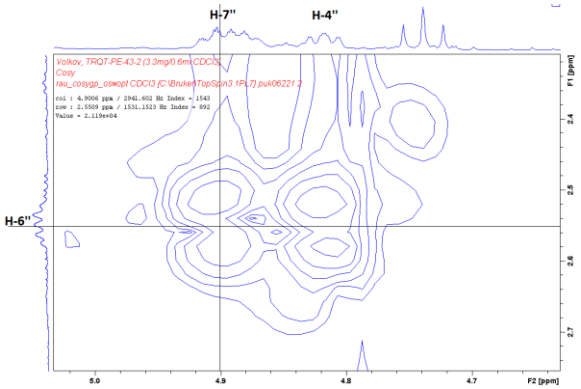

Fig. 69. Clip of COSY experiment of **3**: correlation between H-4'', H-6'' and H-7''.

Carbon at position 4 has an unusually strong down field shift to δ_C 92.4 ppm, whereas the corresponding protons resonated at δ_H 4.71 ppm. Thus, oxygen was assumed to be connected to the carbon in position 4. Nevertheless no HMBC correlations showed any other atoms, which may lie beyond the hetero atom. It was suggested, that only an –OH group is

linked to the carbon in this position. This was later confirmed with a MS experiment, while evaluating the chemical formula of the substance.

In elucidating the structure of compound **3**, almost all the chemical shifts were the same, as for **2**. Molecular mass of both compounds was confirmed the same. However, since both **2** and **3** were isolated from one sub-fraction (PE-4.3) as two separate independent compounds (§ 3.1.2.3), they should possess different chemical structure. NOESY experiment showed that the difference is due to varying configuration at C-2''. The differences in stereochemistry can be noted if comparing both spectra for **2** and **3** (**Fig. 70** and **71**).

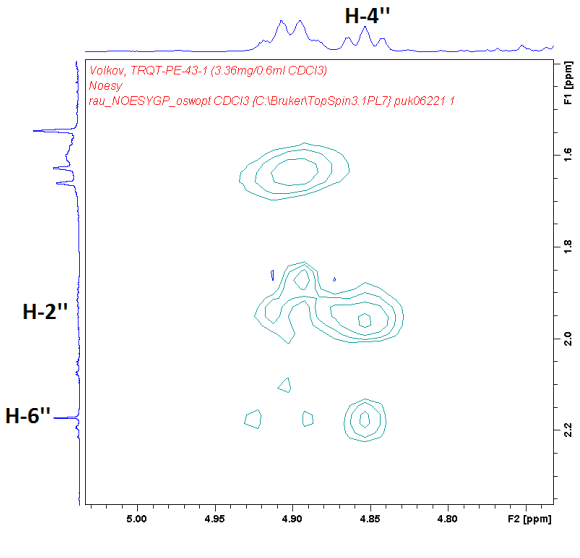

Fig. 70. Part of NOESY spectrum of **2**: correlation between H-2'' and H-4''.

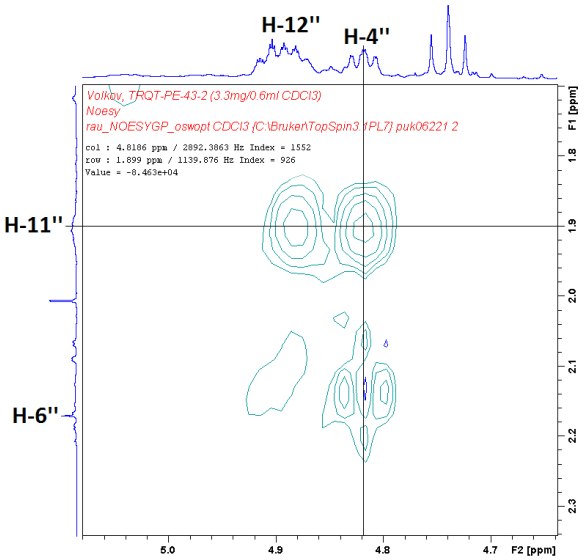

Fig. 71. Part of NOESY spectrum of **3**: correlation between H-4'' and H-11''.

Experimental CD spectra for **2** and **3** are presented in **Fig. 72** and **Fig. 73** respectively.

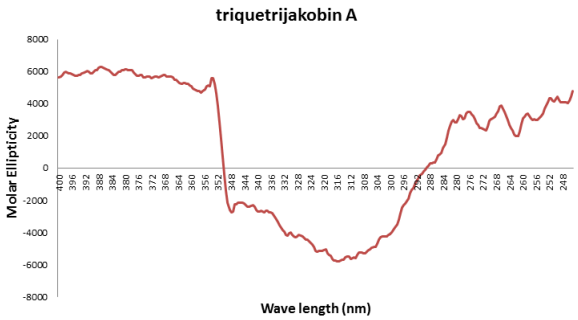

Fig. 72. Experimental CD spectrum of **2.**

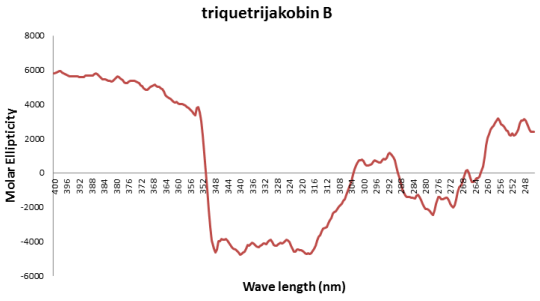

Fig. 73. Experimental CD spectrum of **3.**

Molecular formula for substance **2** was established as $C_{31}H_{47}O_5$ by HRESIMS (*m/z* 499.3418 $[M+H]^+$). The compound was identified as the hitherto unknown (8S, 2''S)-1-[3,3,8-trimethyl-4,5,5-trihydro-4,9-dihydroxy-8-(3,7-dimethyl-2-(3-methylbut-2-en-1-yl)-octyl-3,6-diene)-chroman-5-one-8-yl]-2-methylpropan-1-one and was given the trivial name **Triquetrijakobin A**. Molecular formula for substance **3** was established as $C_{31}H_{47}O_5$ by HRESIMS (*m/z* 499.3418 $[M+H]^+$). The compound was identified as the hitherto unknown (8S, 2''R)-1-[3,3,8-trimethyl-4,5,5-trihydro-4,9-dihydroxy-8-(3,7-dimethyl-2-(3-methylbut-2-en-1-yl)-octyl-3,6-diene)-chroman-5-one-8-yl]-2-methylpropan-1-one and was given the trivial name **Triquetrijakobin B**.

Compounds 4, 5 and 6
(Triquetrireboudin A, B and C)

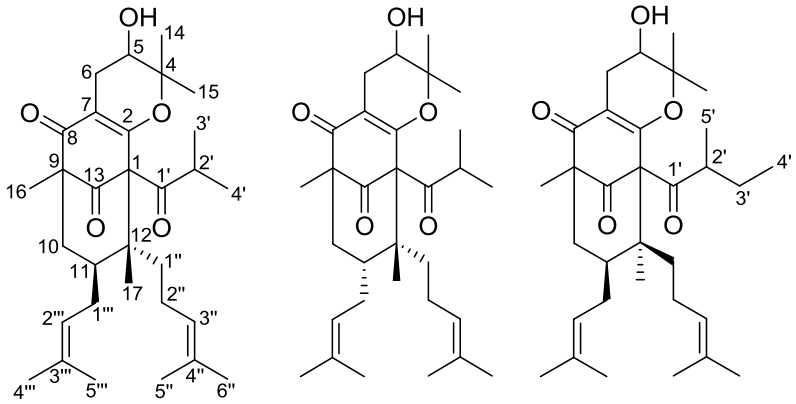

Tab. 13. ^{1}H and ^{13}C data in $CDCl_3$
(^{1}H-NMR 600 MHz, ^{13}C-NMR 150 MHz, 298 K)

	(**4**) Triquetrireboudin A		(**5**) Triquetrireboudin B		(**6**) Triquetrireboudin C	
C/H	δ_C	δ_H mult (*J* in Hz)	δ_C	δ_H mult (*J* in Hz)	δ_C	δ_H mult (*J* in Hz)
1	74.6		74.0		74.6	
2	171.8		171.7		171.9	
4	71.2		71.1		71.2	
5	93.3	4.66 (1H, t, 10.1)	93.9	4.78 (1H, t, 10.7)	93.5	4.62 (1H, t, 10.1)
6	26.7	2.90 (1H, dd, 10.3, 14.9)	26.8	2.97 (2H, dd, 6.0, 10.6)	26.7	2.90 (1H, dd, 10.2, 14.9)
		3.06, (1H, dd, 9.9, 14.9)				3.06 (1H, dd, 10.0, 14.9)
7	119.8		120.3		119.9	
8	191.0		190.9		191.0	
9	59.8		60.1		59.9	
10	41.6	1.29 (1H, m)	41.4	1.30 (1H, m)	41.6	1.29 (1H, m)
		1.93 (1H, dd, 4.5, 13.9)		1.93 (1H, dd, 4.0, 13.6)		1.93 (1H, dd, 4.5, 13.9)
11	44.4	1.60 (1H, m)	42.3	1.71 (1H, m)	44.4	1.60 (1H, m)
12	46.7		47.2		46.8	
13	206.5		206.3		206.5	
14	24.8	1.24 (3H, s)	25.3	1.25 (3H, s)	24.9	1.23 (3H, s)
15	26.3	1.33 (3H, s)	26.6	1.37 (3H, s)	26.6	1.33 (3H, s)
16	15.9	1.22 (3H, s)	15.9	1.22 (3H, s)	15.9	1.23 (3H, s)
17	12.7	1.09 (3H, s)	14.5	1.13 (3H, s)	12.8	1.11 (3H, s)
1‘	209.0		208.8		208.4	
2‘	40.7	2.41 (1H, m)	40.7	2.48 (1H, sept, 6.5)	47.6	2.16 (1H, m)
3‘	20.8	1.17 (3H, d, 6.5)	21.1	1.15 (3H, d, 6.5)	27.0	1.35 (1H, m)
						1.71 (1H, m)
4‘	20.6	1.07 (3H, d, 6.5)	21.1	1.16 (3H, d, 6.5)	11.8	0.88 (3H, t, 7.5)
5‘					17.0	1.17 (3H, d, 6.5)
1‘‘	39.1	1.42 (1H, td, 4.0, 13.6)	38.0	1.59 (1H, m)	39.2	1.42 (1H, m)
		1.82 (1H, td)		1.66 (1H, m)		1.81 (1H, m)
2‘‘	25.2	2.00 (1H, m)	24.3	1.94 (1H, m)	25.2	2.00 (1H, m)
		2.20 (1H, m)		2.02 (1H, m)		2.20 (1H, m)
3‘‘	124.3	5.00 (1H, t, 6.8)	124.3	4.99 (1H, t, 7.0)	124.3	5.00 (1H, t, 6.8)
4‘‘	132.2		131.6		132.2	
5‘‘	17.8	1.59 (3H, s)	17.7	1.57 (3H, s)	17.8	1.59 (3H, s)
6‘‘	25.6	1.66 (3H, s)	25.6	1.65 (3H, s)	25.6	1.68 (3H, m)
1‘‘‘	27.8	1.68 (1H, m)	28.0	1.71 (1H, m)	27.0	1.35 (1H, m)
		2.09 (1H, m)		2.08 (1H, m)		1.71 (1H, m)
2‘‘‘	122.2	4.91 (1H, t, 7.1)	122.2	4.94 (1H, t, 6.6)	122.2	4.91 (1H, m)
3‘‘‘	133.5		133.5		133.5	
4‘‘‘	17.9	1.53 (3H, s)	18.0	1.55 (3H, s)	17.9	1.54 (3H, s)
5‘‘‘	28.5	1.66 (3H, s)	25.9	1.65 (3H, s)	25.8	1.74 (3H, m)

For **4** and **5** ^{13}C-NMR spectrum showed 31 atoms. Out of them, 11 carbons are quaternary, 5 are methines, 5 are $–CH_2–$ and 10 $–CH_3$ groups. Unlike in **1**, **2** and **3**, there were no "*down field shifted*" signals on ^{1}H-NMR spectrum, which means no intramolecular hydrogen bond in this molecule exist and phloroglucinol main core oxygens are present as keto groups or involved in a cyclization. In ^{13}C-NMR spectrum only three carbons resonated between 190 – 207 ppm, one of which is referred to the starter acid, another two are in the main molecule core, while the third phloroglucinol oxygen is either etherized or cyclised. Cyclisation was confirmed as "3-ortho-pyrano" type (**Fig. 16**) with the same not detectable hydroxyl group in position 5, as described for **2** and **3**.

For substance **4** – a clear septet at δ_H 2.41 ppm (δ_C 40.7 ppm) for an aliphatic methin proton, as well as two doublets at δ_H 1.07 ppm and δ_H 1.17 ppm for $–CH_3$ groups confirmed the starter acid as activated isobutyric acid. Two isoprene chains were evaluated with the help of HMBC and COSY experiments, starting from characteristic $=CH–$ protons at δ_H 4.91 ppm and δ_H 5.00 ppm. Same way structures of **5** and **6** were elucidated with the only difference for the latter: its starter acid is 2-methylbutyryl with a pseudo-sextet at δ_H 2.16 ppm (δ_C 47.6 ppm) for an aliphatic methine proton, as well as two $–CH_3$ groups δ_H 1.17 ppm (doublet) and δ_H 0.88 ppm (triplet).

Since **4** and **5** possess same structure, it was suggested, that the difference between two compounds lies in their different stereochemistry. Indeed, while almost all carbons have equal shift values (± 0.3-0.5 ppm), those for atoms C-11, C-17 and C-1'' differ in both substances significantly: C-11 (δ_C 44.4 / 42.3 ppm), C-17 (δ_C 12.7 / 14.5 ppm) and C-1'' (δ_C 39.1 / 38.0 ppm) for **4** / **5** respectively. NOESY experiment confirmed the suggestion (**Fig. 74-76**).

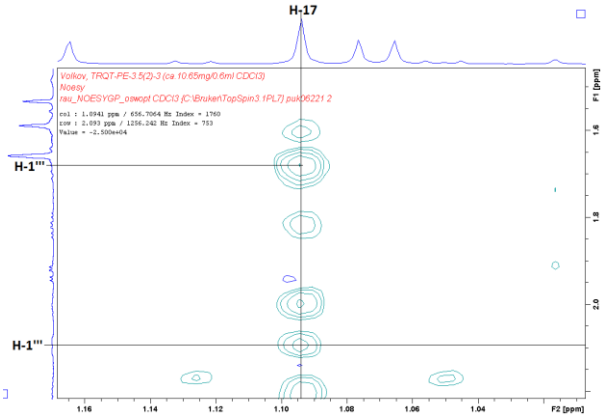

Fig. 74. Clip of NOESY experiment of **4**: correlation between H-17 and H-1’’’.

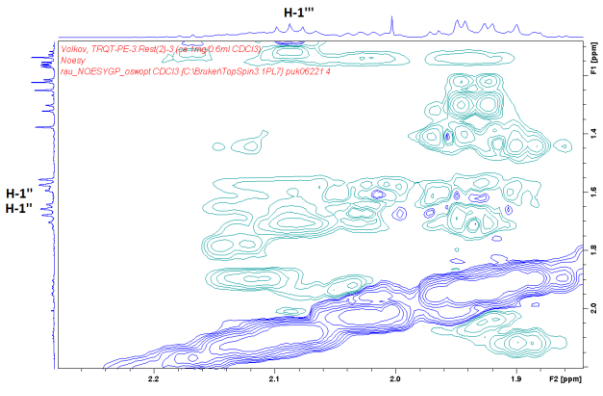

Fig. 75. Clip of NOESY experiment of **5**: correlation between H-1’’’ and H-1’’.

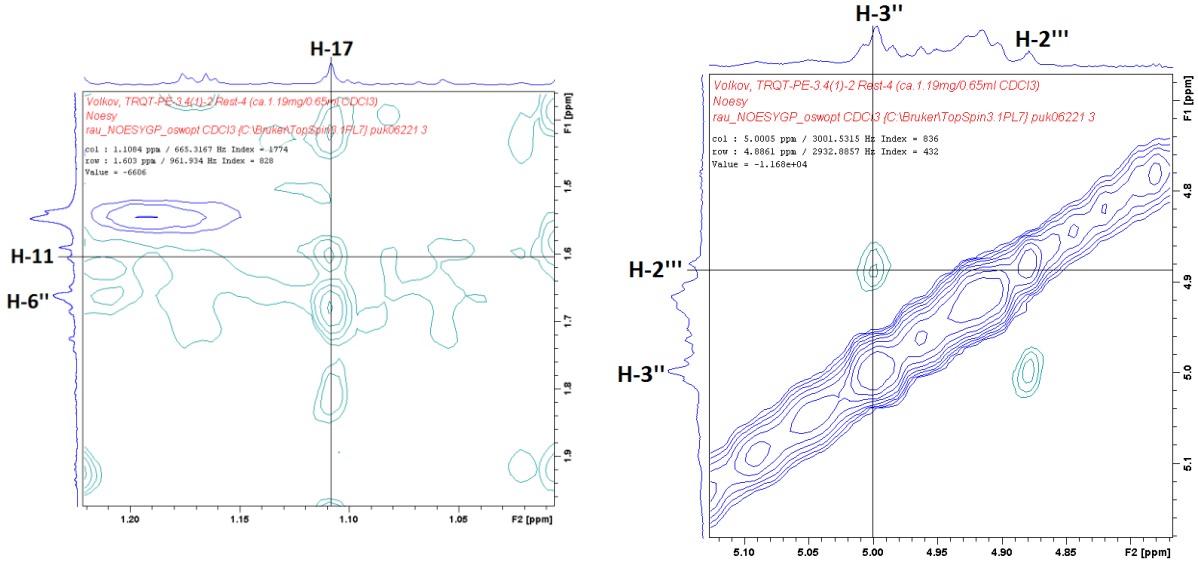

Fig. 76. Clip of NOESY experiment for **6**: correlations between H-17 and H-11 (left) and correlations between H-3’’ and H-2’’’ (right).

Molecular formula for substance **4** was established as $C_{31}H_{47}O_5$ by HRESIMS (*m/z* 499.3418 $[M+H]^+$). The compound was identified as (11S, 12R)-1-isobutyryl-4,4,9,12-tetramethyl-11α-(3-methylbut-2-enyl)-12-(4-methylpent-3-enyl)-3-oxatricyclo-[7.3.1.02,7]- trideca-2(7)-ene-8,13-dione and was given a trivial name **Triquetrireboudin A**. Molecular formula for substance **5** was established as $C_{31}H_{47}O_5$ by HRESIMS (*m/z* 499.3418 [M+H]+). The compound was identified as (11R, 12R)-1-isobutyryl-4,4,9,12-tetramethyl-11α-(3-methylbut-2-enyl)-12-(4-methylpent-3-enyl)-3-oxatricyclo-[7.3.1.02,7]-trideca-2(7)-ene-8,13-dione and was given a trivial name **Triquetrireboudin B**. Molecular formula for substance **6** was established as $C_{32}H_{49}O_5$ by HRESIMS (*m/z* 513.3575 $[M+H]^+$). The compound was identified as (11S, 12S)-1-(2-methylbutanoyl)-4,4,9,12-tetramethyl-11α-(3-methyl-but-2-enyl)-12-(4-methylpent-3-

enyl)-3-oxatricyclo-[7.3.1.02,7]trideca-2(7)-ene-8,13-dione and was given a trivial name **Triquetrireboudin C**.

Experimental CD spectra for **4**, **5** and **6** are presented in **Fig. 77**, **78** and **79** respectively.

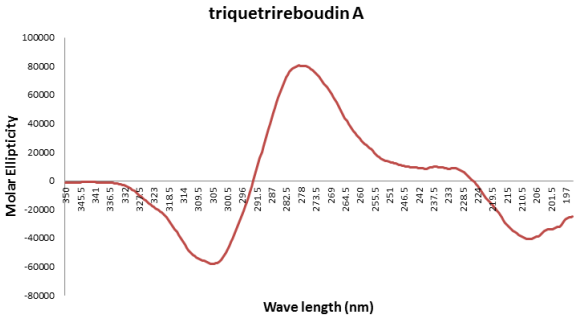

Fig. 77. Experimental CD spectrum of **4.**

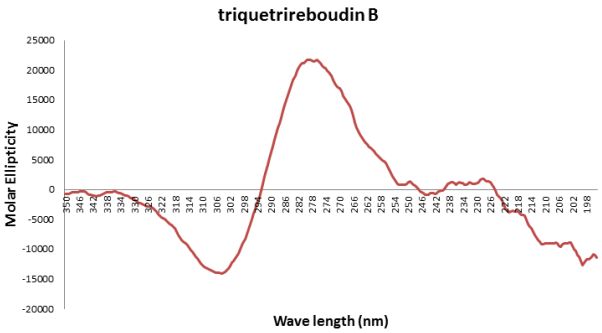

Fig. 78. Experimental CD spectrum of **5.**

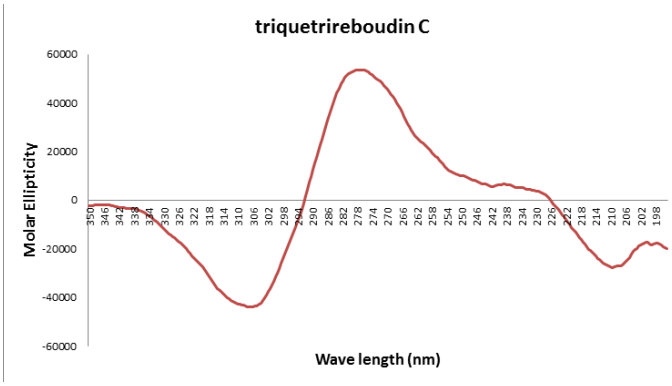

Fig. 79. Experimental CD spectrum of **6.**

Compounds 7, 8 and 9 (Triquetrikotelin A, B and Triquetriroxettin)

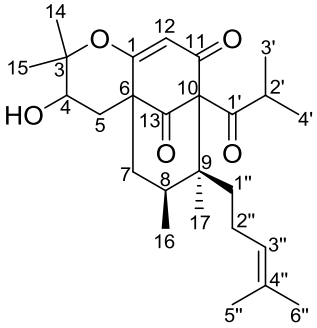

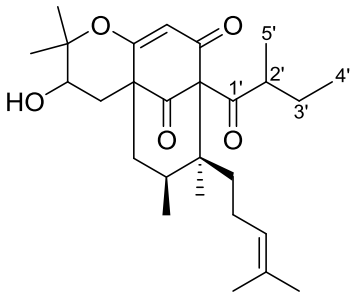

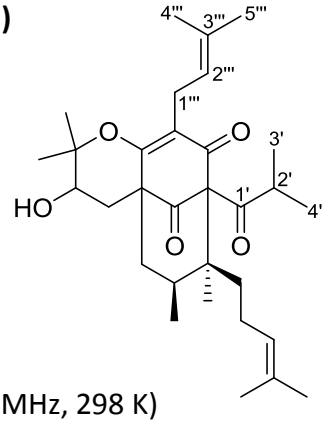

Tab. 14. ^{1}H and ^{13}C data in $CDCl_3$ (^{1}H-NMR 600 MHz, ^{13}C-NMR 150 MHz, 298 K)

	(**7**) Triquetrikotelin A		(**8**) Triquetrikotelin B		(**9**) Triquetriroxettin	
C/H	δ_C	δ_H mult (*J* in Hz)	δ_C	δ_H mult (*J* in Hz)	δ_C	δ_H mult (*J* in Hz)
1	171.8		171.8		166.5	
3	72.7		72.6		72.6	
4	88.2	3.84 (1H, d, 9.7)	88.3	3.86 (1H, d, 9.7)	87.8	3.84 (1H, d, 9.5)
5	23.6	1.59 (1H, m)	23.5	1.59 (1H, m)	24.2	1.58 (1H, m)
		1.82 (1H, m)		1.82 (1H, m)		1.83 (1H, m)
6	61.0		61.0		74.36	
7	33.4	1.93 (1H, dd, 5.2, 14.9)	33.4	1.93 (1H, dd, 5.3, 15.0)	33.2	1.92 (1H, dd, 6.2, 13.8)
		2.53 (1H, m)		2.52 (1H, m)		2.54 (1H, m)
8	36.6	2.09 (1H, m)	36.7	2.09 (1H, m)	36.9	2.04 (1H, m)
9	44.9		45.0		45.0	
10	74.5		74.5		60.6	
11	195.6		195.6		194.5	
12	118.8	6.25 (1H, s)	118.7	6.25 (1H, s)	128.9	
13	207.2		207.2		207.2	
14	25.3	1.240 (1H, m)	25.3	1.24 (3H, s)	25.9	1.24 (3H, m)
15	25.0	1.21 (3H, s)	24.9	1.21 (3H, s)	25.5	1.23 (3H, s)
16	15.7	1.235 (3H, s)	15.7	1.23 (3H, s)	16.4	1.24 (3H, m)
17	16.5	1.02 (3H, s)	16.6	1.02 (3H, s)	16.9	1.01 (3H, s)
1‘	210.9		210.1		211.5	
2‘	41.1	2.52 (1H, sept)	47.9	2.26 (1H, sext)	41.0	2.51 (1H, sept)
3‘	21.6	1.18 (3H, d, 6.5)	26.7	1.37 (1H, m)	21.5	1.17 (3H, d, 6.5)
				1.69 (1H, m)		
4‘	21.0	1.12 (3H, d, 6.5)	11.3	0.86 (3H, t, 7.4)	20.7	1.11 (3H, d, 6.6)
5‘			17.5	1.17 (3H, d, 6.5)		
1‘‘	42.8	1.40 (1H, m)	42.9	1.39 (1H, m)	42.8	1.39 (1H, m)
		2.04 (1H, m)		2.04 (1H, m)		2.03 (1H, m)
2‘‘	26.9	1.60 (1H, m)	26.8	1.59 (1H, m)	26.7	1.58 (1H, m)
		2.06 (1H, m)		2.06 (1H, m)		2.06 (1H, m)
3‘‘	121.8	4.95 (1H, t, 7.2)	121.8	4.95 (1H, t, 7.1)	121.8	4.93 (1H, m)
4‘‘	133.7		133.7		133.6	
5‘‘	17.9	1.55 (3H, s)	17.9	1.54 (3H, s)	17.9	1.55 (3H, s)
6‘‘	25.8	1.67 (3H, s)	25.8	1.67 (3H, s)	25.8	1.67 (3H, s)
1‘‘‘					22.8	3.15 (1H, dd, 6.2, 15.1)
						3.28 (1H, dd, 6.1, 15.1)
2‘‘‘					121.8	4.96 (1H, m)
3‘‘‘					133.6	
4‘‘‘					18.1	1.72 (3H, s)
5‘‘‘					25.5	1.68 (3H, s)

The ^{13}C-NMR spectrum of **7** showed 26 carbons, out of which 9 carbons are quaternary, 5 are CH–, 4 are –CH_2– and 8 –CH_3 groups. Starter acid was confirmed as isobutyric acid with characteristic septet at δ_H 2.52 ppm and two doublets at δ_H 1.12 ppm and δ_H 1.18 ppm for its methyl groups. The substance has only one isoprene rest with =CH– proton at δ_H 4.95 ppm. The cyclisation type was confirmed as type-A 5-para-pyrano (**Fig. 16**) in an only possible way because of the presence of an aromatic proton in the main molecule's core (δ_C 118.8 ppm, δ_H 6.25 ppm).

Difference between **7** and **8** lies in its starter acid structure: isobutyryl *versus* 2-methylbutyryl. In case of **8** a pseudo sextet resonated at δ_H 2.26 ppm characteristic for the methine proton, as well as a doublet at δ_H 1.17 ppm and triplet at δ_H 0.86 ppm for its both –CH_3 groups.

Compound **9** is a derivative of **7**, with isoprene chain connected to C-12 (δ_C 128.9 ppm), which is a quaternary one in this compound. The double bond remains between carbons C-1 and C-12.

Relative stereochemistry of these compounds was confirmed with NOESY experiments (**Fig. 80-82**).

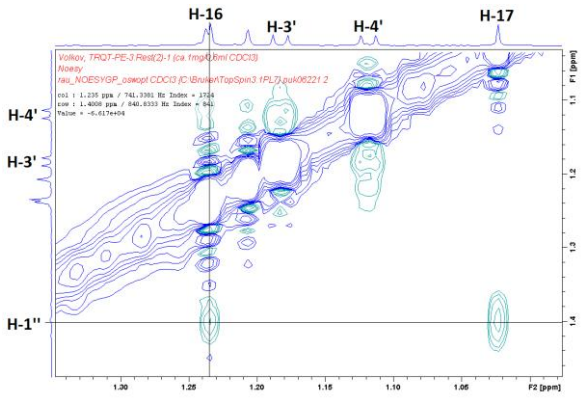

Fig. 80. Clip of NOESY experiment of **7**: correlation between H-16 and H-1''.

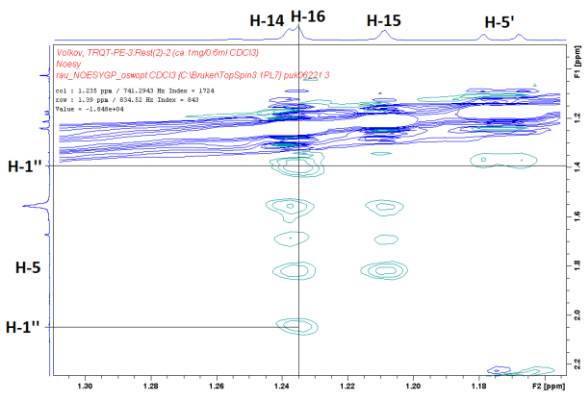

Fig. 81. Clip of NOESY experiment of **8**: correlation between H-16 and H-1''.

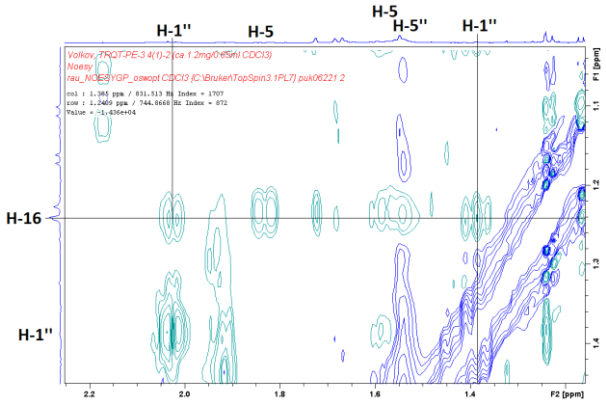

Fig. 82. Clip of NOESY experiment of **9**: correlation between H-16 and H-1''.

Molecular formula of **7** was established as $C_{26}H_{39}O_5$ by HRESIMS (*m/z* 431.2792 $[M+H]^+$). The compound was identified as (8S, 9S)-3,3,8,9-tetramethyl-9-(4-methylpent-3-enyl)-10-isobutyryl-2-oxatricyclo[7.3.1.01,6]-trideca-1(12)ene-11,13-dione and **Triquetrikotelin A** was given as trivial name. Molecular formula for substance **8** was established as $C_{27}H_{41}O_5$ by HRESIMS (*m/z* 445.2949 $[M+H]^+$). The compound was identified as (8S, 9S)-3,3,8,9-tetramethyl-9-(4-methylpent-3-enyl)-10-(2-methylbutanoyl)-2-oxatricyclo[7.3.1.01,6]-trideca-1(12)ene-11,13-dione and was given a trivial name **Triquetrikotelin B**. Molecular formula for substance **9** was established as $C_{31}H_{47}O_5$ by HRESIMS (*m/z* 499.3418 $[M+H]^+$). The compound was identified as (8S, 9S)-3,3,8,9-tetramethyl-9-(4-methylpent-3-enyl)-10-isobutyryl-12-(3-methylbut-2-enyl)-2-oxatricyclo[7.3.1.01,6]-trideca-1(12)ene-11,13-dione and was and was trivially named **Triquetriroxettin**.

Experimental CD spectra for compounds **7**, **8** and **9** are shown on **Fig. 83-85**.

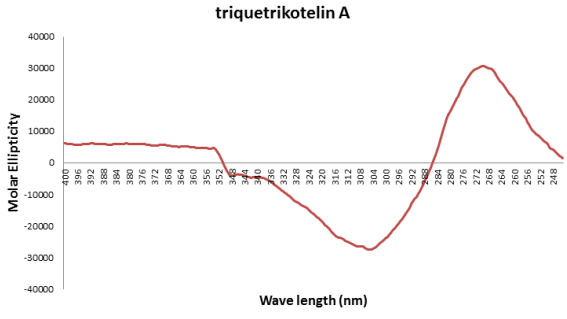

Fig. 83. Experimental CD spectrum of **7.**

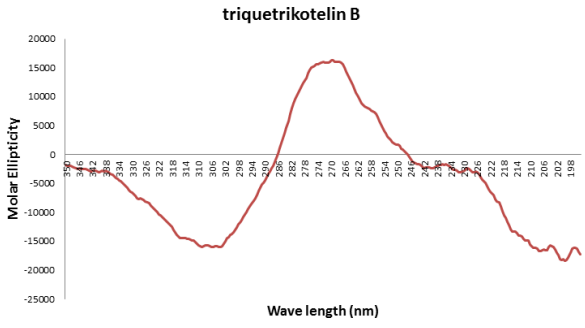

Fig. 84. Experimental CD spectrum of **8.**

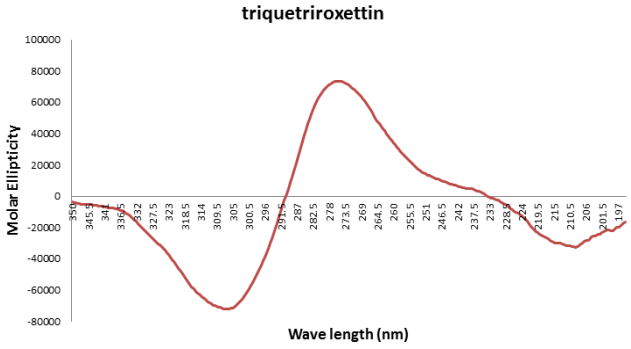

Fig. 85. Experimental CD spectrum of **9.**

Compound 10 (Triquetribavarin)

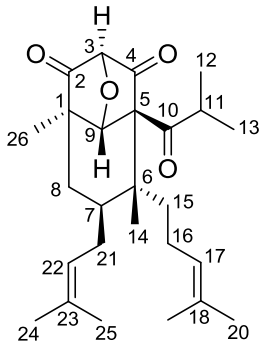

Tab. 15. ^{1}H and ^{13}C data in $CDCl_3$ (^{1}H-NMR 600 MHz, ^{13}C-NMR 150 MHz, 298 K)

C/H	δ_C	δ_H mult (*J* in Hz)
1	55.7	
2	203.5	
3	52.5	3.56 (1H, s)
4	171.8	
5	173.4	
6	44.7	
7	37.9	2.74 (1H, m)
8	38.0	1.20 (1H, m)
		2.66 (1H, dd, 4.0, 14.2)
9	72.4	3.82 (1H, s)
10	208.6	
11	43.1	2.76 (1H, sept)
12	18.5	1.10 (3H, d, 6.8)
13	17.6	1.06 (3H, d, 7.0)
14	18.9	0.78 (1H, s)
15	37.4	1.41 (1H, m)
		1.51 (1H, m)
16	22.5	1.62 (1H, m)
		1.85 (1H, m)
17	123.9	4.95 (1H, t, 13.8)
18	131.8	
19	26.6	1.65 (3H, s)
20	17.7	1.54 (3H, s)
21	27.8	1.62 (1H, m)
		2.20 (1H, m)
22	123.3	5.22 (1H, m)
23	132.4	
24	25.8	1.74 (3H, s)
25	18.0	1.60 (3H, s)
26	23.5	1.27 (3H, s)

Substance **10** was isolated in a very low quantity (< 0.6 mg) and ^{13}C-NMR didn't show all quaternary carbons. Several carbons were allocated with the help of HMBC experiment and added to the list manually. Therefore, 26 carbon atoms were detected, out of which 8 are quaternary, 6 are methines, 4 are $–CH_2–$ and 8 $–CH_3$ groups. Two isoprene chains elucidation started with characteristic protons at δ_H 5.22 ppm and δ_H 4.95 ppm. Further correlations within the chains and their connections to the molecule's main core were established with the help of HMBC and COSY experiments. Starter acid was confirmed as isobutyric acid, with a characteristic septet at δ_H 2.76 ppm (δ_C 43.1 ppm) for an aliphatic CH proton, as well as two doublets δ_H 1.10 ppm and δ_H 1.06 ppm for its both $–CH_3$ groups. Two down field shifted carbons (δ_C 203.5 ppm and δ_C 171.8 ppm) represent two keto groups in positions 2 and 4 respectively. C-3 (δ_C 52.5 ppm, δ_H 3.56 ppm) and C-9 (δ_C 72.4 ppm, δ_H 3.82 ppm) are CH– groups near an oxygen, because of the down field shifted values (**Fig. 86**). No hydroxyl group exist in this compound, especially as the corresponding "*down field shifted*" singlet of a proton is absent in the ^{1}H-NMR spectrum.

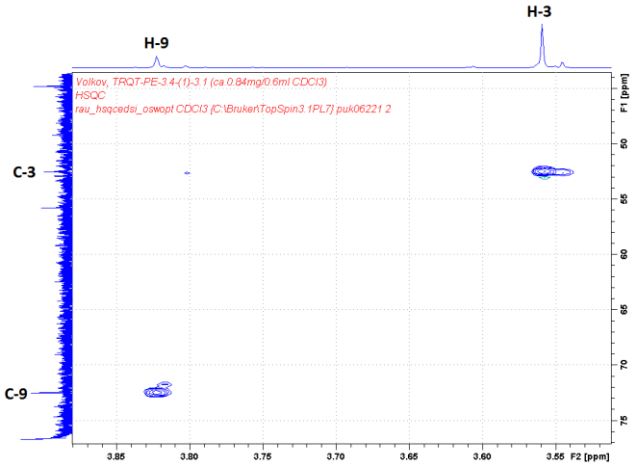

Fig. 86. HSQC correlations between between C-H atoms at C-3 and C-9.

Relative stereochemistry for **10** was confirmed with NOESY experiment (**Fig. 87**). Experimental CD spectrum for **10** is shown in **Fig. 88**.

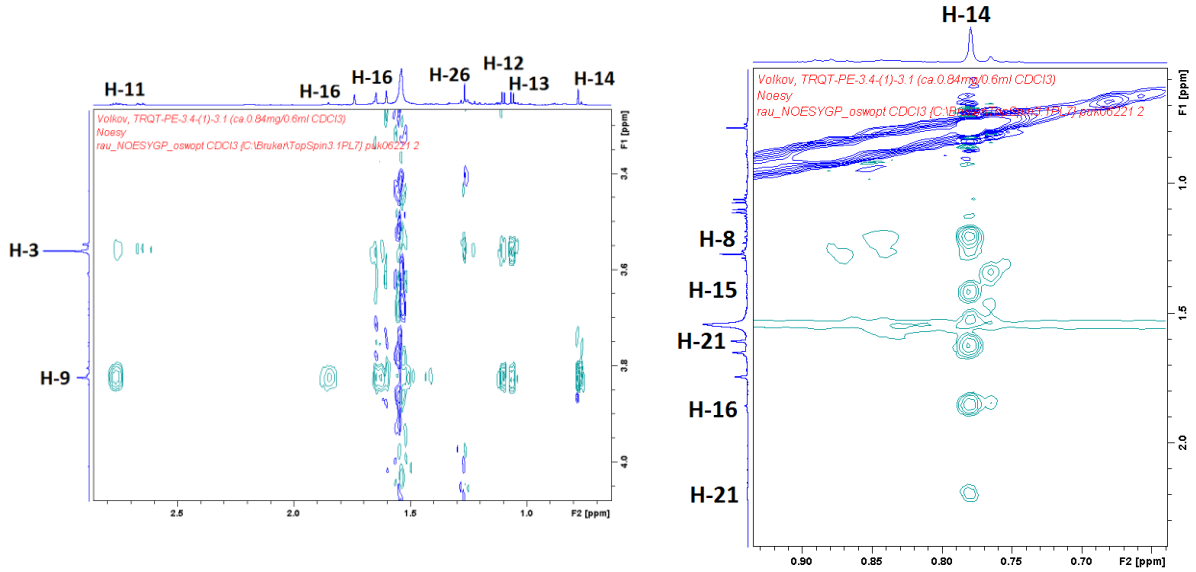

Fig. 87. Clip of NOESY experiment of **10**.

Molecular weight for substance **10** was established by HRESIMS (*m/z* 415.2115 $[M+H]^+$), which is in accordance with the postulated chemical formula $C_{26}H_{28}O_4$. The compound was identified as (1R, 3S, 5R, 6R, 7S, 9S)-1,6-dimethyl-5-isobutyryl-6-(4-methylpent-3-enyl)-7-(3-methylbut-2-enyl)-bicyclo-[3.3.1]-3,9-epoxy-3,9-dihydro-2,4-dione and was given a trivial name **Triquetribavarin**.

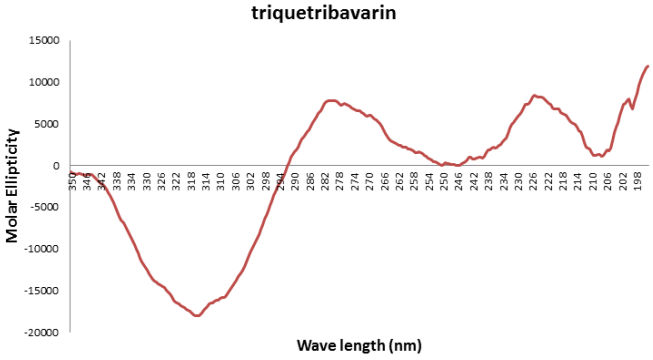

Fig. 88. Experimental CD spectrum of **10.**

3.1.3.3 Possible hyperforin analogues and precursors

Compound 11 and 12 ((+)-Yezo'otogirin C and Triquetriirinon A)

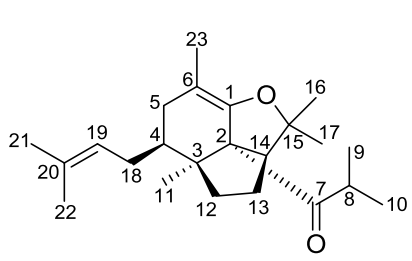

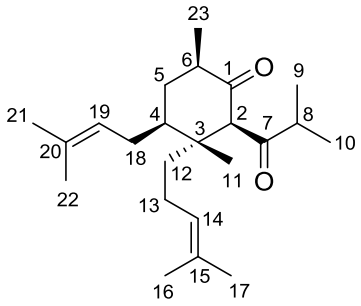

Tab. 16. ^{1}H and ^{13}C data in $CDCl_3$ (^{1}H-NMR 600 MHz, ^{13}C-NMR 150 MHz, 298 K)

	(**11**) (+)-Yezo'otogirin C		(**12**) Triquetriirinon A	
C/H	δ_C	δ_H mult (*J* in Hz)	δ_C	δ_H mult (*J* in Hz)
1	149.3		210.6	
2	73.6		66.7	3.85 (1H, s)
3	48.5		45.5	
4	47.0	1.23 (1H, m)	42.4	1.84 (1H, m)
5	32.7	1.86 (1H, dd, 3.4, 15.5)	36.9	1.22 (1H, dd, 12.8)
		1.95 (1H, m)		2.11 (1H, m)
6	107.5		45.5	2.46 (1H, m)
7	217.5		211.0	
8	38.0	2.96 (1H, sept, 6.7)	42.7	2.47 (1H, m)
9	18.3	1.02 (3H, d, 6.5)	17.7	1.06 (3H, d, 6.7)
10	21.5	1.01 (3H, d, 6.8)	18.5	1.04 (3H, d, 7.0)
11	19.7	0.75 (3H, s)	17.3	1.00 (3H, s)
12	41.5	1.35 (1H, m)	36.6	1.48 (2H, m)
		1.74 (1H, m)		
13	25.4	1.54 (2H, m)	21.9	1.80 (1H, m)
				2.05 (1H, m)
14	54.9	3.19 (1H, dd, 8.9, 9.9)	123.7	4.98 (1H, t, 6.9)
15	83.5		131.7	
16	25.4	1.18 (3H, s)	17.6	1.58(3H, s)
17	29.5	1.14 (3H, s)	25.7	1.66 (3H, s)
18	29.6	1.82 (1H, m)	26.8	1.70 (1H, m)
		1.94 (1H, m)		2.10 (1H, m)
19	124.2	5.11 (1H, t, 7.2)	123.0	5.11 (1H, t, 7.2)
20	132.4		132.9	
21	17.9	1.60 (3H, s)	17.9	1.61 (3H, s)
22	25.9	1.72 (3H, s)	25.9	1.73 (3H, s)
23	16.3	1.71 (3H, s)	14.3	1.01 (3H, d, 6.4)

^{13}C-NMR spectrum for compound **11** showed 23 carbons, out of which 7 are quaternary, 4 are methines, 4 are $–CH_2–$ and 8 $–CH_3$ groups. Starter acid was confirmed as isobutyric acid with an aliphatic CH– proton at δ_H 2.96 ppm and two doublets at δ_H 1.01 ppm and δ_H 1.02 ppm as both $–CH_3$ groups. The presence of only one isoprene rest was confirmed with both HMBC and COSY experiments, starting from its =CH– proton at δ_H 5.11 ppm.

Main core of the molecule was elucidated as octahydroindeno[7,1-*bc*]furan with four methyl groups. Example of HMBC correlations can be observed from **Fig. 89**.

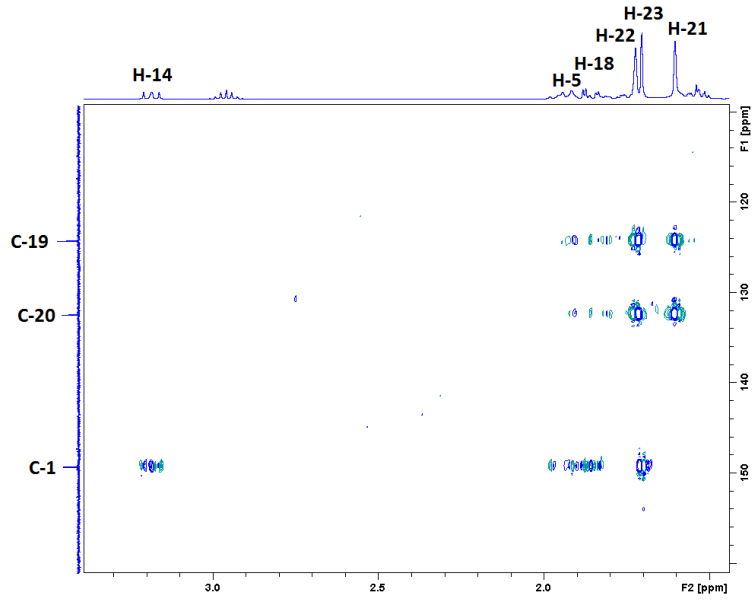

Fig. 89. Clip of HMBC experiment of **11**: example correlations.

Original article describing the first ever elucidation of Yezo'otogirin C (Tanaka et al., 2009) provides molecule atoms' numbering only and does not provide any IUPAC name for the substance. Following articles, which describe Yezo'otogirin C and its possible biosynthesis, etc. (He et al., 2014; Yang et al., 2015a) use only a trivial name of the compound and follow the same atoms' numbering, as was suggested in the original paper by Tanaka et al. In course of the present work **Tab. 16** refers to and still maintains the original numbering for comparison reasons. However, **Fig. 90** presents alternative numbering and the IUPAC name for **11:** (2aS, 2a^{1}R, 4aS, 5S)-2a^1-isobutyryl-2,2,4a,7-tetramethyl-5-(3-methylbut-2-enyl)-2,2a,2a^1,3,4,4a,5,6-octahydroindeno[7,1-*bc*]furan.

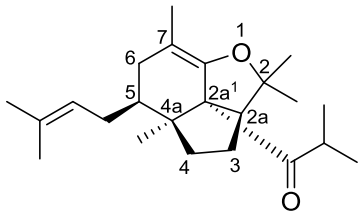

Fig. 90. (+)-Yezo'otogirin C.

Carbon spectrum for **12** comprises 23 carbons as well, out of which 5 are quaternary, 6 are =CH–, 4 are $–CH_2–$ and 8 $–CH_3$ groups. Both isoprene rests were elucidated with HMBC and COSY experiments help, starting from their =CH– protons (δ_H 4.98 ppm and δ_H 5.11 ppm). Starter acid was detected as activated isobutyric acid, because of its septet (δ_C 42.7 ppm, δ_H 2.47 ppm) and two doublets (δ_H 1.04 ppm, δ_H 1.06 ppm) for its $–CH_3$ groups. The only keto group in the main core is proved by a down shifted carbon at δ_C 210.6 ppm.

Stereochemistry was defined according to NOESY spectra (**Fig. 91-92**).

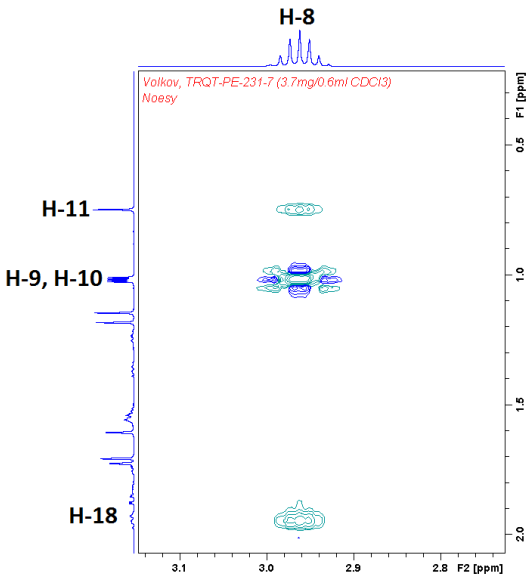

Fig. 91. Clip of NOESY experiment of **11**.

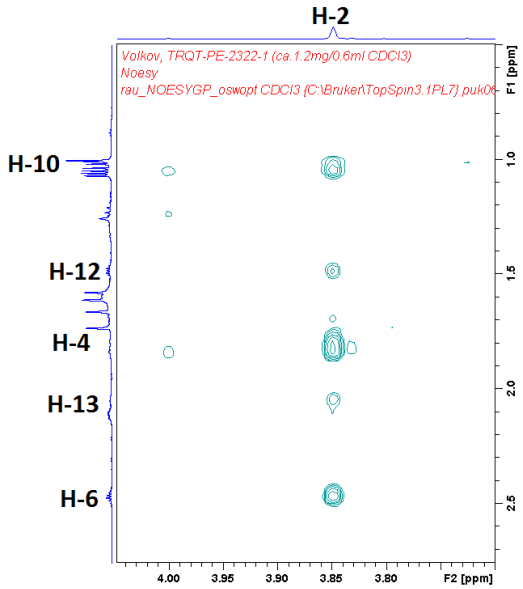

Fig. 92. Clip of NOESY experiment of **12**.

For a better understanding of stereochemistry of **11**, a tridimensional model was build and is presented on **Fig. 93** below.

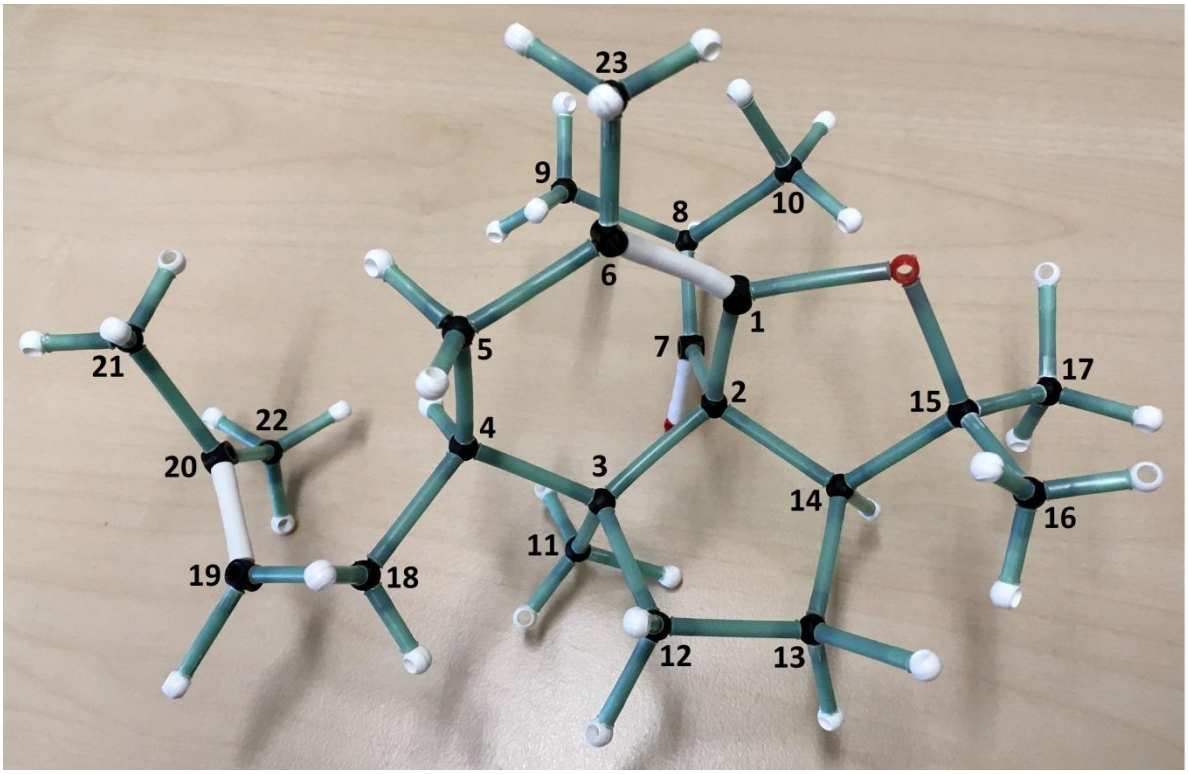

Fig. 93. Modeled structure of **11**.

Experimental CD spectra for **11** and **12** are presented on **Fig. 94** and **Fig. 95** respectively.

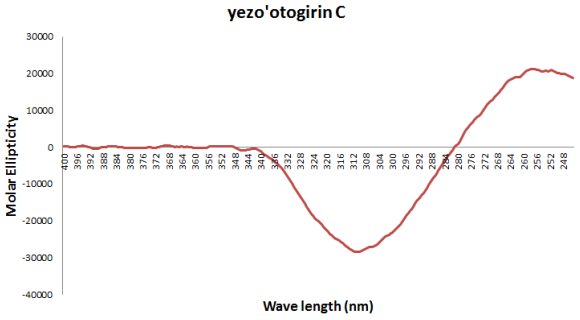

Fig. 94. Experimental CD spectrum of **11.**

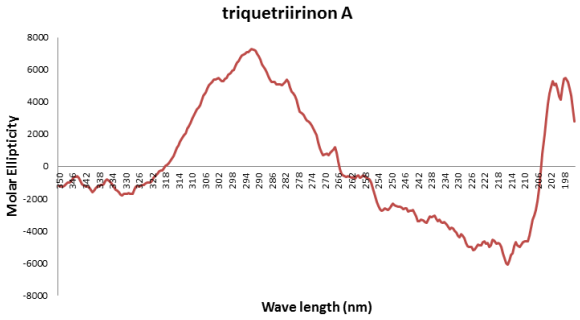

Fig. 95. Experimental CD spectrum of **12.**

Molecular formula for substance **11** was established as $C_{23}H_{37}O_2$ by HRESIMS (*m/z* 345.2788 $[M+H]^+$). Molecular formula for substance **12** was established as $C_{23}H_{39}O_2$ by HRESIMS (*m/z* 347.2945 $[M+H]^+$). The compound was identified as 2-isobutyryl-3,6-dimethyl-3-(4-methylpent-3-en-1-yl)-4-(3-methylbut-2-en-1-yl)-cyclohexan-1-one. It was isolated for the first time and given the trivial name **Triquetriirinon A**.

Compounds 13, 14 and 15 (Triquetriirinon B, C and D)

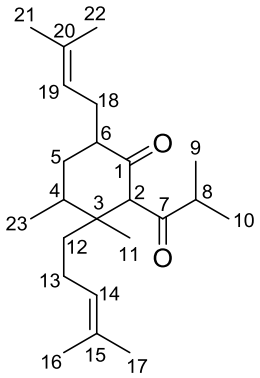

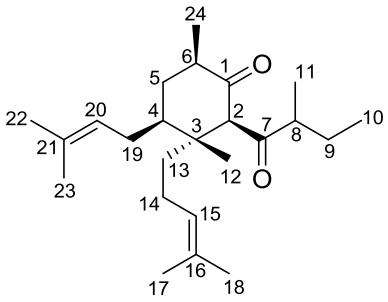

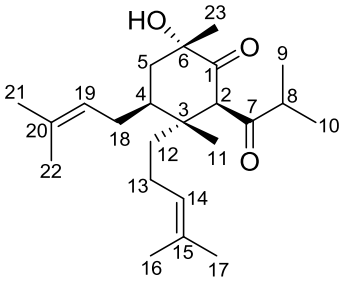

Tab. 17. ^{1}H and ^{13}C data in $CDCl_3$ (^{1}H-NMR 600 MHz, ^{13}C-NMR 150 MHz, 298 K)

	(**13**) Triquetriirinon B		(**14**) Triquetriirinon C		(**15**) Triquetriirinon D	
C/H	δ_C	δ_H mult (*J* in Hz)	δ_C	δ_H mult (*J* in Hz)	δ_C	δ_H mult (*J* in Hz)
1	203.5		210.7		209.0	
2	72.4	3.82 (1H, m)	67.1	3.83 (1H, s)	61.4	4.67 (1H, s)
3	55.7		45.6		45.8	
4	37.9	2.74 (1H, m)	42.5	1.83 (1H)	37.6	2.10 (1H, m)
5	37.4	1.41 (1H, m) 1.50 (1H, m)	36.9	1.21 (1H) 2.10 (1H)	42.2	1.44 (1H, m) 2.01 (1H, m)
6	44.7		45.55	2.46 (1H, m)	75.6	
7	208.5		210.5		211.2	
8	43.1	2.76 (1H, m)	49.6	2.29 (1H, sext)	42.7	2.48 (1H, sept)
9	17.6	1.06 (3H, d, 6.8)	25.4	1.26 (1H, m) 1.64 (1H, m)	17.7	1.07 (1H, d, 6.9)
10	18.5	1.10 (3H, d, 6.9)	11.5	0.88 (3H, t, 7.4)	18.5	1.06 (1H, d, 7.0)
11	23.5	1.27 (3H, s)	14.5	1.04 (3H, d, 6.8)	16.5	0.99 (3H, s)
12	38.0	1.20 (1H, m) 2.66 (1H, dd, 4.0, 14.3)	17.3	1.00 (3H, m)	36.7	1.50 (2H, m)
13	27.8	1.61 (1H, m) 2.19 (1H, m)	36.6	1.48 (2H, m)	22.0	1.83 (1H, m) 2.07 (1H, m)
14	123.3	5.22 (1H, m)	21.9	1.80 (1H, m) 2.06 (1H, m)	123.7	4.98 (1H, t)
15	132.4		123.6	4.97 (1H, m)	131.7	
16	18.0	1.61 (3H, m)	131.7		17.7	1.58 (3H, s)
17	25.8	1.74 (3H, s)	17.7	1.56 (3H, s)	25.7	1.66 (3H, s)
18	22.5	1.63 (1H, m) 1.85 (1H, m)	25.7	1.66 (3H, s)	26.5	1.65 (1H, m) 2.10 (1H, m)
19	123.9	4.95 (1H, m)	26.8	1.70 (1H, m) 2.11 (1H, m)	122.8	5.10 (1H, t)
20	131.8		123.0	5.11 (1H, t, 7.1)	132.9	
21	17.7	1.54 (3H, m)	132.9		18.0	1.60 (3H, s)
22	25.6	1.65 (3H, s)	18.0	1.61 (3H, s)	25.9	1.73 (3H, s)
23	18.9	0.78 (3H, s)	25.9	1.73 (3H, s)	23.9	1.30 (3H, brs)
24			14.3	1.01 (3H, d, 6.4)		

Compound **13** was not separable from **12** and thus elucidated only in a mixture. The signals were separated and therefore the elucidation of both structures from one set of NMR spectra was possible. The only difference between **12** and **13** lie in the fact that substituents (methyl group and prenyl side chain) in positions 4 and 6 are reversed. Compound **14** differs from **12** in its starter acid: activated 2-methyl-butyric acid *versus* isobutyric acid. In this case for **14**, a =CH– group proton is shown as a multiplet (probably an overlaid pseudo sextet) (δ_H 2.29 ppm), while one $-CH_3$ group resonated as a doublet (δ_H 1.04 ppm) and another as a triplet (δ_H 0.88 ppm).

Stereochemistry for **14** was confirmed in NOESY experiments (**Fig. 96**).

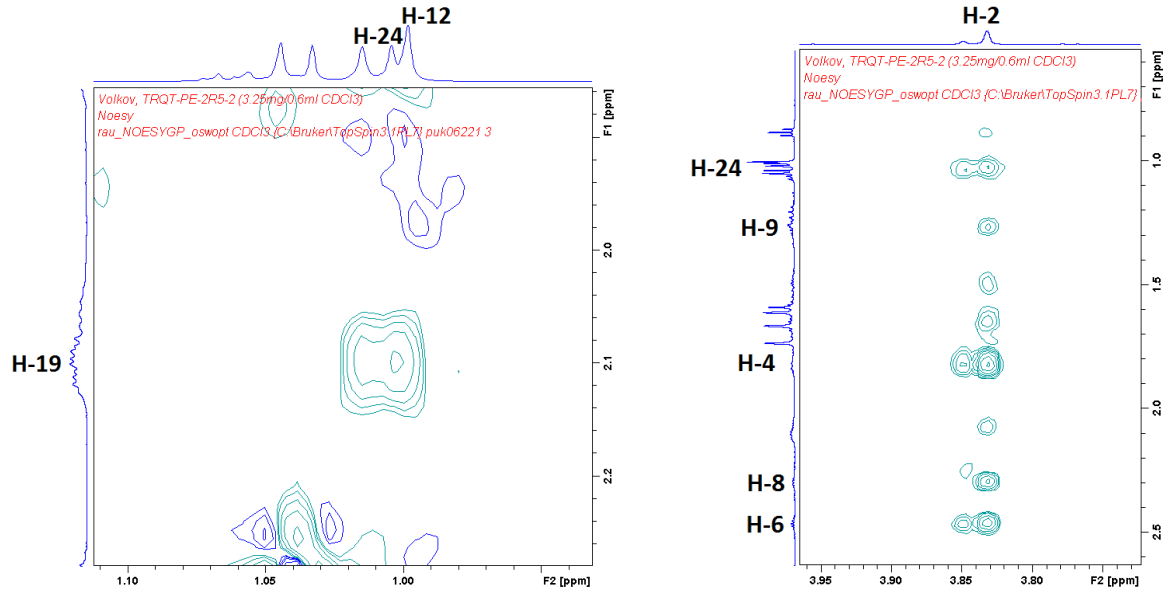

Fig. 96. Clip of NOESY experiment of **14**: most important correlations.

Substance **15** has an additional hydroxyl group in position 6: C-6 is quaternary and resonates at δ_C 75.6 ppm. The proton of the –OH group didn't show any signals in ^{1}H-NMR spectrum, but its presence was confirmed with MS experiment. Several basic HMBC correlations can be observed from **Fig. 97**.

Stereochemistry of **15** was defined with NOESY experiment (**Fig. 98**). Experimental CD spectra for **14** and **15** are presented in **Fig. 99** and **100**.

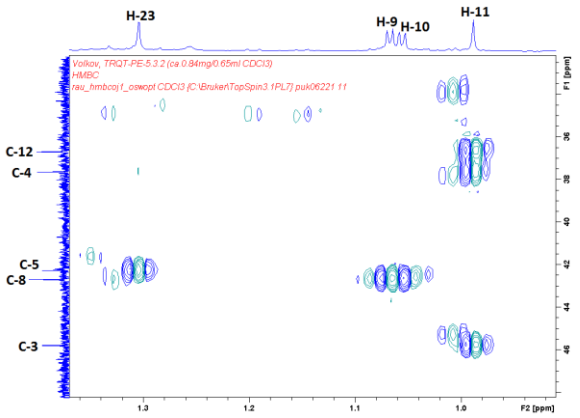

Fig. 97. Clip of HMBC experiment of **15**: several important HMBC correlations.

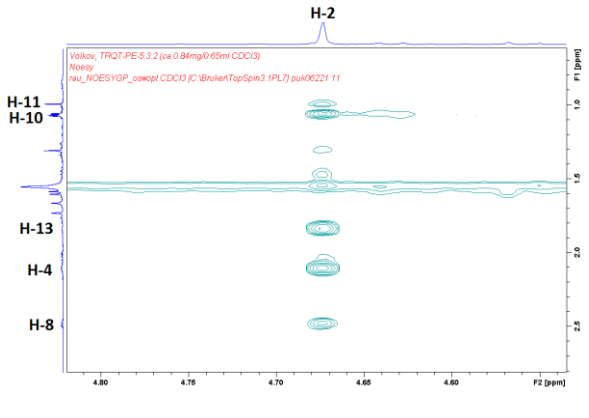

Fig. 98. Clip of NOESY experiment of **15**: correlations between H-2 and H-4 and H-11.

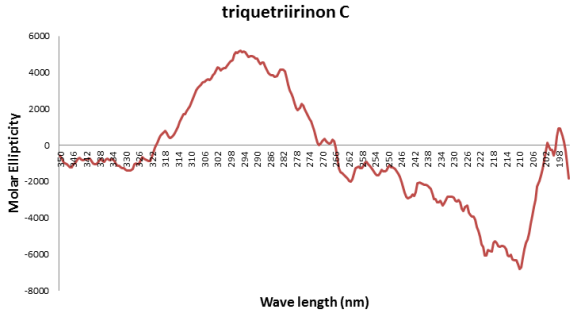

Fig. 99. Experimental CD spectrum of **14.**

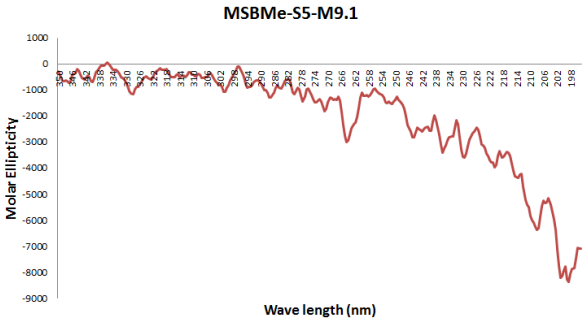

Fig. 100. Experimental CD spectrum of **15.**

Molecular formula for substance **12** was established as $C_{23}H_{39}O_2$ by HRESIMS (*m/z* 347.2945 $[M+H]^+$). The compound was identified as 2-isobutyryl-3,4-dimethyl-3-(4-methylpent-3-en-1-yl)-6-(3-methylbut-2-en-1-yl)-cyclohexan-1-one and was given a trivial name **Triquetriirinon B**. Molecular formula for substance **13** was established as $C_{24}H_{41}O_2$ by HRESIMS (*m/z* 361.3101 $[M+H]^+$). The compound was identified as (2R, 3R, 4S, 6R)-2-(2-methylbutanoyl)-3,6-dimethyl-3-(4-methylpent-3-en-1-yl)-4-(3-methylbut-2-en-1-yl)-cyclohexan-1-one and was given a trivial name **Triquetriirinon C**. Molecular formula for substance **14** was established as $C_{23}H_{39}O_3$ by HRESIMS (*m/z* 363.2894 $[M+H]^+$). The compound was identified as (2R, 3R, 4S, 6S)-2-isobutyryl-3,6-dimethyl-3-(4-methylpent-3-en-1-yl)-4-(3-methylbut-2-en-1-yl)-6-hydroxy-cyclohexan-1-one. The hitherto unknown compound was given the trivial name **Triquetriirinon D**.

3.1.4 Overview of the isolated substances

3.1.4.1 Prenylated acylphloroglucinols

The data presented in this list are: trivial name, IUPAC-name; state of matter (isolated quantity); specific rotation (concentration [g/100 ml], solvent); UV wave length (molar attenuation coefficient's logarithm); NMR data; MS data.

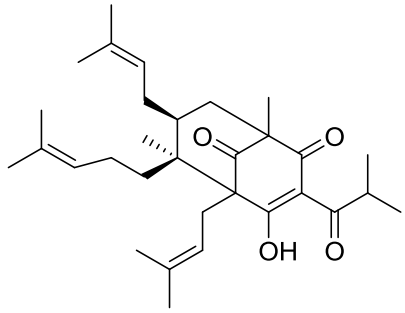	**1 – Triquetriborin**
	(6S, 7S)-4-hydroxy-1,6-dimethyl-3-isobutyryl-5,7-bis(3-methylbut-2-en-1-yl)-6-(4-methylpent-3-en-1-yl)-bicyclo-[3.3.1]non-3-ene-2,9-dione Green oil (1.46 mg); $[\alpha]^{23}_{D}$ +30 (c 0.01, MeOH); UV (MeOH) λ_{max} (log ε) 285 (2.92) nm; ^{1}H- and ^{13}C-NMR data see **Tab. 11**; HRESIMS *m/z* 483.3463 $[M+H]^+$ (calculated for $C_{31}H_{47}O_4$, 483.3469)
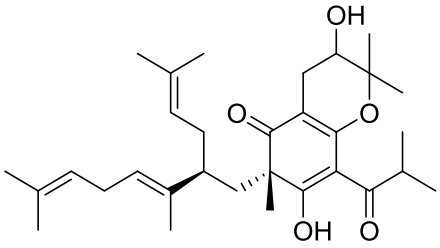	**2 – Triquetrijakobin A**
	(8S, 2''S)-1-[3,3,8-trimethyl-4,5,5-trihydro-4,9-dihydroxy-8-(3,7-dimethyl-2-(3-methylbut-2-en-1-yl)-octyl-3,6-diene)-chroman-5-one-8-yl]-2-methylpropan-1-one Green oil (3.36 mg); $[\alpha]^{23}_{D}$ -21 (c 0.05, MeOH); UV (MeOH) λ_{max} (log ε) 269 (3.62), 314 (3.48) nm; ^{1}H- and ^{13}C-NMR data see **Tab. 12**; HRESIMS *m/z* 499.3423 $[M+H]^+$ (calculated for $C_{31}H_{47}O_5$, 499.3418)
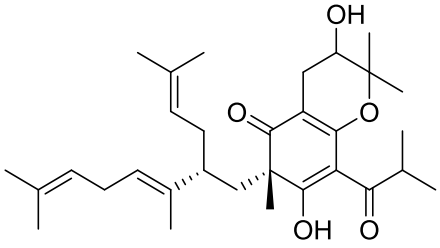	**3 – Triquetrijakobin B**
	(8S, 2''R)-1-[3,3,8-trimethyl-4,5,5-trihydro-4,9-dihydroxy-8-(3,7-dimethyl-2-(3-methylbut-2-en-1-yl)-octyl-3,6-diene)-chroman-5-one-8-yl]-2-methylpropan-1-one Green oil (3.30 mg); $[\alpha]^{23}_{D}$ +140 (c 0.05, MeOH); UV (MeOH) λ_{max} (log ε) 272 (3.63), 315 (3.55) nm; ^{1}H- and ^{13}C-NMR data see **Tab. 12**; HRESIMS *m/z* 499.3420 $[M+H]^+$ (calculated for $C_{31}H_{47}O_5$, 499.3418)
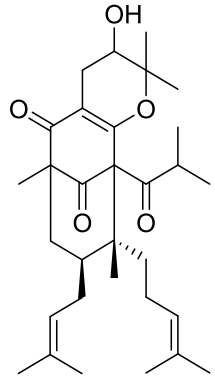	**4 – Triquetrireboudin A**
	(11S, 12R)-1-isobutyryl-4,4,9,12-tetramethyl-11α-(3-methylbut-2-enyl)-12-(4-methylpent-3-enyl)-3-oxatricyclo-[7.3.1.0^{2,7}]- trideca-2(7)-ene-8,13-dione Greenish oil (10.95 mg); $[\alpha]^{23}_{D}$ +118 (c 0.05, MeOH); UV (MeOH) λ_{max} (log ε) 280 (4.18) nm; ^{1}H- and ^{13}C-NMR data see **Tab. 13**; HRESIMS *m/z* 499.3418 $[M+H]^+$ (calculated for $C_{31}H_{47}O_5$, 499.3418)

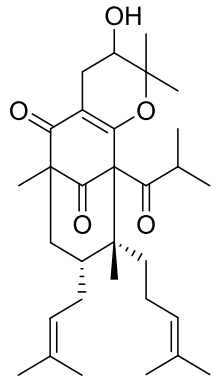	**5 – Triquetriroboudin B** *(11R, 12R)-1-isobutyryl-4,4,9,12-tetramethyl-11α-(3-methylbut-2-enyl)-12-(4-methylpent-3-enyl)-3-oxatricyclo-[7.3.1.0^{2,7}]-trideca-2(7)-ene-8,13-dione* Greenish oil (29.21 mg); $[\alpha]^{23}_{D}$ +166 (c 0.05, MeOH); UV (MeOH) λ_{max} (log ε) 280 (3.48) nm; ^{1}H- and ^{13}C-NMR data see **Tab. 13**; HRESIMS *m/z* 499.3425 $[M+H]^{+}$ (calculated for $C_{31}H_{47}O_5$, 499.3418)
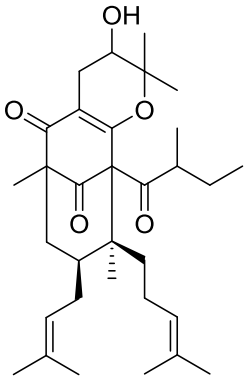	**6 – Triquetriroboudin C** *(11S, 12S)-1-(2-methylbutanoyl)-4,4,9,12-tetramethyl-11α-(3-methyl-but-2-enyl)-12-(4-methylpent-3-enyl)-3-oxatricyclo-[7.3.1.0^{2,7}]trideca-2(7)-ene-8,13-dione* Greenish oil (1.19 mg); $[\alpha]^{23}_{D}$ -60 (c 0.05, MeOH); UV (MeOH) λ_{max} (log ε) 280 (3.88) nm; ^{1}H- and ^{13}C-NMR data see **Tab. 13**; HRESIMS *m/z* 513.3577 $[M+H]^{+}$ (calculated for $C_{32}H_{49}O_5$, 513.3575)
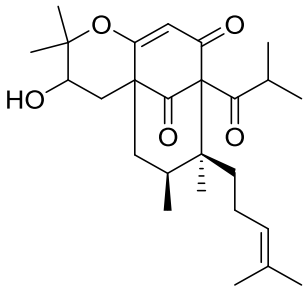	**7 – Triquetrikotelin A** *(8S, 9S)-3,3,8,9-tetramethyl-9-(4-methylpent-3-enyl)-10-isobutyryl-2-oxatricyclo[7.3.1.0^{1,6}]-trideca-1(12)ene-11,13-dione* Greenish oil (4.52 mg); $[\alpha]^{23}_{D}$ -138 (c 0.05, MeOH); UV (MeOH) λ_{max} (log ε) 270 (3.58) nm; ^{1}H- and ^{13}C-NMR data see **Tab. 14**; HRESIMS *m/z* 431.2796 $[M+H]^{+}$ (calculated for $C_{26}H_{39}O_5$, 431.2792)
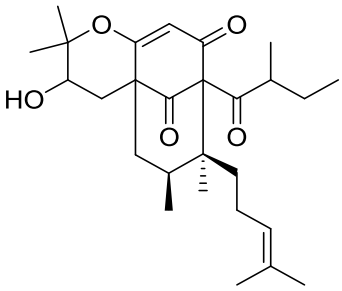	**8 – Triquetrikotelin B** *(8S, 9S)-3,3,8,9-tetramethyl-9-(4-methylpent-3-enyl)-10-(2-methylbutanoyl)-2-oxatricyclo[7.3.1.0^{1,6}]-trideca-1(12)ene-11,13-dione* Greenish oil (1.54 mg); $[\alpha]^{23}_{D}$ -104 (c 0.05, MeOH); UV (MeOH) λ_{max} (log ε) 270 (3.40) nm; ^{1}H- and ^{13}C-NMR data see **Tab. 14**; HRESIMS *m/z* 445.2952 $[M+H]^{+}$ (calculated for $C_{27}H_{41}O_5$, 445.2949)
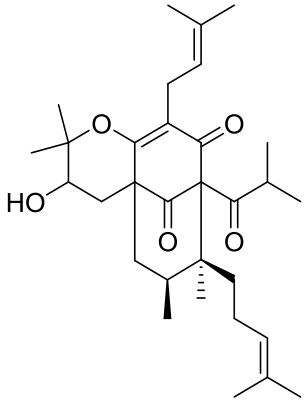	**9 – Triquetriroxettin** *(8S, 9S)-3,3,8,9-tetramethyl-9-(4-methylpent-3-enyl)-10-isobutyryl-12-(3-methylbut-2-enyl)-2-oxatricyclo[7.3.1.0^{1,6}]-trideca-1(12)ene-11,13-dione* Greenish oil (2.24 mg); $[\alpha]^{23}_{D}$ -116 (c 0.05, MeOH); UV (MeOH) λ_{max} (log ε) 275 (3.97) nm; ^{1}H- and ^{13}C-NMR data see **Tab. 14**; HRESIMS *m/z* 499.3424 $[M+H]^{+}$ (calculated for $C_{31}H_{47}O_5$, 499.3418)

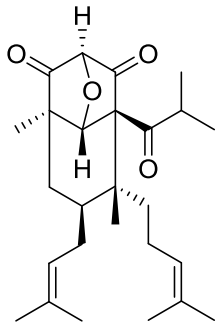	**10 – Triquetribavarin** *(1R, 3S, 5R, 6R, 7S, 9S)-1,6-dimethyl-5-isobutyryl-6-(4-methylpent-3-enyl)-7-(3-methylbut-2-enyl)-bicyclo-[3.3.1]-3,9-epoxy-3,9-dihydro-2,4-dione* Greenish oil (0.59 mg); $[\alpha]^{23}_{D}$ -58 (c 0.05, MeOH); UV (MeOH) λ_{max} (log ε) 280 (3.22) nm; ^{1}H- and ^{13}C-NMR data see **Tab. 15**

3.1.4.2 Possible hyperforin analogues and precursors

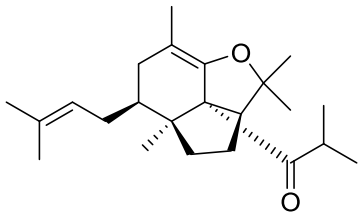	**11 – (+)-Yezo'otogirin C** *(2aS, 2a^{1}R, 4aS, 5S)-2a^{1}-isobutyryl-2,2,4a,7-tetramethyl-5-(3-methylbut-2-enyl)-2,2a,2a^{1},3,4,4a,5,6-octahydroindeno[7,1-*bc*]furan* Colourless oil (14.53 mg); $[\alpha]^{23}_{D}$ +56 (c 0.01, MeOH); UV (MeOH) λ_{max} (log ε) 275 (3.34) nm; ^{1}H- and ^{13}C-NMR data see **Tab. X**; HRESIMS *m/z* 345.2787 $[M+H]^{+}$ (calculated for $C_{23}H_{37}O_2$, 345.2788)
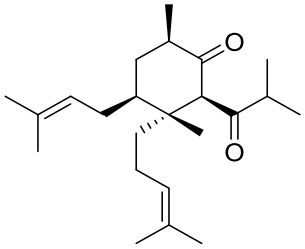	**12 – Triquetriirinon A** *(2R, 3R, 4S, 6R)-2-isobutyryl-3,6-dimethyl-3-(4-methylpent-3-en-1-yl)-4-(3-methylbut-2-en-1-yl)-cyclohexan-1-one* Colourless or slightly greenish oil; $[\alpha]^{23}_{D}$ +170 (c 0.01, MeOH); UV (MeOH) λ_{max} (log ε) 289 (3.36) nm; ^{1}H- and ^{13}C-NMR data see **Tab. 16**; HRESIMS *m/z* 347.2950 $[M+H]^{+}$ (calculated for $C_{23}H_{39}O_2$, 347.2945)
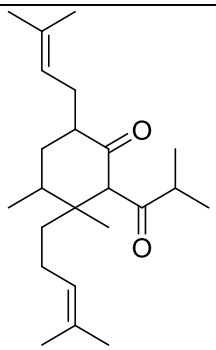	**13 – Triquetriirinon B** *2-isobutyryl-3,4-dimethyl-3-(4-methylpent-3-en-1-yl)-6-(3-methylbut-2-en-1-yl)-cyclohexan-1-one* Colourless oil; substance elucidated only in a mixture with (**12**); ^{1}H- and ^{13}C-NMR data see **Tab. 17**; HRESIMS *m/z* 347.2948 $[M+H]^{+}$ (calculated for $C_{23}H_{39}O_2$, 347.2945)
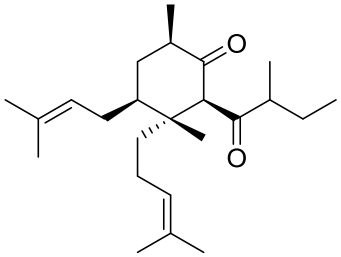	**14 – Triquetriirinon C** *(2R, 3R, 4S, 6R)-2-(2-methylbutanoyl)-3,6-dimethyl-3-(4-methylpent-3-en-1-yl)-4-(3-methylbut-2-en-1-yl)-cyclohexan-1-one* Greenish oil (3.25 mg); $[\alpha]^{23}_{D}$ -60 (c 0.05, MeOH); UV (MeOH) λ_{max} (log ε) 275 (2.91) nm; ^{1}H- and ^{13}C-NMR data see **Tab. 17**; HRESIMS *m/z* 361.3102 $[M+H]^{+}$ (calculated for $C_{24}H_{41}O_2$, 361.3101)

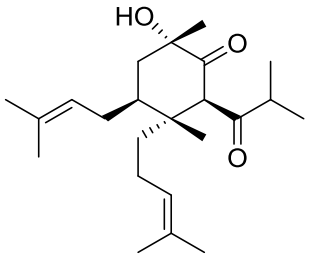	**15 – Triquetriirinon D** *(2R, 3R, 4S, 6S)-2-isobutyryl-3,6-dimethyl-3-(4-methylpent-3-en-1-yl)-4-(3-methylbut-2-en-1-yl)-6-hydroxy-cyclohexan-1-one* Greenish oil (0.64 mg); $[\alpha]^{24}_{D}$ +38 (c 0.05, MeOH); UV (MeOH) λ_{max} (log ε) 280 (3.21) nm; ^{1}H- and ^{13}C-NMR data see **Tab. 17**; HRESIMS *m/z* 363.2899 $[M+H]^{+}$ (calculated for $C_{23}H_{39}O_3$, 363.2894)

3.1.4.3 Other compounds

In addition to the above described substances, other substances were also isolated from *H. triquetrifolium* in course of the present work. They are: two fatty acids and three flavonoids. All these compounds were previously isolated from the species and are therefore known to be present in the plant.

16 – α-Linolenic acid (ω-3, C18:3)
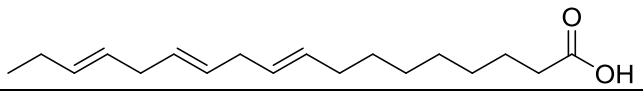
17 – Linoleic acid (ω-6, C18:2)
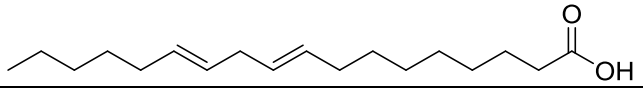

18 – Rutin *Quercetin-3-O-rutinoside*	**19 – Astragalin** *Kaempferol 3-O-glucoside*	**20 – Hyperoside** *Quercetin-3-O-galactoside*
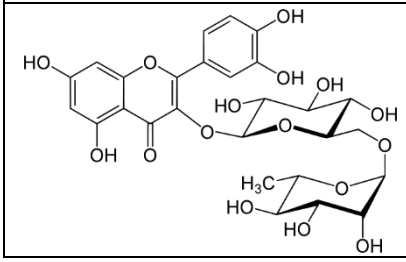	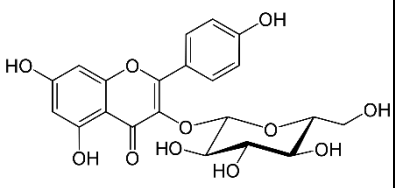	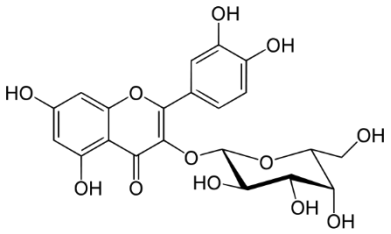

3.1.5 Discussion of isolation and structure elucidation

Compound **1** (Triquetriborin) refers to type B(I) acylphloroglucinol (**Fig. 15**). However, according to (Dakanali and Theodorakis, 2011) type B(I) compounds have got a quaternary carbon and two methyl groups, attached to it in position 8 as in clusianone, unlike Triquetriborin (**Fig. 101**).

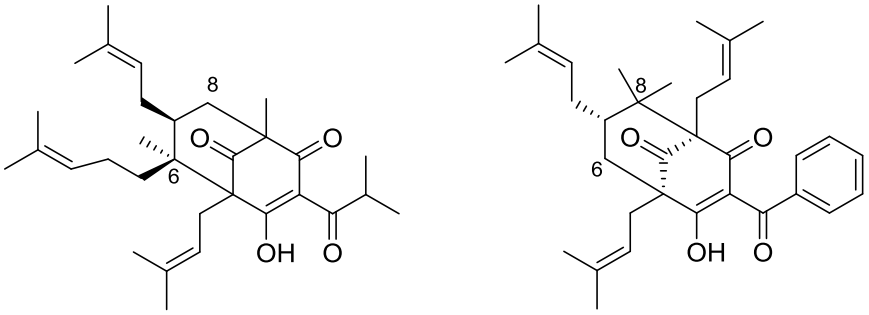

Triquetriborin **Clusianone**

Fig. 101. Comparison of structures of Triquetriborin and Clusianone.

Compounds of B(I) type were previously reported in *Hypericum* herbs, belonging to sections 17, 20, 26, 27 and sub-section 9c (Schmidt and Heilmann, 2013). The latter comprises one representative, *H. sampsonii*, which accumulates clusianone (Hu and Sim, 2000) (**Fig. 101**). This is the first ever report of type B(I) acylphloroglucinol presence in *Hypericum*, belonging to section 9. This also confirms chemotaxonomic relations between herbs from sections 9 and 9c. Therefore, the first principal difference between **1** and clusianone lies in the character of the starter acid (aliphatic or aromatic), type of main core structure cyclisation and stereo configuration. The main structural difference regarding the carbon skeleton is the ring closing from C-1 to C-5 which started in clusianone most probably from a precursor substituted at C-5 with two prenyl rests, whereas the precursor of triquetriborin started from a prenyl group substituted at C-1.

Compounds **2** and **3** (Triquetrijakobin A and B) are bicyclic acylphloroglucinols with 3-ortho-pyrano cyclisation type (**Fig. 16**). They both have a hydroxyl group in the main core, which builds a hydrogen bond with the oxygen of a starter acid's keto group. These compounds possess a specific and unusual aliphatic side chain, built of three isoprene rests: it consists of a "long chain" (1'' – 10'') and a "short chain" (11'' – 15''). The long chain consists of 10

carbons, but it is not a geranyl rest. Each separate isoprene rest is numbered in blue, red and black for better overview (**Fig. 102**). This unusual aliphatic side chain discovered during this work shall receive a trivial name "*evgenyl*".

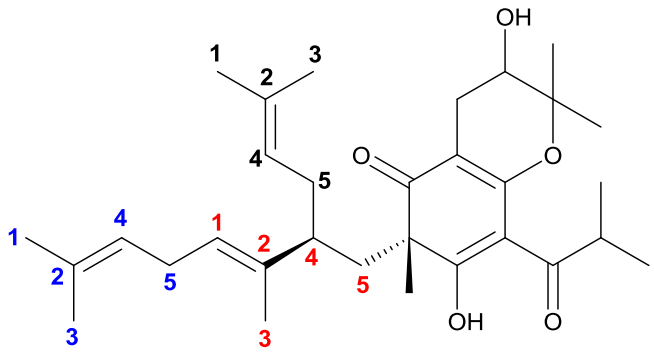

Fig. 102. Overview of Triquetrijakobin A's aliphatic side chain.

Compound with similar structure was isolated from *H. erectum* (Ishida et al., 2010) (section 9), and is called otogirinin G (**Fig. 103**). This compound has similar main core (hydroxyl group in position 7 instead of keto group in Triquetrijakobins), but differs in aromatic starter acid and geranyl rest in position 8. The structural similarity of both secondary metabolites isolated from two species of the same section once again proves the chemotaxonomical relation between both species.

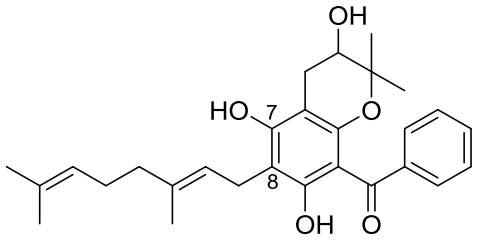

Fig. 103. Structural formula of Orotiginin G, isolated from *H. erectum* (section 9).

Compounds **4**, **5** and **6** (Triquetrireboudin A, B and C) belong to type A 3-ortho-pyrano polycyclic acylphloroglucinols (**Fig. 15** and **16**). Their structure reminds hyperforin a lot (**Fig. 11**) with only two differences: methyl group in position 9 instead of an isoprene, as well as cyclised isoprene in position 7. Thus these compounds might possess high biological activity like hyperforin itself, what has to be proven in further assays.

Compounds **7**, **8** and **9** (Triquetrikotelin A, B and Triquetriroxettin) are also type A polycyclic acylphloroglucinols, but their cyclisation happens to form a rare 5-para-pyrano system (**Fig.**

16). All three compounds are very much the same, with the only difference in **8**: 2-methylbutyric acid as a starter acid and **9**: isoprene chain in position 12.

Compound **10** (Triquetribavarin) is a type A polycyclic acylphloroglucinol with 7-oxabicyclo[2.2.1]heptane-2,6-dione core. This structure is unusual, however already known: at least two substances with the similar configuration were previously isolated (**Fig. 104**). An oxidated hyperforin analogue 8-hydroxyhyperforin 8,1-hemiacetal was isolated from *H. perforatum* (section 9) (Verotta et al., 2000). Hyperfoliatin was first isolated from *H. perfoliatum* (section 13) (Benkiki et al., 2003); a year later the same substance was also isolated under the name "Hyperibone J" from *H. scabrum* (section 17) (Tanaka et al., 2004). These two compounds are oxidated hyperforin analogues. Hyperibine J isolated from *H. triquetrifolium* (Mitsopoulou et al., 2015) is an obvious precursor of hyperibone J, which in turn can be a precursor of **10**.

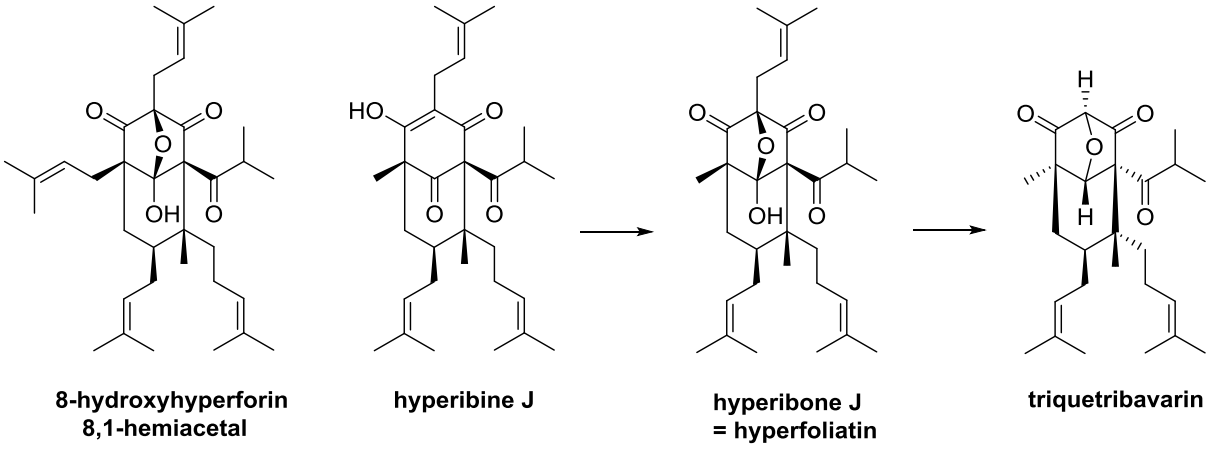

Fig. 104. Comparison of structural similarities between 8-hydroxyhyperforin 8,1-hemiacetal, Hyperibine J, Hyperibone J (Hyperfoliatin) and Triquetribavarin.

(-)-Yezo'otogirin C was first-ever isolated from *H. yezoense* MAXIM. (Tanaka et al., 2009). This herb belongs to Section 9 along with *H. perforatum* and *H. triquetrifolium* (§ 1.1.2, **Fig. 2**).

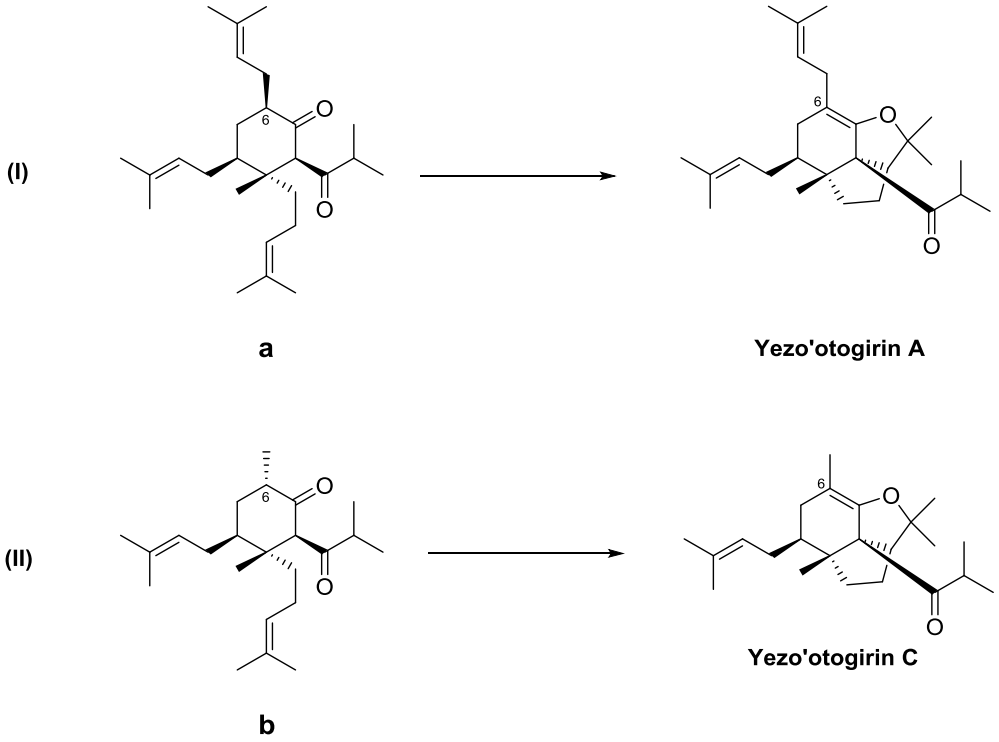

Fig. 105. Proposed theories of yezo'otogirin A and C biosynthesis (Tanaka et al., 2009; He et al., 2014).

Compound depicted on **Fig. 105**, **a** was first-ever isolated from *H. perforatum* as a hyperforine analogue (Shan et al., 2001) and later also from *H. yezoense* alongside yezo'otogirins A-C (Tanaka et al., 2009). Tanaka et al. suggested a plausible biogenetic pathway, where yezo'otogirin A derives from (**a**) via an intramolecular cyclization (**Fig. 105**, **(I)**).

Inspired by this idea, a group of Chinese scientists developed a biomimetic synthesis of (±)-yezo'otogirin C via an oxidative cascade cyclization (He et al., 2014). A substrate (**Fig. 105**, **b**) was initially synthesized from 3-methyl-4-isoprene-cyclohex-2-en-1-one. Since the originally proposed synthesis was conducted via 2 pathways, one of which led to formation of highly instable intermediates, the same working group improved their theory and presented another vision of the same process (Yang et al., 2015a). In the latter case, the substrate synthesis is suggested from cyclohexane-1,3-dione and biomimetic pathways to yezo'otogirin C were investigated under aerobic and anaerobic conditions, both are found to be feasible pathways to the natural product depending on the physiological conditions. A

shortened scheme of the improved yezo'otogirin C biosynthesis theory is presented in **Fig. 106**.

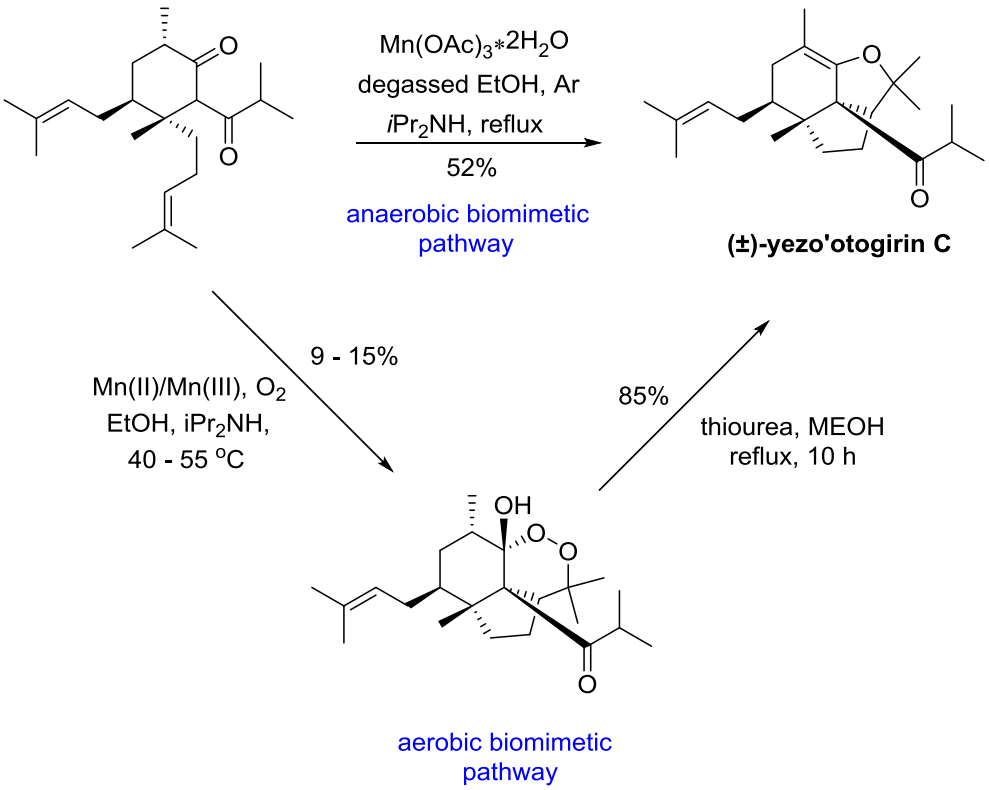

Fig. 106. Schematic biosynthesis theory of Yezo'otogirin C (Yang et al., 2015a).

Therefore, the initial substrates for yezo'otogirins A and C (**Fig. 105**) differ in substituents in position 6 – isoprene- or methyl-group respectively. The substrate for yezo'otogirin A was isolated from the living plant, while the one for yezo'otogirin C was synthesised organically.

In the course of this work, substance (**Fig. 105**, **b**) was isolated from the living herb for the first time. It was isolated from a sub-fraction close to that, from which yezo'otogirin C was isolated as well. This confirms the suggestion of He et al. and proves that (**Fig. 105**, **b**) which received a trivial name of **Triquetriirinon A** in the course of the present work, must really be a biosynthetic precursor of yezo'otogirin C, one of the main constituents of several *Hypericum* herbs of section 9.

It should be also noted, that unlike isolated from *H. yezoense* (-)-yezo'otogirin C, the one isolated from *H. triquetrifolium* possesses different stereo configuration, according to its

NOESY spectra and is (+)-yezo'otogirin C. According to the literature research, this is the first report of a (+)-yezo'otogirin C isolation from a living herb.

A group of substances **12-15** (Triquetriirinons A-D) was also isolated from *H. triquetrifolium* for the first time. Compound **13** (Triquetriirinon B) was only isolated in a mixture with **12**. The only difference between **12** and **13** is the reversed position of an isoprene rest and a $–CH_3$ group. Chemical **14** differs from **12** in a character of its starter acid, while **15** does also possess a hydroxyl group in position 6. All these compounds are believed to be phloroglucinol analogues and/or precursors.

Biosynthesis of **15** is believed to be mostly the same as for acylphloroglucinols, with the only one difference: malonate and acetate react with each other in this case in ratio 1:1 (**Fig. 107**).

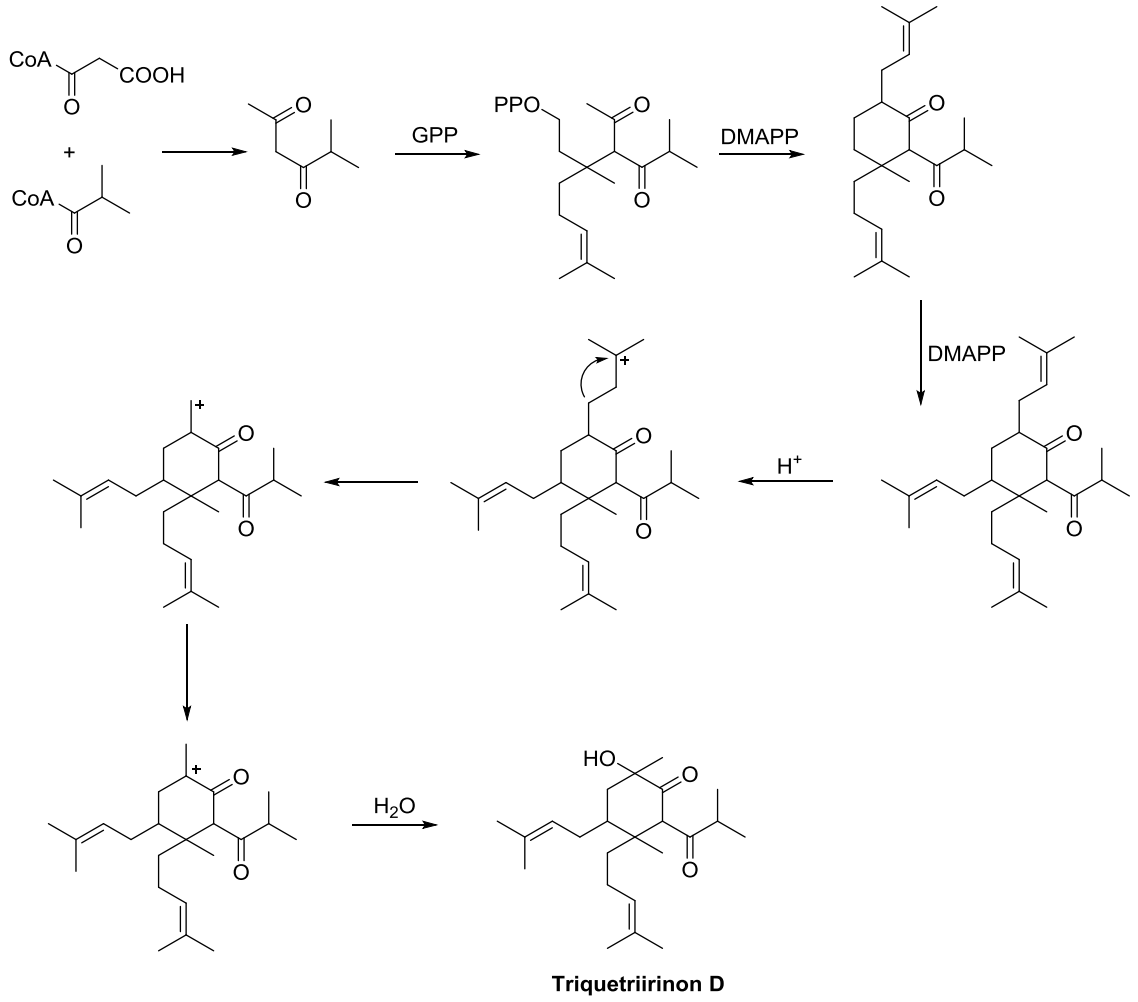

Fig. 107. Proposed biosynthesis of Triquetriirinon D; inspired by (Gao et al., 2016).

Omega-3 and omega-6 fatty acids are rare in herbs, however known for several representatives of the genus *Hypericum*. Acids **16** (α-Linolenic) and **17** (Linoleic) were isolated by (Hosni et al., 2007). Flavonoid **18** (Rutin) was described in *H. triquetrifolium* by (Cirak et al., 2011) while **19** (Astragalin) and **20** (Hyperoside) were found in this herb by (Conforti et al., 2002).

3.1.6 Conclusion and summary on phytochemical experiments

Hypericum triquetrifolium TURRA belongs to section 9 along with *H. perforatum*, the most famous and widely used today representative of the genus. Several studies were conducted on *H. triquetrifolium*'s phenolic constituents and its essential oil composition; however its acylphloroglucinol spectrum was poorly explored.

For this purpose, *H. triquetrifolium* was collected in summer 2012 on Golan Heights, Israel from wild nature. It was dried and subsequently extracted with different solvents. Petroleum ether extract was separated using various chromatographic methods (CPC, Flash column chromatograph, RP-HPLC), yielding in 17 compounds: 10 acylphloroglucinols, 5 hyperforin analogues and 2 fatty acids. Also 3 flavonoids from methanolic extract were obtained.

All isolated acylphloroglucinols are new, previously unknown compounds. They belong to different phloroglucinol types, characteristic for section 9, therefore, confirming taxonomic relationship between species. Moreover, a compound of type B(I) was isolated: this phloroglucinol type was previously unknown for the section. Isolated B(I) type compound possesses unusual rare structure, thus leaving food for reflection and further studies and investigations.

During the isolation and separation process CPC showed very inspiring results: method resulted in numerous diverse sub-fractions, which were almost clear and ready to final stage separation on semi-preparative HPLC. It is positively suggested to use CPC for future works with PE extracts. Semi-preparative RP-HPLC method with water and MeCN (20:80, MeCN → 100%) is also noted as a good enough one for isolation of acylphloroglucinols. The herb undoubtedly comprises much wider spectrum of phloroglucinol derivatives, ca. 30-40 more compounds might be isolated, thus completing the knowledge about its unpolar phenolic constituents.

3.2 Cell culture experiments

In order to pharmacologically characterise newly isolated substances from *H. triquetrifolium*, they were tested in MTT assays on neurotoxicity and neuroprotection on HT-22 cells. This continues a row of acylphloroglucinols' neuroprotection studies, conducted on Pharmaceutical Biology department of the University of Regensburg (Pitzl et al., 2015).

3.2.1 General amendments: solvent's influence on the cells

Pure DMSO solution for molecular biology (§ 2.2.2) was used to solve the investigated substances and to prepare 0.1 M stock solutions (stored in freezer). Straight before conducting a single experiment, each stock solution was diluted with growth medium in ratio 1:2000 in order to prepare a 50 µM stock solution. The latter was then used to produce a dilution series 1 µM, 5 µM, 10 µM and 25 µM, which were the investigated concentrations. DMSO concentration in each case was, therefore, 0.001%, 0.005%, 0.01% and 0.025% respectively.

In order to evaluate the influence of the solvent on the HT-22 cells, three independent successive experiments were performed with DMSO concentrations 0.01%, 0.025% and 0.05% in growth medium (**Fig. 108**). Data analysis shows no significant influence of DMSO on the cells in its highest used concentration (0.025%) and lower. Therefore, the impact of the solvent during the tests may be neglected.

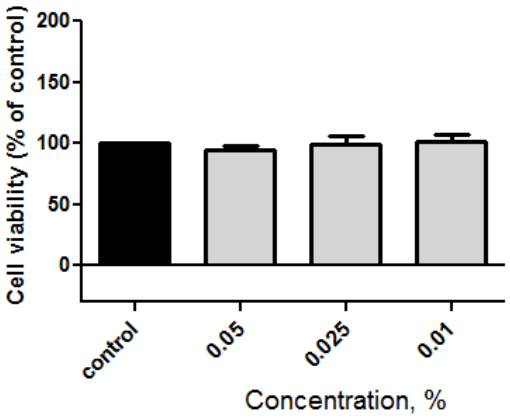

Fig. 108. Impact of DMSO on HT-22 cells.

3.2.2 Neurotoxicity and neuroprotection of acylphloroglucinols

Isolated acylphloroglucinols were tested on neurotoxicity and neuroprotection *in vitro* (§ 2.2).

Desired are low or absence of any toxicity in highest tested concentration (25 µM), as well as high neuroprotective potency in lowest tested concentrations (1-5 µM). Neuroprotection effect of the investigated compounds should be close to or exceed the one of quercetin (positive control). Obtained data results may be observed from **Tab. 18**.

Tab. 18. Neurotoxicity and neuroprotection assays for isolated acylphloroglucinols.

Neurotoxicity assay	Neuroprotection assay
(1) Triquetriborin	
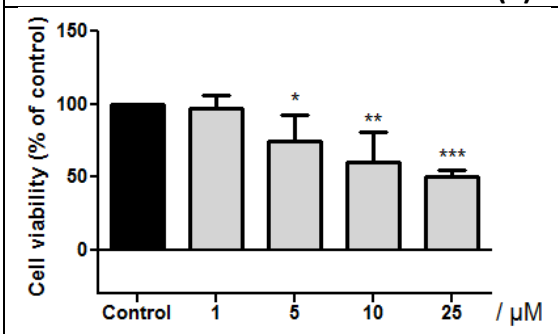	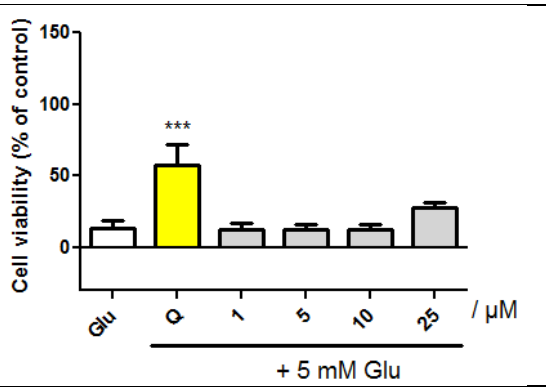
(2) Triquetrijakobin A	
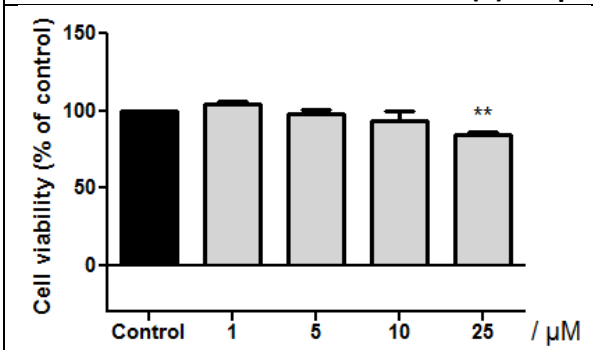	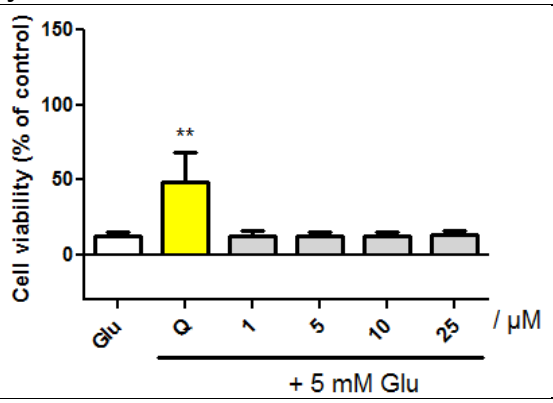

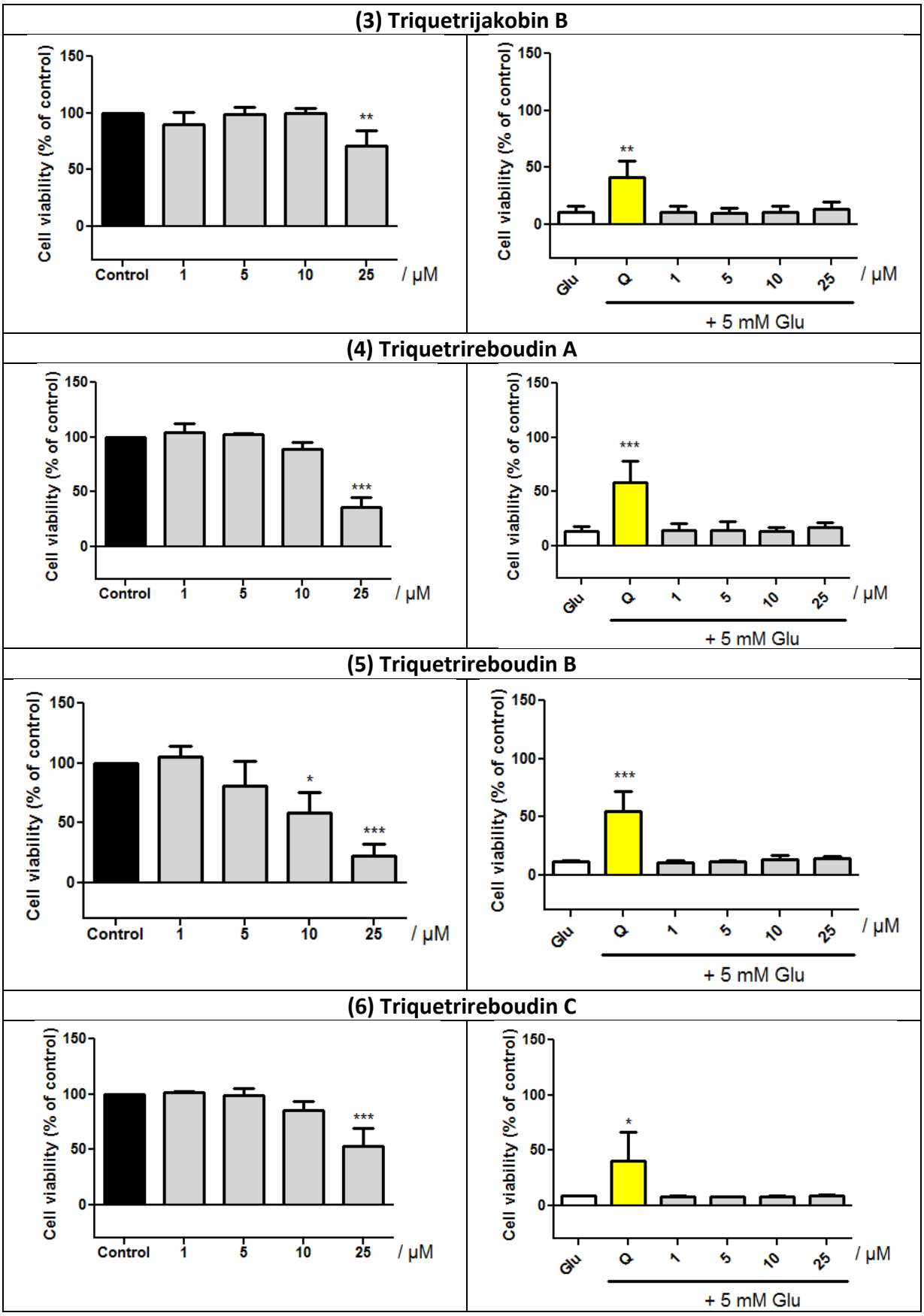
(3) Triquetrijakobin B
Cell viability (% of control)
150
100
50
0
**
Control
1
5
10
25
/ µM
Glu
Q
1
5
10
25
/ µM
+ 5 mM Glu
(4) Triquetrireboudin A
***
(5) Triquetrireboudin B
*
***
(6) Triquetrireboudin C

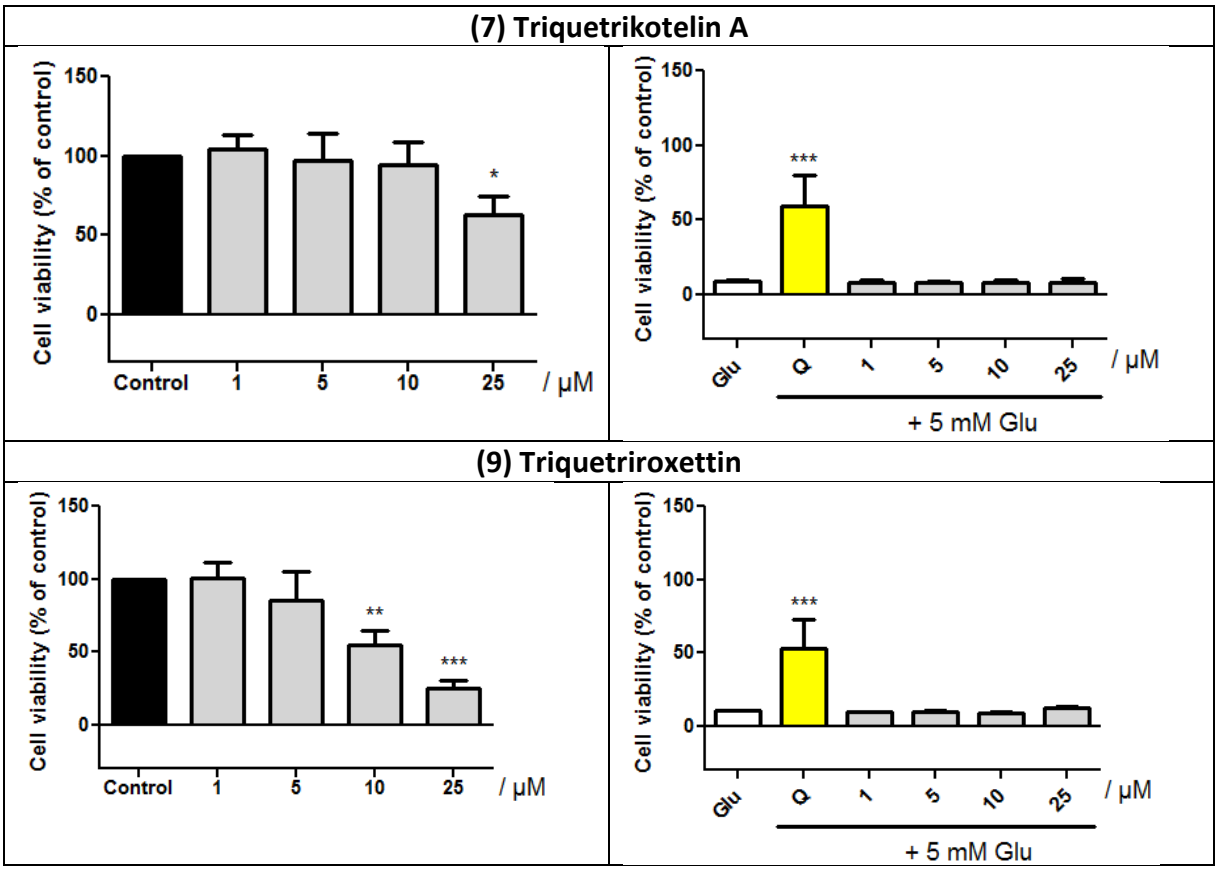

Control – untreated cells, taken as 100%. 1, 5, 10, 25 µM – concentrations of the investigated compounds. Glu – 5 mM glutamate [negative control]. Q – quercetin in DMSO with 5 mM glutamate in growth medium [positive control]. In neuroprotection assay all means are expressed as percent to control, i.e. untreated cells, taken as 100%.

Data were subjected to one-way ANOVA followed by Dunnett's multiple comparison post-test using GraphPad Prism 5.03 software. Levels of significance are: $p < 0.05$ (*), $p < 0.01$ (**) and $p < 0.001$ (***).

3.2.2.1 Evaluation of results and discussion

All investigated acylphloroglucinols express dose-dependent in-vitro toxicity on HT-22 cells. Tested compounds may be divided in two groups. First group unites compounds, which are toxic in low concentrations (≥ 5 µM) and their toxicity rises drastically with the rise of the concentration (**1**, **5** and **9**). Substances of the second group show almost no influence on the cells at ≤ 10 µM, but are significantly toxic at 25 µM (**2**, **3**, **4, 6** and **7**). When compared to work of Pitzl et al. (Appendix, § 7.2), compounds **UR-QS-7**, **UR-QS-8** and **UR-QS-14** may be refered to the first group, while **UR-QS-2** and **UR-QS-4** refer to the second. Furthermore, Pitzl et al. has some phloroglucinols which are not toxic for HT-22 cells in concentrations ≤ 25 µM (**UR-QS-1** and **UR-QS-12**).

By comparing similar structures and their effect, for example, **7** and **9** – additional isoprene rest (lipophilic aliphatic chain) in position 12 seems to make **9** more toxic. In addition, stereo

chemistry of various chiral centers is not clear, e.g. positions 4, 6 and 10, which may also change the look of the molecule critically and therefore its effects on the cells. Consequently the spatial arrangement of atoms plays a key role in substances' biological effects, when comparing **4** and **5**. Both compounds possess the same skeleton, but differ in stereo chemistry. Their influence on the HT-22 cells is also very diverse. However, **4** and **6** seem to be quite similar, and an additional $–CH_2–$ group in starter acid of **6** does not play any important role in exhibiting the chemical's toxicity.

None of the tested compounds exhibit any neuroprotective properties in the model used, except for **1**. It possesses very slight protective activity at 25 µM. However, **1** is shown to be toxic in high concentrations and its protectivity action is apparently overlaid by its deleterious effect.

When compared to the results of (Pitzl et al., 2015) (Appendix, § 7.2), where several acylphloroglucinols show protective effects, the structural difference between the investigated chemicals should be noted. Most compounds tested by Pitzl et al. exhibit neuroprotective effects at ≥ 25 µM, however, at the same time, some of them are toxic for HT-22 cells at ≥ 10 µM and their protective effects do not overcome the one of quercetin, as positive control.

Among non-toxic protective compounds are simple monocyclic acylphloroglucinols with long aliphatic geranyl chain (**UR-QS-1**) and two similar bicyclic (5-para-pyrano type, **Fig. 16**) non-prenylated chemicals with substituted aromatic started acid (**UR-QS-12** and **UR-QS-14**). These compounds differ from those, tested in the course of the present work. And despite the fact that substances **7** and **9** are also 5-para-pyrano type acylphloroglucinols, they are PPAPs and also possess additional ring and 1 or 2 isoprene chains, which may increase the lipophilicity of the molecule.

Non-prenylated compounds with hydroxylated and/or methoxylated aromatic starter acid (**UR-QS-12** and **UR-QS-14**) look very much like flavonoids, for example, quercetin. In this case, starter acid aromatic ring may play the role of flavonoid's "B"-ring. Therefore, these substances exhibit their neuroprotective properties most probably in the same way as flavonoids.

Interesting is to compare the results of toxicity tests of **2** with **UR-QS-1**. Both compounds posess long aliphatic lypophilic side chain, which *inter alia* may be responsible for non-toxicity of the substances.

Tested by Pitzl et al. **UR-QS-4** is a 3-ortho-pyrano bicyclic phloroglucinol with intramolecular hydrogen bond, compared to **2** and **3**. These compounds are the same in being non-toxic at ≤ 10 µM and slightly toxic or really toxic at ≥ 25 µM. **UR-QS-4** however expresses insufficient protection effects (< 50%), while **2** and **3** are non-protective at all. Compounds **4** and **6** of the same bicyclic 3-ortho-pyrano type express almost the same toxicity as **UR-QS-4**, but protection tests are once again different. Compound **5** differs in its toxicity properties from **UR-QS-4** most probably because of its odd stereo configuration.

All in all *in-vitro* neurotoxicity effects of acylphloroglucinols are very difficult to predict. Sometimes the issue is about substituents in aromatic starter acid (**UR-QS-7** *versus* **UR-QS-12**) or in stereo configuration (**4** *versus* **5**, and probably **7** *versus* **9** [?]). Good protective properties exhibit small mono- or bicyclic compounds either non-prenylated or those, possessing a long aliphatic chain. Polyhydroxylated/methoxylated aromatic starter acids play a critical role in exhibiting strong protective activity alongside a relative absence of neurotoxicity.

Important is also to note that prenylated acylphloroglucinols are recently proved to exhibit significant neuroprotection *in vitro* (Gao et al., 2016). These assays were however conducted on SK-N-SH cells (human neuroblastoma cell line) and not on HT-22 (mouse hippocampal cell line). Although the cells types differ, it may be suggested to test the same compounds on SK-N-SH model to ensure their biological potency character and to compare the results to those, obtained on HT-22 cells.

3.2.3 Neurotoxicity and neuroprotection of possible precursors

Current paragraph presents results of neurotoxicity and neuroprotection MTT assays on HT-22 cells for isolated possible acylphloroglucinol precursors. Graphs may be observed from **Tab. 19**.

Tab. 19. Neurotoxicity and neuroprotection assays for possible phloroglucinol precursors.

Neurotoxicity assay	Neuroprotection assay
(11) (+)-Yezo'otogirin C	
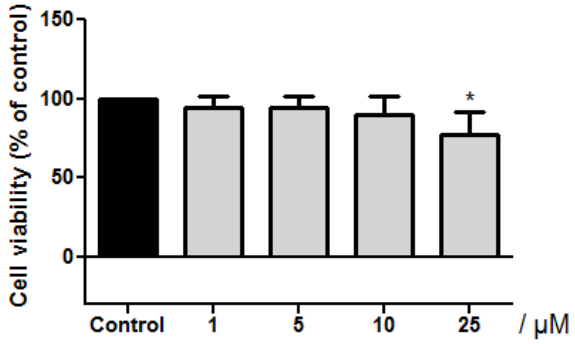	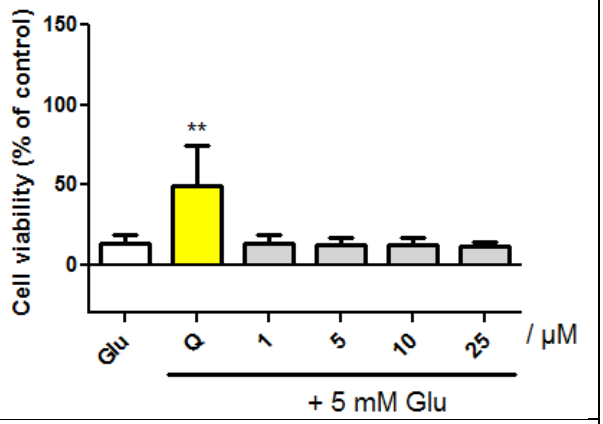
(12) Triquetriirinon A	
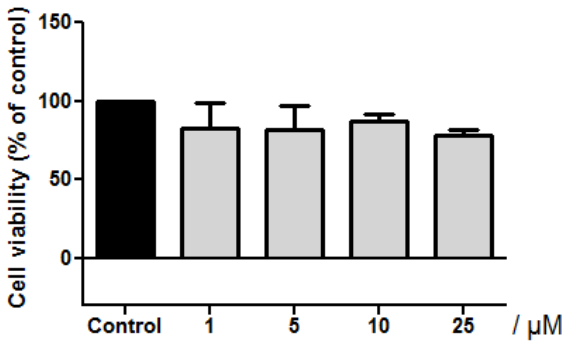	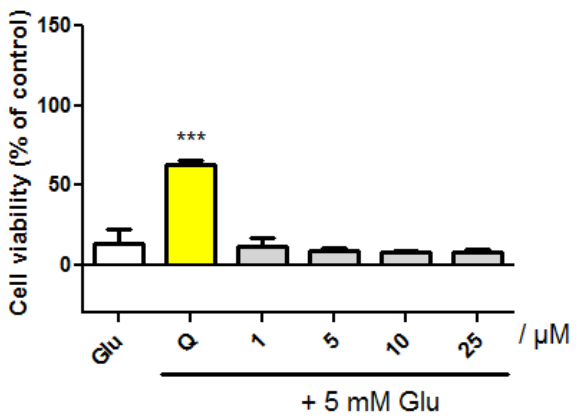
(14) Triquetriirinon C	
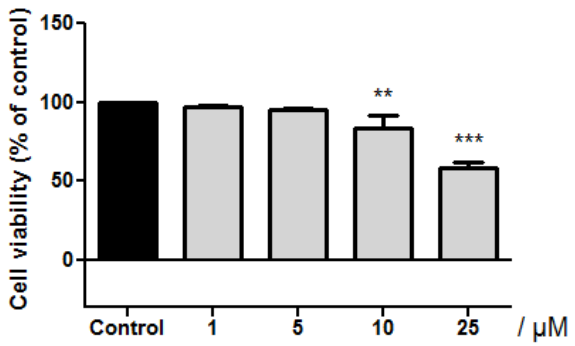	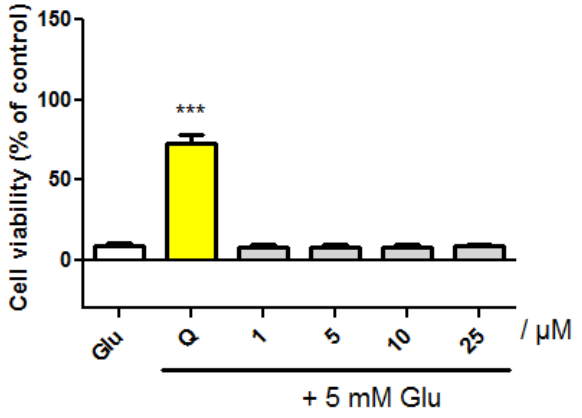

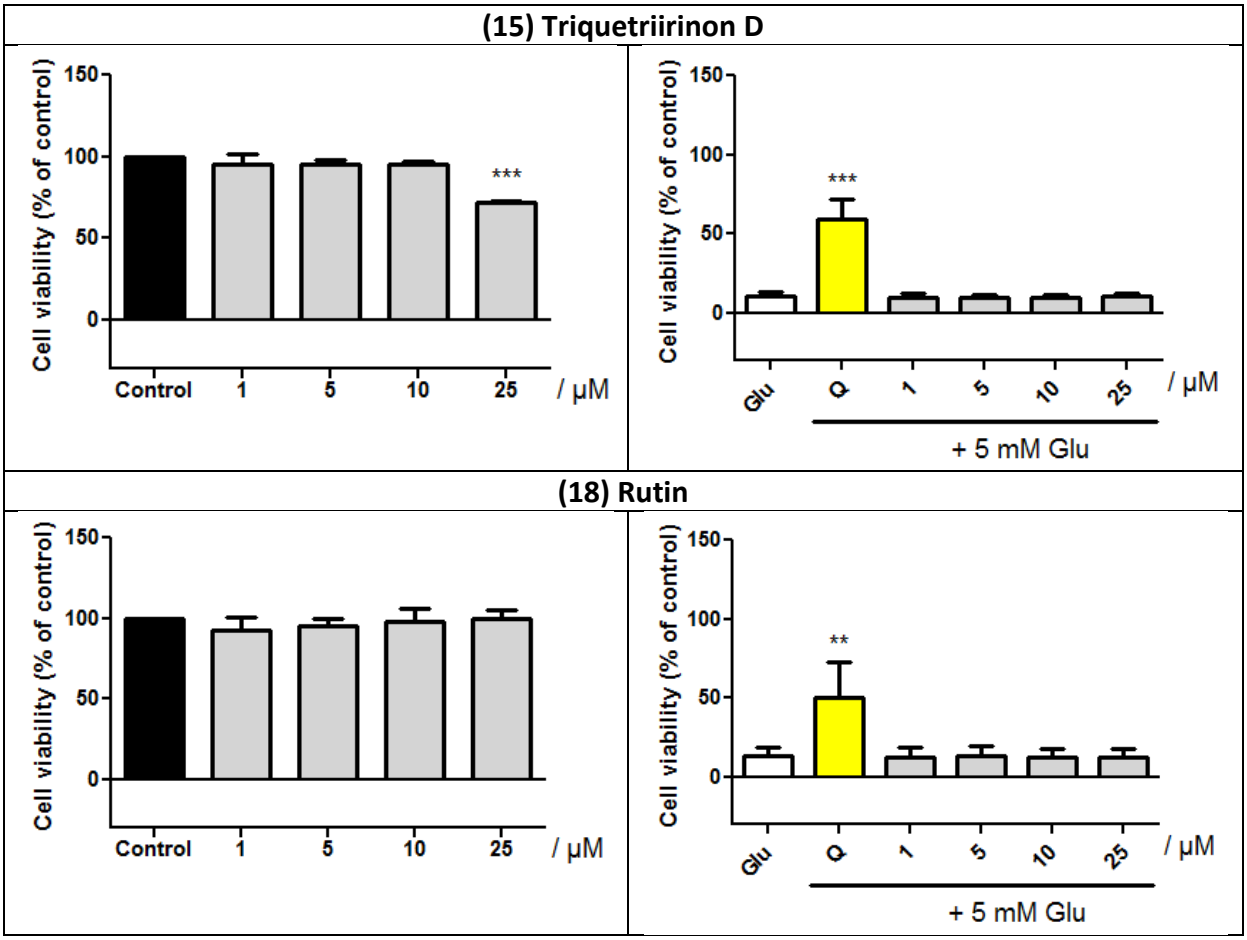

Control – untreated cells, taken as 100%. 1, 5, 10, 25 µM – concentrations of the investigated compounds. Glu – 5 mM glutamate. Q – quercetin in DMSO with 5 mM glutamate in growth medium. In neuroprotection assay all means are expressed as percent to control, i.e. untreated cells, taken as 100%.
Data were subjected to one-way ANOVA followed by Dunnett's multiple comparison post-test using GraphPad Prism 5.03 software. Levels of significance are: $p < 0.05$ (*), $p < 0.01$ (**) and $p < 0.001$ (***).

3.2.3.1 Evaluation of results and discussion

All tested possible phloroglucinol precursors are almost non toxic at ≤ 10 µM, while 25 µM might be slightly toxic. Flavonoid rutin (**18**), as might be expected, shows no toxicity in tested concentrations. As well as in acylphloroglucinols, toxicity of their possible precursors is dose-dependent. None of the investigated compounds exhibit protective activity in Glu-induced neurotoxicity assay.

If comparing tested possible phloroglucinol precursors with tested prenylated acylphloroglucinols (§ 3.2.2), the latter possess more complicated structure. Hyperforin analogues (Triquetriirinons) are simple monocyclic compounds with two isoprene rests, while yezo'otogirin C is tricyclic condensed and rutin is a glycoside between the flavonol

quercetin and the disaccharide rutinose. These chemicals' uncomplicated structure might be the reason of their neurotoxicity mild expression.

Despite their low toxicity, precursors, however, do not possess any neuroprotective properties on the investigated model. When compared to potent monocyclic acylphloroglucinols tested by (Pitzl et al., 2015), the latter differ in aromatic character of the main phloroglucinol core, long aliphatic side chain (geranyl) and large number of hydroxyl groups. As such, **UR-QS-1** tested by Pitzl at el. is not toxic for HT-22 cells at ≤ 25µM, but unlike tested possible phloroglucinol precursors it exhibits strong protective effect at 25 µM.

Apparently for showing fine protective properties, a molecule should posess an aromatic main core, long aliphatic lipophilic chain and hydroxylated-methoxylated aromatic starter acid (thus reminding the structure of a flavonoid, e.g. quercetin, used as a positive control for the tests).

3.2.4 Conclusion and summary on cell culture experiments

Prenylated acylphloroglucinols isolated in course of the present work express low to moderate toxicity, however, they show no protection effects. Possible phloroglucinol analogues isolated during this work were also tested on the same model. They are almost non toxic for these cells, but at the same time do not express any neuroprotectivity either.

When compared to work conducted on Pharmaceutical Biology department of the University of Regensburg (Pitzl et al., 2015) before, some structural differences between tested substances can be noted. However, a clear distinction between the structure and its biological properties is yet very difficult to make.

Possible is to obtain compounds via organical synthesis, which might structurally be a "mean" between the tested non-toxical and efficient protective chemicals. This, however, requires a vast list, i. e. database of already tested compounds.

Advice for the future work includes testing the isolated and/or similar compounds on human neuroblastoma SK-N-SH cells. This line was established from metastatic tumor in the bone marrow of a 5-year-old girl who had consistently elevated urinary vanillylmandelic acid and catecholamine excretion (Helson et al., 1975). Several studies on neuroprotection and antioxidation have already been conducted with this model (Bar-Am et al., 2009).

Acylphloroglucinols exhibit neuroprotection effects in concentration 10 μM on these cells (Gao et al., 2016), while flavonoids, e. g. astragalin, are proved to reduce oxidative stress in SK-N-SH model as well (Chung et al., 2016) and can be used as positive control. Interesting is to conduct parallel tests of acylphloroglucinols and their possible precursors on both SK-N-SH and HT-22 cells at the same time, thus comparing two models.

4 Summary

Herbs of the genus *Hypericum* are widely spread all around the world and are being used in both traditional and officinal medicine in most countries and territories of the planet. Native to the Mediterranean region *Hypericum triquetrifolium* TURRA, a close relative to the most famous member of the genus *Hypericum perforatum* L., is well studied on flavonoids and especially on its essential oil composition. However, its acylphloroglucinol derivatives spectrum was almost unknown.

The herb's aerial parts were collected, dried and extracted. With the help of NMR-guided fractionation strategy, petroleum ether and methanolic extracts underwent further separation by means of various chromatography methods like CPC, Si-gel and RP-18 Flash column chromatography, as well as semi-preparative reversed-phase HPLC. Obtained are twenty compounds of different structure, including previously unknown prenylated acylphloroglucinols of several types, their possible precursors, hyperforin analogues, fatty acids and flavonoids. Compounds' structures were elucidated with 1D- and 2D-NMR methods and confirmed with MS. Newly isolated chemicals were characterised by means of UV and specific rotation, as well as by CD spectra.

The spectrum of isolated compounds corresponds with the one, known for other representatives of the section, thus confirming taxonomic relationships between species. PPAP of type B(I) was also isolated, and this is the first report of such a compound for section 9 representatives. Biosynthesis of yezo'otogirin C, one of the main constituents of the herbs from section 9 was also confirmed: its theoretically proposed precursor was isolated from the living plant for the first time from the sub-fraction close to that of the yezo'otogirin C itself.

Isolated in sufficient quantities phloroglucinols were tested on neurotoxicity and neuroprotection on HT-22 cells in MTT assays. Neurotoxicity of the tested compounds differs from low to moderate, however none of them expresses any neuroprotective properties in this model.

5 List of abbreviations

1D – one-dimentional
12-LOX – 12-lipoxygenase
2D – two-dimensional
Å – ångström
AAR – anisaldehyde reagent in sulfuric acid = derivatized with anisaldehyde/H_2SO_4 reagent
Aβ – amyloid-β
AChE – acetylcholinesterase
AD – Alzheimer's disease
ADP – adenosine diphosphate
AIF – apoptosis-inducing factor
ALS – amyotrophic lateral sclerosis
AMPA – α-amino-3-hydroxy-5-methyl-4-isoxazolepropionic acid
ATP – adenosine triphosphate
BPAPs – bicyclic polyprenylated acylphloroglucinols
ca. – from Latin *circa* = "around" = "about"
cat. no. – catalogue number
CD – circular dichroism
$CDCl_3$ – deuterated chloroform
cGMP – cyclic guanosine monophosphate
CJD – Creutzfeld-Jakob disease
CNS – central nervous system
CoA – coenzyme A
COSY – correlation spectroscopy
CPC – centrifugal partition chromatography
δ – chemical shift, ppm
DLB – dementia with Lewy bodies
DMAPP – dimethylallyl pyrophosphate = dimethylallyl diphosphate
DMEM – Dulbecco's Modified Eagle Medium
DMSO – dimethyl sulfoxide
DNA – deoxyribonucleic acid
DOXP – 1-deoxy-D-xylulose 5-phosphate
EDTA – ethylenediaminetetraacetic acid = ethylenediaminetetraacetate
e.g. – from Latin *exempli gratia* = "for example"
et al. – from Latin *et alii* = and others
etc. – from Latin *et cetera* = "and other things" = "and so forth"
EtOAc – ethyl acetate
EtOH – ethanol
EU – European Union
FCS – fetal calf serum = fetal bovine serum

FCS HI – heat-inactivated fetal calf serum
Fig. – figure
Glu – glutamate = glutamic acid
GPP – geranyl diphosphate
GSH – glutathione
GTP – guanosine triphosphate
h – hour, hours
H. – *Hypericum*
HIV – human immunodeficiency virus
HMBC – heteronuclear multiple-bond correlation spectroscopy
HPLC – high-performance liquid chromatography
HSQC – heteronuclear single-quantum correlation spectroscopy
Hz – hertz
i.e. – from Latin *id est* = "in other words" = "which means"
iNOS – cytokine-inducible nitric oxide synthase
IPP – isopentenyl pyrophosphate
IUPAC – International Union of Pure and Applied Chemistry
J – coupling constant, Hz
JPND – EU Joint Programme – Neurodegenerative Disease Research
K – Kelvin
L – liter
LC_{50} – lethal concentration 50
MAPK – mitogen-activated protein kinase
ME – methanolic extract
MeCN – acetonitrile
MeOH – methanol
MEP – 2-methylerythritol 4-phosphate
MHz – megahertz
MIT – Massachusetts Institute of Technology
MPAPs – monocyclic prenylated acylphloroglucinols
MS – mass spectrometry
MTT – 3-(4,5-dimethylthiazol-2-yl)-2,5-diphenyltetrazolium bromide
mult – multiplicity
m/z – mass-to-charge ratio
MVA – mevalonic acid
NADH – nicotinamide adenine dinucleotide
NADPH – nicotinamide adenine dinucleotide phosphate
NDs – neurodegenerative diseases = neurodegenerative disorders
NMDA – N-methyl-D-aspartate
NMR – nuclear magnetic resonance

NOESY – nuclear Overhauser effect spectroscopy
p.a. – for analysis
PBS – phosphate buffered saline
PE – petroleum ether, petroleum ether extract
PKS – polyketide synthase
PPAPs – polycyclic prenylated acylphloroglucinols
ppm – parts per million
PRC – People's Republic of China
PT – prenyltransferase
R_f – retardation factor = retention factor
RNS – reactive nitrogen species
ROS – reactive oxygen species
RP-18 – reversed-phase octadecyl carbon chain (C18)-bonded silica gel
rpm – revolutions per minute
RT – room temperature
sGC – soluble guanylylcyclase
SDS – sodium dodecyl sulphate
Si-gel – silica gel
subsect. – subsection
Tab. – table
TCM – traditional Chinese medicine
TLC – thin-layer chromatography
TNF-α – tumor necrosis factor alpha
t_R – retention time
TRPC6 – transient receptor potential cation channel, subfamily C, member 6
US – United States [of America]
USA – United States of America
UV – ultraviolet

6 List of references

Abbott A. (2016): More evidence emerges for 'transmissible Alzheimer's' theory. *Nature*, Published online 26 January 2016 , doi:10.1038/nature.2016.19229.

Abu-Irmaileh B., (1982): Weeds of Jordan. University of Jordan, Amman, Jordan. 433 pp.

Åkerborg Ö., Lang A., Wimo A., Sköldunger A., Fratiglioni L., Gaudig M., Rosenlund M. (2016): Cost of Dementia and Its Correlation With Dependence. *J. Aging Health.*, pii: 0898264315624899. [Epub ahead of print]

Al-Bakri A. G., Afifi F. U. (2007): Evaluation of antimicrobial activity of selected plant extracts by rapid XTT colotimetry and bacterial enumeration. *J. Microbiol. Methods*, 68(1): 19-25.

Al-Chalabi A., Leigh P. N. (2000): Recent advances in amyotrophic lateral sclerosis. *Current Opinion in Neurology*, 13(4): 397–405.

Alali F. Q., Tawaha K. (2009): Dereplication of bioactive constituents of the genus *Hypericum* using LC-(+,-)-ESI-MS and LC-PDA techniques: *Hypericum triquetrifolium* as a case of study. *Saudi Pharm. J.*, 17: 269-274.

Alfaro R. A., Gomez-Sandoval Z., Mammino L. (2014): Evaluation of the antiradical activity of hyperjovinol-A utilizing donor-acceptor maps. *J. Mol. Model.*, 20(7): 2337.

Altundag E., Ozturk M. (2011): Ethnomedicinal studies on the plant resources of east Anatolia, Turkey. *Proc. Soc. Behav. Sci.*, 19: 756-77.

AMR (2004): *Hypericum perforatum* Monograph. *Alter. Med. Rev.*, 9(3): 318-325.

Andlin-Sobocki P., Jönsson B., Wittchen H.-U., Olesen J. (2005): Costs of Disorders of the Brain in Europe. *Eur. J. Neur.*, 12(1): 1-27.

Apaydin S., Zeybek U., Ince I., Elgin G., Karamenderes C., Ozturk B., Tuglular I. (1999): *Hypericum triquetrifolium* Turra extract exhibits antinociceptive activity in the mouse. *J. Ethnopharmacol.*, 67(3): 307-12.

Avato P. (2005): A survey on the *Hypericum* genus: secondary metabolites and bioactivity, *Bioact. Nat. Prod.*, 30: 603-634.

Ballard C., Gauthier S., Corbett A., Brayne C., Aarsland D., Jones E. (2011): Alzheimer's disease. *Lancet*, 377(9770): 1019-31.

Bar-Am O., Weinreb O., Amit T., Youdim M. B. (2009): The novel cholinesterase-monoamine oxidase inhibitor and antioxidant, ladostigil, confers neuroprotection in neuroblastoma cells and aged rats. *J. Mol. Neurosci.*, 37(2): 135-45.

Bartzokis G. (2011): Alzheimer's disease as homeostatic responses to age-related myelin breakdown. *Neurobiology of Aging*, 32(8): 1341-71.

Battistini S., Ricci C., Lotti E. M., Benigni M., Gagliardi S., Zucco R., Bondavalli M., Marcello N., Ceroni M., Cereda C. (2010): Severe familial ALS with a novel exon 4 mutation (L106F) in the SOD1 gene. *J. Neurol. Sci.*, 293(1): 112–115.

Beerhues L. (2006): Molecules of Interest. Hyperforin. *Phytochemistry*, 67: 2201-7.

Ben-Gedalya T., Moll L., Bejerano-Sagie M., Frere S., Cabral W. A., Friedmann-Morvinski D., Slutsky I., Burstyn-Cohen T., Marini J. C., Cohen E. (2015): Alzheimer's disease-causing proline substitutions lead to presenilin 1 aggregation and malfunction. *EMBO J.*, 34(22): 2820-39.

Benkiki N., Kabouche Z., Tillequin F., Vérité P., Chosson E., Seguin E. (2003): A new polyisoprenylated phloroglucinol derivative from *Hypericum perfoliatum* (Clusiaceae). *Z. Naturforsch. C.*, 58(9-10): 655-8.

Berridge M. V., Tan A. S. (1993): Characterization of the cellular reduction of 3-(4,5-dimethylthiazol-2-yl)-2,5-diphenyltetrazolium bromide (MTT): subcellular localization, substrate dependence and involvement of mitochondrial electron transport in MTT reduction, *Arch. Biochem. Biophys.*, 303: 474-482.

Berridge M. V., Herst P. M., Tan A. S. (2005): Tetrazolium dyes as tools in cell biology: new insights into their cellular reduction, *Biotechnol. Annu. Rev.*, 11: 127-152.

Bongiorno P., LoGiudice P. (2010): *Hypericum* for depression. *Nat. Med. J.*, 2(12): 3-9.

Boxberger H. J. (2007): Leitfaden für die Zell- und Gewebekultur. Einführung in Grundlagen und Techniken. Weinheim: Wiley-VCH.

Brewer G. J. (2012): Copper excess, zinc deficiency, and cognition loss in Alzheimer's disease. *BioFactors*, 38(2): 107-113.

Budzikiewicz H., Schäfer M. (2012): Massenspektrometrie. Eine Einführung. 6., vollst. überarb. und aktualis. Auflage. Weinheim: Wiley-VCH.

Burns A., Iliffe S. (2009): Alzheimer's disease. *BMJ*, 338: b158.

Cacciapuoti F. (2016): Oxidative Stress as “Mother” of Many Human Diseases at Strong Clinical Impact. *J. Cardiovasc. Med. Cardiol.*, 3(1): 001-006.

Cakilcioglu U., Khatun S., Turkoglu I., Hayta S. (2011): Ethnopharmacological survey of medicinal plants in Maden (Elazig-Turkey). *J. Ethnopharmacol.*, 137(1): 469-86.

Cataldo J. K., Prochaska J. J., Glantz S. A. (2010): Cigarette smoking is a risk factor for Alzheimer's disease: An analysis controlling for tobacco industry affiliation. *J. Alzheimer's disease*, 19(2): 465-480.

Chen X. Q., Li Y., Li K. Z., Peng L. Y., He J., Wang K., Pan Z. H., Cheng X., Li M. M., Zhao Q. S., Xu G. (2011): Spirocyclic acylphloroglucinol derivatives from *Hypericum beanii*. *Chem. Pharm. Bull.* (Tokyo), 59(10): 1250-3.

Chen J. K., Chen T. T. (2012): Chinesische Pharmakologie I. Verlag Systemische Medizin AG. p. 216.

Choi D. W. (1988): Glutamate neurotoxicity and diseases of the nervous system. *Neuron.*, 1(8): 623-34.

Chung M. J., Lee S., Park Y. I., Lee J., Kwon K. H. (2016): Neuroprotective effects of phytosterols and flavonoids from *Cirsium setidens* and *Aster scaber* in human brain neuroblastoma SK-N-SH cells. *Life Sci.*, 148: 173-82.

Cirak C., Radusiene J., Janulis V., Ivanauskas L., Camas N. (2011): Phenolic Constituents of *Hypericum triquetrifolium* Turra (Guttiferae) growing in Turkey: variation among populations and plant parts. *Turk. J. Biol.*, 35: 449-456.

Conforti F., Statti G. A., Tundis R., Menichini F., Houghton P. (2002): Antioxidant activity of methanolic extract of *Hypericum triquetrifolium* Turra aerial parts. *Fitoterapia*, 73(6): 479-83.

Conforti F., Loizzo M. R., Statti A. G., Menichini F. (2007): Cytotoxic activity of antioxidant constituents from *Hypericum triquetrifolium* Turra. *Nat. Prod. Res.*, 21(1): 42-6.

Correa, M.P. (1984): Dicionario das Plantas Uteis do Brasil e das Exoticas Cultivadas. Instituto Brasileiro de Desenvolvimento Florestal, Rio de Janeiro.

Couladis M., Badisa R. B., Baziou P., Chaudhuri S. K., Pilarinou E., Verykokidou E., Harvala C. (2002): Antioxidant and cytotoxic activities of *Hypericum* sp. on brine shrimps and human cancer cell lines. *Phytother. Res.*, 16(8): 719-22.

Coyle J., Puttfarcken P. (1993): Oxidative stress, glutamate, and neurodegenerative disorders. *Science*, 262(5134): 689-95.

Crockett S. L., Schaneberg B., Khan I. (2005): Phytochemical profiling of New and Old World *Hypericum* (St. John's wort) species. *Phytochem. Anal.*, 16: 479–485.

Crockett S. L., Wenzig E. M., Kunert O., Bauer R. (2008): Anti-inflammatory phloroglucinol derivatives from *Hypericum empetrifolium*. *Phytochem. Lett.*, 1(1): 37-43.

Crockett S. L., Eberhardt M., Kunert O., Schuhly W. (2010): *Hypericum* species in the Paramos of Central and South America: a special focus upon *H. irazuense* Kuntze ex N. Robson. *Phytochem. Rev.*, 9: 255–269.

Crockett S. L., Robson N. K. B. (2011): Taxonomy and chemotaxonomy of the genus *Hypericum*. *Med. Aromat. Plant Sci. Biotechnol.* 5 (Special issue 1), pp. 1-13.

Culpeper N. (1652): The English Physician, or an Astrologo-physical Discourse on the Vulgar Herbs of this Nation. London, England: Nathanial Brook.

Cummings C. J., Zoghbi H. Y. (2000): Trinucleotide repeats: mechanisms and pathophysiology. *Annu. Rev. Genomics Hum. Genet.*, 1: 281–328.

Dakanali M., Theodorakis E. A. (2011): 12. Polyprenylated phloroglucinols and xanthones. In book: Erwan Poupon und Bastien Nay. *Biometric organic synthesis.* Weinheim: Wiley-VCH Verlag GmbH & Co. KGaA, pp. 433-467.

Danielson N. B., Kaifosh P., Zaremba J. D., Lovett-Barron M., Tsai J., Denny C. A., Balough E. M., Goldberg A. R., Drew L. J., Hen R., Losonczy A., Kheirbek M. A. (2016): Distinct contribution of adult-born hippocampal granule cells to context encoding. *Neuron*, 90: 1–12.

Danino O., Grossman S., Fischer B. (2015): ATP-γ-S-(α,β-CH2) protects against oxidative stress and amyloid beta toxicity in neuronal culture. *Biochem. Biophys. Res. Commun.*, 460(2): 446-50.

Davis J. B., Maher P. (1994): Protein kinase C activation inhibits glutamate-induced cytotoxicity in a neuronal cell line, *Brain Res.*, 652: 169-173.

Decosterd L. A., Hoffman E., Kyburz R., Bray D., Hostettmann K. (1991): A new phloroglucinol derivative from *Hypericum calycinum* with antifungal and in vitro antimalarial activity. *Planta Med.*, 57(6): 548-51.

Decosterd L. A., Stoeckli-Evans H., Chapuis J.-C., Sordat B., Hostettmann K. (1989): New cell growth-inhibitory cyclohexadienone derivatives from *Hypericum calycinum* L. *Helvetica Chimica Acta*, 72(8): 1833-1845.

Dinamarca M. C., Cerpa W., Garrido J., Hancke J. L., Inestrosa N. C. (2006): Hyperforin prevents beta-amyloid neurotoxicity and spatial memory impairments by disaggregation of Alzheimer's amyloid-beta-deposits. *Mol. Psychiatry*, 11(11): 1032-48.

Dodel R., Neff F., Noelker C., Pul R., Du Y., Bacher M., Oertel W. (2010): Intravenous immunoglobulins as a treatment for Alzheimer's disease: rationale and current evidence. *Drugs*, 70(5): 513-28.

Dok-Go H., Lee K. H., Kim H. K., Lee E. H., Lee J., Song Y. S., Lee Y., Jin C., Lee Y. S., Cho J. (2003): Neuroprotective effects of antioxidative flavonoids, quercetin, (+)-dihydroquercetin and quercetin-3-methylether, isolated from *Opuntia ficus-indica* var. *saboten*. *Brain Res.*, 965: 130-136.

Dörks M., Langner I., Dittmann U., Timmer A., Garbe E. (2013): Antidepressant drug use and off-label prescribing in children and adolescents in Germany: results from a large population-based cohort study. *European child & adolescent psychiatry*, 22(8): 511–518.

Dos Santos M. Z., Dalcol I. I., Adolpho L., Teixidó M., Tarragó T., Morel A., Giralt E. (2015): Chemical composition and inhibitory effects of *Hypericum brasiliense* and *H. connatum* on prolyloligopeptidase and acetylcholinesterase activities. *Med. Chem.*, 12(5): 457-463.

Dos Santos K. C., Borges T. V., Olescowicz G., Ludka F. K., de Moraes Santos C. A., Molz S. (2016): *Passiflora actinia* hydroalcoholic extract and its major constituent, isovitexin, are neuroprotective against glutamate-induced cell damage in mice hippocampal slices. *J. Pharm. Pharmacol.*, 68: 282-291.

Dranovsky A., Picchini A. M., Moadel T., Sisti A. C., Yamada A., Kimura S., Leonardo E. D., Hen R. (2011): Experience dictates stem cell fate in the adult hippocampus. *Neuron*, 70: 908–923.

Edgecombe W. S. (1970): Weeds of Lebanon (3rd). American University of Beirut, Beirut, Lebanon. 457 pp.

Elbaz A., Carcaillon L., Kab S., Moisan F. (2016): Epidemiology of Parkinson's disease. *Rev. Neurol. (Paris)*, 172(1): 14-26.

Ellman G. L., Courtney K. D., Andres V. Jr., Featherstone R. M. (1961): A new and rapid colorimetric determination of acetylcholinesterase activity. *Biochem. Pharmacol.*, 7: 88-95.

Ely C. V., Boldrini I. I., de Loreto Bordignon S. A. (2015): A new species of *Hypericum* (Hypericaceae) from Southern Brazil. *Phytotaxa*. 192(4): 290-295.

Eubanks L. M., Rogers C. J., Beuscher A. E., Koob G. F., Olson A. J., Dickerson T. J., Janda K. D. (2006): A molecular link between the active component of marijuana and Alzheimer's disease pathology. *Mol. Pharm.*, 3(6): 773-777.

Fegert J. M., Kölch M., Zito J. M., Glaeske G., Janhsen K. (2006): Antidepressant use in children and adolescents in Germany. *J. Child. Adolesc. Psychopharmacol.*, 16(1-2): 197–206.

Fisel J., Gäbler H., Schwöbel H., Trunzler G. (1966): Haronga madagascariensis CHOISY: botanik, pharmakognosie, chemie und therapeutische Anwendung. *Dtsch. Apoth. Z.*, 106: 1053-60.

Fobofou S. A., Franke K., Sanna G., Porzel A., Bullita E., La Colla P., Wessjohann L. A. (2015): Isolation and anticancer, anthelminthic, and antiviral (HIV) activity of acylphloroglucinols, and regioselective synthesis of empetrifranzinans from Hypericum roeperianum. *Bioorg. Med. Chem.*, 23(19): 6327-34.

Fowler G. (2002): Distribution map. USDA, APHIS, PPQ, Center for Plant Health Science and Technology, Raleigh, NC, USA.

Francis P. T., Palmer A. M., Snape M., Wilcock G. K. (1999): The Cholinergic Hypothesis of Alzheimer's Disease: a Review of Progress. *Journal of Neurology, Neurosurgery, and Psychiatry*, 66(2): 137–47.

Freiherr J., Hallschmid M., Frey W. H., Brünner Y. F., Chapman C. D., Hölscher C., Craft S., de Felice F. G., Benedict C. (2013): Intranasal insulin as a treatment for Alzheimer's disease: a review of basic research and clinical evidence. *CNS Drugs*, 27(7): 505-514.

Friesen J. B., McAlpine J. B., Chen S.-N., Pauli G. F. (2015): Countercurrent Separation of Natural Products: An Update. *J. Nat. Prod.*, 78(7): 1765–1796.

Frontzek K., Lutz M. I., Aguzzi A., Kovacs G. G., Budka H. (2016): Amyloid-β pathology and cerebral amyloid angiopathy are frequent in iatrogenic Creutzfeldt-Jakob disease after dural grafting. *Swiss Medical Weekly*, 146: w14287.

Fukui M., Song J. H., Choi J., Choi H. J., Zhu B. T. (2009): Mechanism of glutamate-induced neurotoxicity in HT22 mouse hippocampal cells, *Eur. J. Pharmacol.*, 617(1-3): 1-11.

Gao W., Hou W.-Z., Zhao J., Xu F., Li L., Xu F., Sun H., Xing J.-G., Peng Y., Wang X.-L., Ji T.-F., Gu Z.-Y. (2016): Polycyclic Polyprenylated Acylphloroglucinol Congeners from *Hypericum scabrum*. *J. Nat. Prod*., 79 (6): 1538–1547.

García I., Ballesta S., Gilaberte Y., Rezusta A., Pascual Á. (2015): Antimicrobial photodynamic activity of hypericin against methicillin-susceptible and resistant Staphylococcus aureus biofilms. *Future Microbiol.*, 10(3): 347-56.

Gatz M., Reynolds C. A., Fratiglioni L. (2006): Role of genes and environments for explaining Alzheimer disease. *Arch. Gen. Psychiatry*, 63(2): 168-174.

Ghorbani A. (2005): Studies on pharmaceutical ethnobotany in the region of Turkmen Sahra, north of Iran (Part I): general results. *J. Ethnopharmacol*., 102(1): 58-68.

Goedert M., Spillantini M. G., Crowther R. A. (1991): Tau Proteins and neurofibrillary degeneration. *Brain Pathology*, 1(4): 279-286.

Gómez del Rio M. A., Sánchez-Reus M. I., Iglesias I., Pozo M. A., García-Arencibia M., Fernández-Ruiz J., García-García L., Delgado M., Benedí J. (2013): Neuroprotective Properties of Standardized Extracts of *Hypericum perforatum* on Rotenone Model of Parkinson's Disease. *CNS Neurol. Disord. Drug Targets*, 12(5): 665-79.

Griffith T. N., Varela-Nallar L., Dinamarca M. C., Inestrosa N. C. (2016): Neurobiological Effects of Hyperforin and its Potential in Alzheimers Disease Therapy. *Current Medicinal Chemistry*, 17(5): 391-406.

Hahn G. (1992): *Hypericum perforatum* (St. John's wort) – a medicinal herb used in antiquity and still of interest today. *J. Naturopat. Med.*, 3: 94–96.

Hashida W., Tanaka N., Kashiwada Y., Sekiya M., Ikeshiro Y., Takaishi Y. (2002): Tomoeones A-H, cytotoxic phloroglucinol derivatives from *Hypericum ascyron*. *Phytochemistry*, 69(11): 2225-2230.

Hashimoto M., Rockenstein E., Crews L., Masliah E. (2003): Role of protein aggregation in mitochondrial dysfunction and neurodegeneration in Alzheimer's and Parkinson's diseases. *NeuroMolecular Med.*, 4(1): 21-35.

He S., Yang W., Zhu L., Du G., Lee C. S. (2014): Bioinspired total synthesis of (±)-yezo'otogirin C. *Org. Lett.*, 16(2): 496-9.

Helson L., Das S. K., Hajdu S. I. (1975): Human neuroblastoma in nude mice. *Cancer Res.*, 35(9): 2594-9.

Henry G. E., Campbell M. S., Zelinsky A. A., Liu Y., Bowen-Forbes C. S., Li L., Nair M. G., Rowley D. C., Seeram N. P. (2009): Bioactive acylphloroglucinols from *Hypericum densiflorum*. *Phytother. Res.*, 23(12): 1759-62.

Holm L. G., Pancho J. V., Herberger J. P., Plucknett D. L. (1979): A geographical atlas of the world weeds. *Wiley*, New York, 391 pp.

Hölzl J., Petersen M. (2003): 6. Chemical constituents of *Hypericum* spp. In: Ernst E.: *Hypericum*: The genus *Hypericum*. London, New York: Taylor and Francis.

Hosni K., Msaada K., Marzouk B. (2007): Comparative study on *Hypericum triquetrifolium* Turra fatty acids. *Asian J. Plant Sci.*, 6(2): 384-388.

Hu L.-H., Sim K.-Y. (2000): Sampsoniones A–M, a Unique Family of Caged Polyprenylated Benzoylphloroglucinol Derivatives, from *Hypericum sampsonii*. *Tetrahedron*, 56(10): 1379-1386.

Hu L., Xue Y., Zhang J., Zhu H., Chen C., Li X. N., Liu J., Wang Z., Zhang Y., Zhang Y. (2016): (±)-Japonicols A-D, Acylphloroglucinol-Based Meroterpenoid Enantiomers with Anti-KSHV Activities from *Hypericum japonicum*. *J. Nat. Prod.*, 79(5): 1322-8.

Hudson J. B., Lopez-Bazzocchi I., Towers G. H. (1991): Antiviral activities of hypericin. *Antiviral Res.*, 15(2): 101-12.

Hung C. W., Chen Y. C., Hsieh W. L., Chiou S. H., Kao C. L. (2010): Ageing and neurodegenerative diseases. *Ageing Res Rev.*, 9 Suppl 1: S36-46

Idolo M., Motti R., Mazzoleni S. (2010): Ethnobotanical and phytomedicinal knowledge in a long-history protected area, the Abruzzo, Lazio and Molise National Park (Italian Apennines). *J. Ethnopharmacol*., 127(2): 379-95.

Iqbal K., Alonso Adel C., Chen S. (2005): Tau Pathology in Alzheimer Disease and Other Tauopathies. *Biochimica et Biophysica Acta*, 1739(2–3): 198–210.

Ishida Y., Shirota O., Sekita S., Someya K., Tokita F., Nakane T., Kuroyanagi M. (2010): Polyprenylated benzoylphloroglucinol-type derivatives including novel cage compounds from *Hypericum erectum*. *Chem. Pharm. Bull. (Tokyo)*, 58(3): 336-343.

Ishige K., Schubert D., Sagara Y. (2001): Flavonoids protect neuronal cells from oxidative stress by three distinct mechanisms. *Free Radic. Biol. Med.*, 30(4): 433-46.

Ittner L. M., Götz J. (2011): Amyloid-β and tau — a toxic *pas de deux* in Alzheimer's disease. *Nature Reviews Neuroscience*, 12: 67-72.

Itzhaki R. F., Wozniak M. A. (2008): Herpes Simplex Virus Type 1 in Alzheimer's Disease: The Enemy Within. *J. Alzheimer's Dis.*, 13(4): 393-405.

Jensen A. G., Hansen S. H., Nielsen E. O. (2001): Adhyperforin as a contributor to the effect of *Hypericum perforatum* L. in biochemical models of antidepressant activity. *Life Sci.*, 68(14): 1593-605.

Karim H., Kamel M., Mouna B. T., Thouraya C., Brahim M. (2007): Essential oil composition of *Hypericum triquetrifolium* Turra aerial parts. *Ital. J. Biochem.*, 56(1): 40-6.

Karioti A., Bilia A. R. (2010): Hypericins as Potential Leads for New Therapeutics. *Int. J. Mol. Sci.*, 11: 562-594.

Kenna K. P., van Doormaal P. T., Dekker A. M., Ticozzi N., Kenna B. J., Diekstra F. P., van Rheenen W., van Eijk K. R., Jones A. R., Keagle P., Shatunov A., Sproviero W., Smith B. N., van Es M. A., Topp S. D., Kenna A., Miller J. W., Fallini C., Tiloca C., McLaughlin R. L., Vance C., Troakes C., Colombrita C., Mora G., Calvo A., Verde F., Al-Sarraj S., King A., Calini D., de Belleroche J., Baas F., van der Kooi A. J., de Visser M., Ten Asbroek A. L., Sapp P. C., McKenna-Yasek D., Polak M., Asress S., Muñoz-Blanco J. L., Strom T. M., Meitinger T., Morrison K. E.; SLAGEN Consortium, Lauria G., Williams K. L., Leigh P. N., Nicholson G. A., Blair I. P., Leblond C. S., Dion P. A., Rouleau G. A., Pall H., Shaw P. J., Turner M. R., Talbot K., Taroni F., Boylan K. B., Van Blitterswijk M., Rademakers R., Esteban-Pérez J., García-Redondo A., Van Damme P., Robberecht W., Chio A., Gellera C., Drepper C., Sendtner M., Ratti A., Glass J. D., Mora J. S., Basak N. A., Hardiman O., Ludolph A. C., Andersen P. M., Weishaupt J. H., Brown R. H. Jr., Al-Chalabi A., Silani V., Shaw C. E., van den Berg L. H., Veldink J. H., Landers J. E. (2016): NEK1 variants confer susceptibility to amyotrophic lateral sclerosis. *Nat. Genet.*, 48(9): 1037-42.

Keogh-Brown M. R., Jensen H. T., Arrighi H. M., Smith R. D. (2015): The Impact of Alzheimer's Disease on the Chinese Economy. *EBioMedicine*, 4: 184-90.

Kiernan M. C., Vucic S., Cheah B. C., Turner M. R., Eisen A., Hardiman O., Burrel J. R., Zoing M. C. (2011): Amyotrophic lateral sclerosis. *The Lancet*, 377(9769): 942-955.

Kling B. (2015): Monitoring neurotoxicity, neuroprotection and CB_2 receptor signalling *in vitro*: comparative analysis of conventional versus impedance-based assays. Dissertation. University of Regensburg, Germany.

Klingauf P., Beuerle T., Mellenthin A., El-Moghazy S. A., Boubakir Z., Beerhues L. (2005): Biosynthesis of the hyperforin skeleton in *Hypericum calycinum* cell cultures. *Phytochemistry*, 66(2): 139-45.

Kraus B., Wolff H., Heilmann J., Elstner E. F. (2007): Influence of *Hypericum perforatum* extract and its single compounds on amyloid-β mediated toxicity in microglial cells. *Life Sciences*, 81: 884-894.

Kritis A. A., Stamoula E. G., Paniskaki K. A., Vavilis T. D. (2015): Researching glutamate – induced cytotoxicity in different cell lines: a comparative/collective analysis/study. *Front. Cell. Neurosci.*, 9: 91.

Kumar B., Vijayakumar M., Govindaranjan R., Pushpangadan P. (2007): Ethnopharmacological approaches to wound healing – exploring medicinal plants of India. *J. Ethnopharmacol*., 114(2): 103-13.

LaFerla F. M., Green K. N., Oddo S. (2007): Intracellular amyloid-β in Alzheimer's disease. *Nature Reviews Neuroscience*, 8: 499-509.

Lee B., Weon J. B., Eom M. R., Jung Y. S., Ma C. J. (2015): Neuroprotective compounds of *Tilia amurensis*. *Pharmacogn. Mag.*, 11(Suppl 2): S303–S307.

Leinenga G., Götz J. (2015): Scanning ultrasound removes amyloid-β and restores memory in an Alzheimer's disease mouse model. *Sci. Translational Med.*, 7(278): 278ra33.

Leuner K., Kazanski V., Müller M., Essin K., Henke B., Gollasch M., Harteneck C., Müller W. E. Hyperforin – a key constituent of St. John's wort specifically activates TRPC6 channels. *FASEB J.*, 21(14): 4101-11.

Linde K., Berner M. M., Kriston L. (2008): St John's wort for major depression. *Cochrane Database Syst. Rev.*, (4): CD000448.

Lipton S. A., Rosenberg P. A. (1994): Excitatory amino acids as a final common pathway for neurologic disorders. *N. Engl. J. Med., 330(9): 613-22.*

Liu X., Yang X. W., Chen C. Q., Wu C. Y., Zhang J. J., Ma J. Z., Wang H., Yang L. X., Xu G. (2013): Bioactive polyprenylated acylphloroglucinol derivatives from *Hypericum cohaerens*. *J. Nat. Prod.*, 76(9): 1612-8.

Loeb M. B., Molloy D. W., Smieja M., Standish T., Goldsmith C. H., Mahony J., Smith S., Borrie M., Decoteau E., Davidson W., McDougall A., Gnarpe J., O'Donnell M., Chernesky M. (2004): A randomized, controlled trial of doxycycline and rifampin for patients with Alzheimer's disease. *J. Am. Geriatr. Soc.*, 52(3): 381-7.

Maher P., Davis J. B. (1996): The role of monoamine metabolism in oxidative glutamate toxicity. *J. Neurosci.*, 16: 6394-6401.

Maher P., Schubert D. (2000): Signaling by reactive oxygen species in the nervous system, *Cell. Mol. Life Sci.*, *57(8-9):1287-305*.

Mander B. A., Marks S. M., Vogel J. W., Rao V., Lu B., Saletin J. M., Ancoli-Israel S., Jagust W. J., Walker M. P. (2015): β-amyloid disrupts human NREM slow waves and related hippocampus-dependent memory consolidation. *Nat. Neurosci.*, 18: 1051–1057.

Marešová P., Mohelská H., Dolejš J., Kuča K. (2015): Socio-economic aspects of Alzheimer's disease. *Curr. Alzheimer Res.*, 12(9): 903-11.

Mark K. A., Dumas K. J., Bhaumik D., Schilling B., Davis S., Oron T. R., Sorensen D. J., Lucanic M., Brem R. B., Melov S., Ramanathan A., Gibson B. W. (2016): Vitamin D Promotes Protein Homeostasis and Longevity via the Stress Response Pathway Genes *skn-1*, *ire-1* and *xbp-1*. *Cell Reports*, 17: 1227–1237.

Mártonfi P., Repcák M., Zanvit P. (2006): Secondary metabolites variation in *Hypericum maculatum* and its relatives. *Biochemical Systematics and Ecology*, 34: 56–59.

Mattson M. P., Magnus T. (2006): Aging and Neuronal Vulnerability. *Nat. Rev. Neurosci.*, 7(4): 278-294.

Medeiros M. S., Schumacher-Schuh A., Machado Cardoso A., Vargas Bochi G., Baldissarelli J., Kegler A., Santana D., Soares Chaves C. M. M. B., Schetinger M. R. C., Moresco R. N., Rieder C. R. M., Fighera M. R. (2016): Iron and Oxidative Stress in Parkinson's Disease: An Observational Study of Injury Biomarkers. *PLoS One*, 11(1): e0146129. doi: 10.1371/journal.pone.0146129. eCollection 2016.

Meek P. D., McKeithan K., Schumock G. T. (1998): Economic considerations in Alzheimer's disease. *Pharmacotherapy*, 18(2 Pt 2): 68-73; discussion 79-82.

Meldrum B. S. (2000): Glutamate as a neurotransmitter in the brain: review of physiology and pathology. *J. Nutr.*, 130(4S Suppl): 1007S-15S.

Mentz L. A., Lutzemberger L. C., Schenkel E. P. (1997): Da flora medicinal do Rio Grande do Sul: Notas sobre a obra de D'Avila (1910). *Caderno de Farmácia*, 13(1): 25–48.

Mitsopoulou K. P., Vidali V. P., Koliopoulos G., Couladouros E. A., Michaelakis A. (2014): Hyperforin and deoxycohumulone as a larvicidal agent against *Culex pipiens* (Diptera: Culicidae). *Chemosphere*, 100: 124-9.

Mitsopoulou K. P., Vidali V. P., Maranti A., Couladouros E. A. (2015): Isolation and Structure Elucidation of Hyperibine J [Revised Structure of Adhyperfirin (7-Deprenyl-13-methylhyperforin)]: Synthesis of Hyperibone J. *Eur. J. Org. Chem.*, 2015(2): 287–290

Montecinos-Oliva C., Schüller A., Inestrosa N. C. (2015): Tetrahydrohyperforin: a neuroprotective modified natural compound against Alzheimer's disease. *Neural Regen Res.*, 10(4): 552–554.

Morimoto B. H., Koshland D. E. Jr. (1990): Introduction and expression of long- and short-term neurosecretory potentiation in a neural cell line. *Neuron.*, 5: 875-880.

Mosaddegh M., Naghibi F., Moazzeni H., Pirani A., Esmaeili S. (2012): Ethnobotanical survey of herbal remedies traditionally used in Kohghiluyeh va Boyer Ahmad province of Iran. *J. Ethnopharmacol*., 141(1): 80-95.

Moulton P. V., Yang W. (2012): Air Pollution, Oxidative Stress, and Alzheimer's disease. *Journal of Environmental and Public Health*, 2012: Article ID 472751, 9 pages.

Muchowski P. J. (2002): Protein misfolding, amyloid formation, and neurodegeneration: a critical role for molecular chaperones? *Neuron.*, 35: 9-12.

Murphy T. H., Miyamoto M., Sastre A., Schnaar R. L., Coyle J. T. (1989): Glutamate toxicity in a neuronal cell line involves inhibition of cystine transport leading to oxidative stress. *Neuron.,* 2(6): 1547-58.

NGRP (2002): Wirld Economic Plants in GRIN (Germplasm Resources Information Network). United States Department of Agriculture, Agricultural Resources Service, National Germplasm Resources Program (NGRP). Beltsville. Last accessed 2009.

Noyce A. J., Bestwick J. P., Silveira-Moriyama L., Hawkes C. H., Giovannoni G., Lees A. J., Schrag A. (2012): Meta-analysis of early non-motor features and risk factors for Parkinson disease. *Annals of Neurology*, 72(6): 893-901.

Nürk N. M. (2011): Phylogenetic analyses in St. John's wort (*Hypericum*). Inferring character evolution and historical biogeography. Dissertation. Freie Universität Berlin, Germany.

Nussbaum J. M., Seward M. E., Bloom G. S. (2013): Alzheimer disease. *Prion*, 7(1): 14-19.

Olesen J., Gustavsson A., Svensson M., Wittchen H.-U., Jönsson B. on behalf of the CDBE2010 study group and the European Brain Council. (2012): The economic cost of brain disorders in Europe. *Eur. J. Neurol.*, 19: 155–162.

Ozturk B., Apaydin S., Goldeli E., Ince I., Zeybeck U. (2002): *Hypericum triquetrifolium* Turra extract enhibits anti-inflammatory activity in the rat. *J. Ethnopharmacol.*, 80(2-3): 207-9.

Parker W. L., Johnson F. (1968): The strcture determination of antibiotic compounds from *Hypericum uliginosum*. *J. Am. Chem. Soc.*, 90(17): 4716-4723.

Parsons W. T., Cuthbertson E. G. (1992): Noxious weeds of Australia. *Inkata Press*, Melbourne, 692 pp.

Piccinelli A. L., Cuesta-Rubio O., Chica M. B., Mahmood N., Pagano B., Pavone M., Barone V., Rastrelli L. (2005): Structural revision of clusianone and 7-*epi*-clusianone and anti-HIV activity of polyisoprenylated benzophenones. *Tetrahedron*, 61: 8206-8211.

Pinhatti A. V., de Barros F. M., de Farias C. B., Schwartsmann G., Poser G. L., Abujamra A. L. (2013): Antiproliferative activity of the dimeric phloroglucinol and benzophenone derivatives of *Hypericum* spp. native to southern Brazil. *Anticancer Drugs,* 24(7): 699-703.

Pitzl S., Kling B., Heilmann J. (2015): *In vitro* Untersuchungen von Acylphloroglucinolen auf Neurotoxizität und Neuroprotektivität mittels MTT-Testungen. *Forschungsbericht im Rahmen des Masterstudiengangs Chemie an der Universität Regensburg.* University of Regensburg, Germany. Unpublished internal data (Data presented in Appendix § 7.2).

Plinius Secundus G. (1967): Natural History. In: Warmington M. A., editor. *Natural History*. 5 ed. Cambridge, Massachusetts: Harvard University Press. p. 381.

Pompella A., Visvikis A., Paolicchi A., De Tata V., Casini A. F. (2003): The changing faces of glutathione, a cellular protagonist. *Biochem. Pharmacol.*, 66(8): 1499-503.

Reed C. F. (1977): Economically important foreign weeds: Potential problems in the United States. Agricultural research service, animal and plant health inspection service, US Dept. of Agriculture, Washington, DC. 746 pp.

van Rheenen W., Shatunov A., Dekker A. M., McLaughlin R. L., Diekstra F. P., Pulit S. L., van der Spek R. A., Võsa U., de Jong S., Robinson M. R., Yang J., Fogh I., van Doormaal P. T., Tazelaar G. H., Koppers M., Blokhuis A. M., Sproviero W., Jones A. R., Kenna K. P., van Eijk K. R., Harschnitz O., Schellevis R. D., Brands W. J., Medic J., Menelaou A., Vajda A., Ticozzi N.,

Lin K., Rogelj B., Vrabec K., Ravnik-Glavač M., Koritnik B., Zidar J., Leonardis L., Grošelj L. D., Millecamps S., Salachas F., Meininger V., de Carvalho M., Pinto S., Mora J. S., Rojas-García R., Polak M., Chandran S., Colville S., Swingler R., Morrison K. E., Shaw P. J., Hardy J., Orrell R. W., Pittman A., Sidle K., Fratta P., Malaspina A., Topp S., Petri S., Abdulla S., Drepper C., Sendtner M., Meyer T., Ophoff R. A., Staats K. A., Wiedau-Pazos M., Lomen-Hoerth C., Van Deerlin V. M., Trojanowski J. Q., Elman L., McCluskey L., Basak A. N., Tunca C., Hamzeiy H., Parman Y., Meitinger T., Lichtner P., Radivojkov-Blagojevic M., Andres C. R., Maurel C., Bensimon G., Landwehrmeyer B., Brice A., Payan C. A., Saker-Delye S., Dürr A., Wood N. W., Tittmann L., Lieb W., Franke A., Rietschel M., Cichon S., Nöthen M. M., Amouyel P., Tzourio C., Dartigues J. F., Uitterlinden A. G., Rivadeneira F., Estrada K., Hofman A., Curtis C., Blauw H. M., van der Kooi A. J., de Visser M., Goris A., Weber M., Shaw C. E., Smith B. N., Pansarasa O., Cereda C., Del Bo R., Comi G. P., D'Alfonso S., Bertolin C., Sorarù G., Mazzini L., Pensato V., Gellera C., Tiloca C., Ratti A., Calvo A., Moglia C., Brunetti M., Arcuti S., Capozzo R., Zecca C., Lunetta C., Penco S., Riva N., Padovani A., Filosto M., Muller B., Stuit R. J.; PARALS Registry; SLALOM Group; SLAP Registry; FALS Sequencing Consortium; SLAGEN Consortium; NNIPPS Study Group, Blair I., Zhang K., McCann E. P., Fifita J. A., Nicholson G. A., Rowe D. B., Pamphlett R., Kiernan M. C., Grosskreutz J., Witte O. W., Ringer T., Prell T., Stubendorff B., Kurth I., Hübner C. A., Leigh P. N., Casale F., Chio A., Beghi E., Pupillo E., Tortelli R., Logroscino G., Powell J., Ludolph A. C., Weishaupt J. H., Robberecht W., Van Damme P., Franke L., Pers T. H., Brown R. H., Glass J. D., Landers J. E., Hardiman O., Andersen P. M., Corcia P., Vourc'h P., Silani V., Wray N. R., Visscher P. M., de Bakker P. I., van Es M. A., Pasterkamp R. J., Lewis C. M., Breen G., Al-Chalabi A., van den Berg L. H., Veldink J. H. (2016): Genome-wide association analyses identify new risk variants and the genetic architecture of amyotrophic lateral sclerosis. *Nat. Genet.*, 48(9): 1043-1048.

Robson N. K. B. (1977): Studies in the genus *Hypericum* L. (Guttiferae). 1. Infrageneric classification. In: *Bull. Brit. Mus. Nat. Hist. (Botany)* (5): 291–355.

Robson N. K. B. (2002): Studies in the genus *Hypericum* L. (Guttiferae) 4(2). Section 9. *Hypericum* sensu lato (part 2): subsection 1. *Hypericum* series 1. *Hypericum*. *Bull. nat, Hist. Mus. Lond.* (Bot.) 32(2): 61-123.

Robson N. K. B. (2003): 1. *Hypericum* botany. In: Ernst E.: *Hypericum*: The genus *Hypericum*. London, New York: Taylor and Francis.

Rocha L., Marston A., Potterat O., Kaplan M. A. C., Stoeckli-Evans H., Hostettmann K. (1995): Antibacterial phloroglucinols and flavonoids from *Hypericum brasiliense*. *Phytochemistry*, 40(5): 1447-1452.

Rouis Z., Elaissi A., Abid N. B., Lassoued M. A., Cioni P. L., Flamini G., Aouni M. (2012): Chemical composition and intraspecific variability of the essential oils of five populations of *Hypericum triquetrifolium* Turra growing in North Tunisia. *Chem. Biodivers.*, 9(4): 806-16.

Rouis Z., Abid N., Koudja S., Yangui T., Elaissi A., Cioni P. L., Flamini G., Aouni M. (2013): Evaluation of the cytotoxic effect and antibacterial, antifungal, and antiviral activities of

Hypericum triquetrifolium Turra essential oils from Tunisia. *BMC Complement Altern. Med.*, 13(1): 24.

Roy D. S., Arons A., Mitchell T. I., Pignatelli M., Ryan T. J., Tonegawa S. (2016): Memory retrieval by activating engram cells in mouse models of early Alzheimer's disease. *Nature*, 531: 508–512.

Rücker G., Neugebauer M., Willems G. G. (2008): Instrumentelle Analytik für Pharmazeuten. Lehrbuch zu spektroskopischen, chromatographischen, elektrochemischen und thermischen Analysenmethoden. 4., durchges. und aktualis. Aufl. Stuttgart: Wiss. Verl.-Ges.

Saad B., Abouatta B. S., Basha W., Hmade A., Kmail A., Khasib S., Said O. (2011): *Hypericum triquetrifolium*-derived factors downregulate the production levels of LPS-induced Nitric Oxide and TNF-α in THP-1 cells. *Evid. Based Complement. Alternat. Med.*, 2011.

Sajjadi S. E., Mehregan I., Taheri M. (2015) Essential oil composition of *Hypericum triquetrifolium* Turra growing wild in Iran. *Res. Pharm. Sci.*, 10(1): 90-94.

Samii A., Nutt J. G., Ransom B. R. (2004): Parkinson's disease. *The Lancet*, 363(9423): 1783-1193.

Schmidt S., Jürgenliemk G., Skaltsa H., Heilmann J. (2012): Phloroglucinol derivatives from *Hypericum empetrifolium* with antiproliferative activity on endothelial cells. *Phytochemistry*, 77: 218-25.

Schmidt S., Heilmann J. (2013): Review: The genus *Hypericum* and its acylphloroglucinols. Unpublished internal data.

Schmidt S. (2013): Phytochemische and pharmakologische *in vitro* Untersuchungen zu *Hypericum empetrifolium* WILLD. Dissertation. University of Regensburg, Germany.

Schmitz S. (2011): Der Experimentator: Zellkultur, 3. Edition; Spektrum Akademischer Verlag: Heidelberg.

Schütt, H.; Schulz, V. (2007): *Hypericum*. In: Blaschek, W.; Ebel, S.; Hackenthal, E.; Holzgrabe, U.; Keller, K.; Reichling J.; Schulz V. (Hg.): Hagers Enzyklopädie der Arzneistoffe und Drogen, Band. 8. 6., neu bearb. und erg. Aufl. Stuttgart: Wiss. Verl.-Ges., pp. 742–780.

Shan M. D., Hu L. H., Chen Z. L. (2001): Three New Hyperforin Analogues from *Hypericum perforatum*. *J. Nat. Prod.*, 64: 127–130.

Shiu W. K. P., Gibbons S. (2006): Anti-staphylococcal acylphloroglucinols from *Hypericum beanii*. *Phytochemistry*, 67(23): 2568-2572.

Silbert L. C., Dodge H. H., Lahna D., Promjunyakul N., Austin D., Mattek N., Erten-Lyons D., Kaye J. A. (2016): Less Daily Computer Use is Related to Smaller Hippocampal Volumes in Cognitively Intact Elderly. *J. Alzheimer's Dis.*, 52(2): 713-7.

Singh I. P., Bharate S. B. (2006): Phloroglucinol compounds of natural origin. *Nat. Prod. Rep.*, 23: 558-591.

Stein A. C., Viana A. F., Müller L. G., Nunes J. M., Stolz E. D., Do Rego J. C., Costentin J., von Poser G. L., Rates S. M. (2012): Uliginosin B, a phloroglucinol derivative from *Hypericum polyanthemum*: a promising new molecular pattern for the development of antidepressant drugs. *Behav. Brain Res.*, 228(1): 66-73.

Stevens P. F. (2007): Hypericaceae. In: The families and genera of vascular plants, Vol. 9: 194-201.

Stevenson N. R., Lenard J. (1993): Antiretroviral activities of hypericin and rose bengal: photodynamic effects on Friend leukemia virus infection of mice. *Antiviral Res.*, 21(2): 119-27.

Stojanovic G., Dordevic A., Smelcerovic A. (2013): Do other *Hypericum* species have medicinal potential as St. John's wort (*Hypericum perforatum*)? *Curr. Med. Chem.*, 20(18): 2273-95.

Stolz E. D., Hasse D. R., von Poser G. L., Rates S. M. (2014): Uliginosin B, a natural phloroglucinol derivative, presents a multimediated antinociceptive effect in mice. *J. Pharm. Pharmacol.*, 66(12): 1774-85.

Stolz E. D., da Costa P. F., Medeiros L. F., Souza A., Battastini A. M., von Poser G. L., Bonan C., Torres I. L., Rates S. M. (2016): Uliginosin B, a Possible New Analgesic Drug, Acts by Modulating the Adenosinergic System. *Evid. Based Complement. Alternat. Med.*, doi: 10.1155/2016/5890590. Epub 2016 Mar 21.

Sun Q., Schmidt S., Tremmel M., Heilmann J., König B. (2014): Synthesis of natural-like acylphloroglucinols with anti-proliferative, anti-oxidative and tube-formation inhibitory activity. *Eur. J. Med. Chem.*, 85: 621-628.

Tala M. F., Talontsi F .M., Zeng G. Z., Wabo H. K., Tan N. H., Spiteller M., Tane P. (2015): Antimicrobial and cytotoxic constituents from native Cameroonian medicinal plant *Hypericum riparium*. *Fitoterapia*, 102: 149-55.

Tan S., Sagara Y., Liu Y., Maher P., Schubert D. (1998a): The Regulation of Reactive Oxygen Species Production during Programmed Cell Death*, J. Cell. Biol.*, 141(6): 1423–1432.

Tan S., Wood M., Maher P. (1998b): Oxidative stress induces a form of programmed cell death with characteristics of both apoptosis and necrosis in neuronal cells. *J. Neurochem.*, 71: 95-105.

Tan S., Schubert D., Maher P. (2001): Oxytosis: a novel form of programmed cell death. *Curr. Top Med. Chem.*, 1: 497-506.

Tanaka N., Takaishi Y., Shikishima Y., Nakanishi Y., Bastow K., Lee K. H., Honda G., Ito M., Takeda Y., Kodzhimatov O. K., Ashurmetov O. (2004): Prenylated benzophenones and xanthones from *Hypericum scabrum*. *J. Nat. Prod.*, 67(11): 1870-1875.

Tanaka N., Kubota T., Ishiyama H., Araki A., Kashiwada Y., Takaishi Y., Mikami Y., Kobayashi J. (2008): Petiolins A-C, phloroglucinol derivatives from *Hypericum pseudopetiolatum* var. *kiusianum*. *Bioorg. Med. Chem.*, 16(10): 5619-23.

Tanaka N., Kakuguchi Y., Ishiyama I., Kubota T., Kobayashi J. (2009): Yezo'otogirins A–C, new tricyclic terpenoids from *Hypericum yezoense*. *Tetrahedron Letters*, 50: 4747–4750.

Tanaka N., Mamemura T., Shibazaki A., Gonoi T., Kobayashi J. (2011): Yojironins E-I, prenylated acylphloroglucinols from *Hypericum yojiroanum*. *Bioorg. Med. Chem. Lett.*, 21(18): 5393-7.

Tracy T. E., Sohn P. D., Minami S. S., Wang C., Min S.-W., Li Y., Zhou Y., Le D., Lo I., Ponnusamy R., Cong X., Schilling B., Ellerby L. M., Huganir R. L., Gan L. (2016): Acetylated Tau Obstructs KIBRA-Mediated Signaling in Synaptic Plasticity and Promotes Tauopathy-Related Memory Loss. *Neuron*, 90(2): 245-60.

Vandal M., White P. J., Tremblay C., St-Amour I., Chevrier G., Emond V., Lefrançois D., Virgili J., Planel E., Giguere Y., Marette A., Calon F. (2014): Insulin reverses the high-fat diet-induced increase in brain Aβ and improves memory in an animal model of Alzheimer disease. *Diabetes*, 63(12): 4291-301.

Verotta L., Appendino G., Jakupovic J., Bombardelli E. (2000): Hyperforin analogues from St. John's wort (*Hypericum perforatum*). *J. Nat. Prod.*, 63(3): 412-415.

Vieira P. M. de S., Marques B. S., Ludovico P., Dias A. C. P. (2011): Evaluation of the protective effect of *Hypericum perforatum* phenolics compounds, in the toxicity induced by heterologous expression of α-synuclein. Universidade do Minho.

Wagner H., Bladt S., Zgainski E. M. (1983): Drogenanalyse. Dünnschichtchromatographische Analyse von Arzneidrogen. Berlin, New York: Springer.

Walker F. O. (2007): Huntington's disease. *The Lancet*, 369(9557): 218-228.

Wang Y., Shi X., Qi Z. (2010): Hypericin prolongs action potential duration in hippocampal neurons by acting on K^+ channels. *Br. J. Pharmacol.*, 159(7): 1402–1407.

Whitfield J. F. (2007): The road to LOAD: late-onset Alzheimer's disease and a possible way to block it. *Expert. Opin. Ther. Targets*, 11(10): 1257-60.

Wilson R. S., Barral S., Lee J. H. (2011): Heritability of different forms of memory in the Late Onset Alzheimer's Disease Family Study. *Journal of Alzheimer's disease*, 23(2): 249-255.

Wu Q. L., Wang S. P., Liao Y. H., Du L. J., Yang J. S., Xiao P. G. (1998): New Phloroglucinol Glycosides from *Hypericum japonicum*. *Chin. Chem. Lett.*, 9(5): 469-470.

Wu C. C., Yen M. H., Yang S. C., Lin C. N. (2008): Phloroglucinols with antioxidant activity and xanthonolignoids from the heartwood of *Hypericum geminiflorum*. *J. Nat. Prod.*, 71(6): 1027-31.

Yang J.-L., Sykova P., Wilson D. M., Mattson M. P., Bohr V. A. (2011): The Excitatory Neurotransmitter Glutamate Stimulates DNA Repair to Increase Neuronal Resiliency, *Mech. Ageing Dev.*, 132(8-9): 405-411.

Yang W., Cao J., Zhang M., Lan R., Zhu L., Du G., He S., Lee C. S. (2015a): Systemic study on the biogenic pathways of yezo'otogirins: total synthesis and antitumor activities of (±)-yezo'otogirin C and its structural analogues. *J. Org. Chem.*, 80(2): 836-46.

Yang X.-W., Li M.-M., Liu X., Ferreira D., Ding Y., Zhang J.-J., Liao Y., Qin H.-B., Xu G. (2015b): Polycyclic polyprenylated acylphloroglucinols congeners possessing diverse structures from *Hypericum henryi*. *J. Nat. Prod.*, 78(4): 885-895.

Yuce E., Bagci E. (2012): The essential oils of the aerial parts of two *Hypericum* taxa (*Hypericum triquetrifolium* and *Hypericum aviculariifolium* subsp. *depilatum* var. *depilatum* (*Clusiaceae*)) from Turkey. *Nat. Prod. Res*., 26(21): 1985-90.

Zaulyanov L. L., Green P. S., Simpkins J. W. (1999): Glutamate receptor requirement for neuronal death from anoxia-reoxygenation: an in Vitro model for assessment of the neuroprotective effects of estrogens. *Cell. Mol. Neurobiol.*, 19(6): 705-18.

Zhang J.-J., Yang X.-W., Liu X., Ma J.-Z., Liao Y., Xu G. (2015): 1,9-*seco*-Bicyclic Polyprenylated Acylphloroglucinols from *Hypericum uralum*. *J. Nat. Prod.*, 78(12): 3075–3079.

Zhang Z., Hu F., Liu Y., Ma B., Chen X., Zhu K., Shi Y., Wei T., Xing Y., Gao Y., Lu H., Liu Y., Kang Q. (2016): Activation of type 5 metabotropic glutamate receptor promotes the proliferation of rat retinal progenitor cell via activation of the PI-3-K and MAPK signaling pathways. *Neuroscience*, 322: 138-151.

Zhao C., Deng W., Gage F. H. (2008): Mechanisms and Functional Implications of Adult Neurogenesis. *Cell*, 132: 645–660.

Zhou J., Xie G., Yan X. (2011): Encyclopaedia of Traditional Chinese Medicines molecular structures, pharmacological activities, natural sources and applications. Springer. ISBN 978-3-642-16744-7.

Zhou Z., Zhang Y., Pan K., Luo J., Kong L. (2014): Cytotoxic polycyclic polyprenylated acylphloroglucinols from *Hypericum attenuatum*. *Fitoterapia*, 95: 1-7.

Zurbriggen A., Kirst H., Melis A. (2012): Isoprene production via the mevalonic acid pathway in *Escherichia coli* (Bacteria). *Bioenerg. Res.*, 5: 814-828.

7 Appendix

7.1 Voucher specimens

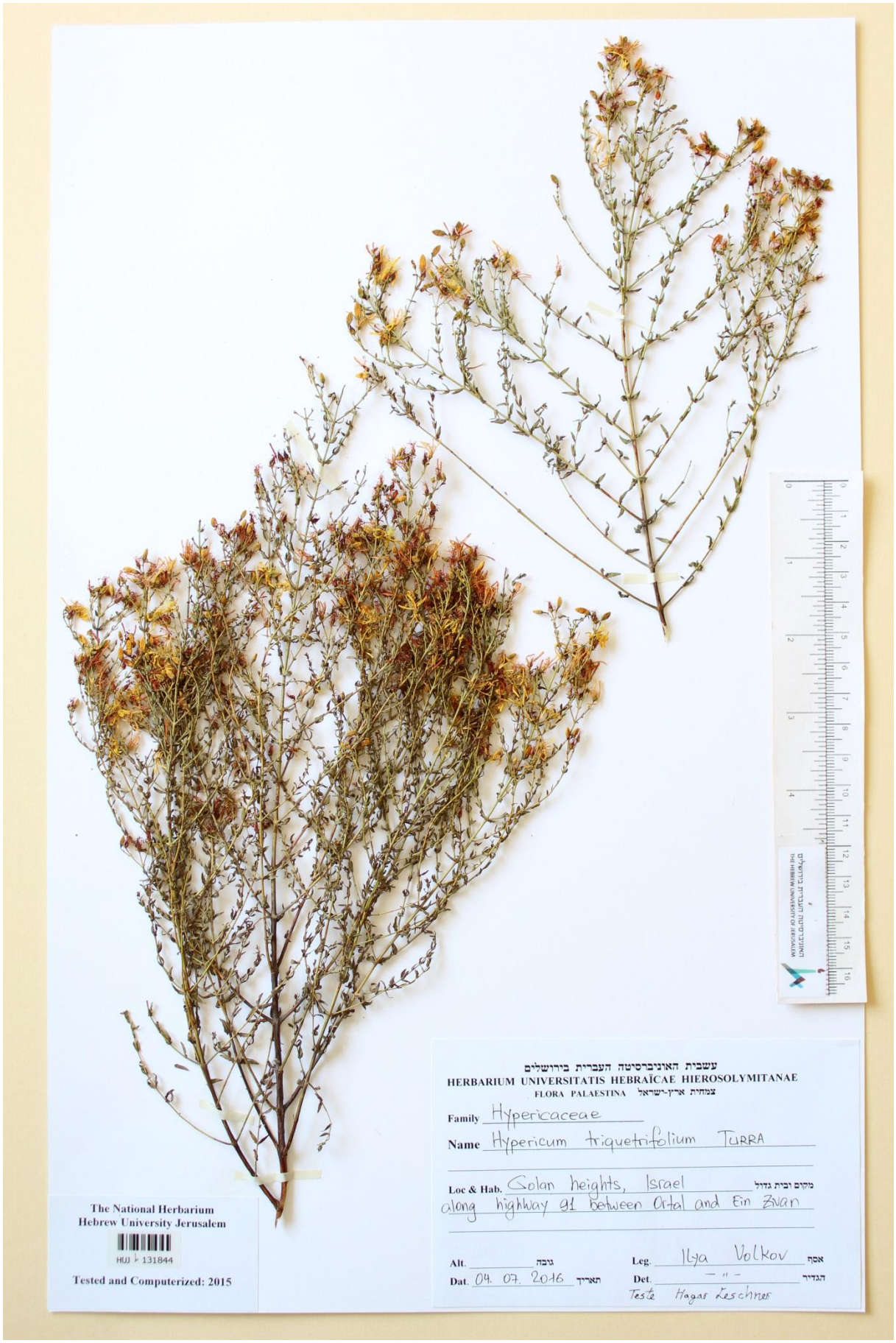
עשבית האוניברסיטה העברית בירושלים
HERBARIUM UNIVERSITATIS HEBRAÏCAE HIEROSOLYMITANAE
FLORA PALAESTINA צמחית ארץ-ישראל
Family Hypericaceae
Name Hypericum triquetrifolium TURRA
Loc & Hab. Golan heights, Israel מקום ובית גדול
along highway 91 between Ortal and Ein Zivan
Alt. גבה
Leg. Ilya Volkov אסף
Dat. 04. 07. 2016 תאריך
Det. — " — הגדיר
Teste Hagar Reschner
The National Herbarium
Hebrew University Jerusalem
HUJ 131844
Tested and Computerized: 2015


I/II
עשבית האוניברסיטה העברית בירושלים
HERBARIUM UNIVERSITATIS HEBRAÏCAE HIEROSOLYMITANAE
FLORA PALAESTINA צמחית ארץ-ישראל
Family Hypericaceae
Name Hypericum triquetrifolium TURRA
Loc & Hab. Golan Heights, Israel מקום ובית גדול
along highway 91 between Ortal and Ein Zivan
Alt. גבה
Dat. 04.07.2016 תאריך
Leg. Ilya Volkov אסף
Det. — " — הגדיר
Taste: Hagar Reschner
The National Herbarium
Hebrew University Jerusalem
HUJ 131845
Tested and Computerized: 2015

7.2 Work of Sebastian Pitzl on neurotoxicity and neuroprotection

The following paragraph presents the internal unpublished data, obtained by Mr. Sebastian Pitzl during his Master thesis work on Pharmaceutical Biology department of the University of Regensburg, Germany. His work on neurotoxicity and neuroprotection on HT-22 cells was supervised by Dr. Beata Kling and Prof. Dr. Jörg Heilmann. These data is specified here with the kind permission of Mr. Sebastian Pitzl.

7.2.1 Structural formulas of the tested substances

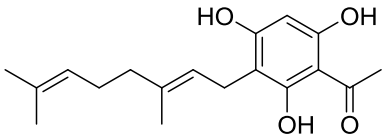

UR-QS-1

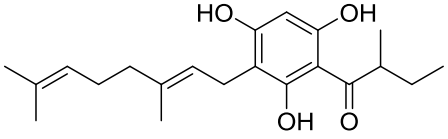

UR-QS-2

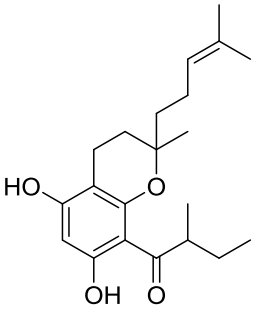

UR-QS-4

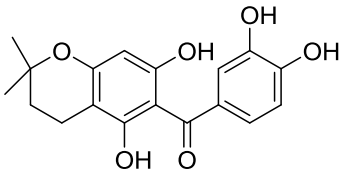

UR-QS-7

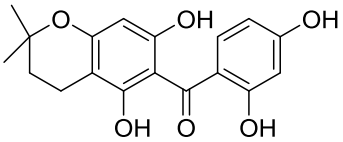

UR-QS-8

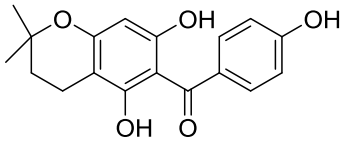

UR-QS-9

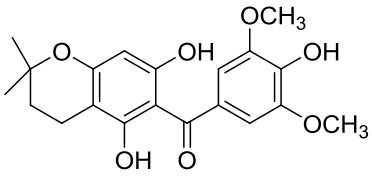

UR-QS-12

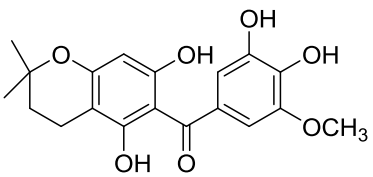

UR-QS-14

7.2.2 Results

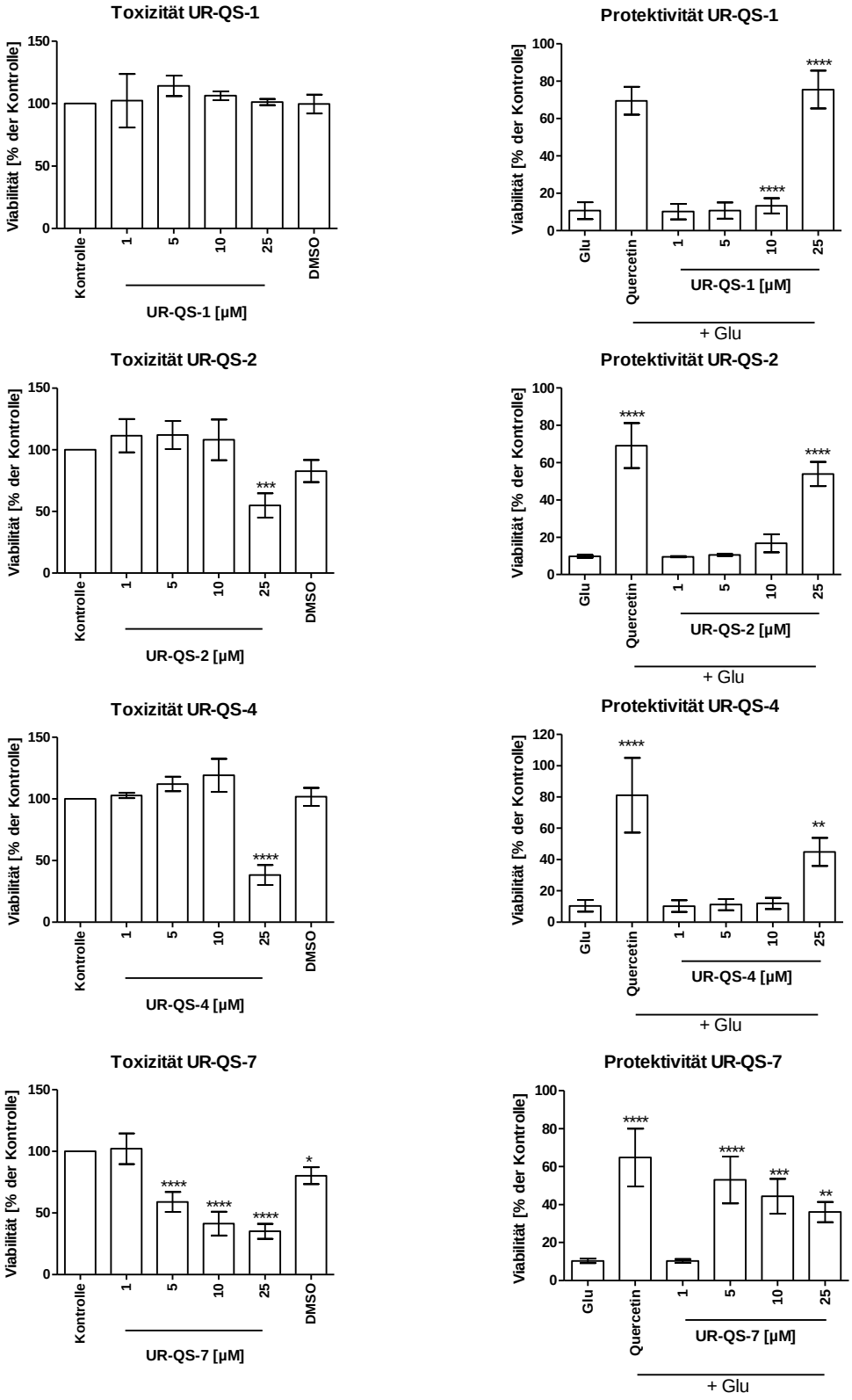

Evaluation of neurotoxicity and neuroprotection of **UR-QS-8**, **UR-QS-9**, **UR-QS-12** und **UR-QS-14**
Level of significance: $p < 0,05$ (*), $p < 0,01$ (**), $p < 0,001$ (***), $p < 0,0001$ (****)

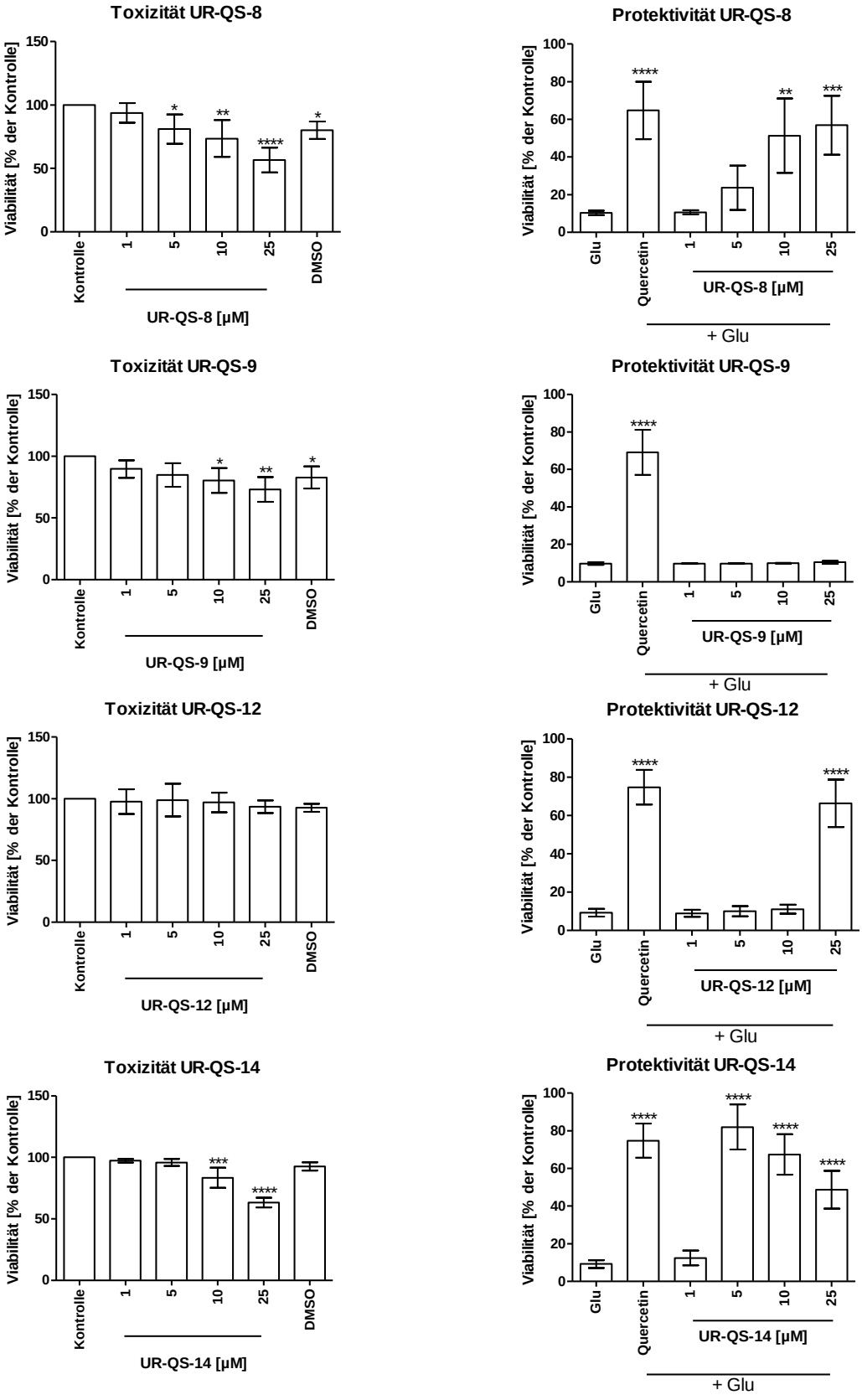

Evaluation of neurotoxicity and neuroprotection of **UR-QS-8**, **UR-QS-9**, **UR-QS-12** und **UR-QS-14**
Level of significance: $p < 0,05$ (*), $p < 0,01$ (**), $p < 0,001$ (***), $p < 0,0001$ (****)

7.3 NMR spectra

^{1}H-NMR (**1**)

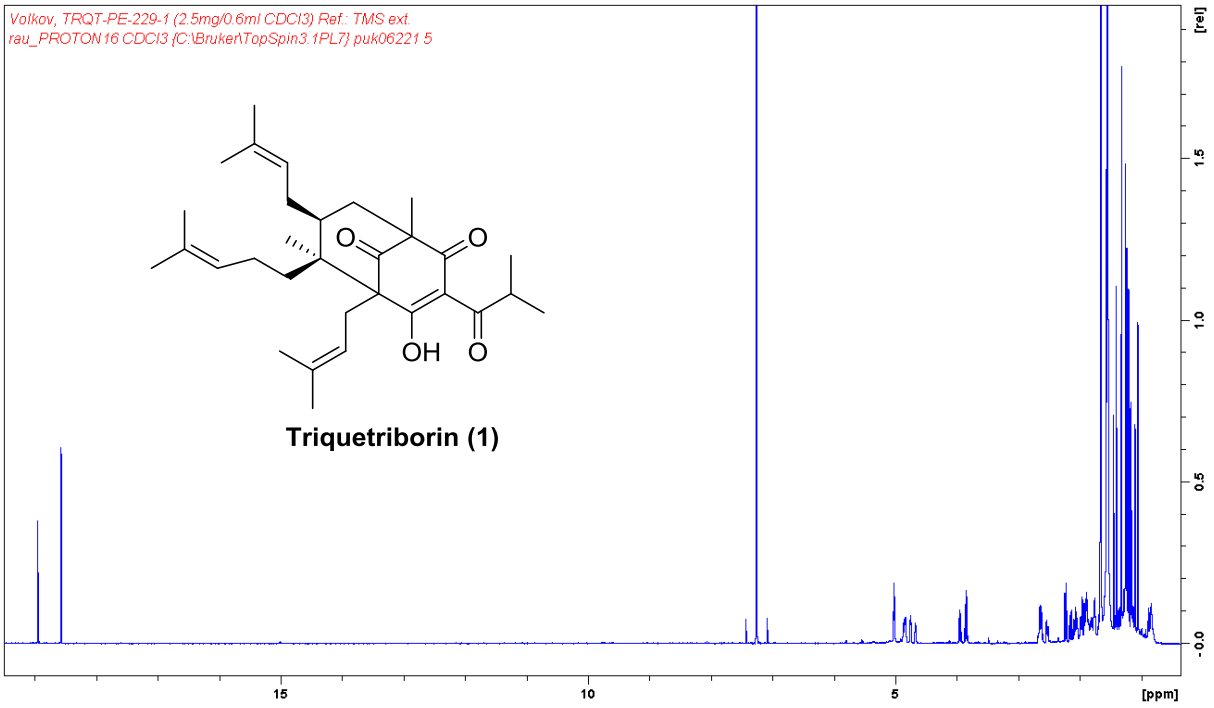

^{13}C-NMR (**1**)

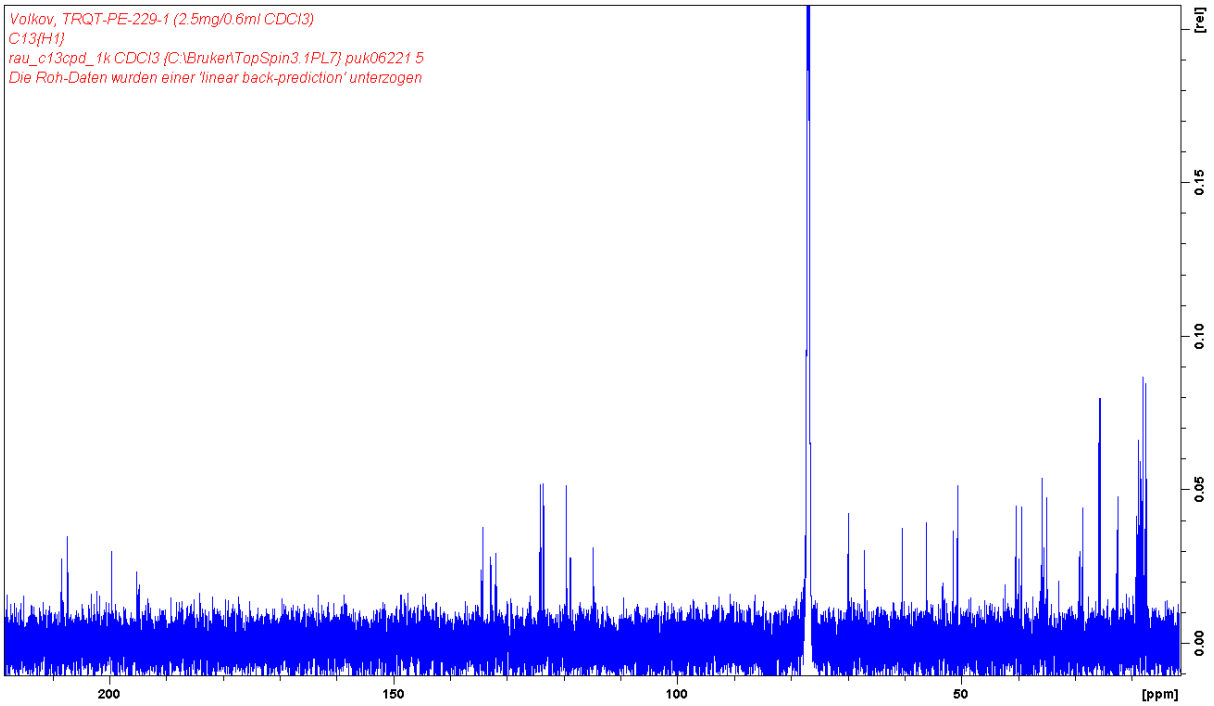

^{1}H-NMR (**2**)

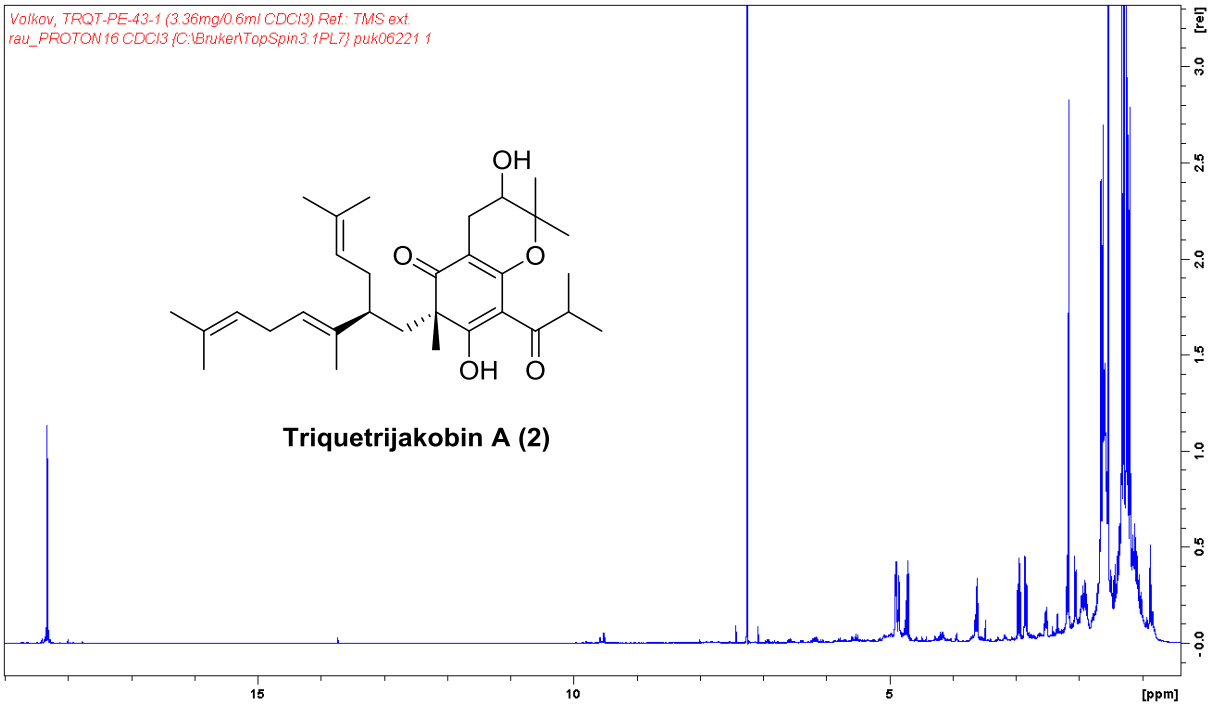

^{13}C-NMR (**2**)

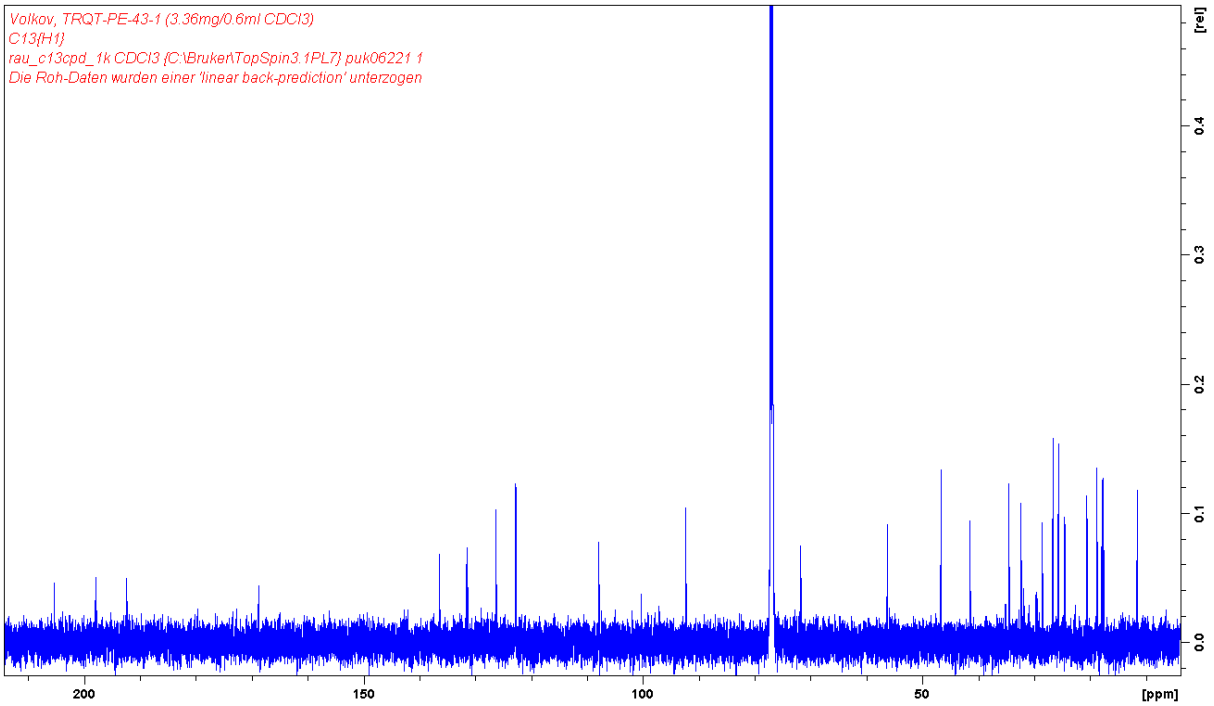

^{1}H-NMR (**3**)

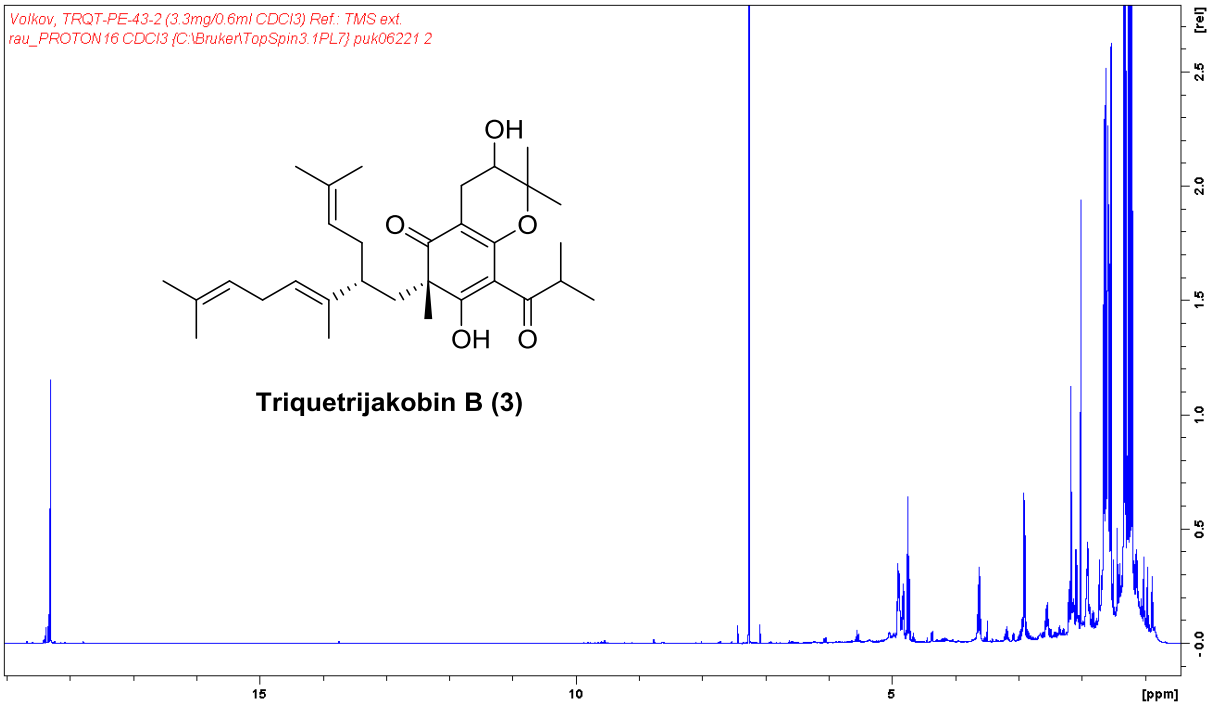

^{13}C-NMR (**3**)

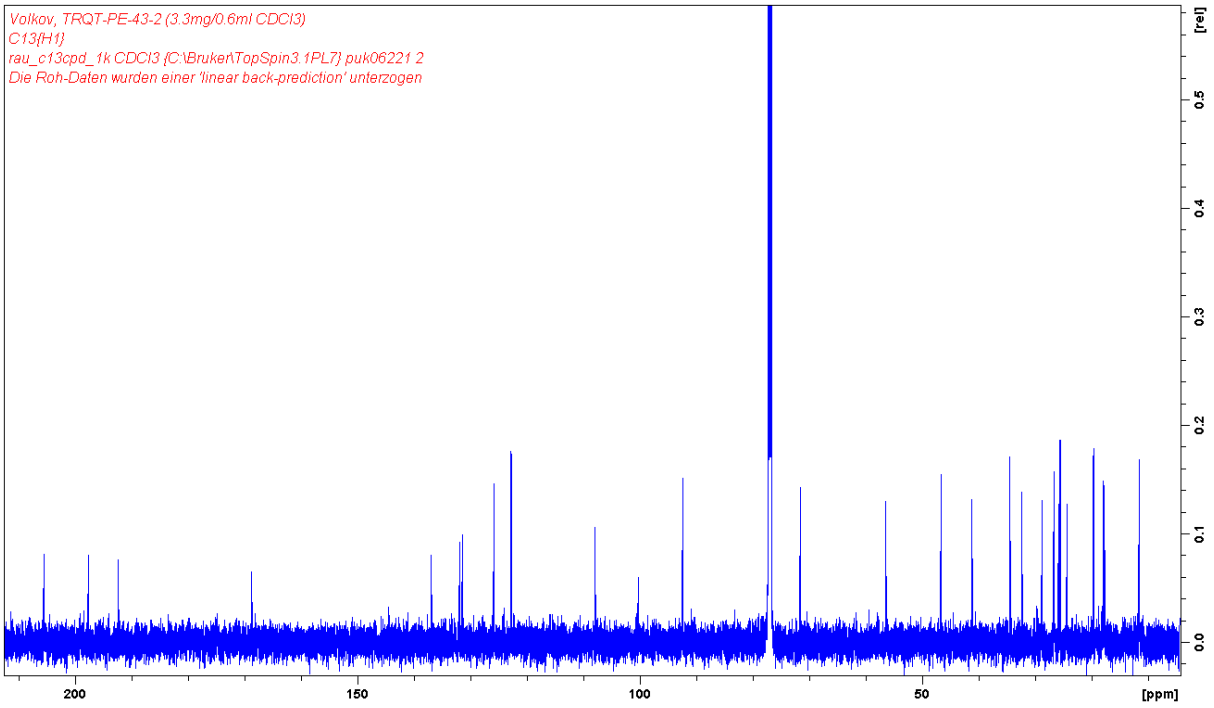

^{1}H-NMR (**4**)

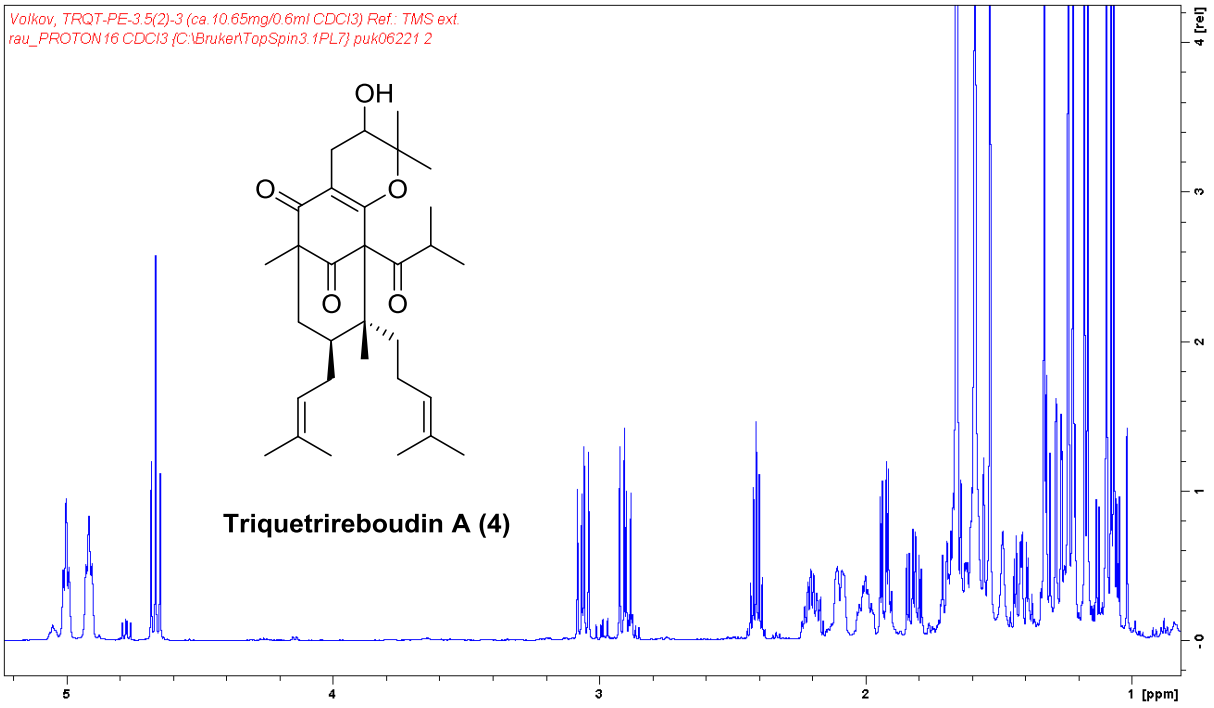

^{13}C-NMR (**4**)

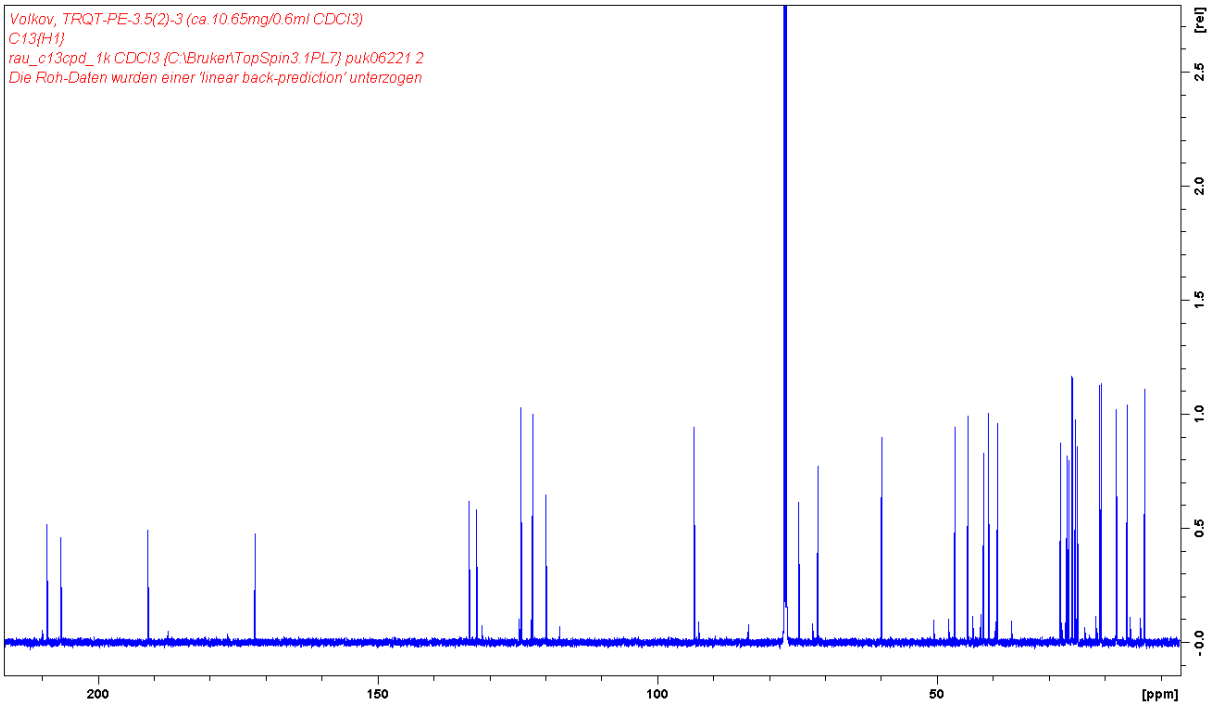

^{1}H-NMR (**5**)

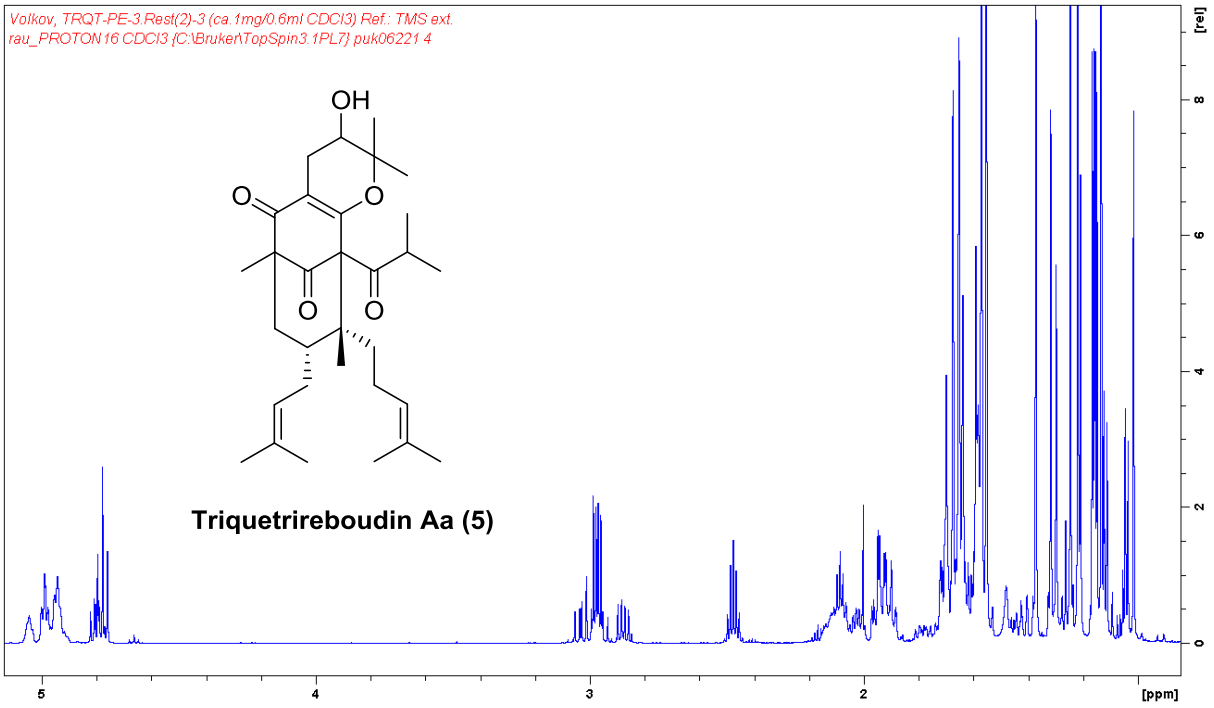

^{13}C-NMR (**5**)

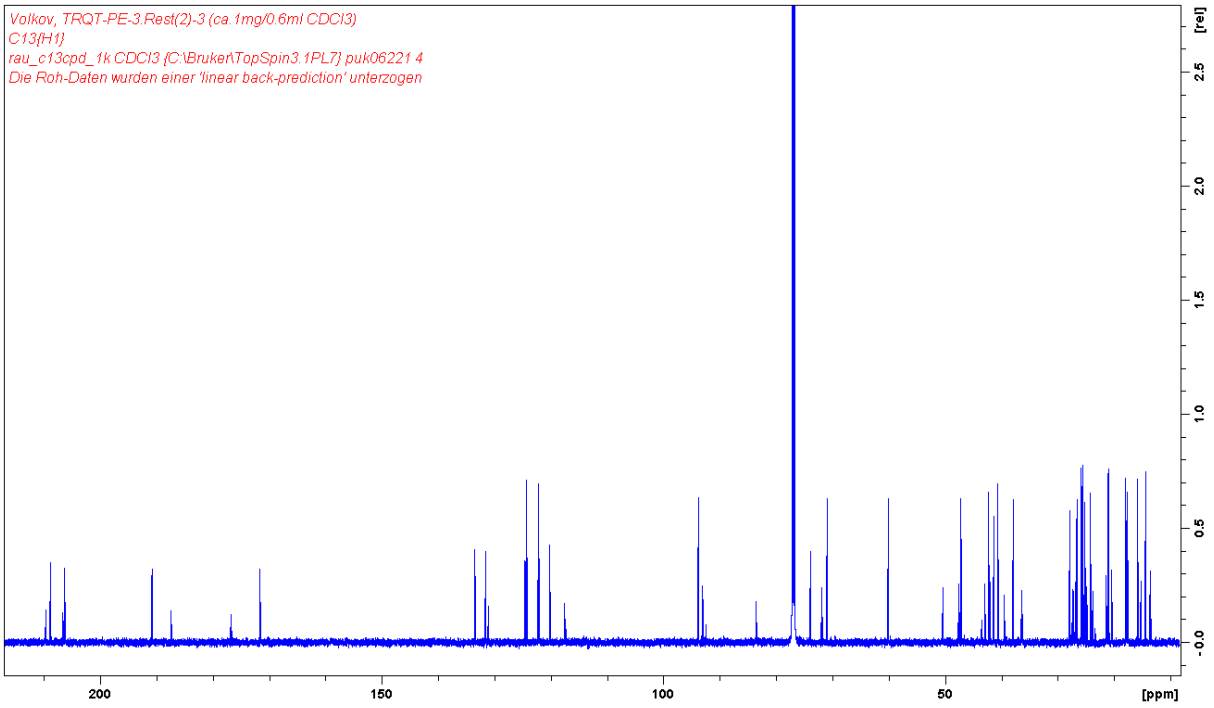

^{1}H-NMR (**6**)

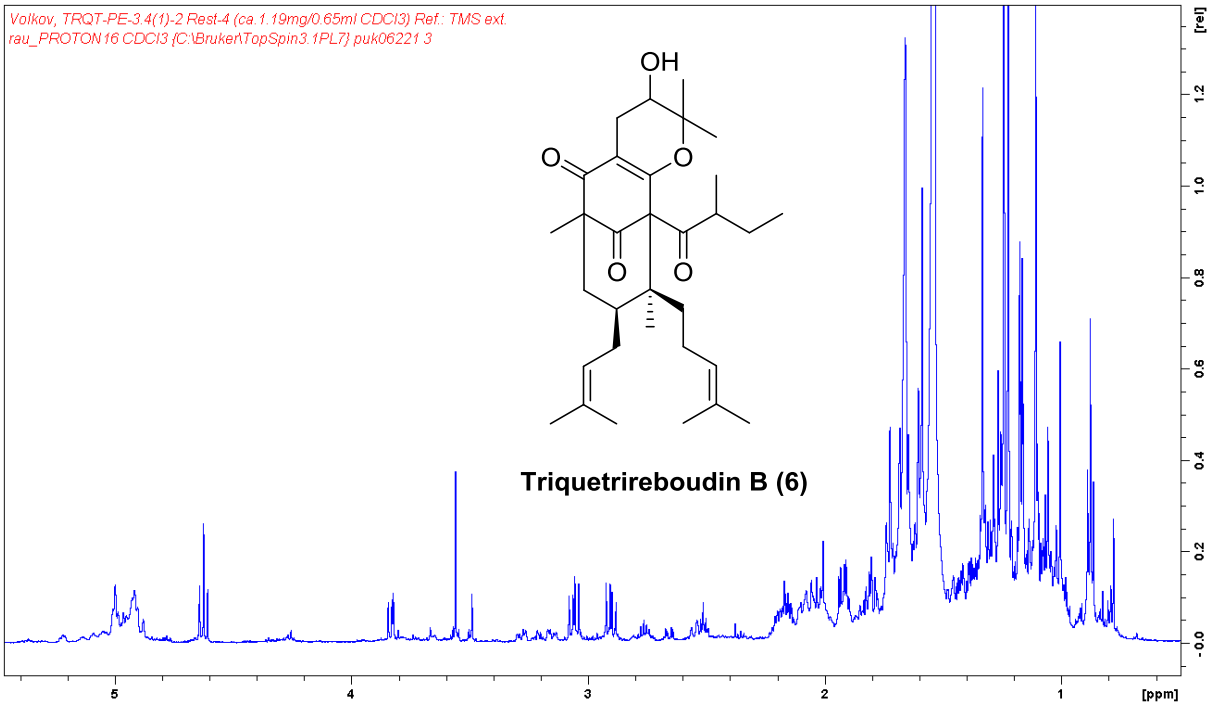

^{13}C-NMR (**6**)

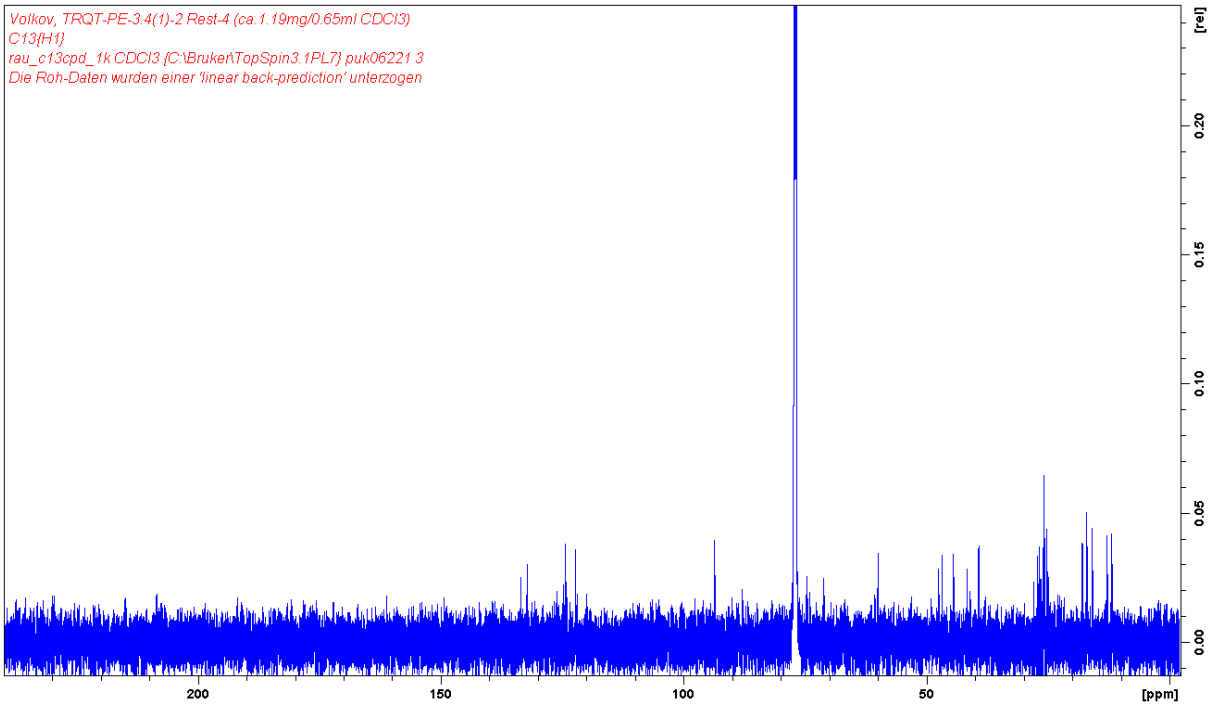

^{1}H-NMR (**7**)

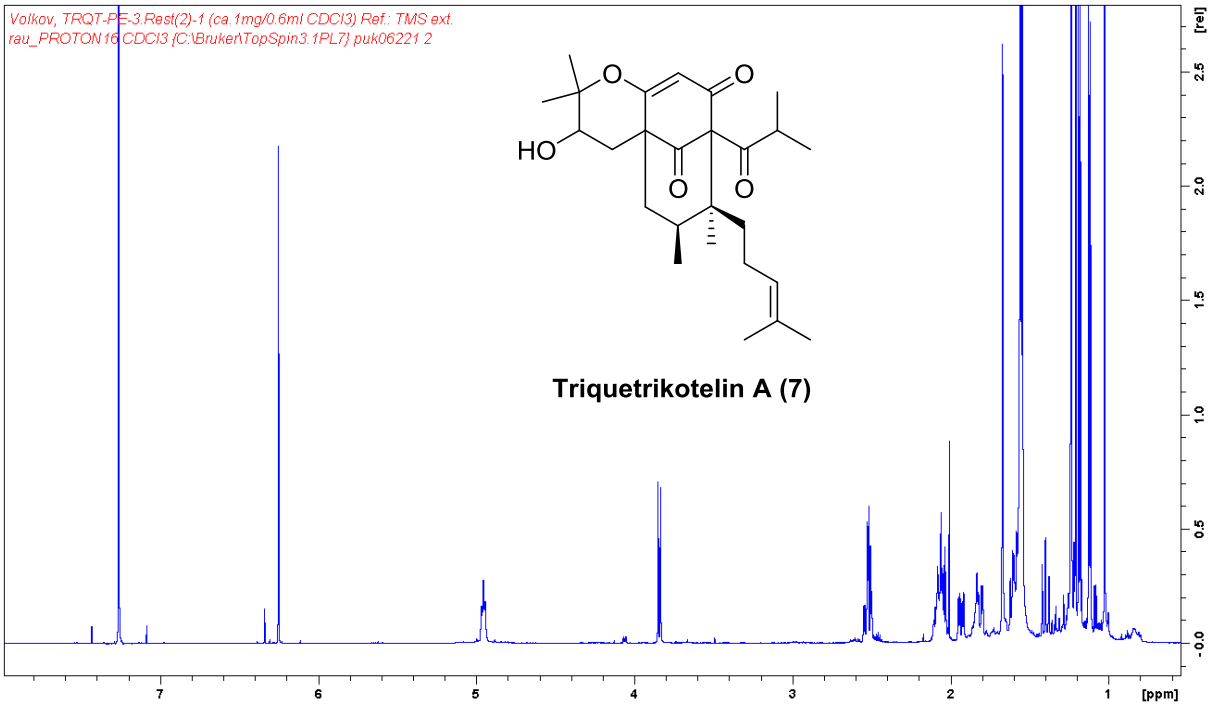

^{13}C-NMR (**7**)

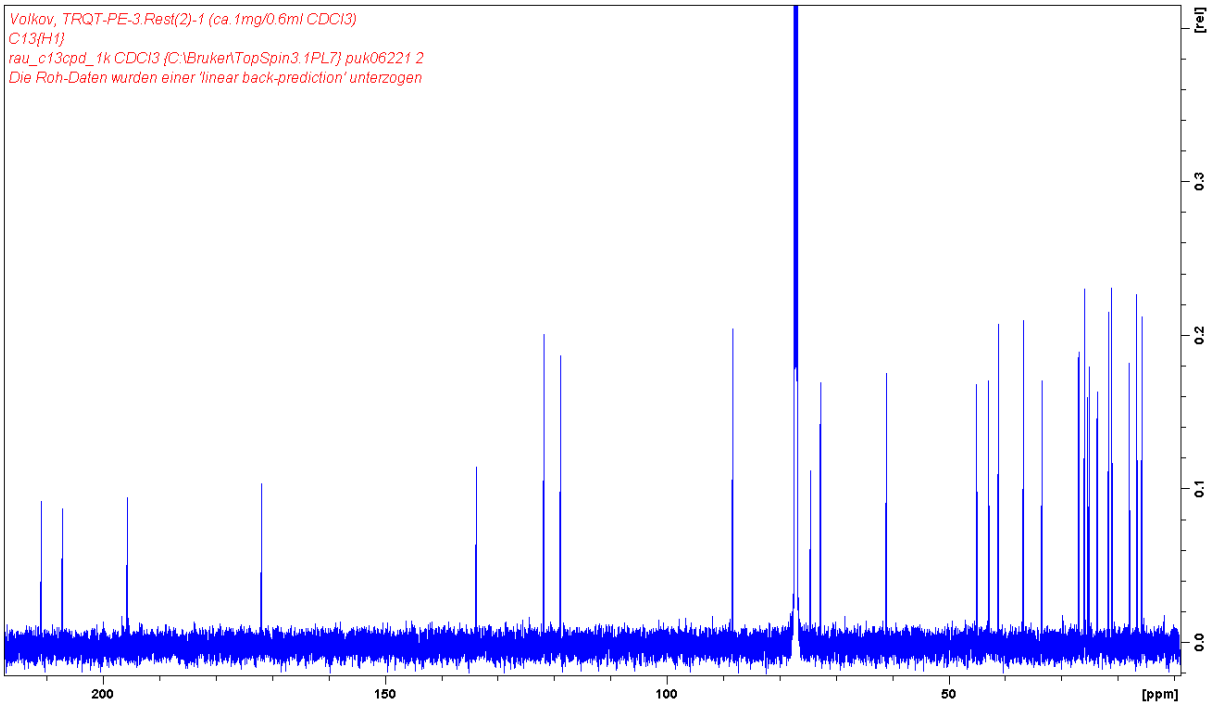

^{1}H-NMR (**8**)

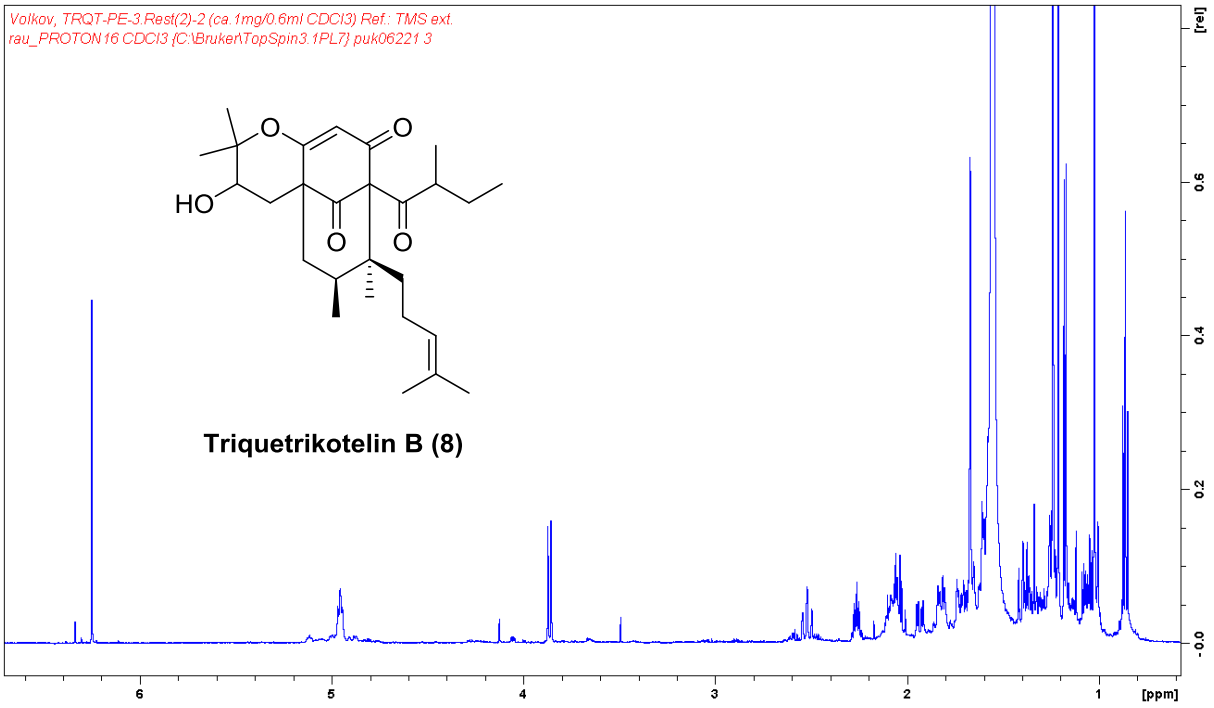

^{13}C-NMR (**8**)

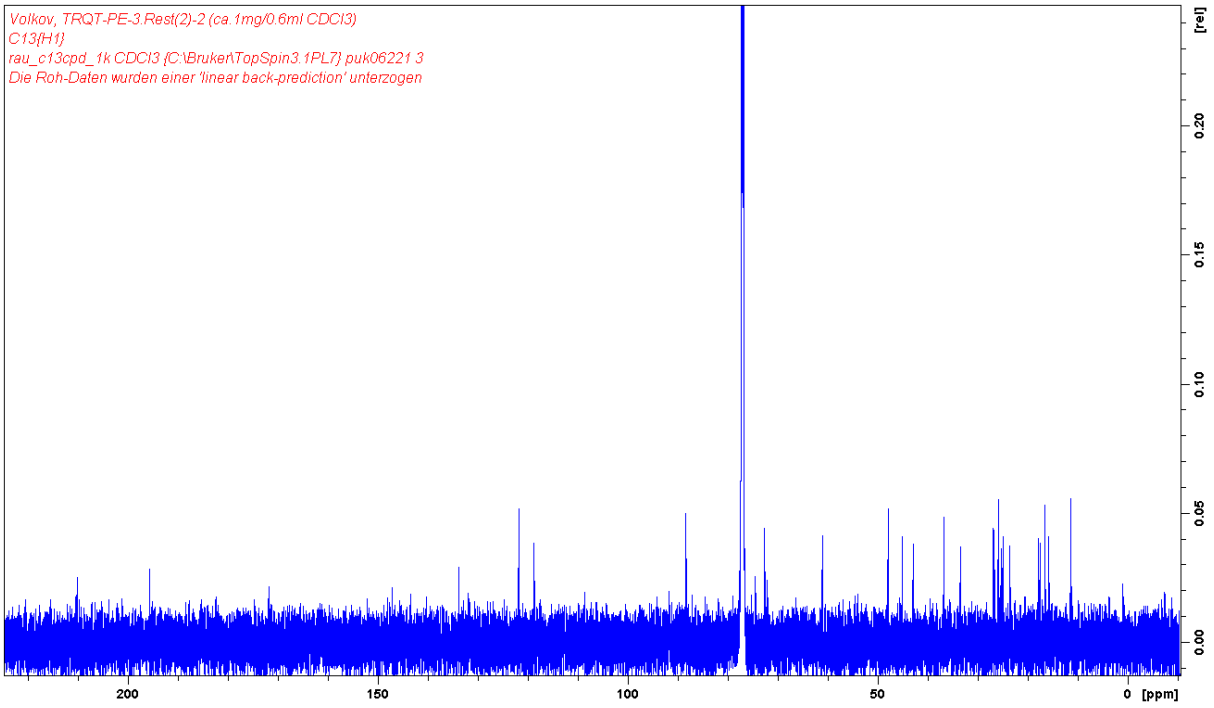

^{1}H-NMR (**9**)

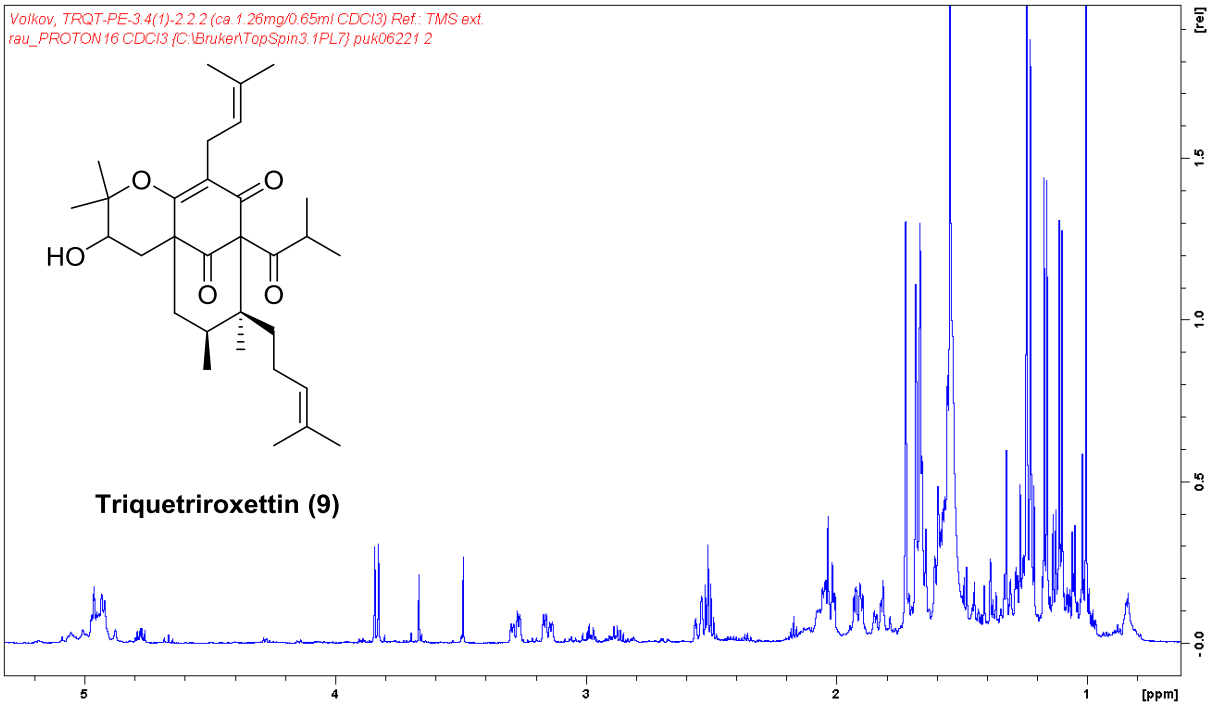

^{13}C-NMR (**9**)

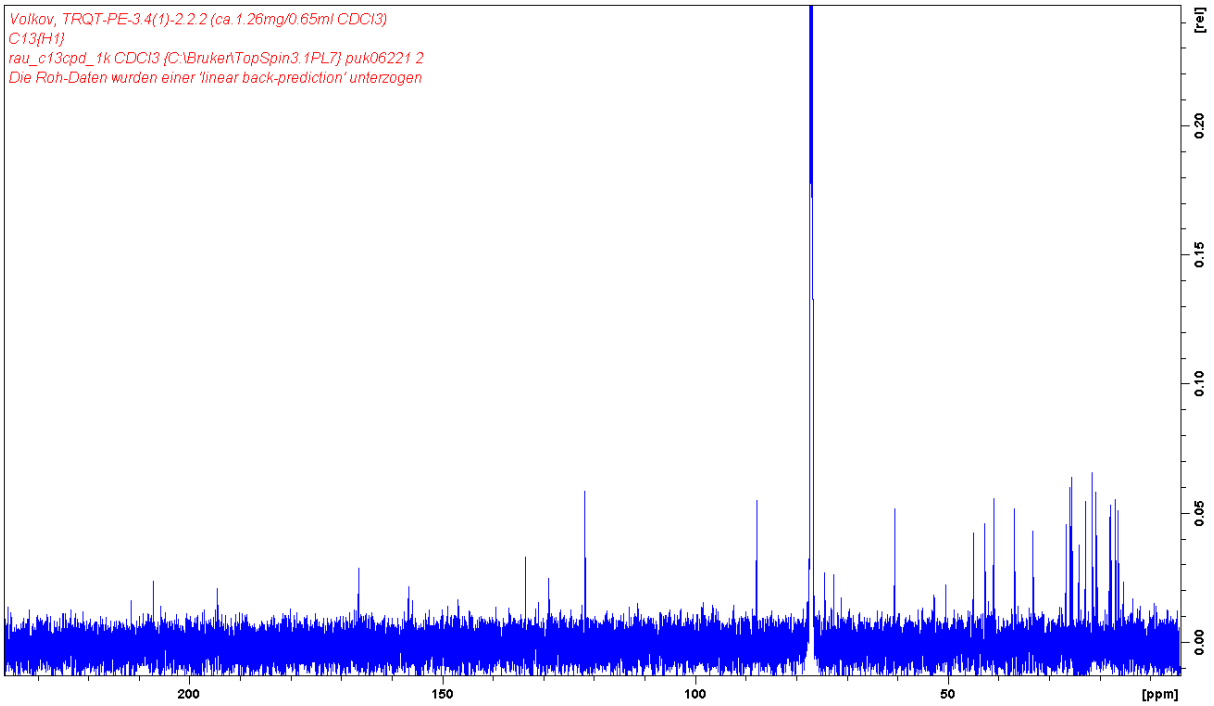

^{1}H-NMR (**10**)

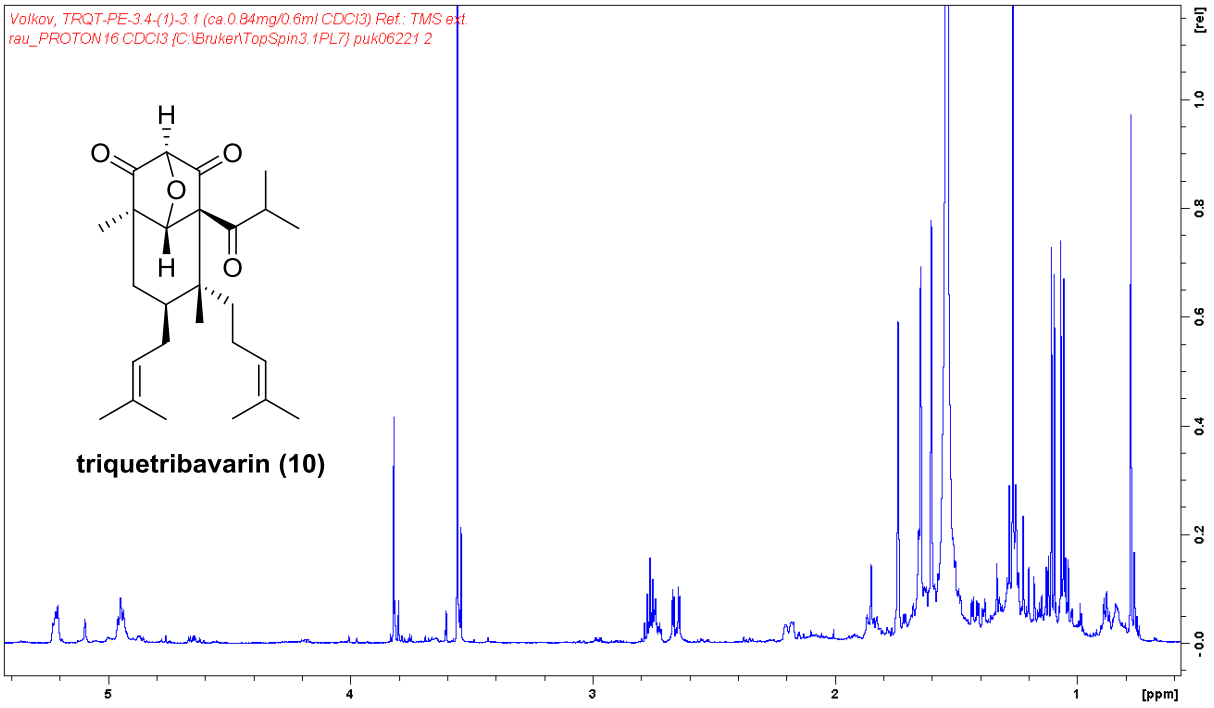

^{13}C-NMR (**10**)

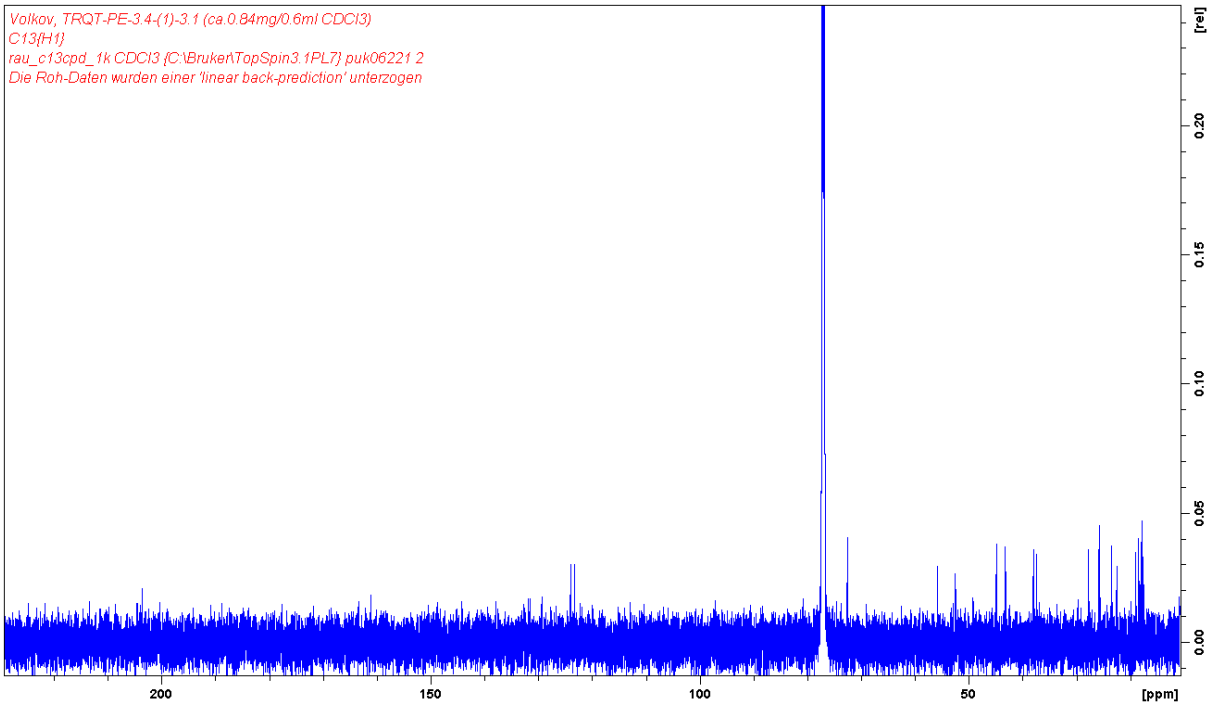

^{1}H-NMR (**11**)

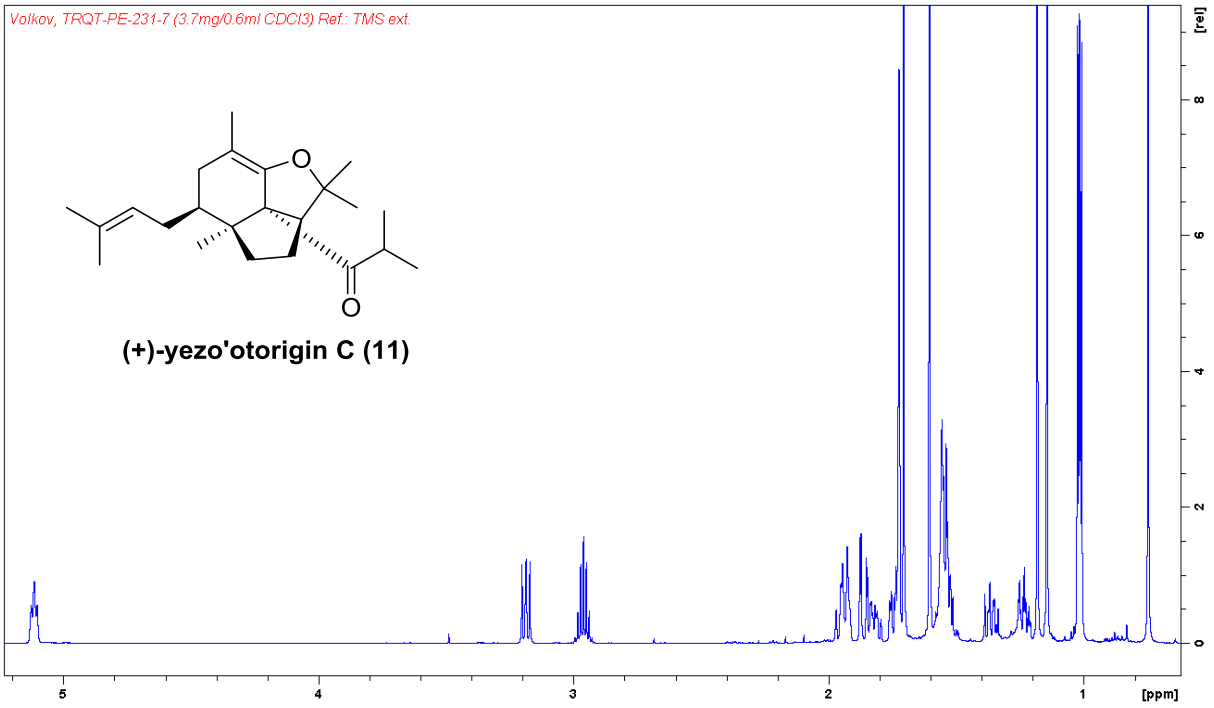

^{13}C-NMR (**11**)

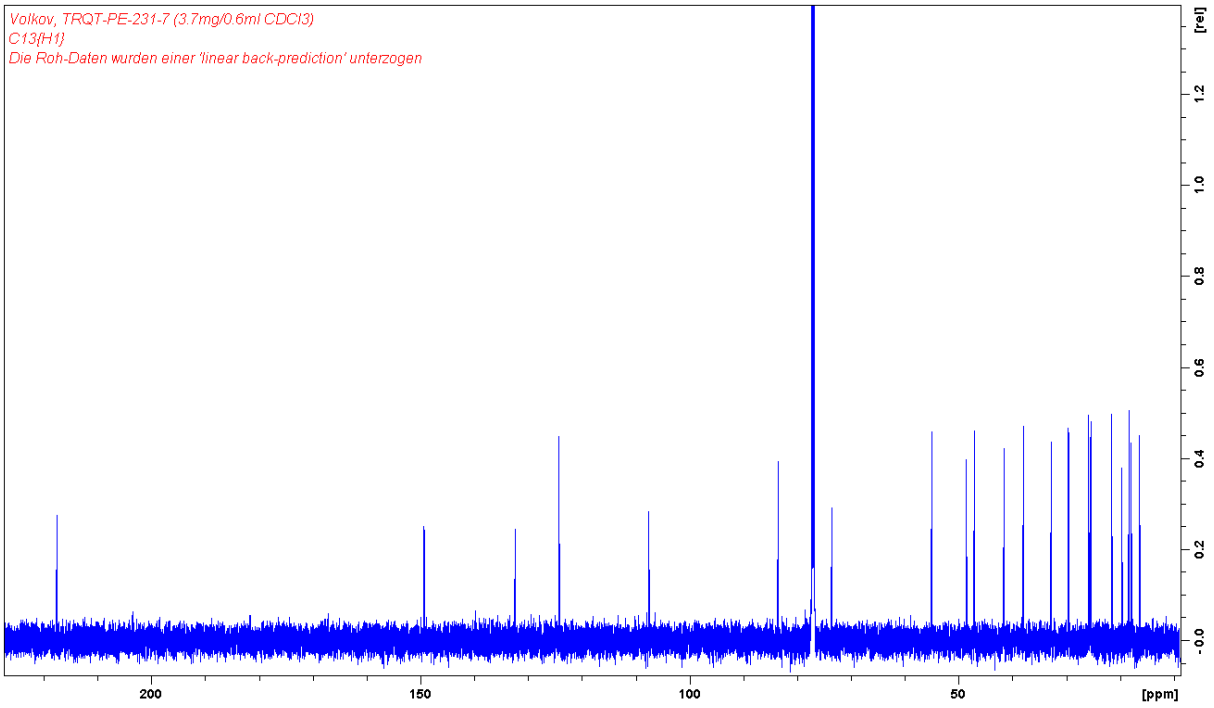

^{1}H-NMR (**12**)

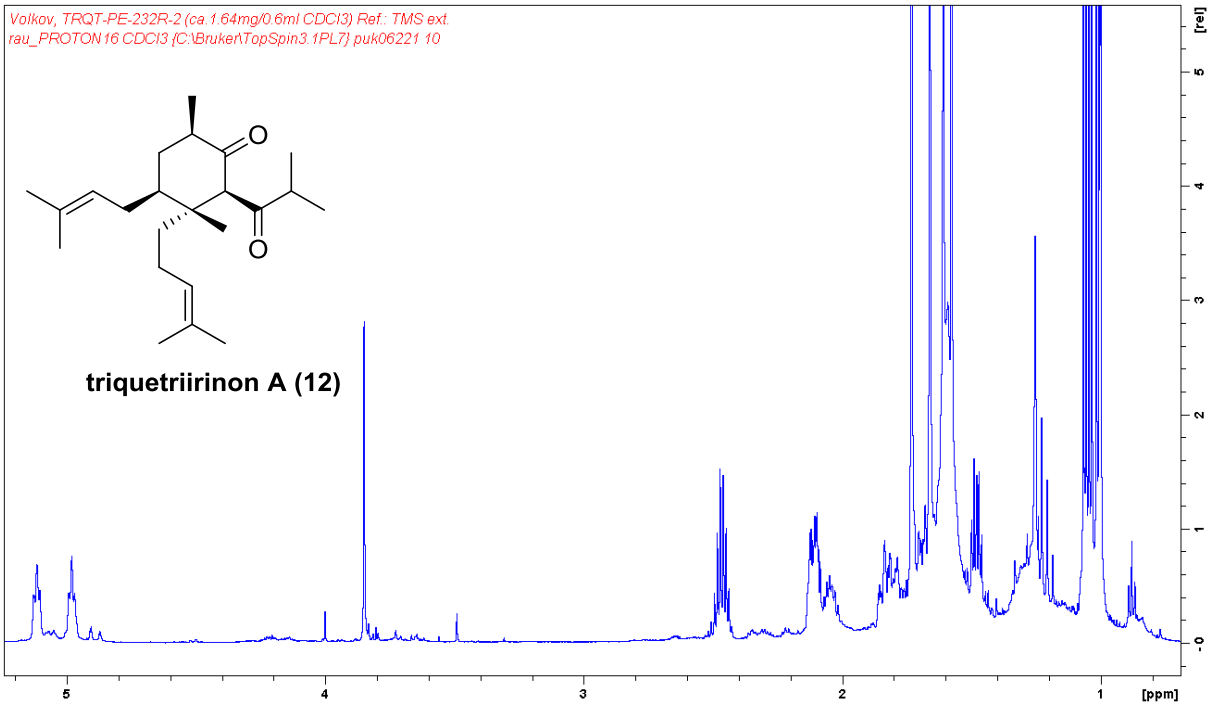

^{13}C-NMR (**12**)

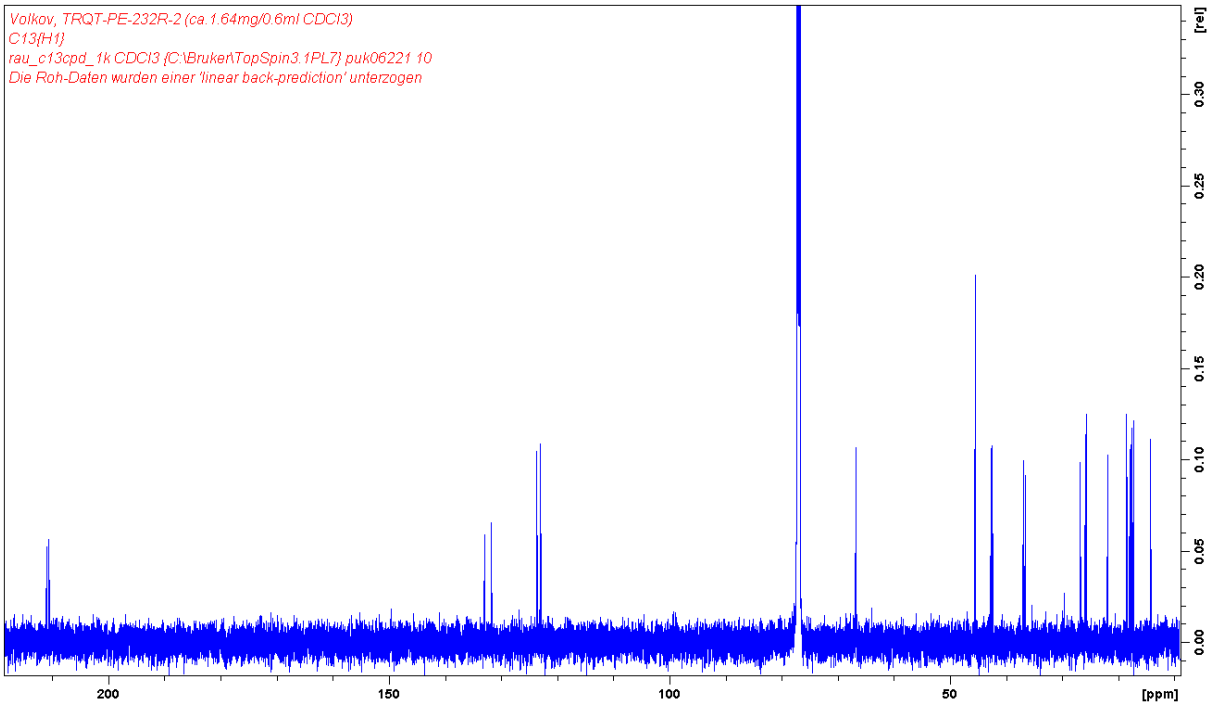

^{1}H-NMR (**12+13**)

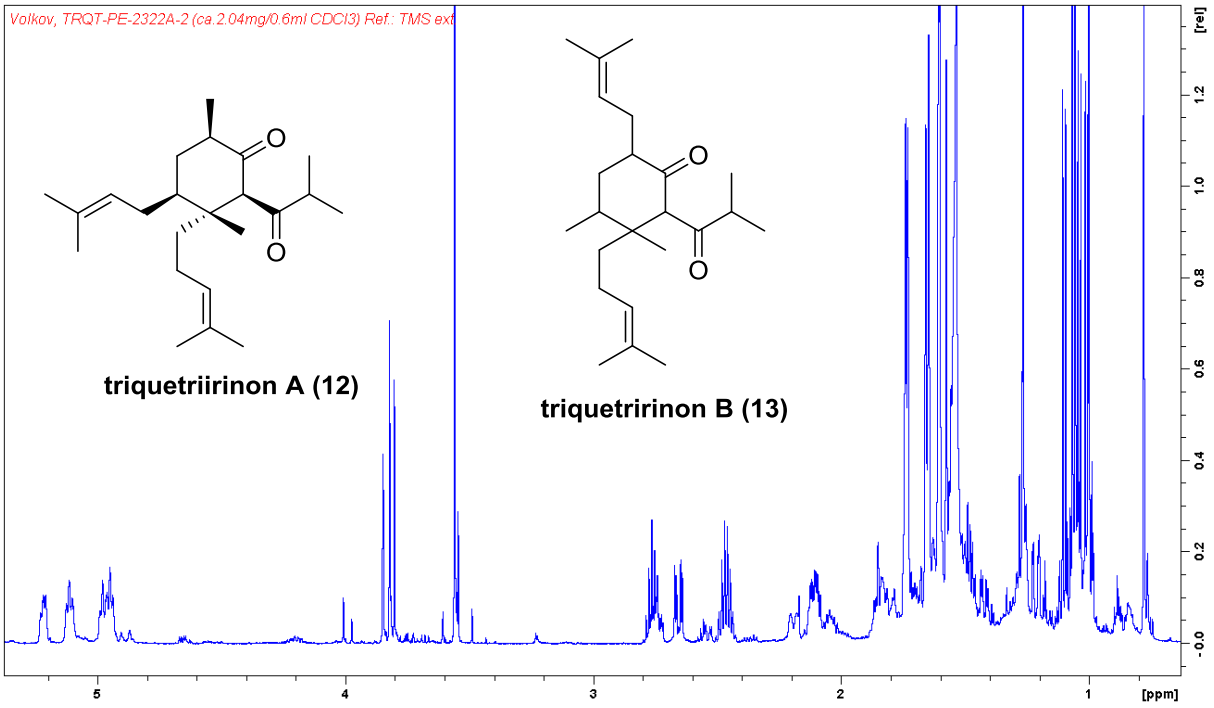

^{13}C-NMR (**12+13**)

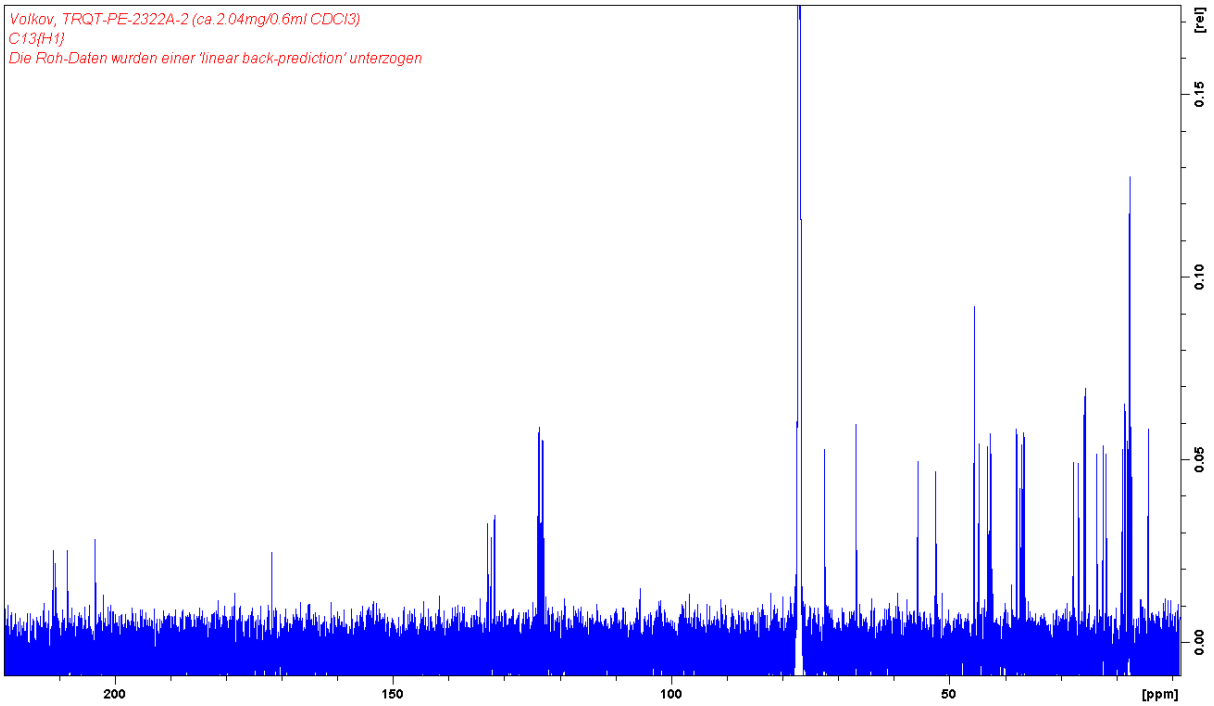

^{1}H-NMR (**14**)

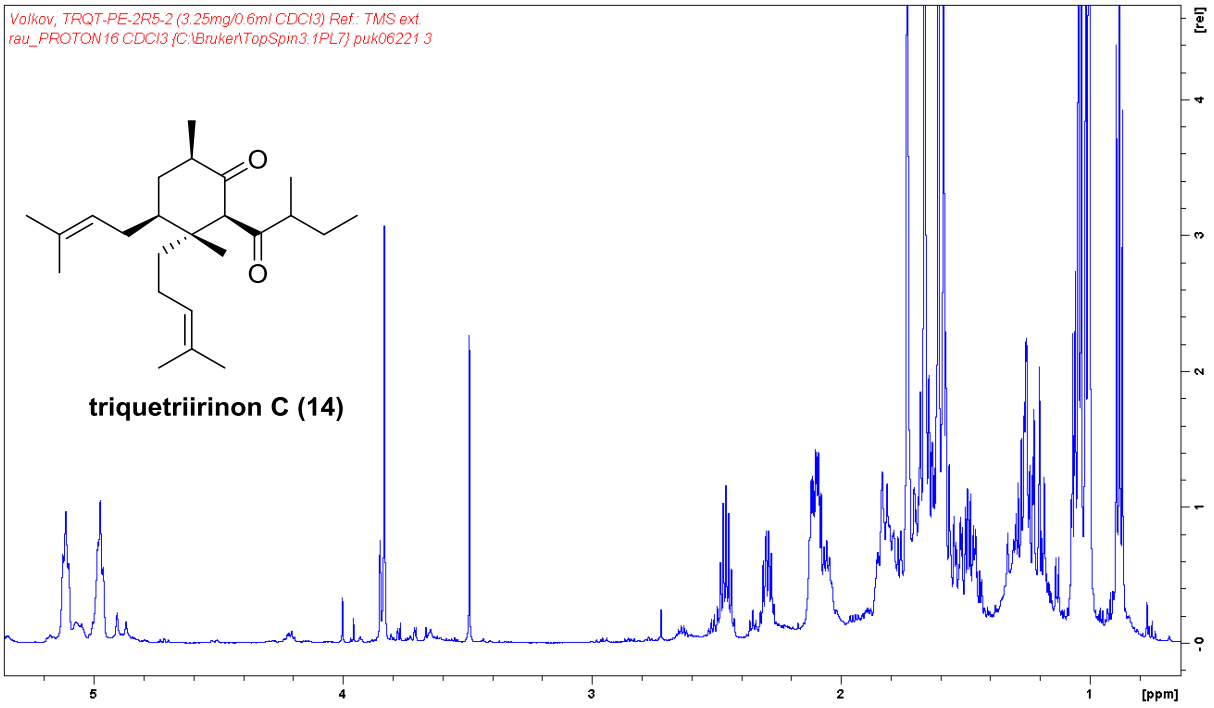

^{13}C-NMR (**14**)

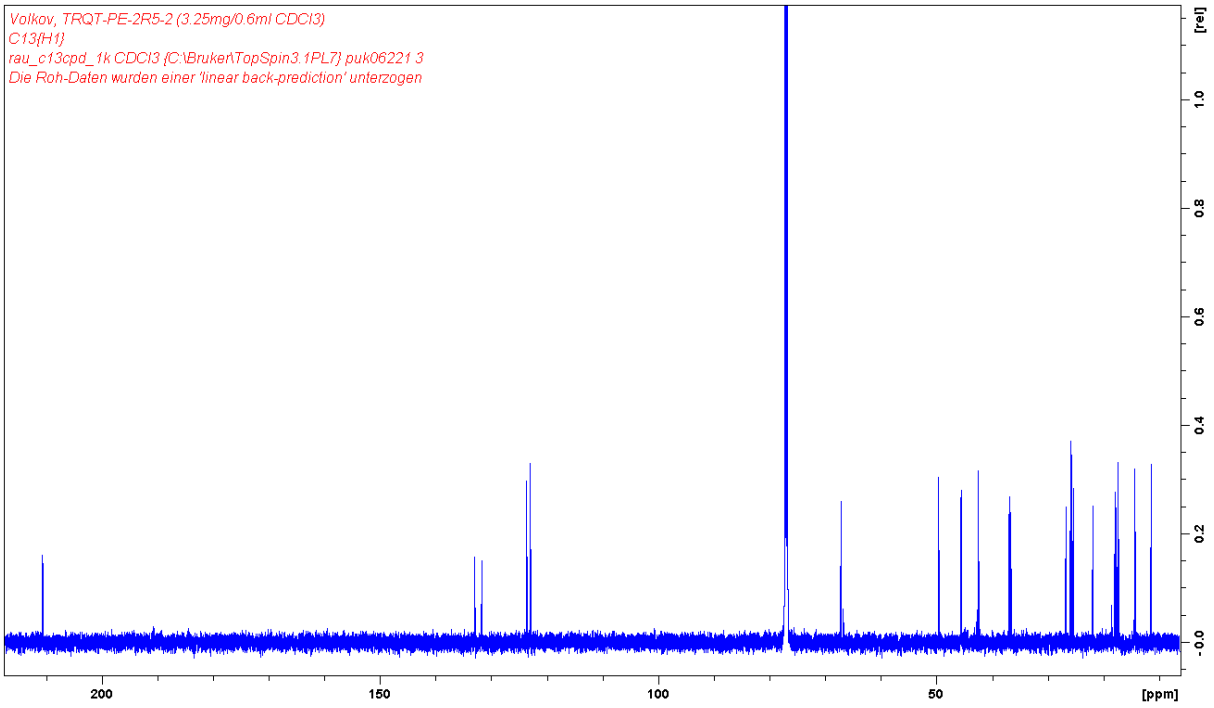

^{1}H-NMR (**15**)

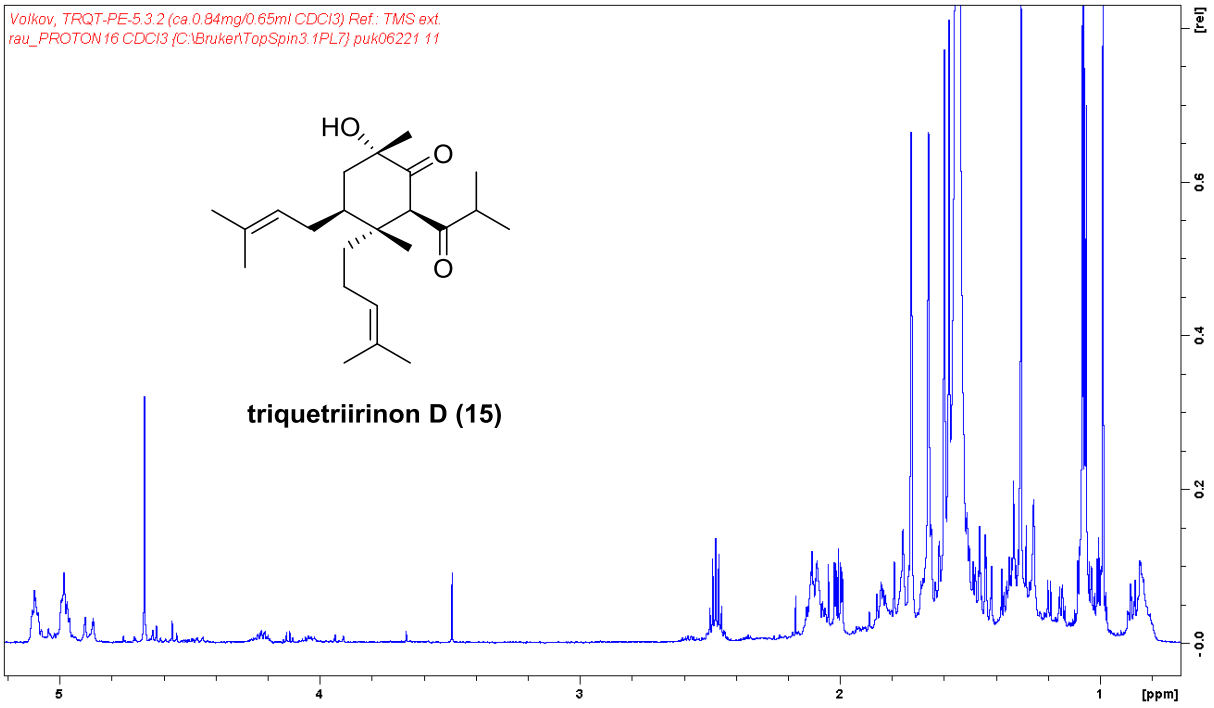

^{13}C-NMR (**15**)